SPECTROSCOPY, SOLVATION AND REACTIVITY OF TRANSITION METAL COMPLEXES WITH π-ACCEPTOR LIGANDS

A THESIS

submitted by

RAZAK BIN ALI

for the

Degree of Doctor of Philosophy

University of Leicester

November, 1986.

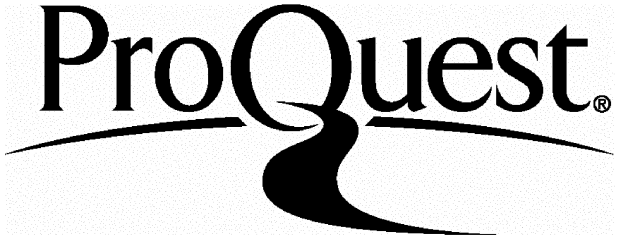

ACKNOWLEDGEMENTS

The work described in this thesis was carried out in the Chemistry Laboratory of the University of Leicester, between October 1983 to November 1986, under the supervision of Dr. J. Burgess, to whom I am deeply grateful, for his continued guidance and encouragement.

I would also like to thank Dr. A. E. Smith and My wife for their helps.

I am indebted to the Commonwealth Commission and the University of Technology Malaysia for awarding me a scholarship for these studies.

Department of Chemistry,
University of Leicester,
Leicester

TO

HASNIZA, MOHAMAD NIZUAN

AND KHAIRUL NISAA'

CONTENTS

CHAPTER 1

Introduction

1-1. π-Acceptor Ligands

The most interesting feature of d-group transition metals is their ability to form complexes with a variety of neutral ligands such as carbon monoxide, nitric oxide, 1,10-phenanthroline, 2,2'-bipyridine, etc. The formation of complexes is well explained by molecular orbital theory.[1,2] Two types of bonds appear in the complex. The first is σ-bonding, which is formed from the donation of a lone pair electrons of ligand to metal. The second is π-bonding which occurs due to the presence of a vacant π^*-orbital of the ligand. The orientation and sufficiently low energy level of π^*-orbital allows it to interact with t_{2g}-orbital of metal in an octahedral complex through π-interaction. This interaction provides for the ligands to accept electron density from the metal into their π^*-orbital. Such type of ligand is often said to have π-acceptor ability (π-acceptor ligand).

Now there are a lot of such ligands, monodentate to chelate. Most of them show similar features; among these the ability to stabilize the lower oxidation state (lower-positive, zero and even negative) of metals. The complex normally tends to have a low-spin configuration which, according to crystal field theory, produces a very stable complex. The complex is substitutionally inert. It requires a large energy to break the metal-ligand bond so that the substitution process by other ligands is rather difficult. Some features of the complexes can be obtained from a study on metal-carbonyl complexes. A lot of these complexes are commercially available and now widely used as starting

compounds to synthesize other complexes especially involving lower oxidation states. The schematic diagram for the formation of the metal-carbonyl bond and the relative energy levels of the molecular orbitals are as shown in Figures [1-1] and [1-2] respectively.

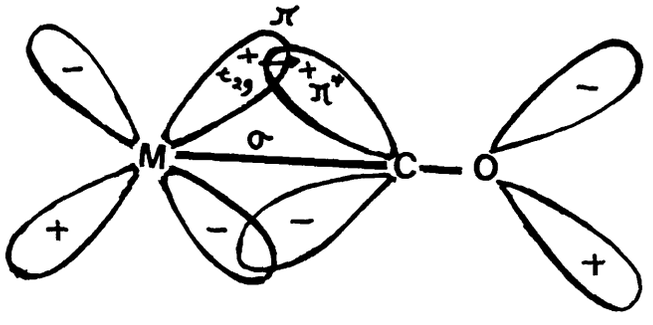

Figure [1-1] Schematic diagram of metal-carbonyl interaction

The objective of the present study is to investigate some characteristic features of complexes in solution involving metals and π-acceptor ligands. These features include spectroscopy, kinetics, and solvation. In general, our study focuses on the complexes which are mainly classified into three groups depending on a type of π-acceptor ligand as well as metal present. The first group, which makes a large contribution to the present study, consists of metal-d^6 and α-diimine ligand complexes. The majority of them are concerned with molybdenum(0), with a very limited number of manganese(I) complexes. The second group involves the

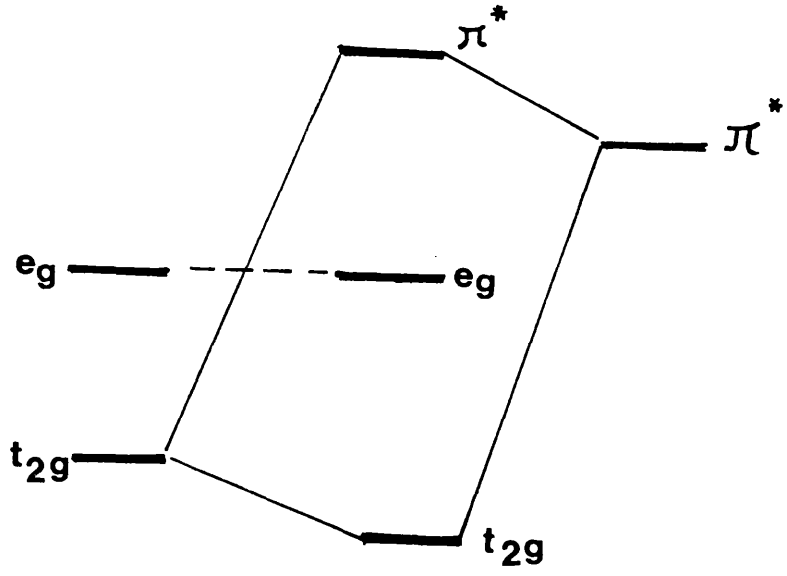

Figure [1-2] Energy level diagram for the molecular orbital in an octahedral complexes where π-bonding occurs.

complexes which are normally known as metallocene dichlorides, $M(Cp)_2Cl_2$. The system of these complexes is totally different from the first in that their π -acceptor ligand, cyclopentadiene (Cp), and chloride atom are bonded to metal atom with low d-electron density but high formal charge; titanium(IV)-d^0, vanadium(IV)-d^1 and zirconium(IV)-d^0. The study of the behaviour of these complexes mainly concerns reactivity in substitution of chlorides. Details of reactions of these complexes are discussed in Chapter 8. The third group is identified as binuclear complexes with π-acceptor bridging ligands such as pyrazine, 2,2'-bipyrimidine, etc with metal-d^6. In many cases, such complexes provide a system in which the intramolecular elecron transfer process can take place as described in the last chapter of this report.

1-2. Metal-Diimine Complexes

Diimines are a group of compounds which are usually considered as good π-acceptor ligands.[3] The most common forms are α-diimines. These compounds have a basic structure as shown in 1 in which two nitrogen atoms are separated by two carbon atoms. There are two type of bonds, σ and π ,

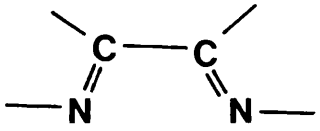

1

present in the system which make it different from ordinary amines (i.e. only σ-bond present). Many of these compounds have been identified; all of them are potentially bidentate. Examples of such compounds include 1,10-phenanthroline, 2;[4] 2,2'-bipyridine, 3;[4] and Schiff bases such as pyridine-2-ketone derivatives, 4; and 1,4-diazabutadienes, 5.[5,6]

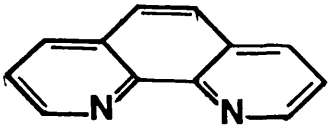

2

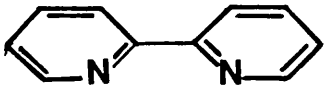

3

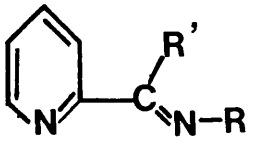

R = H, Alkyl, or Aryl
R'= H, Alkyl, or Aryl

4

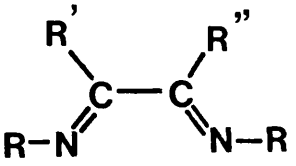

R = H, Alkyl, or Aryl
R'= H, Alkyl, or Aryl
R"= H, Alkyl, or Aryl

5

In general, we can classify all these diimine compounds into three groups depending on two, one and no ligating nitrogens incorporated into aromatic rings. Thus 1,10-phenanthroline and 2,2'-bipyridine are included in the first group. Most of which are commercially available. The second and third groups consist of series of structures 4 and 5 respectively. Both groups can be prepared by condensation of pyridine-2-ketone, pyridine-2-aldehyde, or 1,2-diketones with amines according to the equations below;

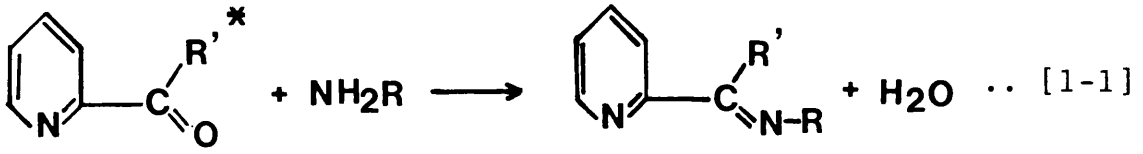

.. [1-1]

pyridine-2-ketone

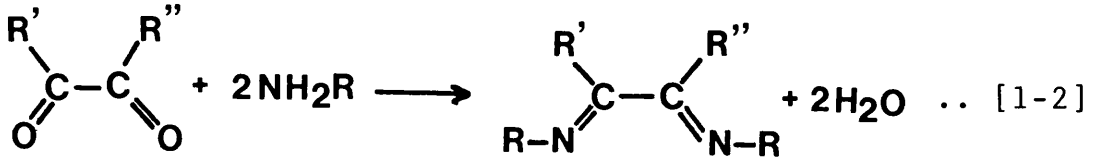

.. [1-2]

"diketone"

* If R' = H is called pyridine-2-aldehyde.

The ligand has the lowest unoccupied molecular orbital, π^*, whose orientation and energy are suitable to interact with t_{2g}-orbitals of metals in octahedral coordination to form metal to ligand back donation.[7] Previous studies have shown that these compounds give stable complexes with metal-d^6 including iron(II)[8] and ruthenium(II)[9,10] (group VIIIB), chromium(0), molybdenum(0) and tungsten(0)[11-13] (group VIB) and manganese(I)[14-16] (group VB). The complexes are low-spin and diamagnetic. In solution, they give very intense colour in solution. All these behaviours are associated with back bonding interactions.

In the present work, we shall undertake to study the behaviour of metal-diimine (neutral) complexes mainly involving molybdenum(0). The syntheses of the complexes are previously reported - by refluxing $Mo(CO)_6$ with the required ligand in an inert solvent leading to replacement of two carbonyl groups (Eq [1-3]).

$$Mo(CO)_6 + N\widehat{\ }N \longrightarrow Mo(CO)_4(N\widehat{\ }N) + 2CO \qquad \ldots [1\text{-}3]$$

Darensbourg and Kump[17] used a similar technique for monodentate substituted ligands such as piperidine (pip) leading to formation of cis-$Mo(CO)_4(pip)_2$ (Eq. [1-4]).

$$Mo(CO)_6 + 2pip \longrightarrow cis\text{-}Mo(CO)_4(pip)_2 + 2CO \qquad \ldots [1\text{-}4]$$

This complex is rather labile and requires little energy to break the metal-piperidine bond. The substitution process is quicker, making cis-$Mo(CO)_4(pip)_2$ convenient to be used as a starting compound, especially to prepare heat sensitive complexes. In Chapter 2, we shall discuss the experimental techniques leading to the synthesis of a series of molybdenum(0) diimine complexes. The complexes are stable in inert solvents (e.g. toluene, benzene, heptane etc) but quickly decompose upon exposure to light (photo-sensitive). In highly polar solvents the complex steadily solvolyse. Kinetics of the nucleophilic attack by incoming ligands such as cyanide, hydroxide, and substituted phosphine on this complex are found to suggest S_N2 mechanism.[18] Our kinetics measurements, discussed in Chapter 5, show that the rate of the reaction involving cyanide attack varies according to the diimine and solvent present.

The complexes exhibit a very intense band in the visible region which is associated with metal to ligand charge transfer. The solvatochromism of the band attracted great interest of among researchers.[12,19-22] These charge transfer spectra are also pressure and temperature dependent.[22,23] Several other features which are related to the properties of the complex in solution can be obtained from measuring the stretching frequency of the carbonyl[24,25] (Infrared technique), ^1H, ^{13}C and ^{95}Mo chemical shifts (NMR technique)[25,26] and solubility. It is found that all those features show similar behaviour; sensitive to solvent. We regard the effect as the result of a variation in solvation of the complex in different solvents.

1-3. Kinetics and Solvation

Following the development of kinetic theory, several information about the characteristic behaviour of reacting molecules in solution can be estimated. In earlier work, people have used only the classical rate law to predict the mechanistic character of the substitution reaction. It is known that there are two types of mechanisms established for substitution reactions, unimolecular and bimolecular. As an example, we consider the reaction of Equation [1-5] below,

$$A + B \longrightarrow \text{product} \qquad \ldots [1\text{-}5]$$

The reaction has a first order rate law if the rate of the reaction is proportional to a concentration of one of the reactants (e.g. A) or a second order rate law if the rate is proportional to both (e.g. A and B). A first order rate laws are often associated with unimolecular, second order with bimolecular, proceses. Based on transition state theory,[27] the unimolecular process is defined as in which only one reactant is involved in forming the activated complex, whereas in bimolecular process both reactants come together to form the activated complex. The rate of the reaction depends on the rate for the activated complex to reach the top of energy barrier (transition state).

In some cases, especially for the reaction where one of the reactants (e.g. B in Eq.[1-5]) always appears in excess,

such as in aquation and solvent exchange processes, it is not possible to establish the order with respect to [B] directly. The estimation of the mechanism based only on rate law leads to uncertain results. Therefore many of the predicted mechanisms are now supported by information from activation parameters, especially $\Delta S^{\ddagger}$ and $\Delta V^{\ddagger}$ as well as $\Delta H^{\ddagger}$ and $\Delta G^{\ddagger}$. These parameters, which are derived from transition state theory, explain the intrinsic difference between physical behaviours of the reacted molecules (initial state) to form the activated complex (transition state), [Eq. 1-6].

$$\Delta X^{\ddagger} = X_{TS} - X_{IS} \qquad \ldots [1\text{-}6]$$

In this case, two physical changes are normally taken into consideration. The first involves the change of the order (i.e. its degree of distribution) and the other includes the change of the size. The former corresponds to the value of $\Delta S^{\ddagger}$ whereas the latter is associated with $\Delta V^{\ddagger}$. Schematic diagrams showing these changes are illustrated in Figure [1-3]. In many cases, negative values of $\Delta S^{\ddagger}$ and $\Delta V^{\ddagger}$ are said to indicate associative (bimolecular) processes, whereas positive values correspond to dissociative (unimolecular) processes.

In practice both parameters can be directly determined. For entropies, the values are readily obtainable from the temperature variation of the reaction rates by using the Arrhenius Equation and transition state theory. Volumes of

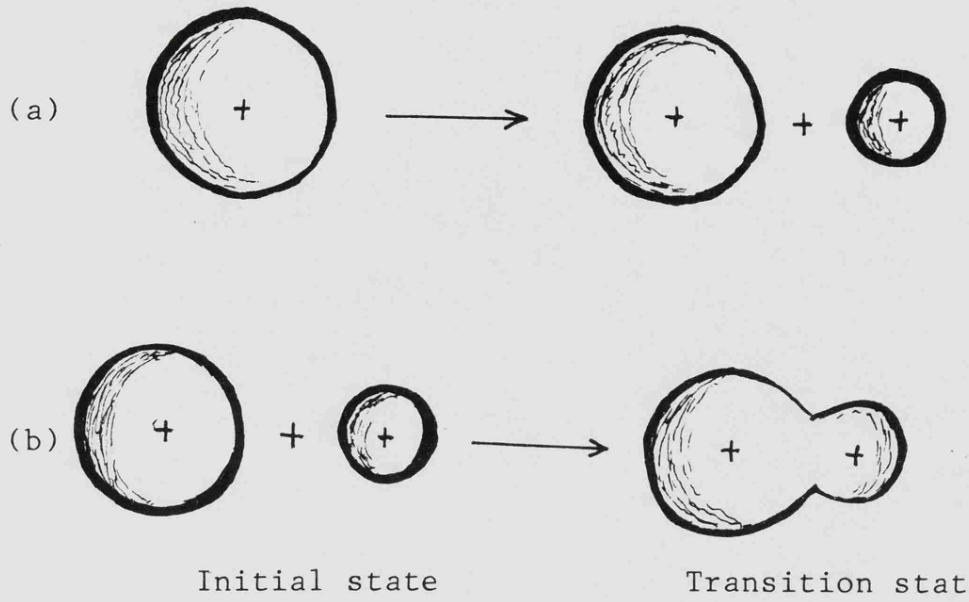

Figure [1-3] Physical changes on transition state formation for (a) dissociative and (b) associative

activation are determined by pressure variation of rate of the reaction according to Equation [1-7] below:

$$\frac{d\ \ln k}{dp} = -\frac{\Delta V^{\ddagger}}{RT} \qquad \ldots \quad [1\text{-}7]$$

In general, establishing the pressure variation on rate is technically more difficult but the $\Delta V^{\ddagger}$ obtained from this experiment is rather easier to visualise. Experimental determination and calculation of $\Delta V^{\ddagger}$ are explained in Chapter 2.

Information from activation parameters has also been used to interpret the solvent effect on reactivity of a particular

reaction. The most common is $\Delta G^{\ddagger}$ because it has a direct relation to rate constant. Previously, analysis of solvent effects on rate constants was carried out by comparing with solvent parameters,[28-34] but the technique does not show any relation between rate constants and the behaviour of the reacting molecules on moving from one solvent to another. A recent trend of interpretation of solvent effects on rate constants is carried out by analysing into initial-state and transition state contributions.[35,36] Analysis using this technique can also tell us which of the reactants, for example in bimolecular process, where two reactants are involved in contributing to transition state, is the most influential in determining the direction of the rate. In Figure [1-4] we summarize three possible situations of $\Delta G^{\ddagger}$ for a particular reaction on changing to another solvent related to the initial and transition states. The first (Figure [1-4](a)) shows how, on going to a second solvent, an increase in rate constant (i.e. $\Delta G^{\ddagger}$ decrease at constant temperature and pressure) can stem from either (i) a destabilization of both states with the initial state being destabilized to a larger extent or (ii) a stabilization of both states with the transition state being stabilized to a larger extent. In the second (Figure [1-4](b)) we show that on going to a second solvent the rate constant is unchanged but changing the initial state-transition state trend either (i) both states are equally destabilized, or (ii) both states are equally stabilized. Finally Figure [1-4](c) shows two cases where on changing the solvent, initial states and transition states are affected differently leading to either (i) an increase or (ii) a decrease in $\Delta G^{\ddagger}$.

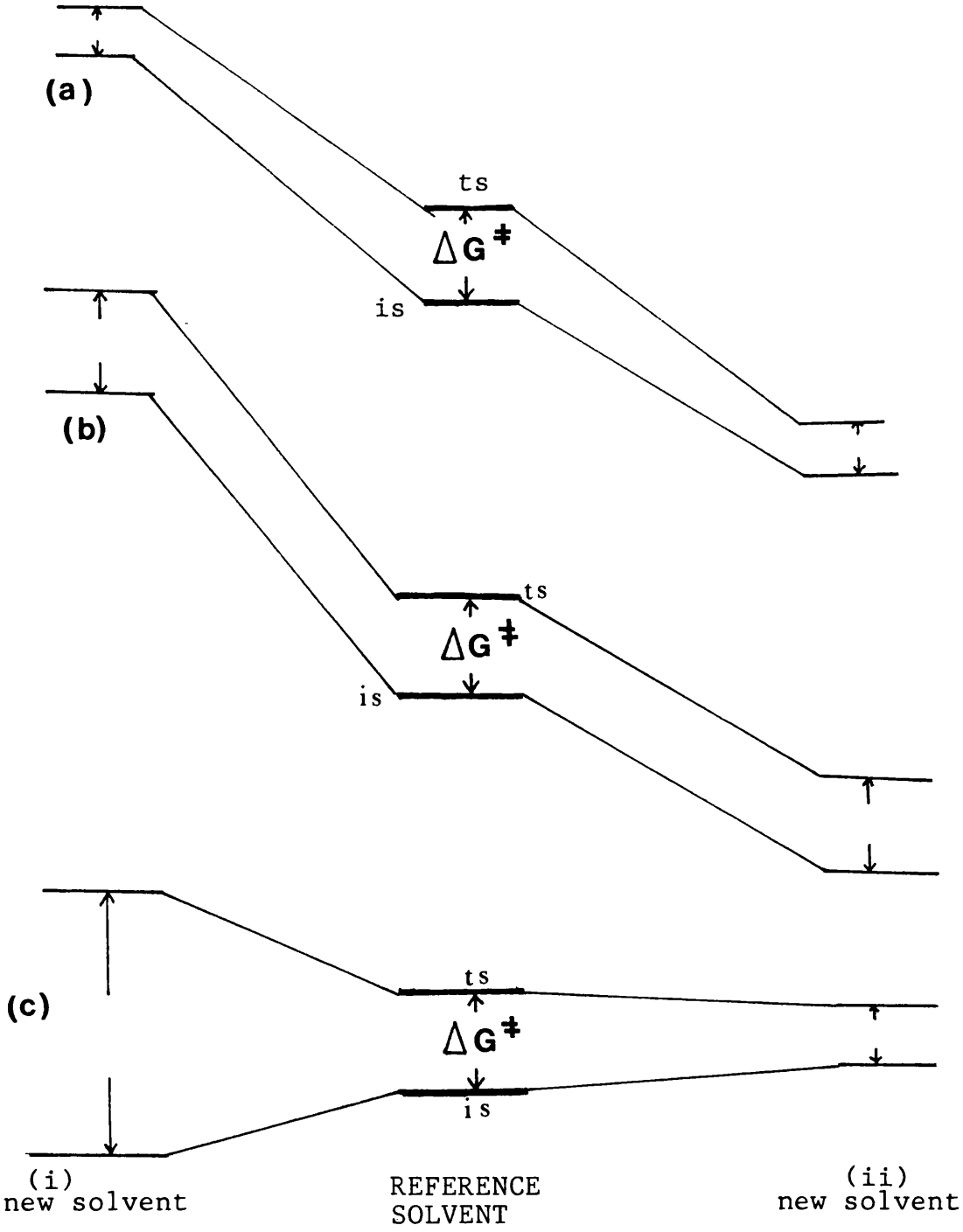

Figure [1-4] Formalised representation of the effect of the solvent on the activation Gibbs function, $\Delta G^{\ddagger}$, and the initial state and transition state; (a) $\Delta G^{\ddagger}$ decreases as a result of (i) destabilization and (ii) stabilization of both states; (b) $\Delta G^{\ddagger}$ unchanges for both states are (i) destabilized (ii) stabilized; (c) $\Delta G^{\ddagger}$ (i) increases and (ii) decreases as a result of differing effects of solvent on initial and transition states.

However, in order to do a complete analysis several requirements have to be fulfilled. These include the establishment of mechanism of a reaction and thermodynamic information (i.e. transfer chemical potential) of the initial state (based on a total of a transfer chemical potentials of all reactants which are contributing to the transition state). The mechanism can be estimated as described earlier whereas the latter is determined separately by several methods. The most common is by measuring solubility. Some experimental techniques and calculations of transfer chemical potentials are given in Chapter 4. In some cases, even though the transfer chemical potentials are difficult to determine, we shall see later that the kinetic trends of the reaction are relevant to the expected pattern of solvation of the most influential reacting compound in the initial state.

1-4. References

1. H. B. Gray and N. A. Beach., J. Amer. Chem. Soc., 85, 2922 (1963)
2. F. A. Cotton and G. Wilkinson,"Advanced Inorganic Chemistry", 4th Edit., Wiley, 1980, p. 632.
3. G. Wilkinson, F. G. A. Stone and E. W. Abel (edts.), "Comprehensive Organometallic Chemistry", Pergamon Press, Vol: 3, 1982, p. 872.
4. W. R. Mcwhinnie and J. D. Miller, Adv. Inorg. Chem. Radiochem., 12, 135 (1969).
5. A. T. T. Hsieh and B. O. West, J. Organomet. Chem., 112, 285 (1976).
6. J. M. Kleiyman and R. K. Barnes, Tetrahedron, 26, 2555 (1970).
7. J. Reinhold, R. Benedix, P. Birner and H. Hennig, Inorg. Chim. Acta, 33, 209 (1979).
8. A. A. Schilt, J. Amer. Chem. Soc., 82, 3000 (1960)
9. J. N. Braddock and T. J. Meyer, J. Amer. Chem. Soc., 95, 3158 (1973).
10. J. B. Godwin and T. J. Meyer, Inorg. Chem., 10, 471 (1971)
11. M. H. B. Stiddard, J. Chem. Soc., 4712 (1962)
12. H. tom Dieck and I. W. Renk, Angew. Chem. Internat. Edn. 5, 520 (1966).
13. E. W. Abel, M. A. Bennett and G. Wilkinson, J. Chem. Soc., 2323 (1959)
14. E. W Abel and G. Wilkinson, J. Chem. Soc., 1501 (1959).

15. G. Schmidt, Diplomarbeit, Technische Hochshule, Darmstadt, 1985.
16. A. G. Osborne and M. H. B. Stiddard, J. Chem. Soc., 4712 (1962)
17. D. J. Darensbourg and R. L. Kump, Inorg. Chem., 17, 2680 (1978)
18. M. J. Blandamer, J. Burgess, J. G. Chambers and A. J. Duffield, Transition. Met. Chem., 6, 156 (1981).
19. H. Saito, J. Fujita and K. Saito, Bull. Chem. Soc. Jap., 41, 863 (1968).
20. J. Burgess, J. Organomet. Chem., 19,218 (1969).
21. J. Burgess, J. G. Chambers and R. I. Haines, Transtion Met. Chem., 6, 145 (1981).
22. H. -T. Macholdt and H. Elias, Inorg. Chem., 23, 4315 (1984).
23. H. -T. Macholdt, R. van Eldik, H. Kelm and H. Elias, Inorg. Chim. Acta, 104, 115 (1985)
24. D. M. Adams, J. Chem. Soc., A, 87 (1969)
25. J. A. Connor and C. Overton, J. Organomet. Chem., 282, 349 (1985)
26. A. F. Masters, R. T. C. Brownlee, M. J. O'Connor, A. G. Wedd and J. D. Cotton, J. Organomet. Chem., 195, C17 (1980).
27. A. A. Frost and R. G. Pearson,"Kinetics and Mechanism", 2nd Edit., Wiley, 1961
28. E. D. Hughes and C. K. Ingold, J. Chem. Soc., 244 (1935)

29. K. A. Cooper, M. L. Dhar, E. D. Hughes, C. K. Ingold, B. J. MacNulty and L. I. Woolf, J. Chem. Soc., 2043 (1948)

30. G. Scatchard, Chem. Rev., 8, 321 (1931).

31. K. J. Laidler and P. A. Landskroener, Trans Faraday Soc., 52, 200 (1956).

32. E. Grunwald and S. Winstein, J. Amer. Chem. Soc., 70, 846 (1948)

33. S. Winstein, E. Grunwald and H. W. Jones, J. Amer. Chem. Soc., 73, 2700 (1951)

34. A. H. Fainberg and S. Winstein, J. Amer. Chem. Soc., 78, 2770 (1956)

35. A. J. Parker, Chem. Rev., 69, 1 (1969)

36. M. J. Blandamer and J. Burgess, Coord. Chem. Rev., 31, 93 (1980).

CHAPTER 2

Experimental

2-1. Preparations

In this section we shall only deal with techniques in the preparation series of molybdenum(0) diimine complexes. The preparations of other complexes are given in their respective chapters. A general preparative outline for these complexes is shown in the Scheme [2-1]. Details are given later in this Chapter.

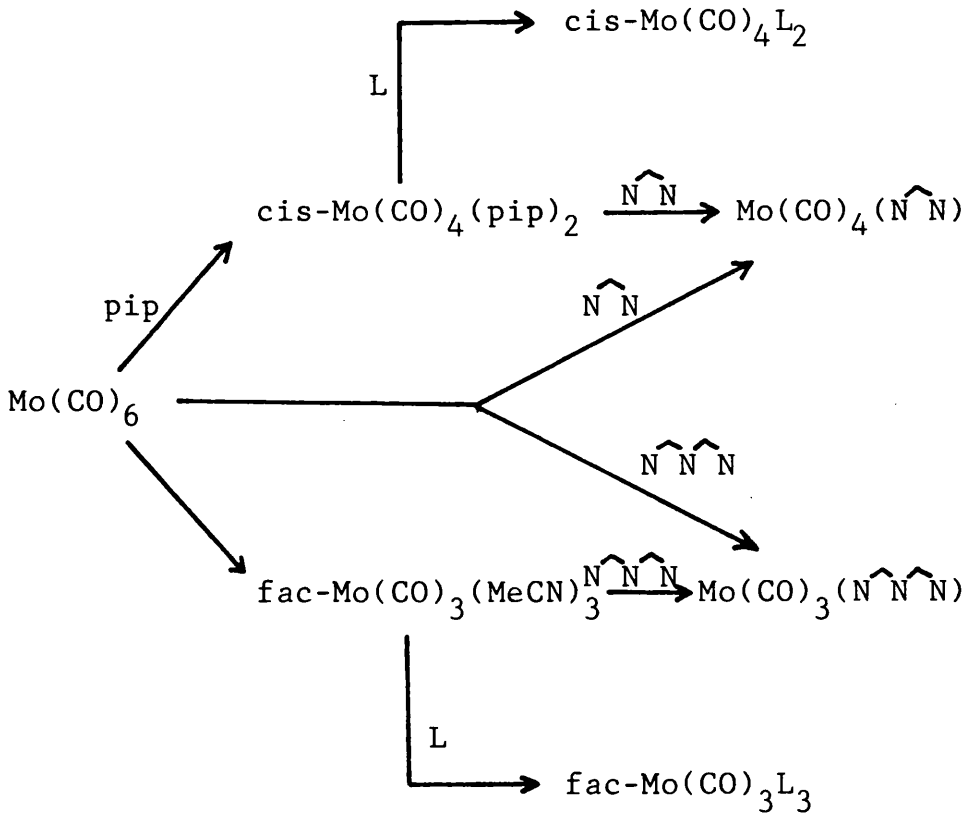

Scheme 2-1

A series of molybdenum(0) diimine complexes, $Mo(CO)_4(N\widehat{\ }N)$, can be synthesized by two routes. The first is direct from molybdenum(0) hexacarbonyl, $Mo(CO)_6$, and the second is via cis-$Mo(CO)_4(pip)_2$[1]. The direct synthesis from $Mo(CO)_6$ is rather slower; it requires a large energy for substitution to take place. In all cases, the reaction is carried out by refluxing the mixture of $Mo(CO)_6$ and appropriate diimine ligand in an inert solvent such as heptane or toluene.[2]

$$Mo(CO)_6 + N\widehat{\ }N \longrightarrow Mo(CO)_4(N\widehat{\ }N) + 2CO. \quad \ldots [2\text{-}1]$$

The second synthesis is rather quicker. This is because the complex cis-$Mo(CO)_4(pip)_2$ is labile; two molecules of piperidine are easily replaced by a diimine ligand even under mild conditions. A similar approach is also applied to preparing $Mo(CO)_3(N\widehat{\ }N\widehat{\ }N)$ complexes from fac-$Mo(CO)_3(MeCN)_3$[3,4]. The second method has been used rather widely to synthesize the present complexes.

Several diimine compounds have been used in this study. Some are available from commercial sources, while others are prepared by condensation of pyridine aldehyde or ketone, or diketone with amines as described in Chapter 1. Unfortunately, some of them cannot be isolated. This group of diimine ligands are usually prepared in situ during the preparation of the corresponding molybdenum complex.

(i) Diimine Compounds

(a) Diacetyl-bis-N-phenylimine (dab)

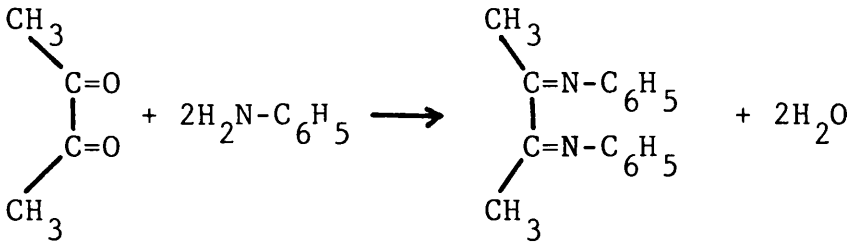

In a 100 cm^3 Quick-fit round-bottomed flask fitted with a reflux condenser, 4.15 cm^3 (46 mmol) aniline and 2 cm^3 (23 mmol) of diacetyl (2,3-butadione) were dissolved in 50 cm^3 of iso-propanol. The reaction mixture was refluxed for about four hours. Then the reaction mixture was concentrated to one-third of its volume by using a rotary evaporator. The mixture was cooled overnight at about -5°C producing a yellow precipitate. The precipitate was twice recrytallized from iso-propanol to form slightly yellow plate-like crystals. A similar method has been used to synthesize other ligands involving diacetyl and several aniline derivatives.

(b) Glyoxal-bis-N-phenylimine (gpi)

To an evaporating dish containing 3.5 cm^3 (22 mmol) of glyoxal (in 40% water) was added dropwise 4 cm^3 (44 mmol) aniline with continuous shaking. The reaction is exothermic and within a few minutes a yellow sticky solution was formed

which finally turned solid. The product was cooled in ice and then the solid was scratched out, ground and washed with water (by decantation) to eliminate excess of glyoxal. The solid was then dried in a vacuum desiccator.

(c) 2,6-Diacetylpyridine-bis-N-phenylimine (dappi)

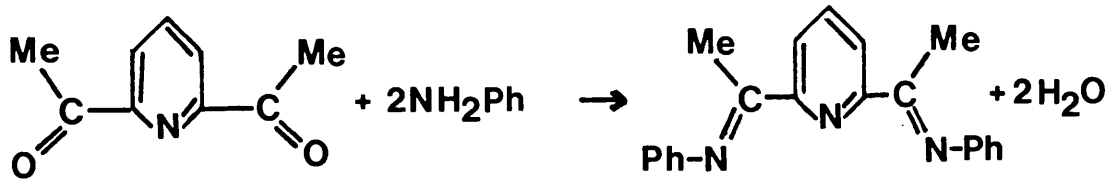

2,6-diacetylpyridine dappi

In a 100 cm^3 Quick-fit round-bottomed flask fitted with a reflux condenser, 1.8 g (11 mmol) of 2,6-diacetylpyridine and 2 cm^3 (22 mmol) of aniline were dissolved in 50 cm^3 of iso-propanol. The reaction mixture was refluxed for about half an hour. Then the reaction mixture was concentrated to 1/2 of its volume by using a rotary evaporator. The mixture was cooled in ice; a greenish-yellow precipitate appeared. The product was filtered and washed twice with 5 cm^3 of iso-propanol and dried in vacuum desiccator. This method was also applied in preparing ligands involving 2,6-diacetylpyridine and other aniline derivatives.

(ii) Molybdenum(0) Complexes

(a) cis-Tetracarbonylbis(piperidine)molybdenum(0);
$cis\text{-}Mo(CO)_4(pip)_2$

$$Mo(CO)_6 + 2pip \longrightarrow cis\text{-}Mo(CO)_4(pip)_2 + 2CO$$

Two grams of molybdenum(0) hexacarbonyl (Aldrich) and 5 cm^3 of piperidine were refluxed in 25 cm^3 of heptane for four hours, during which time the bright yellow product precipitated from the solution. The reaction mixture was filtered hot to remove any heptane-soluble $Mo(CO)_5(pip)$. The isolated yellow solid was washed with cold heptane, dried and kept in a vacuum desiccator in the dark.

Analysis : Calculated %C = 44.44, %H = 5.82, %N = 7.41
Observed %C = 43.95, %H = 5.87, %N = 7.48

(b) fac-Tricarbonyltris(acetonitrile)molybdenum(0);
$fac\text{-}Mo(CO)_3(MeCN)_3$

The $fac\text{-}Mo(CO)_3(MeCN)_3$ was prepared by refluxing a certain amount (3 g) of $Mo(CO)_6$ in excess (30 cm^3) of acetonitrile for about 3-4 hours under nitrogen.

$$Mo(CO)_6 + 3MeCN \longrightarrow fac\text{-}Mo(CO)_3(MeCN)_3 + 3CO$$

The reaction mixture was concentrated to half its volume by using a rotary evaporator and then saturated again with nitrogen. The solution was cooled in ice. Colourless crystals of fac-$Mo(CO)_3(MeCN)_3$ were collected. The solution was quickly filtered, and the solid was dried in a vacuum desiccator. The crystals was kept free from air and light.

(c) Tetracarbonyl(2-benzoylpyridine-N-phenylimine)molybdenum(0); $Mo(CO)_4(bppi)$

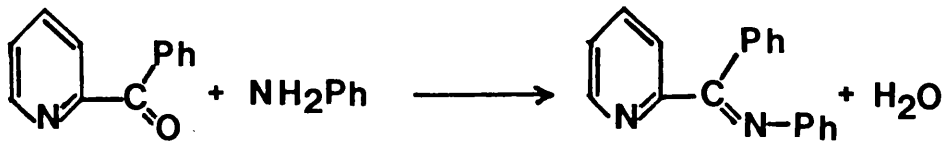

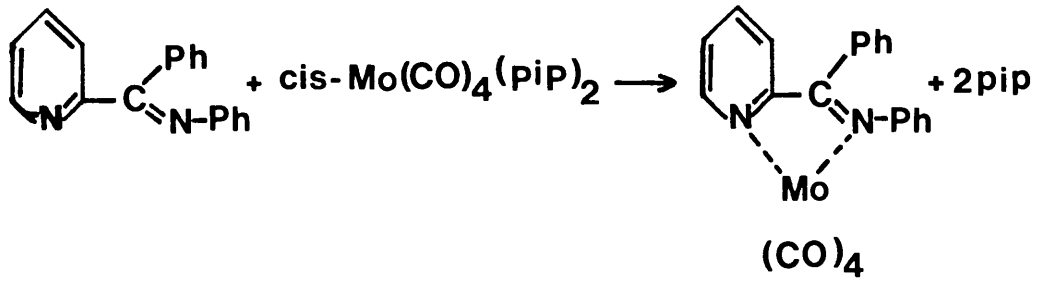

In a 200 cm^3 conical flask 1 g of 2-benzoylpyridine and 0.5 cm^3 of aniline were dissolved in 75 cm^3 of iso-propanol. The mixture was then heated on water bath for about 30 minutes, resulting in the formation of a yellowish solution. To the hot solution 1.5 g of cis-$Mo(CO)_4(pip)_2$ was added slowly with continuous shaking. A red colour was immediately appeared. The solution was heated on a water bath for another 30 minutes and was left to cool overnight at room temperature. A black solid, $Mo(CO)_4(bppi)$, was collected by filtration. The

collected $Mo(CO)_4$(bppi) was not pure. Further recrystallization was carried out by dissolving in large quantities of toluene and then slowly evaporating off the solvent at room temperature. The complex was washed with diethyl ether and dried in a vacuum desiccator.

Analysis: Calculated %C = 56.65, %H = 3.00, %N = 6.01

Observed %C = 56.20, %H = 3.19, %N = 6.13

This procedure has been used to synthesize the majority of other molybdenum(0) tetracarbonyldiimine complexes, especially those of diimines prepared in situ.

(c) Tetracarbonyl-butane-2,3-dimethyliminemolybdenum(0); $Mo(CO)_4$(bmi)

To a 100 cm^3 Quick-fit flask was added 0.7 cm^3 of 2,3-butadione and 0.85 cm^3 of methylamine (40% in water) in 50 cm^3 iso-propanol. The mixture was heated on water bath for 5 minutes and then 1.5 g of cis-$Mo(Co)_4(pip)_2$ was slowly added. A red colour immediately appeared. The solution was refluxed at solvent boiling point for about half an hour, leaving a dark concentrated solution which was then left to cool overnight at room temperature. A clean black crystalline product slowly precipitated. The product was filtered,and the collected solid washed with ether and dried in a vacuum desiccator.

Analysis: Calculated %C = 37.52, %H = 3.78, %N = 8.75

Observed %C = 37.52, %H = 3.81, %N = 8.76

IR($\nu_{C=O}$): 2020, 1917, 1865, and 1815 cm^{-1} (in KBr).

^1H ($CDCl_3$): 3.75 and 2.20 (1:1 intensity)

2-2. Kinetics at High Pressure

(a) Operating Section

The schematic diagram for the high pressure kinetic apparatus used in this work is as shown in Figure [2-1]. For convenience, we shall divide the operating technique into several sections as follows:

(i) Preliminary Checking

Before the measurements are carried out several important points related to the work have to be done and checked:

(1) Turn on relay and heater for bath, with bath full of water

(2) "Bleed" the system to ensure that no air is in the line (i.e. turn on water and run through apparatus). Leave main water tap opened but closed tap E.

(3) Check nitrogen cylinder before use to ensure sufficient supply for entire run.

(ii) Filling Procedures

The required concentrations of all reacting solutions were prepared separately so that the volume should be about 150 cm^3 (the minimum volume required for every run). All solutions were placed into the thermostatted bath at a measured temperature before use and then mixed in a container such as a 250 cm^3 conical flask. After thorough mixing, the solution was poured into the metal cell which was filled to

the top (it is best to have the metal cell at room temperature and standing on absorbent paper). Wet the sides of the plunger, including the black O-rings, with the test solution. Push in the Teflon plunger with even hand pressure. Considerable force may be required to push the plunger into the cell past both rings. If additional force is necessary place a wooden block squarely on top of the plunger, and use a large spanner to strike the block with vigour. After several repetitions of this, the plunger should fit firmly. Place the small O-ring on the top of the remaining cell assembly. Invert the filled cell and fit on to cell assembly. Place the whole cell and valve assembly into the apparatus and tighten down the cell. Valve C should be opened to prevent any air bubbles being trapped. Now close valve C, turn on water tap E and nitrogen supply (tap A), giving the gas pressure about 50 lb/in^2. Turn on tap B (clockwise) to required pressure on gauge, at the same time starting the clock. Aliquots of the solution are withdrawn at required times by slowly opening valve C. The measuring of the changes of concentration of reaction mixture (in this case by measuring absorbance using a Pye-Unicam S.P. 8-100) is carried out soon after the solution was drawn out. There is enough solution in the reaction vessel for 9-11 readings per run.

At the same time the rate of the reaction is also followed at normal pressure by taking some of the reaction mixture solution. So, a reasonable interval for withdrawing solution could be estimated and a direct comparison in rate constants between both conditions obtained.

(iii)Shutting down

When all the sampling is completed, the first task is to remove the source of pressure on the water which is pressurising the cell. Close off the nitrogen supply by closing tap A. Turn tap B anticlockwise until the small gauge (above tap B) reads zero. By now no further pressure could be put on the system, but there is still pressure in the cell. This is released by carefully allowing the solution to pass through valve C. When the large gauge reads zero, the pressure in the cell has become atmospheric. Close tap E. The cell may now be unscrewed, if necessary using water pressure by turning on tap E. Close all water taps.

(b) Calculation of Volumes of Activation

Volumes of activation were estimated by plotting logarithms of the ratio of rate constant at pressure, k_p, to the rate constant at 1 atm (k_p/k_1) against pressure. Since our results are not precise enough to detect any (small) curvature, such plots are normally assumed to be a straight line passing through the origin. The slope was used to evaluate the volume of activation from the equation [5]

$$RT\left(\frac{d \ln k}{dP}\right)_T = -\Delta V^{\ddagger}$$

For all reactions the pressures used were 340, 680 and 1020 atmospheres (345, 690, and 1035 bars; 5000, 10000, and 15000 lb/in^2.

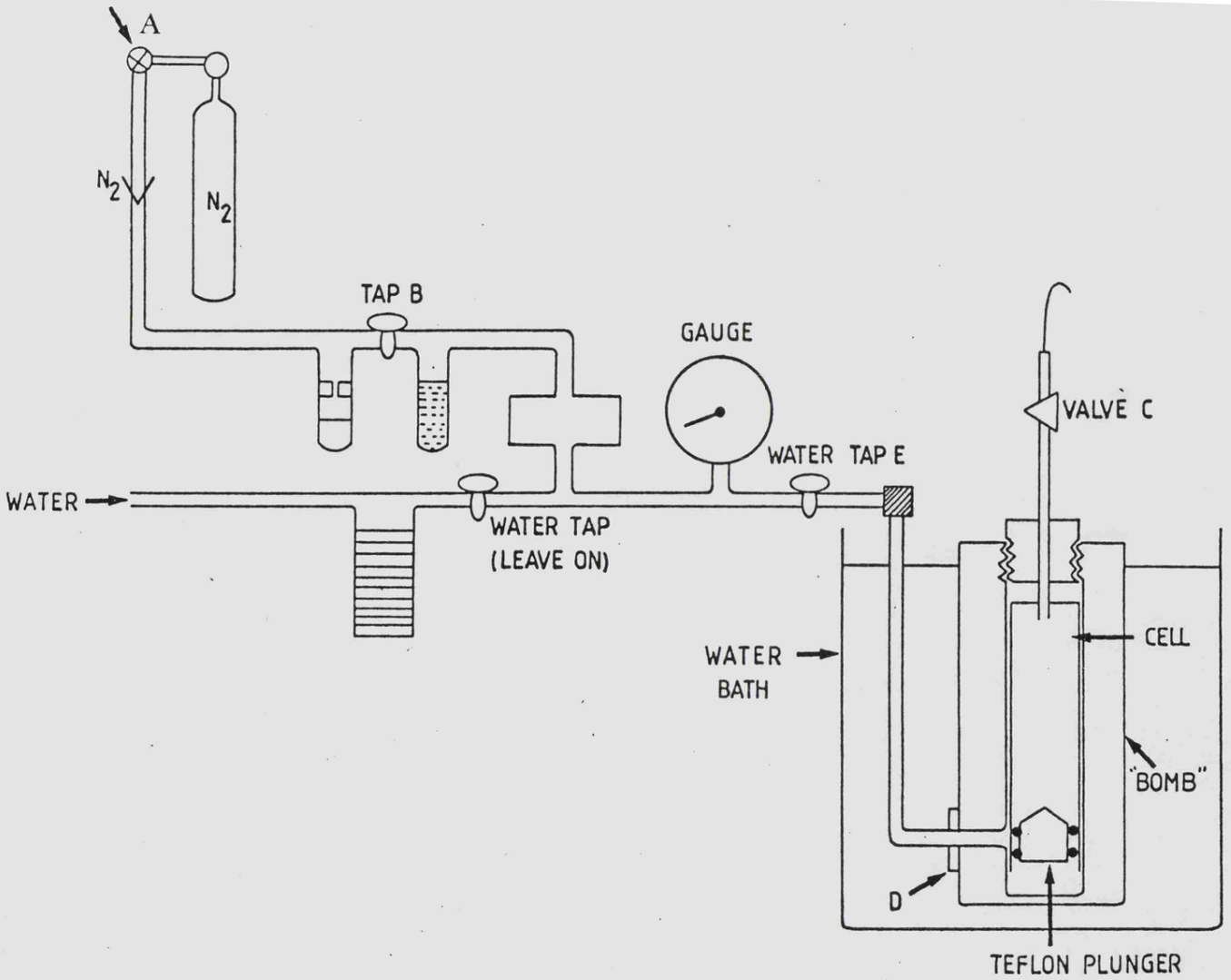

Figure [2-1] Schematic diagram for the high pressure kinetic apparatus.

2-3. References

1. D. J. Darensbourg and R. L. Kump, Inorg. Chem., 17, 2680 (1978)
2. M. H. B. Stiddard, J. Chem. Soc., 4, 712 (1962).
3. D. P. Tate, W. R. Knipple and J. M. Augl, Inorg. Chem., 1, 433 (1962).
4. R. P. M. Werner and T. H. Coffield, 6th. Internat. Conf. on Coord. Chem., Detroit, 1961, Reprint p 534, Macmillan Comp. N.Y.
5. K. R. Brower and Tao-shing Chen, Inorg. Chem., 12, 2198 (1973).

CHAPTER 3

Spectroscopic Studies on Tetracarbonyldiiminemolybdenum(0) Complexes, $Mo(CO)_4(N\widehat{\ }N)$

3-1. Introduction

Studies on the properties of the $M(CO)_{6-2x}(N\widehat{\ }N)_x$ complexes, where M = Cr, Mo and W, $N\widehat{\ }N$ = bidentate diimine ligand and x = 1 or 2, by uv-visible and infrared spectroscopy have been widely reported but very little by NMR techniques. Behrens and Harder[1] first discovered the formation of the intense charge transfer spectra of $M(CO)_2(N\widehat{\ }N)_2$ where M = Cr, Mo or W and $N\widehat{\ }N$ = 2,2'-bipyridine (bipy) or 1,10-phenanthroline (phen). They found that the charge transfer band (λ_{max}) is sensitive to the solvent (i.e. solvatochromic). Later on several other investigations have been carried out to study the effect on other ternary complexes involving Group VI metal carbonyls.[2-7] Most of them concluded that the charge transfer spectra of the complexes always show solvatochromism which is already well-known for π-conjugated organic compounds. Theoretical interpretations on the basis of the electrostatic model on the latter compounds by several workers seem quite successful.[8,9] Saito[10] used this concept to explain the effect on the coordination compounds, $M(CO)_4(N\widehat{\ }N)$. He assumed that the solvent molecule interacts with the complex through the carbonyl group, which leads to changes in the metal-diimine charge transfer energy. This argument is in agreement with the result of relatively large solvent effects on $Fe(CN)_4(bipy)^{2-}$ [11-13] and $Fe(CN)_2(bipy)_2$[14,15] and the very small effect on $Fe(bipy)_3^{2+}$.[16]

Adams[17] monitored the effect of solvent and ligand L on the carbonyl stretching frequency of $Mo(CO)_{6-x}L_x$ and found that it is dependent on both solvent and ligand L. He

postulated that the changes are closely related to charge distribution in the complex. Such changes may be clearly observed when we study some individual nuclei NMR of the complex.

Our aim here is to ascertain some of the effects which influence the charge transfer spectra, stretching frequency of carbonyl, and chemical shift of NMR of several nuclei of $Mo(CO)_4(N\widehat{\ }N)$ complexes. The diimine group , $N\widehat{\ }N$, in the complex can be classified, basically, into two types; aliphatic and aromatic. The detailed description of these ligands is discussed in Chapter 1 and the preparation of their corresponding molybdenum complexes is detailed in Chapter 2.

3-2. Experimental

All tetracarbonyldiimine derivatives of molybdenum(0) were prepared from the tetracarbonylbis(piperidine) complex as described in Chapter 2. The uv-visible spectra of all solutions at room temperature were run on a Pye-Unicam SP 800 recording spectrophotometer, whose wavelength calibration was checked periodically using the holmium glass filter supplied by the manufacturer. Variable temperature and pressure uv-visible spectra were kindly undertaken by R. van Eldik of Frankfurt University. The infrared spectra of the complexes in potassium bromide discs and in solution were monitored using a Perkin Elmer 580. The proton NMR spectra were measured using TMS as reference. ^{13}C NMR was determined using a Bruker AM 300 (75 MHz) and ^{95}Mo NMR spectra were carried out at the University of Warwick by O. Howarth.

3-3. Charge Transfer Spectra

The charge transfer band for these complexes is very intense in the visible region. The existence of the band corresponds to the lower electronic transition energy, which has been identified as arising from charge transfer from t_{2g}-orbital of metal to π^*-orbital of ligands; that is metal - ligand charge transfer (MLCT) spectra. The assignment was based on the low intensity of spectra in the visible region of complexes containing analogous ligands such as ethylenediamine (en) and diethylenetriamiine (dien), where the extremely high energy level σ^*-orbital is the lowest unoccupied orbital in the molecule. The molecular orbital description of these complexes is, similar to metal-carbonyl complexes, given in Chapter 1. The low intensity band is due to a d-d transition. It is found that the wavenumber of maximum absorption, ν_{max}, of charge transfer varies considerably with the nature of the diimine ligand,[18,19] organic solvents,[20-23] and other physical changes such as pressure and temperature.[24] These variables will be discussed separately in the following sections.

(a) Ligand Effect

Wavenumbers of the charge transfer band of several tetracarbonyldiiminemolybdenum(0) complexes have been recorded and are listed in Table [3-1]. It is found that the wavenumber of maximum absorption of charge transfer varies with the nature of the diimine ligand. The results indicate that, in

the majority of solvents, the wavenumber of maximum absorption of the complex increases in the presence of the diimine ligand as follows:

bipy > apmi, 1 > appi, 2 > bmi, 3 > gmi, 4 > dab, 5 > gpi, 6.

Perhaps we can suggest that the most significant factor influencing the trend is given by the "sub-group" such as pyridyl, methyl, phenyl etc, present in the ligand.

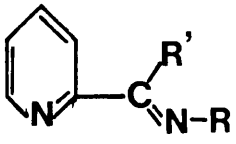

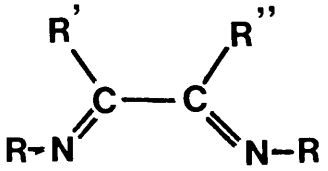

1. R = R' = Me
2. R = Me ; R' = Ph

3. R = R' = R'' = Me
4. R = R' = H; R'' = Me
5. R = R' = Me; R'' = Ph
6. R = R' = H; R'' = Ph

The higher wavenumbers of maximum absorption reported for the complexes with bipy and with apmi suggest that the aromatic pyridyl group gives the strongest effect, followed by methyl, phenyl and hydrogen.

A more detailed explanation of this trend has to take into account several factors. In all cases, these changes are related to factors influencing the energy level of the t_{2g}-orbital of the metal and MLCT excited state orbital in the complex. The energy required depends on the size of the energy separation between the two orbitals. If the ground state orbital (t_{2g}) is stabilized while the MLCT excited state is highly destabilized the largest shift to higher wavenumber (blue shift) is reported. Similarly, if the ground state is destabilized while the excited state is highly stabilized the largest shift to lower wavenumber (red shift) resulted.

The molecular orbital energy diagram described in Figure [1-2] shows that the energy level of the MLCT excited state is associated with the lowest unoccupied molecular orbital (π^*) of the diimine ligand. The result established that the lowest unoccupied molecular orbital (π^*) of the diimine ligand is increasingly stabilized as follows,[18,19]

gpi > gmi > bmi > apmi > bipy .

The trend indicates that the π^* molecular orbital of an aromatic diimine ligand will always be more destabilized than an aliphatic one.

The energy level for the t_{2g}-orbital of a metal in $Mo(CO)_4(\widehat{N\ N})$ complex has not yet been established. But we estimate that this energy level will be stabilized as the complex becomes more stable. This possible relationship is explained according to the crystal field stabilization energy of the complex. Since the number of electrons occupying the t_{2g}-orbitals are equal, the stabilization energy is only determined by the energy level of these orbitals.

The kinetic study of $Mo(CO)_4(\widehat{N\ N})$ complexes discussed in Chapter 5 shows that the inertness of a complex with an aromatic diimine ligand is higher than that of an aliphatic one. This observation suggests that the t_{2g}-orbital will be more stabilized in the aromatic complex. In conclusion, in an aromatic complex the energy level of the MLCT excited state is relatively destabilized while the t_{2g}-orbital is stabilized which leads to a shifting of the absorption to higher wavenumber. The largest blue shift reported, for the $Mo(CO)_4$(bipy) complex, is a good example to illustrate this. The ligand 2,2'-bipyridine (bipy) is aromatic. It gives a large transition energy which corresponds to the ground state and excited state of MLCT respectively being stabilized and destabilized a lot. Similarly, the largest red shift, for the $Mo(CO)_4$(gpi) complex, is related to a small energy gap between the two orbitals involved. The relative lower stability of the complex and the lower energy of the unoccupied molecular orbital of the ligand supports the results observed. A general picture of the changes of the energy level of the orbitals is given in Figure [3-1].

The effect of the substituent group, X (including

hydrogen, methyl, methoxide, and chloride) present in the diimine ligand, as shown in 7, indicates a strong contrast with effects reported on $Mo(CO)_4$(4,4'-XX-2,2'-bipy)[20] and $Mo(CO)_4$(X-phen)[23] complexes. It is found that the substituent groups have little effect on charge transfer bands. Presumably those groups have relatively similar strengths in influencing the electron density in the diimine system.

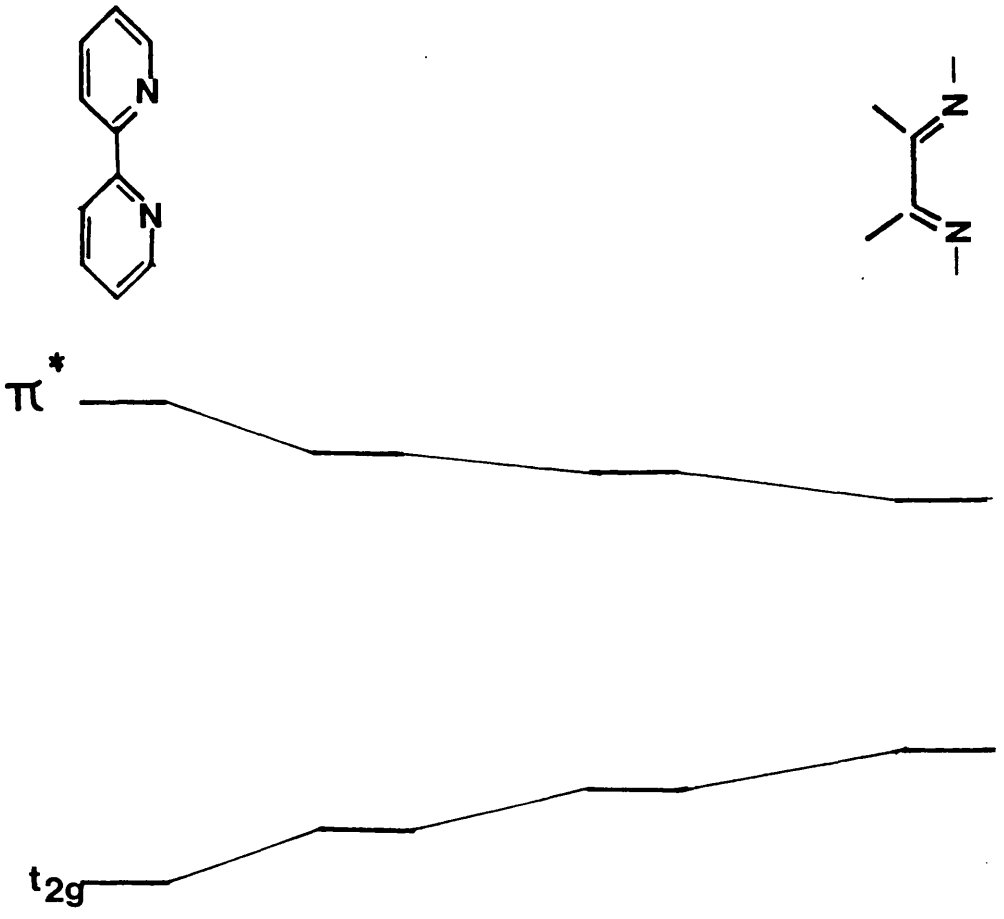

Figure [3-1] Schematic qualitative representation of energy level diagram for the formation of metal to ligand charge transfer (MLCT) spectra.

We have tried to study the charge transfer spectra of complexes with a stronger electron withdrawing group such as NO_2 or COOH. Unfortunately, these types of complex are very unstable and not possible to be isolated.

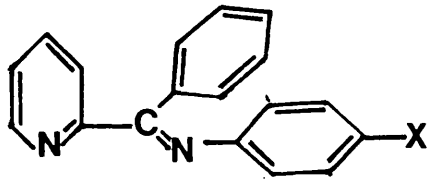

7

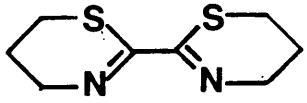

8

(b) Solvent effect

The effects of solvent on the charge transfer spectra of several $Mo(CO)_4(N\widehat{\ }N)$ complexes, where $N\widehat{\ }N$ = 1,10-phenanthroline, 2,2'-bipyridine and 2,2'-bi(4H-5,6-dihydrothiazine) (btz; 8) have been recorded. Similar observations are also reported for analogous complexes with other diimine derivatives. Table [3-1] reports the wavenumbers of maximum absorption for these complexes in various organic solvents. The results show that the complexes are significantly solvatochromic; their wavenumber of maximum absorption increases as the polarity of the solvent increases. The plot of wavenumber of maximum absorption against polarity of solvent (the polarity of solvent is based on E_T values of Reichardt[25] which are measured from the charge transfer energy

of an aromatic betaine) gives two separate lines as shown in Figure [3-2]. The wavenumbers of maximum absorption of the charge transfer bands of these complexes distinguish two different types of solvents, namely protic and aprotic. The protic solvents normally consist of alcohols and those that are able to form hydrogen bonds, whereas aprotic includes other organic solvents which have no potential to form hydrogen bonds. The presence of a hydrogen bond in a protic solvent decreases the effective polarity of the solvent in its interaction with the complex.

The relative solvent sensitivities of the complexes can be estimated roughly from the slope of this plot in which a higher slope reflects a stronger solvent effect (Table [3-2]). But, because this plot always gives two lines, it offers little advantage to be used as a basis for comparison. The alternative method used here is by comparing the absorption of the complex in several solvents with those of one particular complex as a reference. In the present case, $Mo(CO)_4(bipy)$ is chosen as reference because studies on the charge transfer band of this complex are well established. The plot of the wavenumbers of maximum absorption of a given complex against those for $Mo(CO)_4(bipy)$ always gives a single straight line as shown in Figure [3-3]. The slope of the plot varies in the range from 1.11 to 0.41 depending on the complex (Table [3-3]). These extremes correspond to $\Delta\nu_{max}(CCl_4 \rightarrow MeOH)$ of 2300 cm^{-1} for $Mo(CO)_4(bipym)$ (9) but only of 840 cm^{-1} for $Mo(CO)_4(gpi)$. These value may be used as a rough representation of solvent sensitivity. These results show that the solvent sensitivity of the charge transfer spectra is

dependent upon the nature of the diimine ligand in the complex. In general, these natures can be classified in three groups, corresponding to the number (two, one, or none) of the ligating nitrogen atoms incorporated into a pyridyl ring. The first group, including the complexes of bipy, phen, and bipym, have slopes of 1.00 to 1.11. Kaim's data for complexes in this group, $Mo(CO)_4(N\widehat{\ }N)$ with $N\widehat{\ }N$ = bpz (10), bpdz (11), bpm (12), and bipym give slopes in the similar range 0.91 to 1.07 (3 or 4 solvents only).[26]

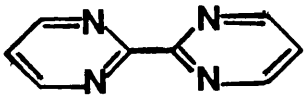

9

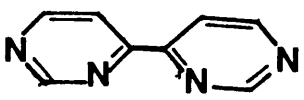

10

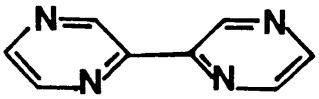

11

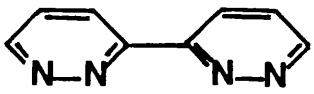

12

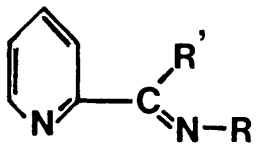

13

For the eight complexes in Table [3-3] of the type 13 with one pyridine ring incorporated into the coordinating diimine moiety, recorded slopes of 0.88 to 0.98 are all just less than the slopes for the first group of complexes with two-pyridyl-diimine ligands. Several published sets of data for other complexes of this group give slopes of similar magnitude. For example, for the complex with R'=H, R=$CH_3C_6H_4$, the slope is 0.95 (16 solvents);[27] with R'=H and R=Ph, the slope is 0.98 (two solvents)[28] or 0.97 (7 solvents);[29] R'=H, R=Et, the slope is 1.01 (seven solvents);[29] with R'=H, R= Pr, the slope is 0.95 or 1.08 depending on the choice of solvent pair.[28,30]

Solvent sensitivity for complexes of the third group, type 14, are summarized and compared in Figure [3-4], which includes our results and values derived from published data. It is apparent that for given R R , solvent sensitivities all follow the same trend as $R'R''$ vary, with $R'R''$=Me giving high solvent sensitivity (strongly marked solvatochromism), $R'R''$=H considerably less and $R'R''$=Ph slightly less again. For constant $R'R''$ there is a similar trend for varying R R :

$$Cx^{*} > Bu > Pr^{*} > Me > Bz^{*} > H > Ph$$

The first four members of this series indicate the importance of steric factors, while the sequence from methyl (Me) to

---

*Cx = cyclohexyl; Pr = propyl; Bz = benzyl.

phenyl (Ph) suggests that in the absence of steric factors, electronic factors have a marked effect. For the latter series, solvent sensitivities are less than for pyridine-ring diimine complexes. They are also affected only a little by interchange of RR and R'R"; for example, the solvent sensitivities for $Mo(CO)_4(N\widehat{\ }N)$ with $N\widehat{\ }N$ = 15 and 5 are 0.55 and 0.67 respectively. It is interesting to note that the solvent sensitivity of $Mo(CO)_4$(btz), 0.82,[4] lies with this group of complexes rather than with bis-pyridine-ligand (bipy and phen) group. Although btz has its donor nitrogen atoms in heterocyclic rings (8), the diimine moiety is not incorporated into aromatic rings.

The pattern of solvent sensitivities described in the preceding paragraphs can be rationalised in term of the relative π-acceptor abilities of the various types of ligands. Solvent sensitivities increase as the π-acceptor potential decreases; π-acceptor abilities are highest for diazabutadiene ligands, lowest for bis-heteroaramatics such as phen and bipy.[19,30] The steric factor noted above and apparent in Figure [3-4] simply operates through the bulky groups R R interfering with orbital overlap and thereby reducing π-acceptor capabilities.

The discussion so far has been restricted to alkyl and aryl groups attached to the diimine framework 16. It is noteworthy that substitution in phenyl rings (R) in compounds of type 13 and 14 has very little effect on solvatochromic properties. This is apparent from published data on glyoxal derivatives (14 with $R'R''=H$ and $R=X\text{-}C_6H_4$)[5,7,32] and from Table [3-3], which shows that solvent sensitivities are unaffected

within experimental uncertainty by the incorporation of para -Me, -OMe or -F substituents into R=C_6H_5 in 13. Again substituent effects are very small for 1,10-phenanthroline derivatives $Mo(CO)_4$(X-phen);[4,23] it is only for the series $Mo(CO)_4$(4,4'-XX'-2,2'-bipy)[33] that significant substituent effects begin to emerge. However if one replaces R = alkyl or aryl in 14 by, e.g., NMe_2, OH, or NH_2, then solvent sensitivities increase markedly, to 0.93, 1.11 and 1.16 respectively for these three complexes.[5,32] These effects are comparable in magnitude to those caused by the presence of bulky groups at R'R'' in 14; effects on π-acceptor properties must therefore be similar.

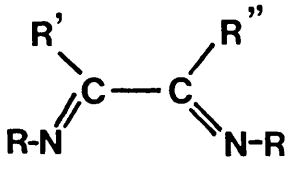

14

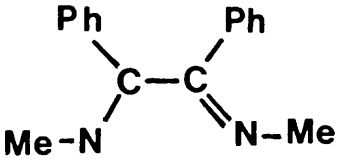

15

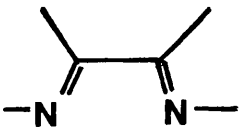

16

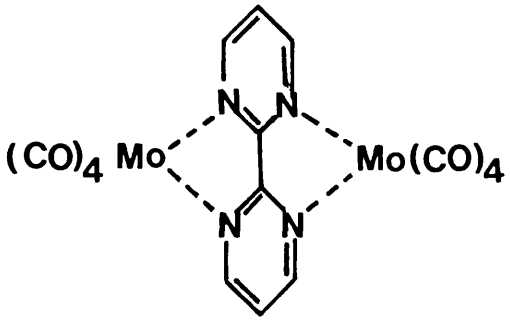

17

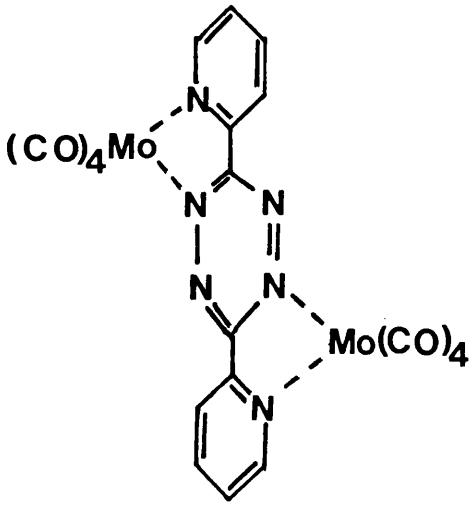

18

The greater delocalization in the terdentate ligand derivatives $Mo(CO)_3(N\widehat{\ }N\widehat{\ }N)$, with $N\widehat{\ }N\widehat{\ }N$ derived from 2,6-diacetylpyridine and two molecules of aniline (Chapter 1), does not affect solvatochromism behaviour greatly. The solvent sensitivity for this complex, 1.12 (Table [3-3]), is only marginally greater than that (1.06) for the bidentate analogue $Mo(CO)_4$(appi). Although increasing ligand denticity and delocalization seem to have only a small effect on solvatochromism, going from a mononuclear complex to a binuclear complex with a bridging diimine (e.g. 17 and 18) has a dramatic effect.[29,34,35] This is consistent with comparable observations in such systems as $W(CO)_5$(pyz) and $(OC)_5W(pyz)W(CO)_5$, where pyz = pyrazine.[36] Further discussion on solvatochromism of the binuclear complexes will be given in Chapter 9.

The overall picture of the solvent effect on charge transfer spectra can be understood by analysing the effect on the ground state and excited state. By using the enthalpies of solution and spectral data (Table [3-4]), the relative solvation of both states are established as displayed in Figure [3-5]. The trend indicates that both states are being stabilized on going from a less to a more polar solvent.

Similar observations are also reported in mixed solvents; in this case toluene-heptane and toluene-methanol. As expected, the wavenumber of maximum absorption of charge transfer of the complex increases as the percentage of the more polar solvent in the solution increases (Table [3-5]). The plot of wavenumbers of maximum absorption of charge transfer against the percentage volume of solvent normally

shows a curve increasing from heptane to pure toluene for toluene-heptane and toluene to methanol for toluene-methanol mixtures. Likewise in pure solvents, spectra are determined by the nature of the diimine ligand. These changes are clearly illustrated in Figure [3-6].

(c) Pressure effect

The pressure dependence of the charge transfer spectra of several molybdenum(0) diimine complexes has been studied in pure toluene and n-butanol at 25°C. The results, as shown in Table [3-6] and Figure [3-7], are clearly piezochromic; the wavenumber of maximum absorption of charge transfer increases as the pressure increases. The effect may be explained by two possible reasons. The first is associated with the changes in the polarity of solvent upon varying the pressure.[37] The present result suggests that the polarity of the solvent increases as the pressure increases which is in good agreement with previously reported work. The second is based on the argument that in complex molecules the ligand will come closer to the metal atom as the pressure is raised and thus increase the interaction between them.

The plot of wavenumber of maximum absorption of charge transfer against pressure, as illustrated in Figure [3-8], gives a straight line, whose slope varies from one complex to another. The calculated slopes are also listed in Table [3-6]. In the following we shall consider the slope of the plot as representing the relative strength of the effect. The results clearly show that the pressure sensitivity of the charge

transfer band varies according to the nature of the diimine ligand present in the complex. It is found that a complex with an aromatic diimine ligand gives a somewhat larger effect. For comparison, in Table [3-6], we also include results of the solvent dependence for corresponding complexes. The trends of both effects are parallel. A plot between them is shown in Figure [3-9]. It is disappointing that it cannot be determined whether the correlation trend in toluene crosses the solvent sensitivity axis or curves asymptotically to this axis at low values of $d\nu/dp$. The only compound in this series which seems likely to have the required lower sensitivity than $Mo(CO)_4$(gpi) is the parent diimine complex $Mo(CO)_4$(HN:CHCH:NH). The ligand, derived simply from glyoxal and ammonia, appears to be known in the iron(II), $Fe(CN)_4(HN:CHCH:NH)^{2-}$,[38] anion and ruthenium(II), $Ru(en)_2(HN:CHCH:NH)^{2+}$,[39,40] cation but unknown for molybdenum. Our efforts to synthesize $Mo(CO)_4$(HN=CHCH=NH) have so far been unsuccessful.

For comparison, the correlation trend for pressure and solvent sensitivity for n-butanol seems to show a line passing through the origin. Presumably less pressure sensitivity in n-butanol forces the line to cross closer the origin.

(d) Temperature effect

Charge transfer spectra of these molybdenum(0) diimine complexes are also temperature dependent (thermochromic). The effect is relatively small; 150-200 cm^{-1} over 40°C. The wavenumber of maximum absorption of the charge transfer band

decreases as temperature increases, Table [3-7], in contrast to the pressure effect. These changes probably follow from the increasing polarity of the solvent as temperature increases, or the ground state is destabilized due to lower stability of the metal-diimine bond upon heating.

3-4. Stretching Frequency of Carbonyl in $Mo(CO)_4(N\widehat{\ }N)$

Studies of the stretching frequency of the carbonyl group in complexes of type $M(CO)_{6-x}L_x$, where M = Cr, Mo or W, have long been undertaken.[41-44] Values have been used to help in the inference of the geometrical structure of the complex. The changes in stretching frequency of carbonyl reflect the change in charge distribution of the complex. For example, the steady fall of the stretching frequency of carbonyl along the series of $Ni(CO)_4$, $Cr(CO)_4^-$ and $Fe(CO)_4^{2-}$ is consistent with an increase in π-electron donation from metal to carbonyl group. A similar situation is also reported when some of carbonyl groups are replaced by other ligands such as phosphines, arsines, amines, sulphides, and isonitriles. It is found that the stretching frequency of carbonyl steadily decreases as a result of a decreasing demand for metal d_π -electrons.[45]

The present work is centered on monitoring the stretching frequency of carbonyl of complexes of type $Mo(CO)_4(N\widehat{\ }N)$, where $N\widehat{\ }N$ is diimine ligand. The objective is to assess solvation effects. The geometry of the molecule indicates there are two types of the carbonyl groups; carbonyl trans to diimine ligand (trans-carbonyl) and cis to diimine group (cis-carbonyl). This type of complex normally gives four stretching frequency bands

(C_{2v} point group). Orgel[46] suggested that two of the bands correspond to the stretching frequency mode of cis-carbonyl; assymetrical B_1 and almost forbidden A_1, whereas the other two are given by vibration of the trans-carbonyls which are associated with stretching modes A_1 and B_2. These stretching modes are displayed diagramatically in Figure [3-10]. According to Cotton and Kraihanzel[47], the stretching frequency of cis-carbonyl should always correspond to a higher stretching force. Therefore, the two highest frequencies of carbonyl are regarded as being due to cis-carbonyl.

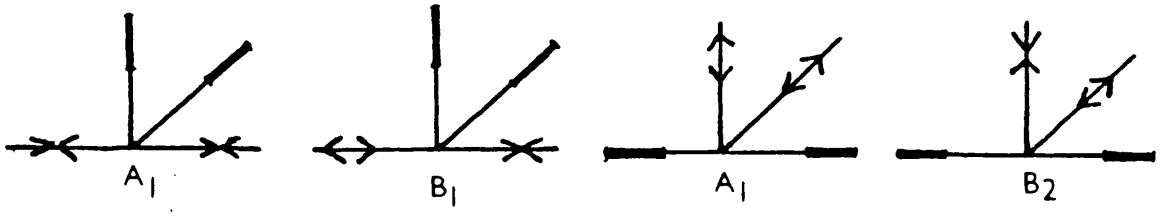

Figure [3-10] The carbonyl stretching frequencies of $Mo(CO)_4(N\widehat{\ }N)$.

In the present, the study of the stretching frequency of carbonyl in $Mo(CO)_4(N\widehat{\ }N)$ has been carried out in two states. The first is in the solid state using potassium bromide and the other is in solution in the range of 2100-1700 cm^{-1}. The former may be useful in monitoring the effect of changing the diimine ligand in the complex on the stretching frequency of carbonyl whereas the latter is used to demonstrate the solvent effect. The results as shown in Table [3-8] and Figure [3-11] give of the stretching frequency of carbonyl of several $Mo(CO)_4(N\widehat{\ }N)$ complexes in the solid state. It is found that

all four carbonyl stretching frequencies are clearly resolved and vary from one complex to another. Figure [3-12] shows a plot of those four stretching frequencies against the corresponding wavenumber of maximum absorption of the charge transfer spectra in methanol. The trend clearly demonstrates that the two higher frequencies of carbonyl are almost unaffected by changing the diimine ligand compared with the other two bands. This observation suggests that changing the diimine ligand in the complex has no significant effect on the carbonyl stretching frequency of the cis-carbonyl. But the situation is different for trans-carbonyls. It is found that the carbonyl stretching frequency increases as the diimine ligand has more demand for metal d_{π}-electrons. For example, in the complex $Mo(CO)_4(ppi)$, where the ligand ppi is considered to be a good π-acceptor (Chapter 5), it attracts more of the d_{π}-electron density of the metal and thus reduces the electron density in π^*-orbital of the carbonyl group trans to it. Such rearrangement provides a stronger C-O bond and increases the carbonyl stretching frequency. Similarly the lower carbonyl stretching frequency of $Mo(CO)_4(bmi)$ corresponds to the lower π-acceptor ability of the bmi ligand.

In solution, the measurement of the carbonyl stretching frequency was carried out on several complexes in various organic solvents. These results, summarized in Table [3-9], also show four bands. But, unlike in the solid state, the second lower frequency band of carbonyl (A_1) of most of the complexes in highly polar solvents eventually forms a shoulder to the second higher frequency band (B_1) and vanishes in less

polar solvents (Figure [3-13]). A similar observation is also reported as we change the diimine ligand in the complex. In this case, we found that the stretching frequency of carbonyl in the A_1 mode tends to vanish in the presence of a stronger π-accepting diimine ligand. The vanishing of the band is due to the overlapping of the stretching frequency band of B_1 mode. A plot of all four CO bands against polarity of solvent (E_T values of Reichardt)[25] is shown in Figure [3-14]. The trend clearly demonstrates that the two higher frequency bands of carbonyl which have been assigned as the stretching frequencies of the two cis-carbonyl are almost unaffected by the nature of the solvent. The other two bands, which originate from the trans-carbonyl, are markedly solvent dependent. Our present results indicate that these two lower frequencies steadily drop as the polarity of the solvent increases. This behaviour probably follows from the increasing interaction between a small negative charge on the carbonyl oxygen with the highly polar solvent. This interaction leads to a weakening of the C-O bond thus decreasing its stretching frequency.

M-C=O .....solvent

However, the smaller decrease of the stretching frequency of carbonyl of all the complexes in methanol relative to its polarity suggests that the solvent sensitivity of the stretching frequency probably distinguishes between the two

types of solvents (protic and aprotic); similar to the effect on charge transfer spectra. In another comparison of solvent dependence, we can plot a graph of the stretching frequency of the A_1 mode of trans-carbonyl of the complex in various solvents against the corresponding carbonyl stretching frequency of carbonyl for $Mo(CO)_4$(bipy), Figure [3-15]. The plot gives a good straight line; slopes are summarized in Table [3-10]. The results show that the solvent sensitivity of the carbonyl stretching frequency for $Mo(CO)_4$(gpi) are the strongest (largest slope), on the other hand, poorest for $Mo(CO)_4$(bipy) (smallest slope) compared to other complexes studied here.

3-5. Nuclear Magnetic Resonance of $Mo(CO)_4(\hat{N}\hat{N})$.

So far we have seen that the solvent molecule has a great influence on the electronic spectra and carbonyl stretching frequencies of molybdenum(0) tetracarbonyl diimine complexes. Since the effect is related to changes in charge distribution in the complex, the solvent may also influence the nuclear spin resonance of the complex. Connor and Overton[48] have monitored the ^1H and ^{13}C NMR of $Mo(CO)_4$(4,4'-XX-2,2'-bipy), where X is a substituent group like methyl, methoxy, chloride etc, in two solvents, chloroform ($CDCl_3$) and dimethylsulphoxide (DMSO-d_6). They found the chemical shifts to be solvent dependent. We now intend to examine the effect involving three types of nucleus (^1H, ^{13}C, and ^{95}Mo) in several solvents. The study will focus on one of the complexes which is structurally simple, so that the problem of spectral

complication can be avoided. However, NMR spectra of some other complexes are also required in helping to assign the resonances. The complex concerned is $Mo(CO)_4(bmi)$ which has the structure shown in 19, where the bmi ligand is thought to be coplanar with the two carbonyls trans to it. The complex is expected to have two pairs of equivalent methyl groups; one pair bonded to carbon ($C-CH_3$) and the other bonded to nitrogen ($N-CH_3$). Figure [3-16](a) shows a proton NMR spectrum of the complex in $CDCl_3$ which clearly displays two equivalent intensity signals at chemical shifts (δ) 3.75 ppm and 2.20 ppm. In an attempt to identify the signals, we ran the proton NMR of $Mo(CO)_4(gmi)$, 20, in chloroform, as indicated in Figure [3-16](b). Its spectrum gives two signals with 3:1 intensities which is in good agreement with the structure of the complex.

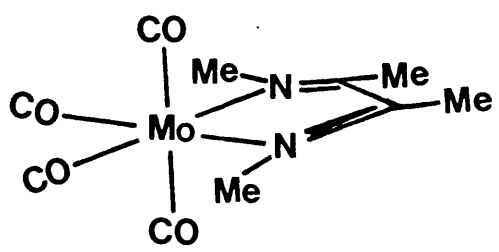

19

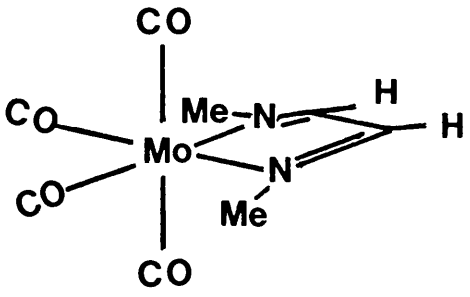

20

The more intense signal appears at δ = 4.0 ppm, and is assigned to a methyl group whereas the lower one, absorbing at δ = 8.02 ppm, is the signal of the single proton. In comparing the signals between two complexes, we found that the chemical

shift of the methyl group of $Mo(CO)_4$(gmi) is close to the signal at δ = 3.75 ppm of $Mo(CO)_4$(bmi). Therefore we conclude that the signal at this chemical shift corresponds to the methyl group bonded to a nitrogen atom whereas the other one (δ = 2.20 ppm) is given by the methyl group bonded to a carbon atom. This order of chemical shift is in agreement with the fact that the nitrogen atom has a stronger electronegativity which will attract more electrons away from the attached methyl group, thus reducing the shielding of the nucleus[49]

It is found that the chemical shifts of both types of methyl groups of $Mo(CO)_4$(bmi) are solvent dependent. They move to a higher chemical shift as the polarity of the solvent increases (Table [3-11] and Figure [3-17]). This observation indicates that the electrons residing around the methyl group are being driven away as the solvent become more polar. However, there is no one solvent parameter which can be used for correlation purposes. The most satisfactory trend is given by $(1/D_{op}-1/D)$ where D_{op} and D are the optical and static dielectric constants respectively (Figure [3-18]). Apart from that, the results reported here reveal that the chemical shift of the methyl group bonded to a carbon atom is more sensitive to solvent than that bonded to a nitrogen atom. This leads to a closer chemical shift between the two signals as the polarity of the solvent increases. For example, in benzene and acetone, the differences between the two signals are 2.29 ppm and 1.42 ppm respectively. Similar changes are also reported for the $Mo(CO)_4$(gmi) complex in which the chemical shift of the single proton exhibits more sensitivity to solvent. This different interaction is probably in accord with the slightly

open and exposed nature of this position facilitating interaction with solvent molecules.

The ^{13}C NMR spectrum of $Mo(CO)_4(bmi)$ consists of five peaks which are associated with five groups of non-equivalent carbon atoms present in the complex, as shown in Figure [3-19]. Two of them originate from the carbonyl carbons (trans- and cis- to bmi) and the rest from bmi carbons. The identification of the chemical shifts of carbonyl carbon in transition metal carbonyls has been widely reported.[50-53] Braterman and co-workers reported that the carbonyl-carbons in $Mo(CO)_{6-x}L_x$ give two signals (δCO (trans) and δCO (cis) to L) which occur at higher chemical shifts compared with the other sources of carbon in the complex. They also established that the δCO (trans) is always higher than δCO (cis). Based on this argument, we conclude that the first two (highest) chemical shifts of carbon in $Mo(CO)_4(bmi)$ are assigned as being due to two carbonyl groups; δCO(trans)= 223.6 and δCO (cis-) = 203.4 ppm in (chloroform).

The other three signals are produced by the three non-equivalent carbon atoms in the bmi ligand (20). As in proton NMR, the identification of these signals also requires determination of other relevant complexes. The most relevant include $Mo(CO)_4(gmi)$ (20) and $Mo(CO)_4(bami)$ (21). But, it is disappointing that the latter complex could not be isolated. For the present purposes, it is sufficient to use $Mo(CO)_4(gpi)$ (22), though the ^{13}C spectrum is rather complicated. The structure of the complex is similar to that of $Mo(CO)_4(bmi)$ and $Mo(CO)_4(gmi)$ in which the gpi ligand is expected to be planar to the carbonyl groups trans to it.

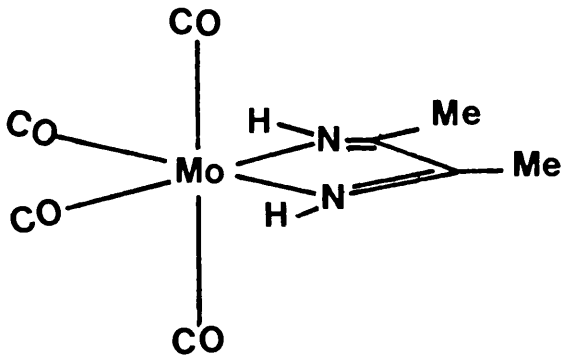

21

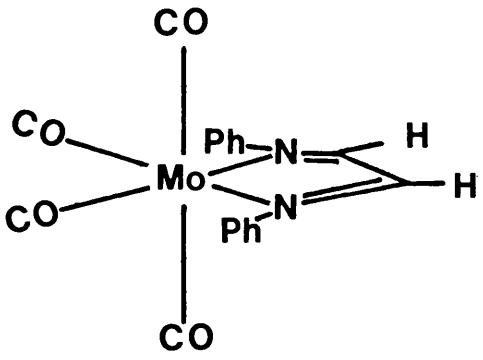

22

Determination of the spectrum of $Mo(CO)_4$(gmi) may also give information about the chemical shift of methyl carbon bonded to diimine carbon (C-CH_3) whereas the spectrum of $Mo(CO)_4$(gpi) may help to identify the chemical shift of C=C of the $Mo(CO)_4$(bmi) complex. The results in chloroform are summarized in Table [3-11]. It is found that $Mo(CO)_4$(gmi) shows no signal at chemical shifts around 17.36 ppm. Thus the signal at this chemical shift for $Mo(CO)_4$(bmi) may be associated with methyl carbon bonded to carbon atom. The ^{13}C NMR spectrum of $Mo(CO)_4$(gpi) is slightly complicated. This is due to the presence of several carbon atoms in the phenyl ring. However, it is found that all signals produced by this complex occur at chemical shifts higher than 100 ppm (157.0, 153.4, 129.3, 128.7 and 122.3 ppm). That there is no signal at lower chemical shift (around δ = 50 and 20 ppm) in $Mo(CO)_4$(gpi) proves that the two lowest signals reported in

$Mo(CO)_4$(bmi) (δ = 47.3 and 17.36 in chloroform) correspond to the chemical shifts of two different methyl groups; $N\text{-}CH_3$ and $C\text{-}CH_3$. From the earlier identification, we can show that the signal at δ = 17.36 ppm is due to the chemical shift of methyl carbon bonded to carbon atom. Therefore the signal at δ = 47.3 ppm is given by methyl carbon bonded to nitrogen atom. The signal at δ = 168.4 ppm of $Mo(CO)_4$(bmi) is probably associated with $\delta_{C=C}$, since the other two complexes also give a signal close to the value ($\delta_{C=C}(Mo(CO)_4(gmi)$ = 158.8 ppm and $\delta_{C=C}(Mo(CO)_4(gpi)$ = 157.0 ppm in chloroform-d_1). Details of these comparisons are listed in Table [3-11].

So, up to this point, we have identified the chemical shift of the particular carbon atoms in the $Mo(CO)_4$(bmi) complex. We are now interested in examining the effect of solvent on these chemical shifts. Data in Table [3-11] also include the chemical shift of ^{13}C NMR of $Mo(CO)_4$(bmi) in three solvents; toluene, chloroform, and acetone. It is found that the effect of solvent on carbon chemical shifts is very small (less than 2 ppm). In general their chemical shifts move to lower field (higher chemical shift) as the polarity of the solvent increases. For example, the chemical shift of the two methyl carbons ($C\text{-}CH_3$ and $N\text{-}CH_3$), C=C, trans-carbonyl and cis-carbonyl move about +1.1, +0.10, +2.25, -0.3 and -0.1 ppm respectively on changing solvent from toluene to acetone. These results suggest that the chemical shift of C=C is the most sensitive to interaction with solvent molecules which is odd as they are not in contact with solvent. Likewise in proton NMR the solvent sensitivity of the methyl carbon to carbon atom is stronger than that of nitrogen bonded of methyl

carbon.

In contrast to proton and ^{13}C NMR, the ^{95}Mo spectrum of $Mo(CO)_4(N\widehat{\ }N)$ consists of a single line as shown in Figure [3-20]. Previous studies on the type of complex $Mo(CO)_{6-x}L_x$ indicate that the ^{95}Mo NMR spectra are dependent on the nature of the substituent ligand L.[54-56] The chemical shift of ^{95}Mo increases as the number and strength of π-acceptor groups, L, increase. This observation proves that the charge distribution in a complex plays an important role in determining the chemical shift of the metal atom in the centre. Thus this technique has been used in diagnosing isomerism and estimating stability of the metal-ligand bond.[57-61] In this work, we shall report how the substituent group and solvent influence the chemical shift of ^{95}Mo of $Mo(CO)_4(N\widehat{\ }N)$. The results are summarized in Table [3-11]. As expected, the ^{95}Mo chemical shifts for $Mo(CO)_4(N\widehat{\ }N)$ are largely shifted to lower field compared to $Mo(CO)_6$ (δ_{Mo} = -1856.7 ppm)[54]. This indicates that the electron density residing around the molybdenum atom is being increased as carbonyl groups are replaced by diimine ligands, presumably due to less demand for the π-electron density of metal by this ligand. The present results show that the δ_{Mo} of $Mo(CO)_4$(bpbui) (23) occurs at higher field than that of $Mo(CO)_4$(bmi) ($\delta_{Mo}(Mo(CO)_4(bpbui))$ = -1177.91 ppm and $\delta_{Mo}(Mo(CO)_4(bmi))$ = -1165.90 ppm in chloroform). This trend suggests that the diimine ligand bpbui is a better π-acceptor than bmi. This order of π-acceptor ability is identical with that expected from the charge transfer spectra of the complexes discussed in Chapter 5 (ν ($Mo(CO)_4$(bpbui) = 19150 cm^{-1} and ν ($Mo(CO)_4$(bmi) = 19800 cm^{-1} in chloroform).

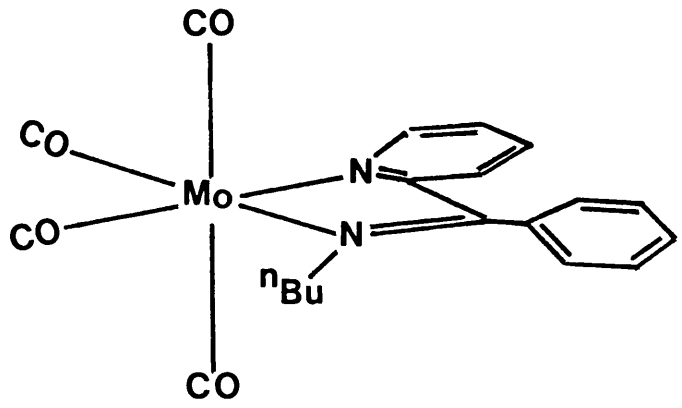

23

Like the ligand substituent, the solvent also influences the δ_{Mo} of $Mo(CO)_4(N\widehat{\ }N)$. It is found that the δ_{Mo} shifts to higher field as the polarity of the solvent increases. For example, δ_{Mo} of $Mo(CO)_4$(bmi) in toluene is -1162.46 ppm shift to -1165.90 ppm in chloroform. The changes suggest that a polar solvent has a tendency to reduce the formation of back-bonding by pulling the ligand molecule further apart from metal atom through electrostatic interaction.

TABLE 3-1(a)

The wavenumbers of maximum absorption, ν_{max}, of $Mo(CO)_4$(bipy) complex in various organic solvents and the corresponding E_T values (kcal mol^{-1}).

No:	Solvent	E_T	ν_{max}
1	Methanol	55.5	21790
2	Ethanol	51.9	21320
3	n-Propanol	50.7	20920
4	i-Propanol	48.6	21000
5	n-Butanol	50.2	20750
6	DMSO	45.0	22780
7	DMF	43.8	22620
8	Nitromethane	46.3	22570
9	Acetonitrile	46.0	22520
10	Acetone	42.5	22080
11	Ethyl methyl-ketone	41.3	21830
12	Acetophenone	41.3	21790
13	Cyclohexanone	40.8	21690
14	1,2-Cl_2 ethane	41.9	21370
15	Dichloromethane	41.1	21230
16	Ethyl acetate	38.1	21230
17	Anisole	37.2	21100
18	Phenetole	36.4	21000
19	Chlorobenzene	37.5	20660
20	Chloroform	39.1	20580
21	Diethyl ether	34.6	20240
22	Toluene	33.9	20120
23	CCl_4	32.5	19500

TABLE 3-1(b)

The wavenumbers of maximum absorption, ν_{max}, of $Mo(CO)_4(N\hat{}N)$ complexes in various organics solvents and the corresponding E_T values (kcal mol^{-1}).

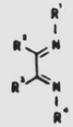

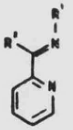

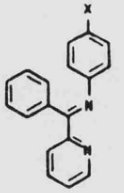

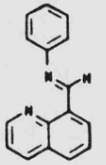

Solvent	E_T	bipym	R^1=Me R^2=Me R^3=Me R^4=Me bmi	Me ⌒ Me cmi	Me H H Me gmi	Me Ph Ph Me bzmi	Ph Me Me Ph dab	Ph ⌒ Ph cpi	Ph Me H Ph ppi	Ph H H Ph gpi	R^1=Me R^4=Me apmi	CH_2CH_2Ph Ph bppei	Bu Ph bpbui	Me Ph bpmi	Ph Me appi	H Ph bpami	Ph H cppi	X = H bppi	Me bppi p-Me	OMe bppi p-OMe	F bppi p-F	cqpi	dappi
1 Methanol	55.5	20400	20750	20100	19300	19050	18980	18350	17920	17240	21050	20100	20100	20100	20000	19350	18850	18900	18990	18970	18850	20150	19850
2 Ethanol	51.9	20200	20330	19700	19050	18790	18650	18150	17700	17040	20650	19600	19650	19650	19500	18990	18500	18580	18600	18600	18450	19600	19400
3 n-Propanol	50.7	19550	20060	19550	18900	18660	18420	17900	17530	16890	20300	19400	19450	19350	19250	18760	18250	18180	18250	18220	18250	19250	19050
4 iso-Propanol	48.6	19600	20020	19500	18950	18600	18450	17900	17520	16890	20300	19400	19400	19300	19200	18730	18200	18180	18200	18220	18250	19400	19080
5 n-Butanol	50.2	19400	19980	19400	18870	18620	18590	17850	17480	16870	20100	19200	19150	19250	19150	18550	18150	18110	18150	18100	18000	19200	18720
6 DMSO	45.0	21740	21740	21050	20200	19820	19840	19150	18650	17820	22150	21000	21150	21100	21100	20360	20000	20050	19920	19960	19850	21050	20900
7 DMF	43.8	21650	21620	20950	19950	19720	19760	19050	18450	17700	21900	20900	20950	20900	20900	20080	19850	19900	19850	19840	19700	20800	20750
8 Nitromethane	46.3	21650	21600	21000	19900	19680	19670	19100	18350	17530	22050	21000	21050	21050	21000	20000	19750	19800	19840	19840	19750	21000	20660
9 Acetonitrile	46.0	21600	21550	20950	19900	19650	19650	19100	18400	17550	22050	20950	21000	21000	20900	20120	19800	19850	19800	19800	19700	20900	20800
10 Acetone	42.5	21100	21100	20550	19650	19380	19340	18800	17850	17450	21450	20550	20550	20500	20350	19700	19350	19380	19420	19400	19300	20400	20350
11 Me Et ketone	41.3	21050	20880	20350	19450	19230	19120	18500	17780	17150	21200	20200	20250	20250	20000	19280	19150	19150	19270	19120	19050	20150	19960
12 Acetophenone	41.3	21270	20790	20100	19350	19120	18980	18400	17850	17300	21000	20150	20200	20150	20100	19340	19000	18980	19050	19050	19000	20050	19840
13 Cyclohexanone	40.8	20830	20870	20200	19400	19180	19080	18450	17890	17210	21000	20000	20050	20050	20000	19250	18950	18900	19030	18980	18900	19850	19800
14 1,2-Cl_2ethane	41.9	21370	20410	19950	19000	18940	18690	18300	17550	17010	20750	19850	19950	19900	19700	18830	18600	18830	18940	18730	18600	19700	19270
15 Dichloromethane	41.1	19800	20290	19850	18850	18870	18600	18150	17480	16950	20600	19700	19700	19650	19500	18760	18450	18620	18680	18590	18550	19600	19120
16 Ethyl acetate	38.1	20300	20410	19850	19200	18900	18750	18250	17700	17060	20600	19600	19650	19550	19450	18640	18300	18590	18650	18590	18550	19600	19270
17 Anisole	37.2	20200	20140	19650	19050	18800	18490	18050	17550	16920	20550	19350	19350	19300	19200	18550	18150	18490	18490	18450	18350	19350	18940
18 Phenetole	36.4	19800	20000	19550	18950	18650	18300	17900	17350	16650	20150	19200	19300	19200	19100	18450	18000	18280	18300	18300	18150	19150	18800
19 Chlorobenzene	37.5	19600	19880	19400	18750	18580	18320	17900	17640	16720	20000	19200	19200	19200	18900	18230	17850	18110	18180	18150	18050	19100	18550
20 Chloroform	39.1	19150	19800	19350	18600	18620	18250	17850	17560	16780	19800	19150	19150	19100	18800	18180	17700	18050	18170	18050	18000	19000	18600
21 Diethyl ether	34.6	19500	19670	19200	18650	18420	18180	17800	17180	16750	19600	18700	18700	18650	18600	17860	17400	17760	17860	17780	17800	18700	18250
22 Toluene	33.9	19200	19620	19150	18550	19300	18090	17700	17150	16700	19400	18650	18550	18550	18400	17850	17300	17700	17730	17750	17650	18450	18100
23 CCl_4	32.5	18100	19050	18550	18100	18100	17700	17400	17000	16400	18500	18300	18300	18300	17800	17300	16750	16950	17000	16950	16850	17200	17150

** This column refers to the tricarbonyl complex $Mo(CO)_3(LLL)$, where LLL is the terdentate ligand

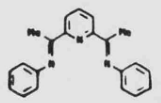

TABLE 3-2

Slopes of plots of wavenumbers of maximum absorption of charge transfer spectra of $Mo(CO)_4(N\widehat{\ }N)$ complexes against E_T (kcal mol^{-1}) values.

No:	N^N	Aprotic[a]	Protic[b]
1	bipy	220±22	141±30
2	bipym	227±30	144±60
3	bmi	177±17	118±21
4	cmi	168±15	100±20
5	gmi	140±15	83±20
6	bzmi	117±10	73±9
7	dab	152±20	79±18
8	cpi	128±20	76±18
9	ppi	90±10	72±10
10	gpi	84±10	70±9
11	cppi	183±15	120±25
12	appi	210±15	115±25
13	apmi	212±15	131±40
14	bppei	210±14	128±25
15	bppbui	213±15	132±25
16	bpmi	211±13	130±24
17	bpami	206±17	107±29
18	bppi	186±13	121±30
19	bppi-4F	185±12	120±30
20	bppi-4Me	187±12	125±30
21	bppi-4OMe	192±15	126±25

a 18 points

b 5 points

TABLE 3-3

Slopes of plots of wavenumbers of maximum absorption of charge transfer spectra of $Mo(CO)_4(\hat{N}\,\hat{N})$ complexes against corresponding wavenumbers for $Mo(CO)_4$(bipy).

No:	N^N	Slope[b]
1	bipy	1.0
2	bipym	1.11+0.07
3	btz[a]	0.82+0.03
4	cqpi	0.95+0.05
5	dappi*	1.12+0.03
6	cppi	0.98+0.03
7	appi	1.06+0.02
8	apmi	1.06+0.02
9	bppei	0.93+0.03
10	bpbui	0.94+0.03
11	bpmi	0.94+0.03
12	bpami	0.96+0.03
13	bppi	0.91+0.02
14	bppi-4Me	0.88+0.03
15	bppi-4OMe	0.90+0.02
16	bppi-4F	0.88+0.02
17	bmi	0.84+0.03
18	cmi	0.77+0.03
19	gmi	0.60+0.03
20	bzmi	0.55+0.02
21	dab	0.67+0.03
22	cpi	0.59+0.03
23	ppi	0.47+0.03
24	gpi	0.41+0.02

(a) reference 4 , (b) for 23 solvents

* tridentate

TABLE 3-4

Ground state-excited state analysis of $Mo(CO)_4$(dab) complex

	Methanol	Toluene	Acetonitrile	DMSO
[a] ΔH_{sol}/kJ mol^{-1}	20.6	20.0	22.1	25.0
$\mathcal{S}_m$ (GS)/kJ mol^{-1}	0	-0.6	+1.5	+4.4
[b] ΔE_{ct}/kJ mol^{-1}	227.0	217.2	234.9	236.8
$\mathcal{S}_m E_{ct}$/kJ mol^{-1}	0	-10.2	+7.9	+9.9
$\mathcal{S}_m$(ES)/kJ mol^{-1}	0	-10.8	+9.4	+14.3

GS = Ground state, ES = Excited state with reference to methanol.

[a] From Table [4-5]

[b] $\Delta E_{ct} = hc\nu_{ct}$

TABLE 3-5

Wavenumber of maximum absorption ($10^{-3}\nu_{max}/cm^{-1}$) of charge transfer spectra of $Mo(CO)_4(\widehat{N\ N})$ in toluene-methanol and toluene-heptane mixtures.

No	$\widehat{N\ N}$	← % (volume) methanol					toluene	% (volume) heptane →				
		100	80	60	40	20	0	20	40	60	80	100
1	bppi	19.01	18.87	18.62	18.45	18.21	17.73	17.60	17.42	17.21	16.95	16.60
2	cppi	18.98	18.76	18.59	18.28	1808	17.58	17.35	17.18	17.00	16.70	16.35
3	appi	20.12	19.92	19.76	19.49	19.20	18.55	18.45	18.29	18.04	17.76	17.35
4	bppi-4OMe	18.94	18.80	18.69	18.45	18.18	17.79	17.65	17.45	17.32	17.05	16.72
5	bmi	20.79	20.66	20.45	20.24	20.04	19.69	19.46	19.32	19.19	18.97	18.64
6	dab	19.05	18.87	18.69	18.55	18.38	18.12	18.20	17.90	17.80	17.71	17.59
7	gpi	17.25	17.09	16.95	16.84	16.76	16.70	16.66	16.62	16.58	16.50	16.38

TABLE 3-6

Pressure dependence on ν_{max} of charge transfer spectra of $Mo(CO)_4(N\widehat{\ }N)$ complexes.

No	N^N	Solvent	ν_{max} /cm^{-1} at P/bar				$(\delta\nu/\delta P)$ /cm^{-1}kbar^{-1}	Solvent sensitivity
			20	500	1000	1500		
1	bppi	Toluene	17860	17920	17990	18050	140±10	0.91
2	cppi	"	17600	17700	17760	17820	150±15	0.98
3	appi	"	18590	18660	18720	19600	160±15	1.06
4	bpbui	"	18870	18940	19050	19160	200±25	0.94
5	bppi-4Me	"	17860	17920	17990	18020	110±15	0.88
6	bppi-4OMe	"	17990	18050	18080	18120	70±15	0.90
7	bmi	"	19760	-	-	19960	130±15	0.84
8	ppi	"	17240	17270	17270	17300	40±10	0.47
9	gpi		no pressure dependence				0	0.41
10	bipy[a]	"					150	1.00
11	phen[a]	"					160	1.00
12	dab[a]	"					80±10	0.67
13	bdhi[b]	"					240±30	1.80
14	bipy[a]	n-BuOH					80	1.00
15	phen[a]	"					70	1.05
16	dab[a]	"					75	0.67
17	bdhi[b]	"					133±40	1.80
18	fz[b]	"					120±10	1.13

[a] reference 24

[b] P. Banerjee, Personal communication, 1986

[b] bdhi,

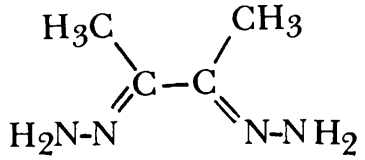

[b] fz,

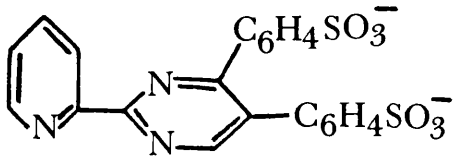

TABLE 3-7

Temperature dependence of charge transfer spectra of $Mo(CO)_4(\widehat{N\ N})$ in various organic solvents.

No	$\widehat{N\ N}$	Solvent	$10^{-3}\,\nu_{max}/cm^{-1}$ in various temp. /°C								$\delta\nu/\delta T$
			15	20	25	30	35	40	45	55	$/cm^{-1}C^{-1}$
1	bppi	toluene	17.92	--	17.86	--	17.86	--	--	17.76	-3.8±0.7
		CH_3CN	19.96		19.92	--	19.88	--	19.80	--	-5.2±0.7
2	bppi-4Me	toluene	17.92	--	17.89	--	17.82	--	17.83	17.76	-3.8±0.7
		heptane	--	16.89	--	16.86	--	16.86	--	--	-1.5±0.9
		methanol	19.08	--	19.08	--	19.01	--	--	--	-3.5±2.0
		CH_3CN		19.92	--	19.88	--	19.84	--	--	-4.0±0.2
3	bmi	toluene	--	19.80	--	--	--	19.72	--	--	-4.0
		methanol	20.92	--	20.88	--	--	20.83	--	--	-3.7±0.2
		CH_3CN	21.74	--	21.69	--	21.65	--	21.60	--	-4.6±0.2

TABLE 3-8

Stretching frequencies of carbonyl of $Mo(CO)_4(\widehat{N\ N})$ complexes in the solid state (KBr), with their corresponding ν_{max} for charge transfer in methanol.

No	$\widehat{N\ N}$	$\nu_{C=O}$(cis)/cm^{-1}		$\nu_{C=O}$(trans)/cm^{-1}		$10^{-3}\nu_{max}$/cm^{-1}
		A_1	B_1	A_1	B_2	in MeOH
1	bppi	2010	1916	1880	1835	18.90
2	cppi	2016	1922	1882	1807	18.85
3	appi	2010	1900	1873	1827	20.00
4	bpmi	2012	1903	1862	1818	20.10
5	bpbui	2016	1908	1867	1922	20.10
6	bppei	2010	1903	1871	1825	20.10
7	bpami	2010	1923	1877	1820	19.35
8	apmi	2011	1910	1852	1802	21.05
9	bppi-4Me	2005	1912	1880	1832	19.00
10	bmi	2020	1917	1865	1815	20.75
11	bzmi	2015	1913	1878	1825	19.05
12	dab	2017	1907	1873	1832	18.98
13	ppi	2017	1913	1880	1840	17.92
14	gpi	2025	1955	1883	1812	17.24
15	btz	2010	1890	1870	1810	20.00

TABLE 3-9

Stretching frequencies of carbonyl of $Mo(CO)_4(\widehat{N\ N})$ complexes in several organic solvents, with their corresponding E_T (kcal mol^{-1}) values.

solvent	E_T	$\widehat{N\ N}$	$\nu_{C=O}$(cis)/cm^{-1}		$\nu_{C=O}$(trans)/cm^{-1}	
			A_1	B_1	A_1	B_2
carbon tetrachloride	32.5	bipy	insoluble			
		bmi	2012	1915	-	1862
		bppi	2021	1908	-	1868
		bzmi	2013	1919	-	1867
		gpi	2021	1938	-	1888
toluene	33.9	bipy	2012	1902	1889	1845
		bmi	2010	1902	-	1853
		bppi	2009	1902	-	1858
		bzmi	2011	1909	-	1863
		gpi	2021	1938	-	1888
diethyl ether	34.6	bipy	2014	1913	1890	1850
		bmi	2012	1908	-	1857
		bppi	2011	1907	-	1859
		bzmi	2012	1916	-	1865
		gpi	2018	1935	-	1880
dioxan	36.0	bipy	2014	1904	1886	1844
		bmi	2009	1903	-	1849
		bppi	2010	1905	-	1854
		bzmi	2011	1911	-	1857
		gpi	2016	1923	-	1870
chloroform	39.1	bipy	2013	1910	1879	1832
		bmi	2012	1912	1888	1842
		bppi	2012	1903	1892	1850
		bzmi	2013	1919	1900	1850
		gpi	2020	1934	-	1868
dichloromethane	41.1	bipy	2014	1904	1878	1830
		bmi	2012	1906	1885	1837
		bppi	2012	1906	1890	1842
		bzmi	2012	1913	1896	1845
		gpi	2018	1928	-	1862

continued

TABLE 3-9

solvent	E_T	N^N	$\nu_{C=O}$(cis)/cm^{-1}		$\nu_{C=O}$(trans)/cm^{-1}	
			A_1	B_1	A_1	B_2
methanol	55.5	bipy	2012	1908	1880	1842
		bmi	2010	1906	1888	1846
		bppi	2011	1906	1894	1853
		bzmi	2012	1916	1904	1861
		gpi	2016	1925	-	1866
aceto-nitrile	46.0	bipy	2016	1904	1874	1830
		bmi	2010	1902	1880	1834
		bppi	2013	1906	1886	1839
		bzmi	2014	1911	1892	1840
		gpi	2014	1920	1900	1854
nitro-methane	46.3	bipy	2014	1907	1875	1830
		bmi	2012	1903	1879	1832
		bppi	2012	1907	1885	1838
		bzmi	2014	1911	1890	1840
		gpi	2015	1920	1900	1852
DMSO	45.0	bipy	2010	1896	1872	1828
		bmi	2008	1896	1877	1828
		bppi	2008	1900	1884	1835
		bzmi	2010	1909	1884	1838
		gpi	2012	1912	1893	1847

TABLE 3-10

Slopes of plots of $\nu_{C=O}$ (A_1 mode) of $Mo(CO)_4(N\widehat{\ }N)$ complexes against corresponding (A_1 mode) for $Mo(CO)_4$(bipy).

No:	N^N	Slope
1	gpi	2.5±1.0
2	bzmi	2.2±0.3
3	bppi	1.3±0.2
4	bmi	1.5±0.2
5	bipy	1.0

TABLE 3-11

Chemical shift of ^{1}H, ^{13}C and ^{95}Mo of $Mo(CO)_4(\widehat{N}N)$ complexes in several organic solvents.

$\widehat{N}N$	solvent	$[1/D_{op}-1/D]$	$^{1}H^{\#}$				$^{13}C^{\#}$					$^{95}Mo^{+}$
			N-CH_3	C-CH_3	C_6H_5	CH	trans-CO	cis-CO	-C=C-	NCH_3	CCH_3	ppm
bmi	benzene	0.009	3.12	0.83								
	toluene	0.029	3.21	1.00	-	-	224.5	205.4	168.95	47.72	16.90	-1162.46
	$CHCl_3$	0.267	3.75	2.20	-	-	223.6	203.4	168.40	47.30	17.36	-1165.90
	CH_2ClCH_2Cl	0.381	3.75	2.20								
	methanol	0.536	3.70	2.23								
	acetone	0.494	3.75	2.33	-	-	224.4	205.1	172.2	47.80	18.00	-
	CH_3CN	0.525	3.67	2.17								
	DMSO	0.438	3.62	2.20								
gmi	$CHCl_3$	0.267	4.00	-	-	8.02	-	-	158.8	53.76	-	-
	toluene	0.029	3.32	-	-	6.55	-	-	-	-	-	-
gpi*	$CHCl_3$	0.267	-	-	7.50	8.45	210.1	203.2	157.0	-	-	-
bpbui	$CHCl_3$	0.267	-	-	-	-	-	-	-	-	-	-1177.91

*
Chemical shift for aromatic carbon is 153.6, 129.3, 128.7 and 122.3 ppm.

$^{\#}$Measured in deuterinated solvent; $^{+}$Measured in non-deuterinated solvent.

TMS was used as reference in ^{1}H and ^{13}C, and MoO_4^{2-} for ^{95}Mo.

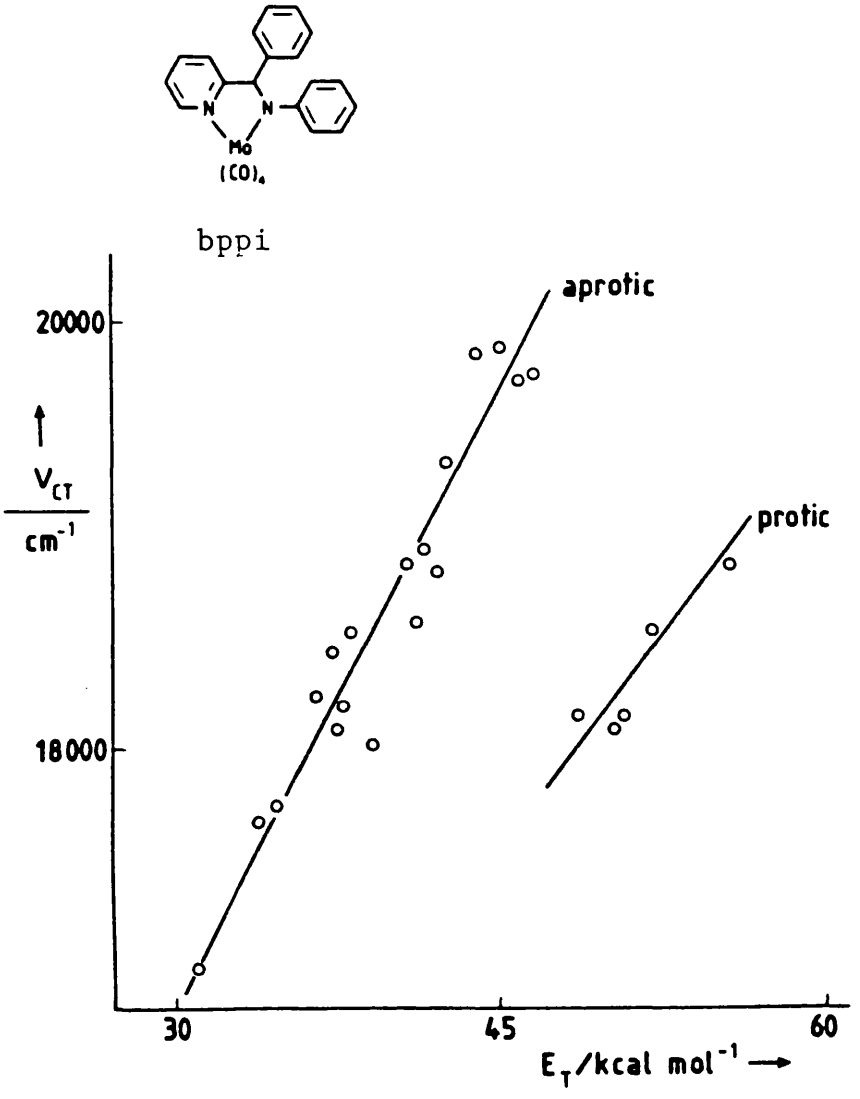

Figure [3-2] Plot of wavenumber of maximum absorption ν_{max} of $Mo(CO)_4$(bppi) against E_T values of solvent.

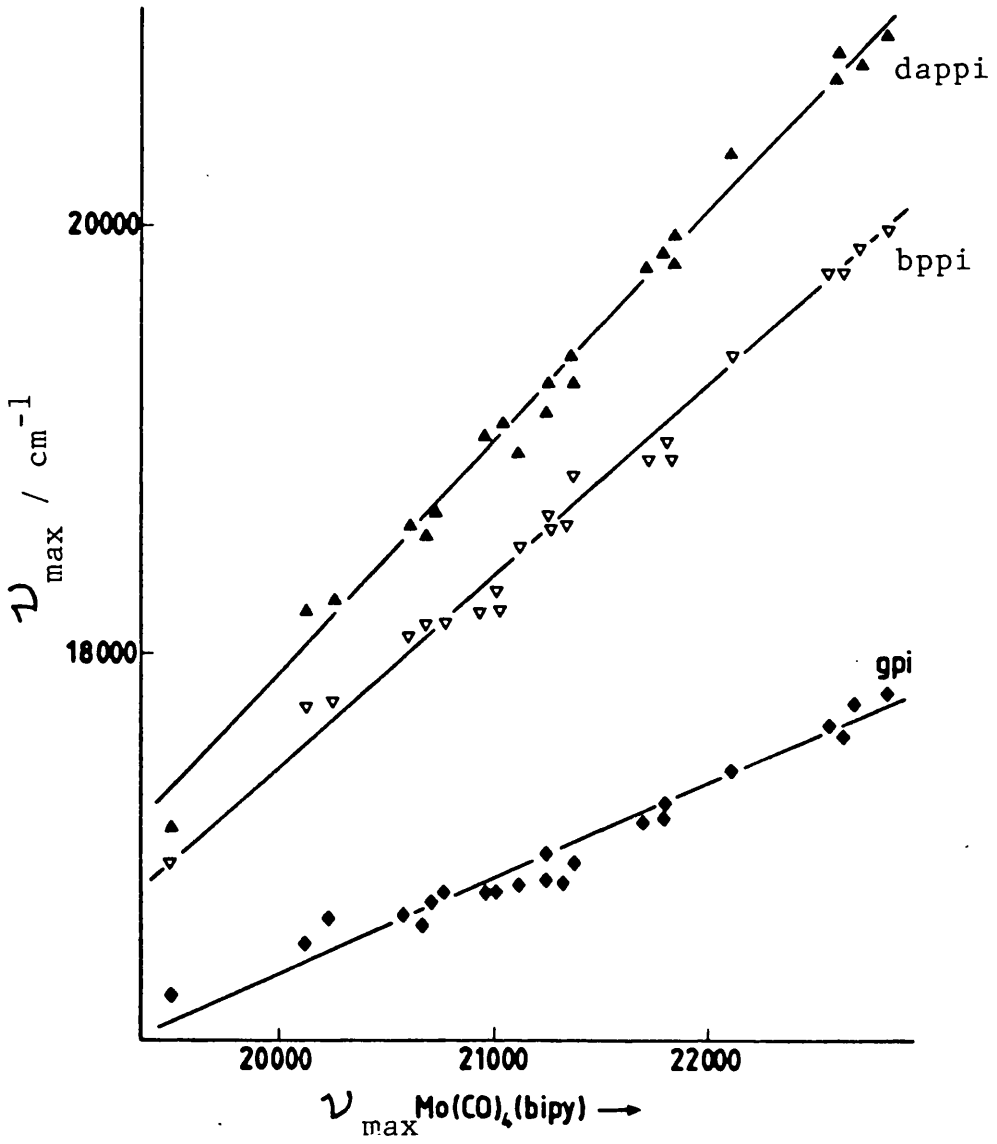

Figure [3-3] Plots of wavenumber of maximum absorption (ν_{max}) of $Mo(CO)_4(N\hat{}N)$ in various solvents versus the corresponding ν_{max} for $Mo(CO)_4$(bipy).

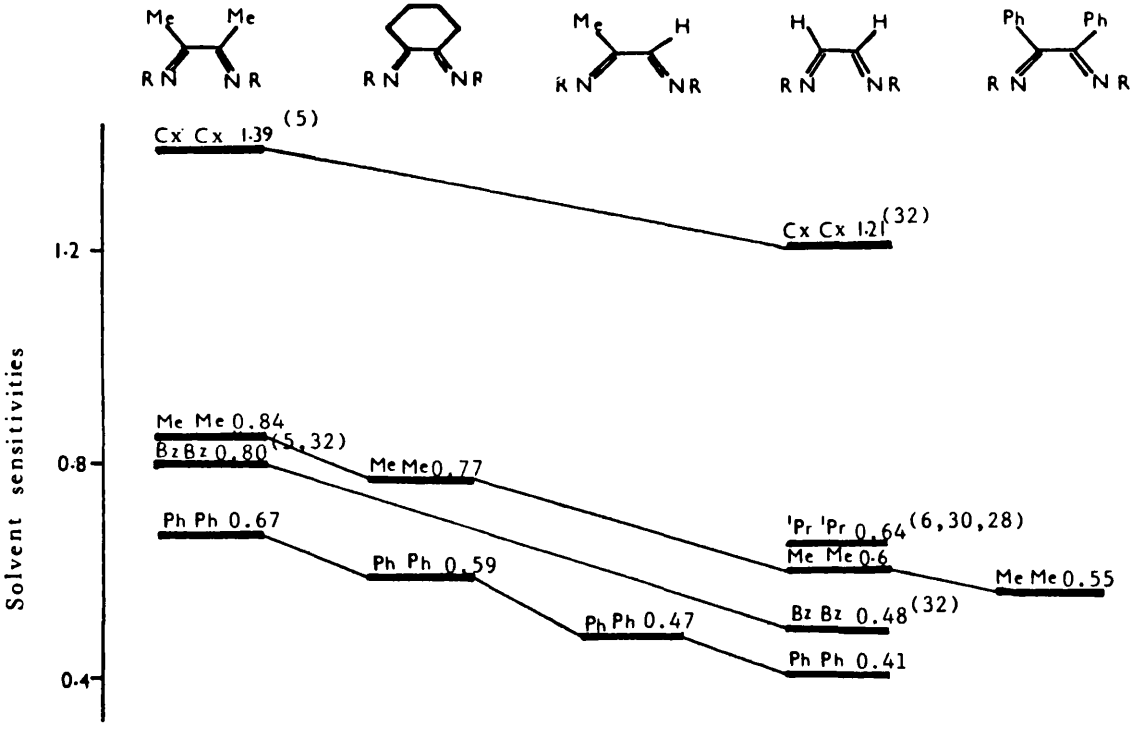

Figure [3-4] Solvent sensitivities (slopes of ν_{max} 14 versus ν_{max} $Mo(CO)_4(bipy)$ plot) each entry gives the groups R'R', the solvent sensitivities and the reference numbers for values derived from published data. Diagonal lines join complexes with identical group R R . Bz = benzyl; Cx = cyclohexyl.

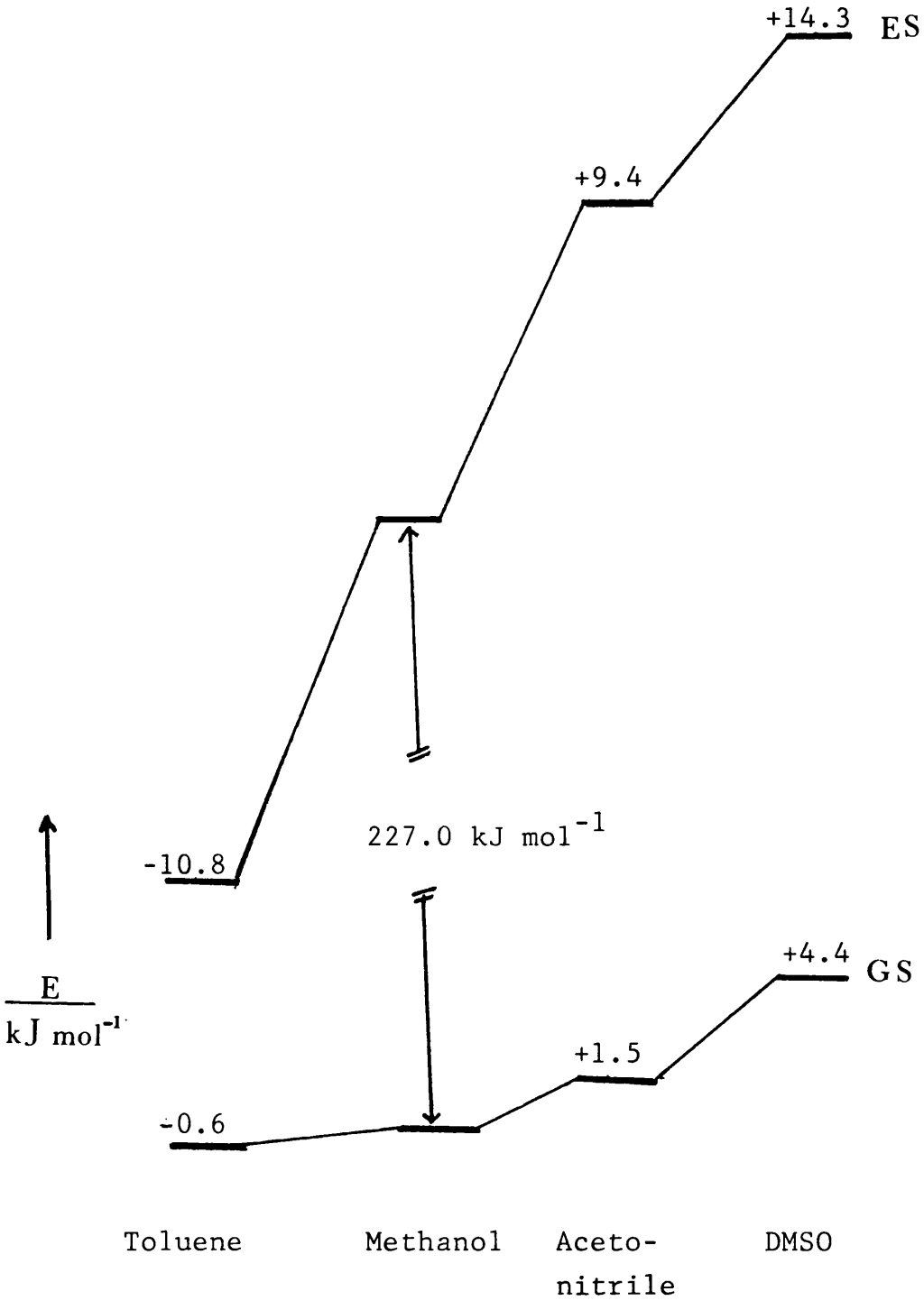

Figure [3-5] Ground state-excited state analysis of solvent effects on charge transfer absorption for $Mo(CO)_4(dab)$; dab = 5.

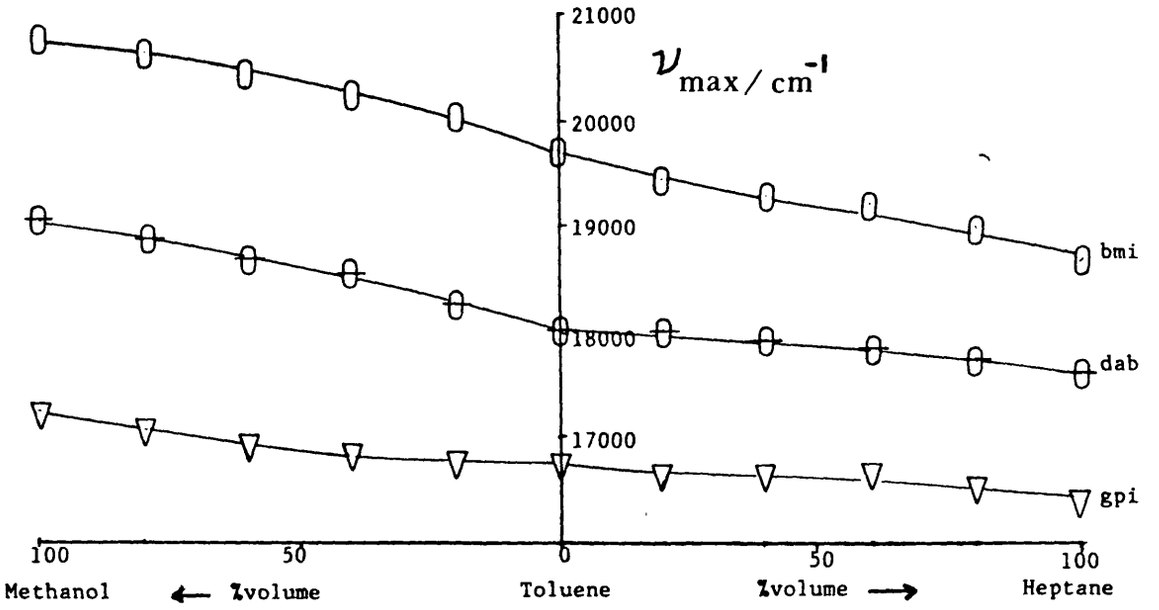

Figure [3-6] Plots of wavenumber of maximum absorption (ν_{max}) of $Mo(CO)_4(N\hat{}N)$ against percentage volume for toluene-heptane, toluene-methanol ; $N\hat{}N$ = bmi, dab and gpi.

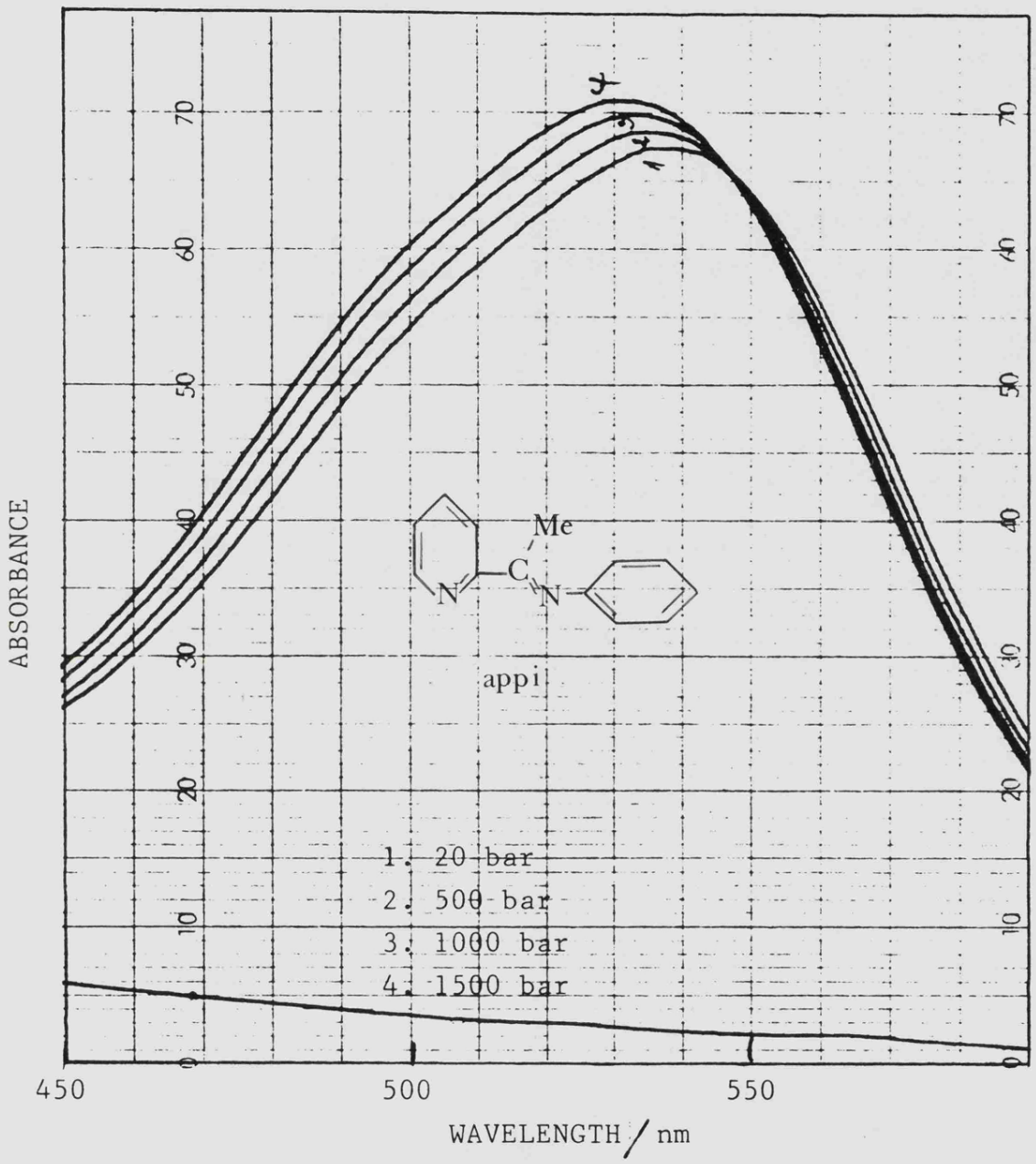

Figure [3-7] Charge transfer spectra of $Mo(CO)_4$(appi) in toluene at various pressures.

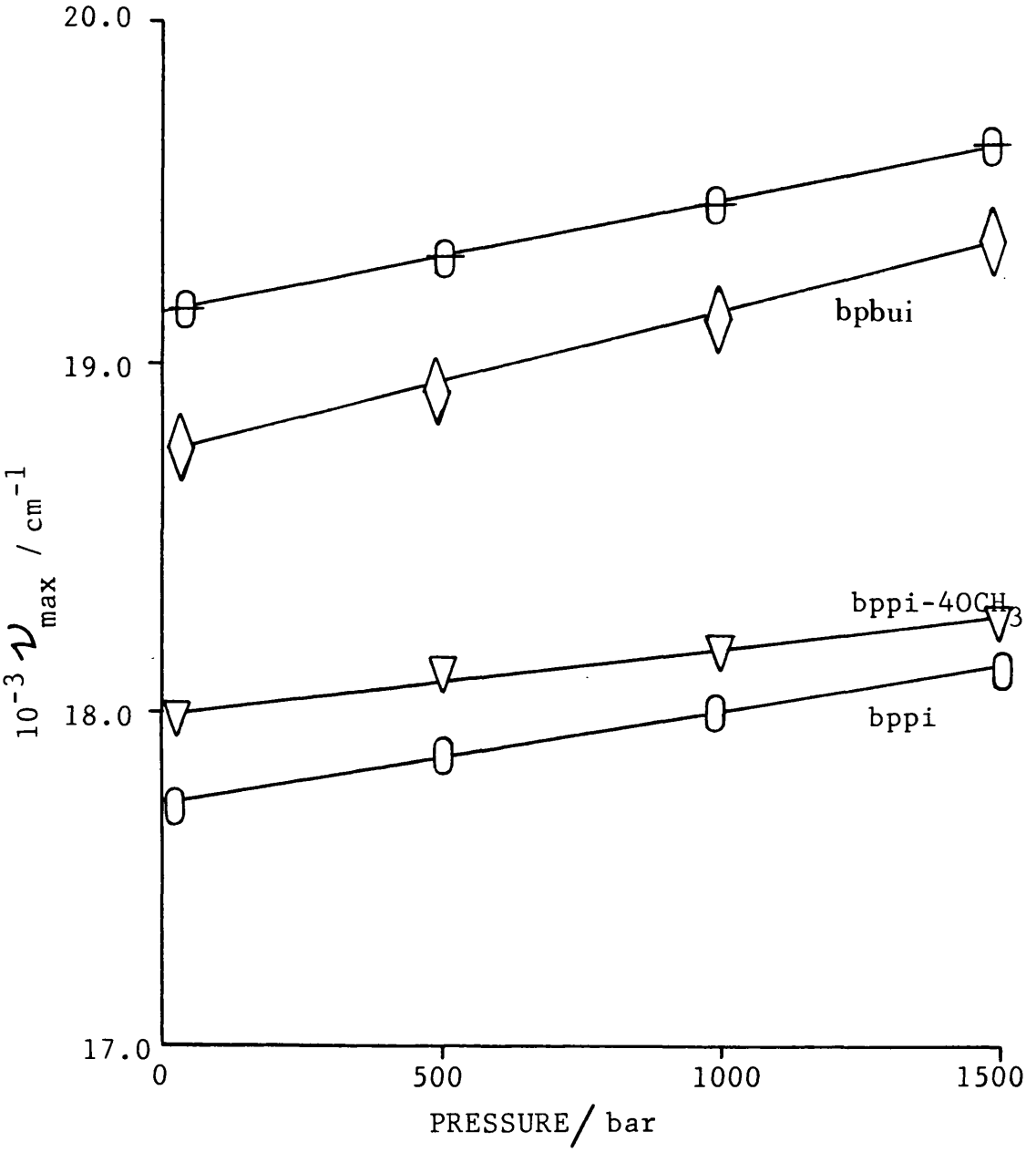

Figure [3-8] A typical plot of the dependence of charge transfer spectra of $Mo(CO)_4(N\hat{}N)$ on pressure.

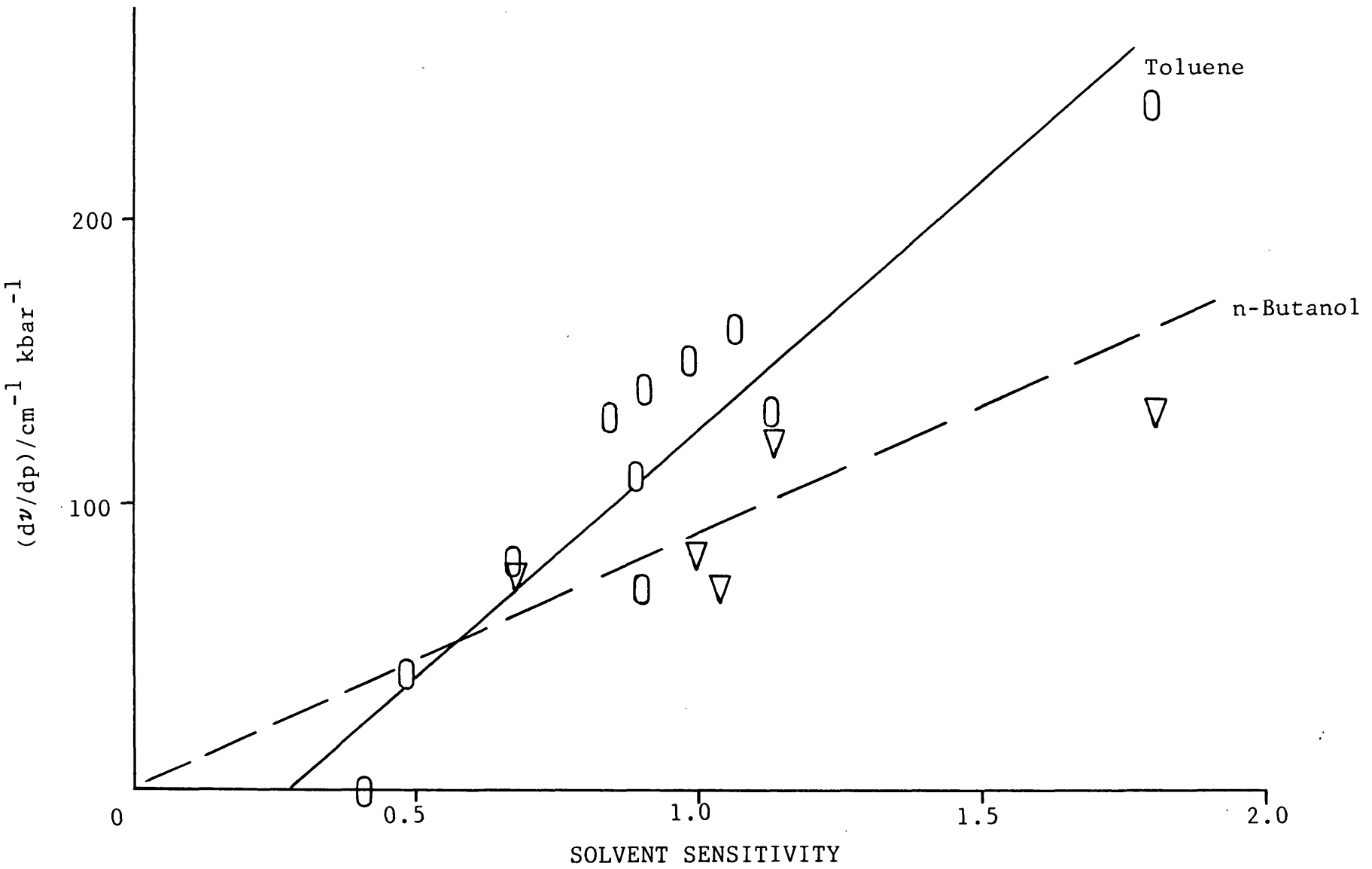

Figure [3-9] Plots of pressure ($d\nu/dp$) against solvent sensitivities (slope of the plot $\nu_{max}(Mo(CO)_4(N\hat{}N)$ against $\nu_{max}(Mo(CO)_4(bipy))$ of charge transfer spectra of $Mo(CO)_4(N\hat{}N)$

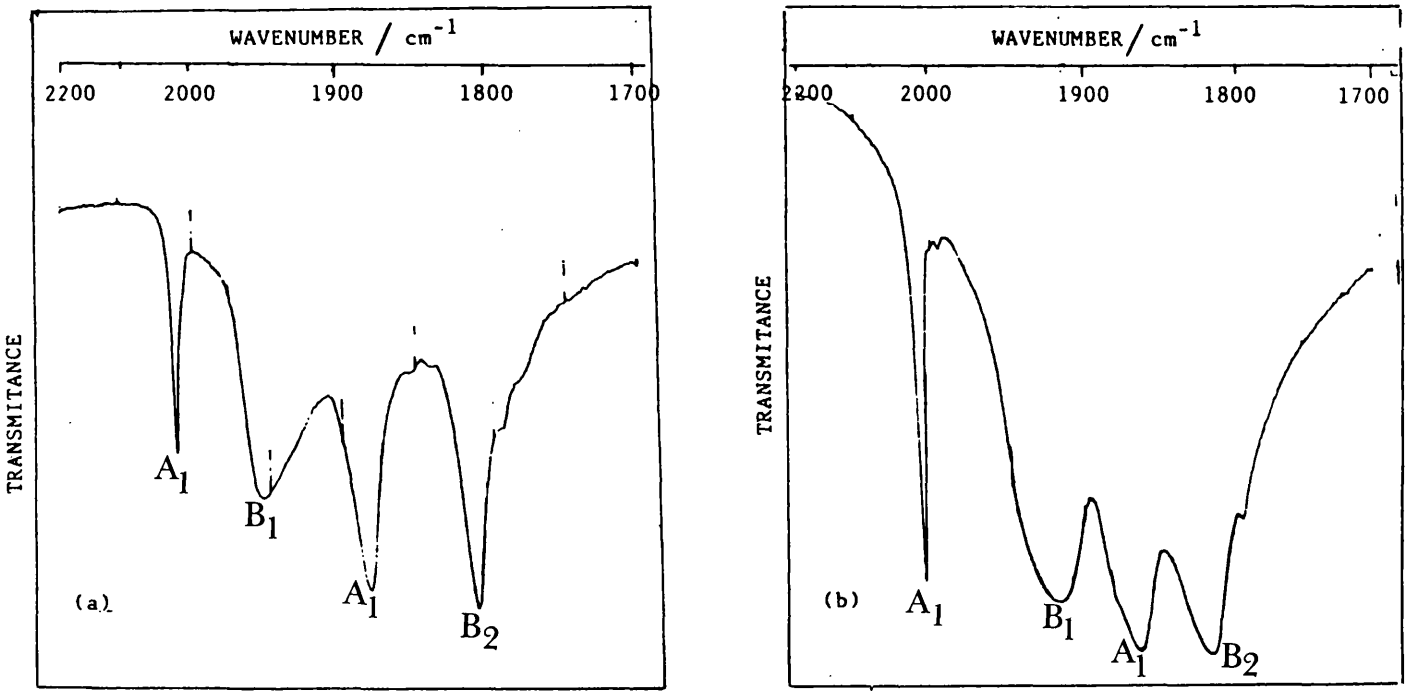

Figure [3-11] The carbonyl stretching region of the infrared spectra in KBr; (a) $Mo(CO)_4$(gpi) and (b) $Mo(CO)_4$(bmi).

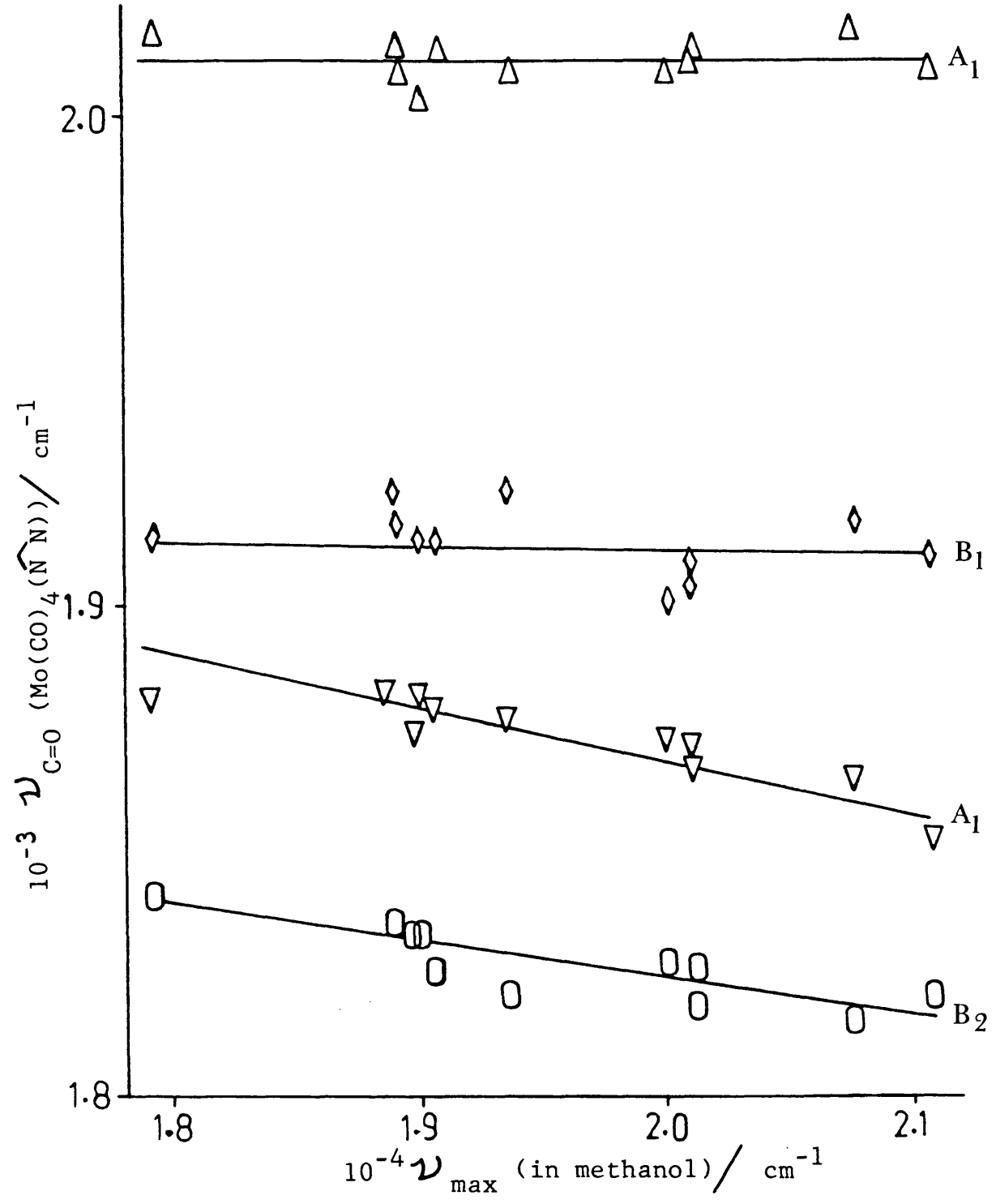

Figure [3-12] Plot of the carbonyl stretching frequencies (4 stretching modes) of several $Mo(CO)_4(N\hat{}N)$ complexes in KBr against the corresponding ν_{max} in methanol.

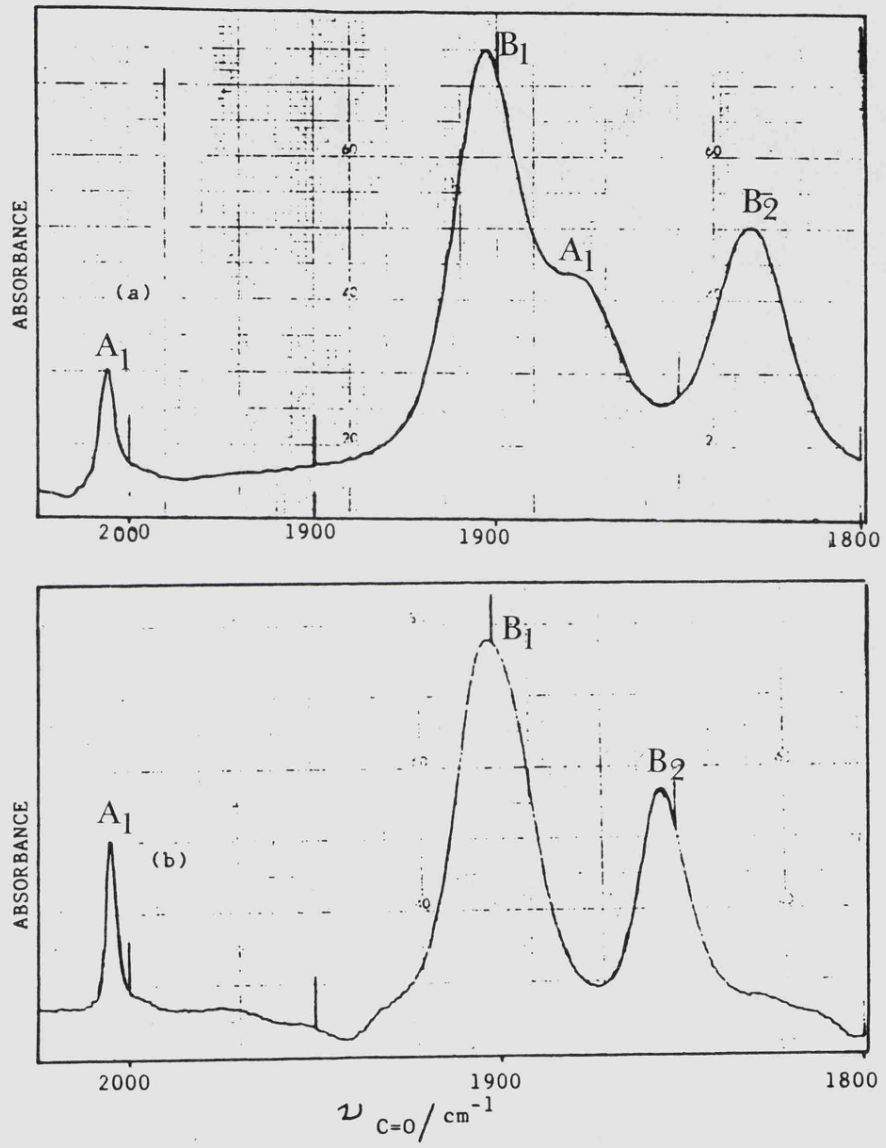

Figure [3-13] The carbonyl stretching region for the infrared spectra of $Mo(CO)_4(bmi)$ in solution; (a) in toluene and (b) in nitromethane.

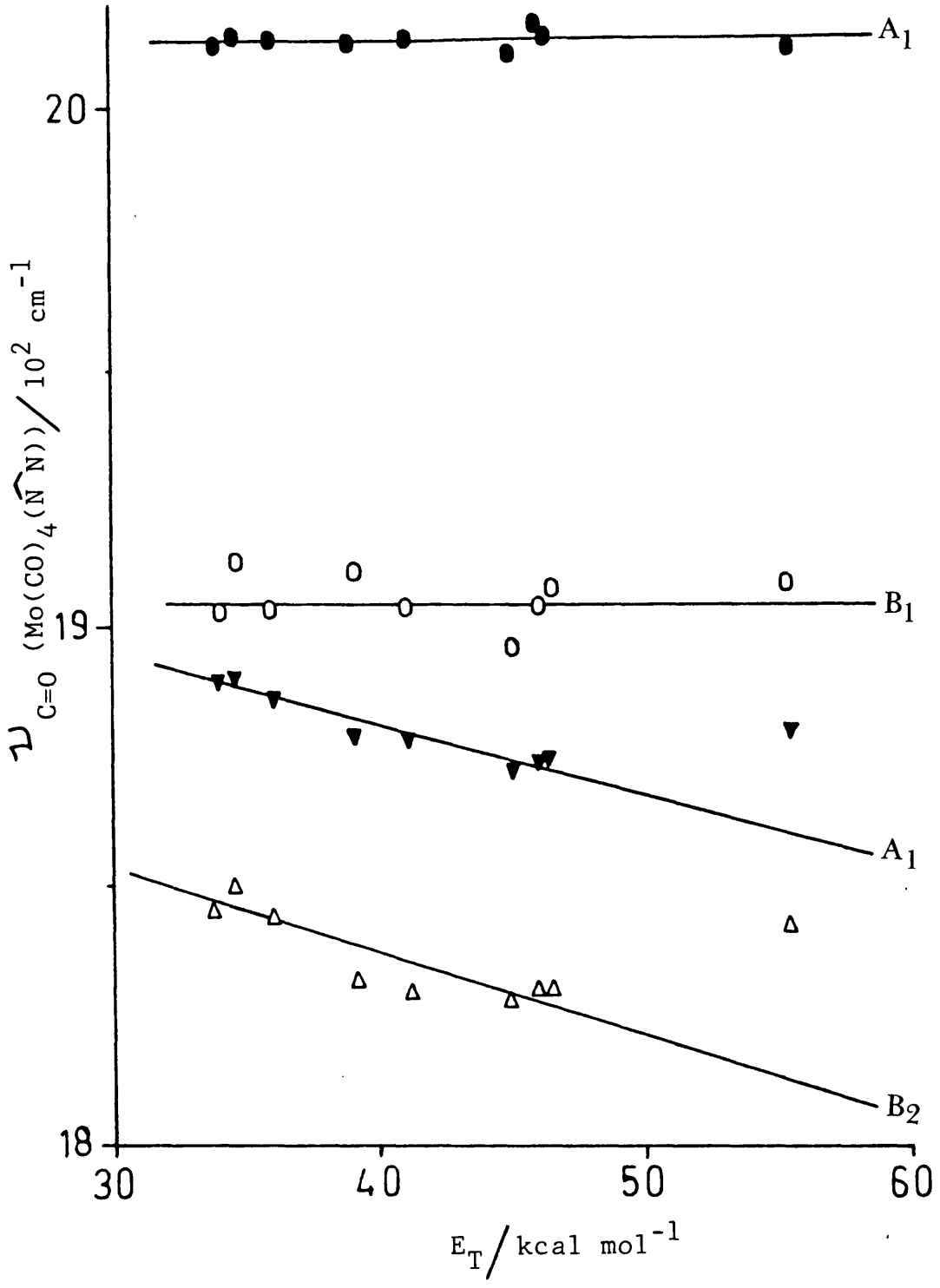

Figure [3-14] Plots of stretching frequencies of carbonyl of $Mo(CO)_4(N\widehat{\ }N)$ against solvent polarities (E_T)

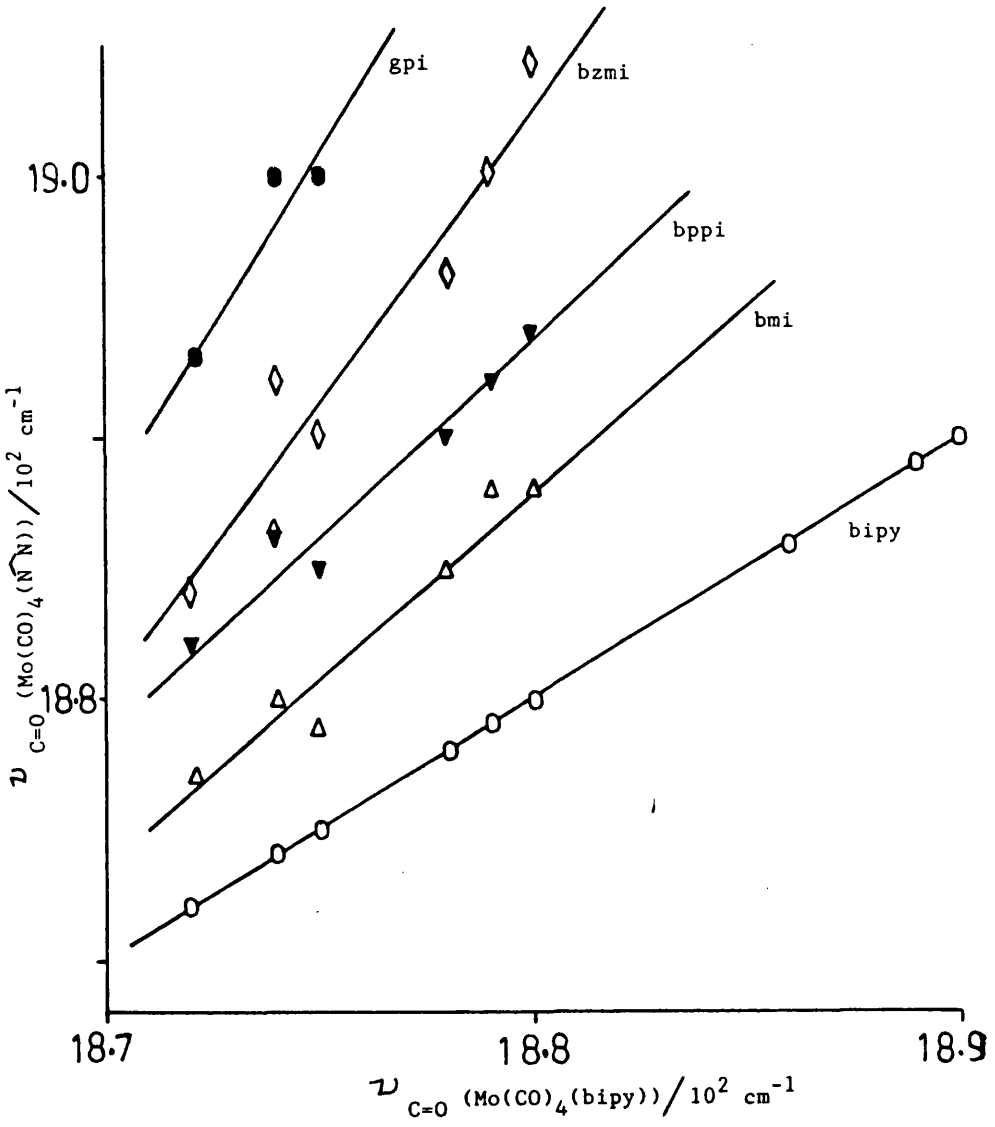

Figure [3-15] Plots of the stretching frequencies of carbonyl for A_1 mode of $Mo(CO)_4(N\widehat{\ }N)$ against the corresponding frequencies for $Mo(CO)_4$(bipy).

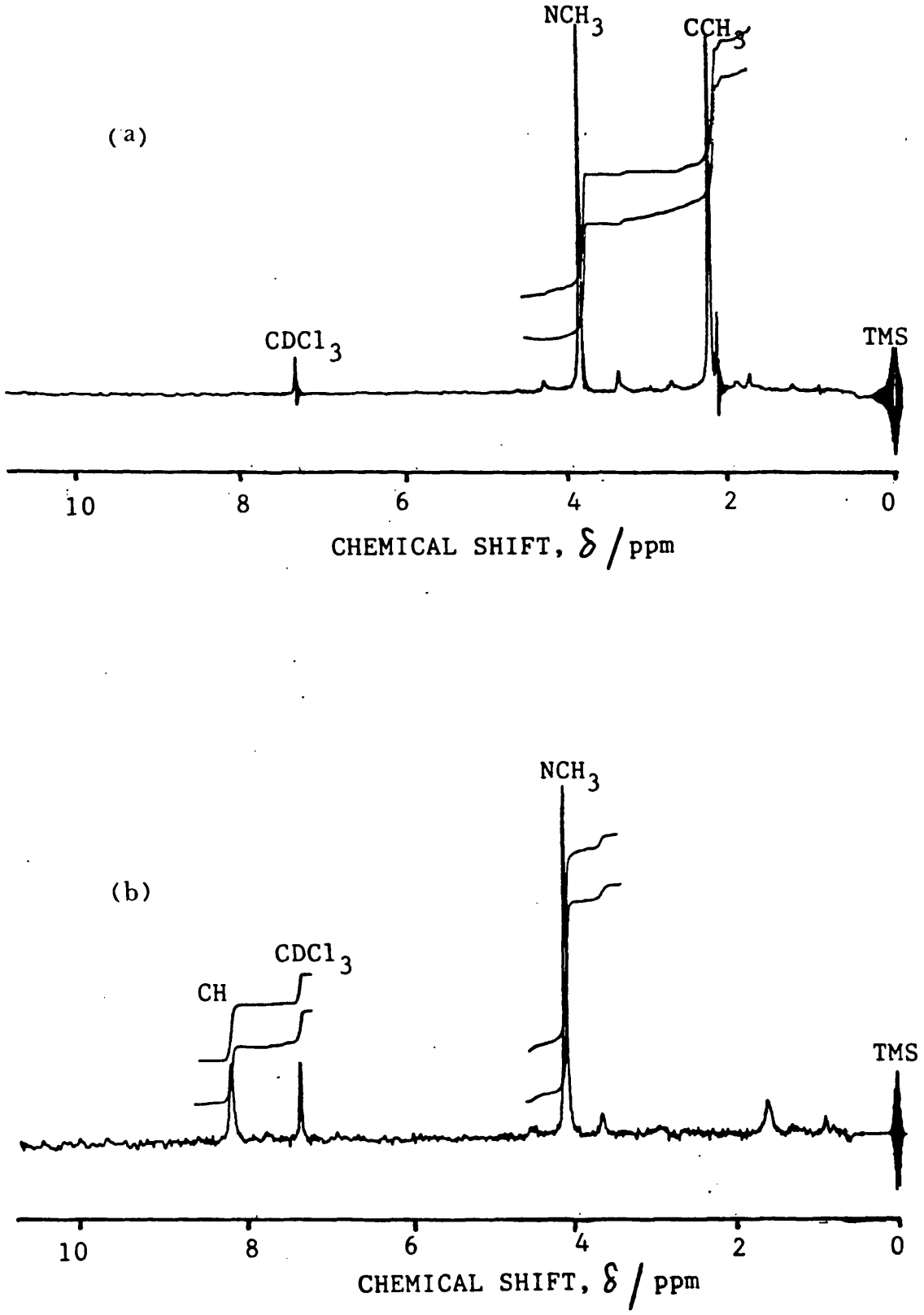

Figure [3-16] Proton NMR spectra of $Mo(CO)_4(N\hat{}N)$ in $CDCl_3$; (a) $Mo(CO)_4$(bmi) and (b) $Mo(CO)_4$(gmi).

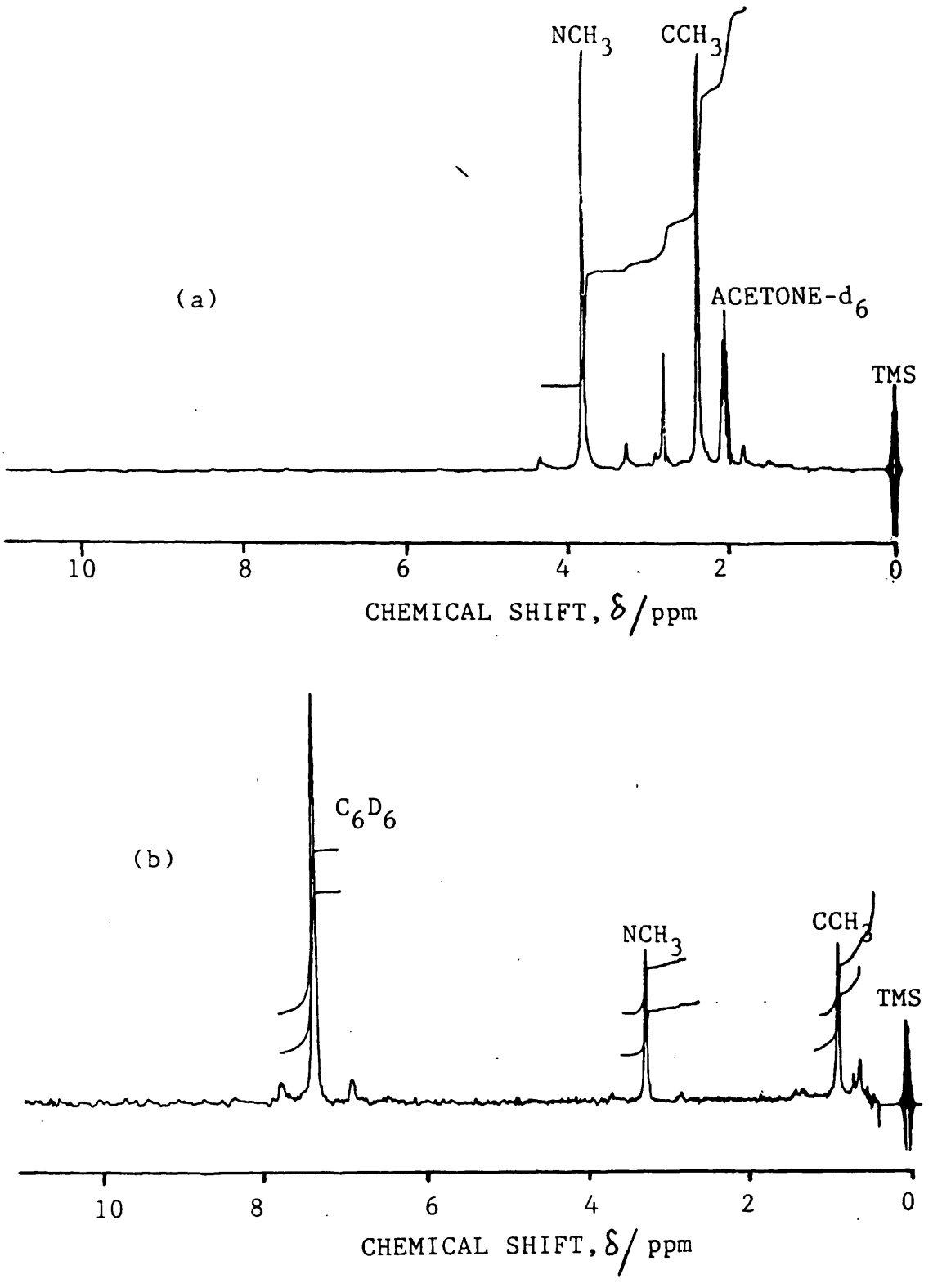

Figure [3-17] Proton NMR spectra of $Mo(CO)_4$(bmi) in (a) acetone-d_6 and (b) benzene-d_6

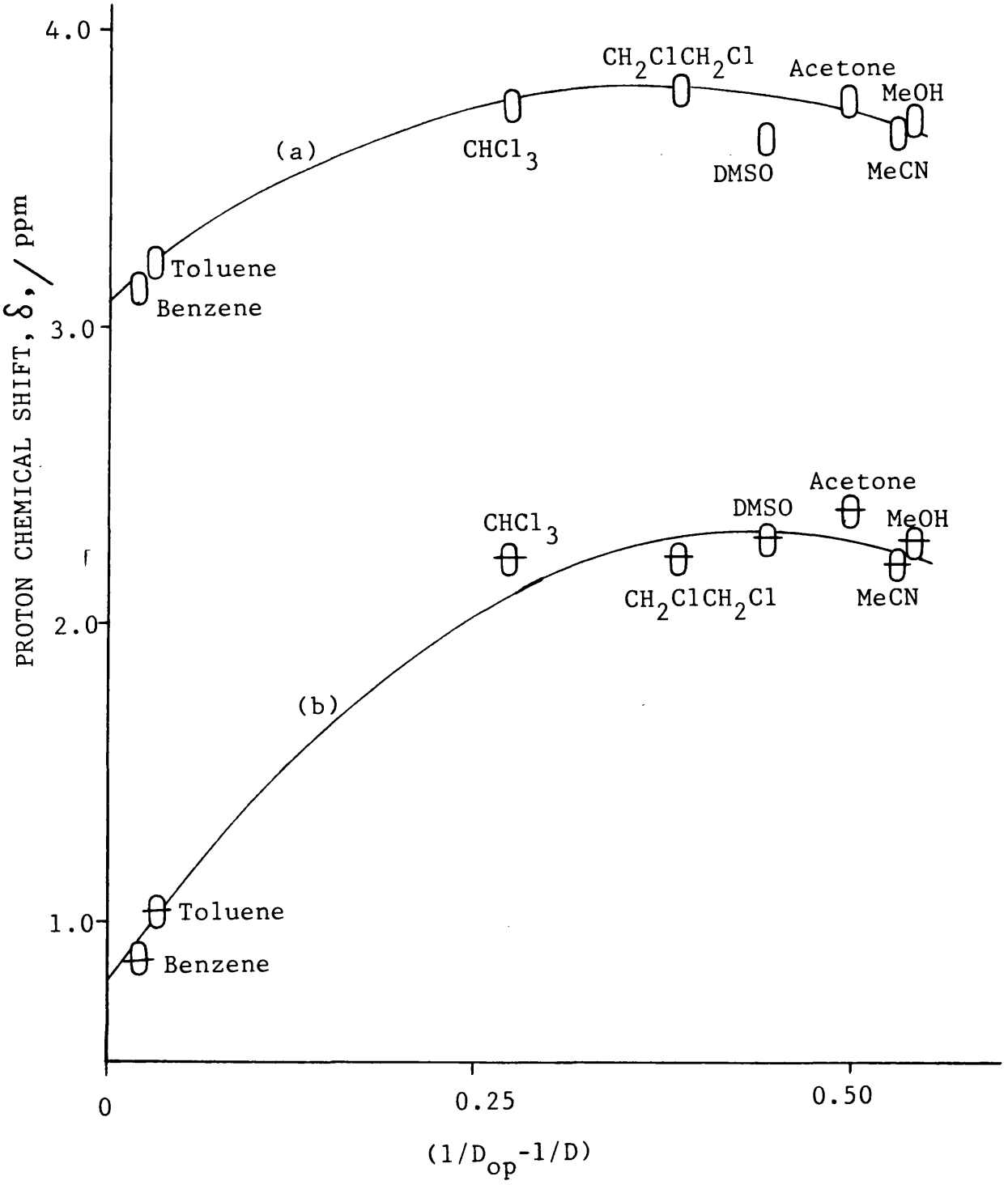

Figure [3-18] Plots of proton chemical shift (δ) of $Mo(CO)_4(bmi)$ against $(1/D_{op}-1/D)$, (a) δ $(N-CH_3)$ and (b) δ $(C-CH_3)$.

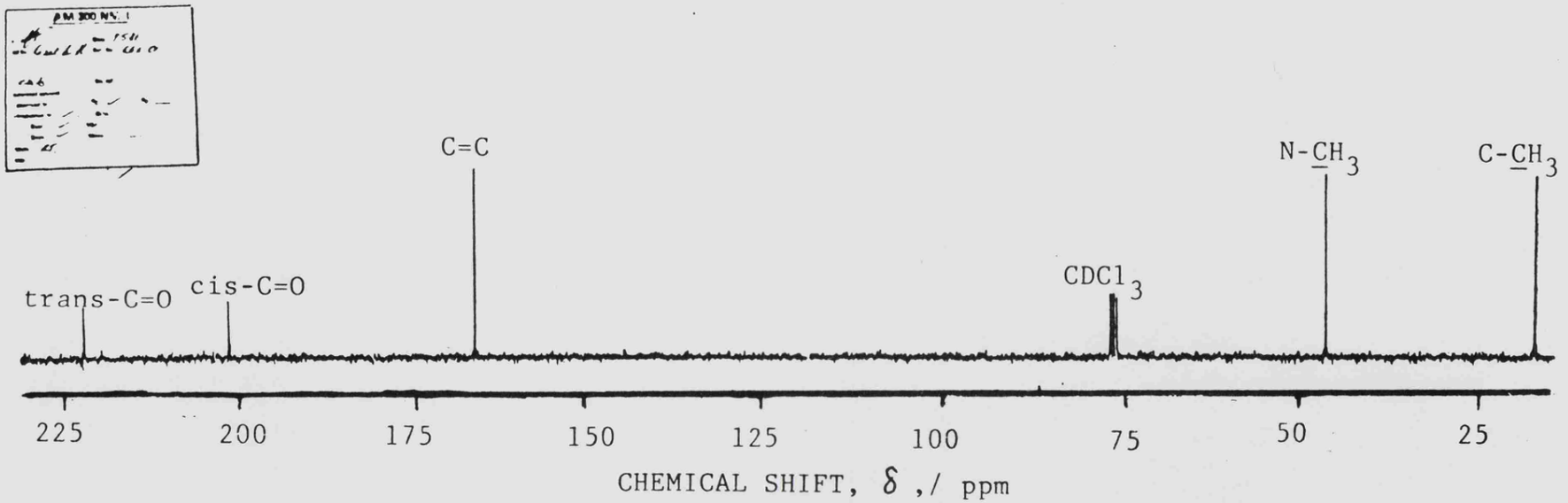

Figure [3-19] ^{13}C NMR spectrum of $Mo(CO)_4$(bmi) in $CDCl_3$.

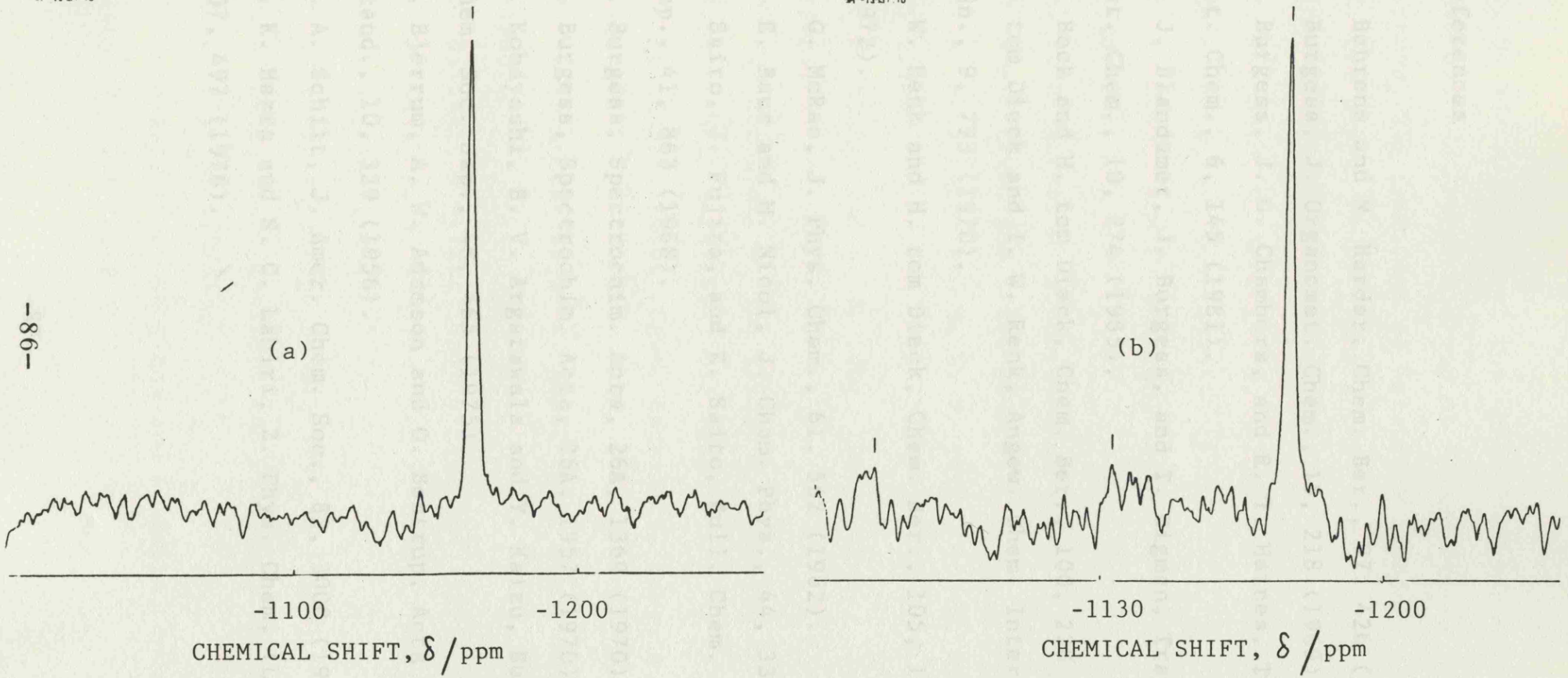

Figure [3-20] ^{95}Mo NMR spectra of $Mo(CO)_4$(bmi) in (a) chloroform and (b) toluene

3-5. References

1. H. Behrens and N. Harder, Chem. Ber., 97, 426 (1964).
2. J. Burgess, J. Organomet. Chem., 19, 218 (1969).
3. J. Burgess, J. G. Chambers, and R. I. Haines, Transition Met. Chem., 6, 145 (1981).
4. M. J. Blandamer, J. Burgess, and T. Digman, Transition Met. Chem., 10, 274 (1985).
5. H. Bock and H. tom Dieck, Chem. Ber., 100, 228 (1967).
6. H. tom Dieck and I. W. Renk, Angew. Chem. Internat. Edn., 9, 793 (1970).
7. I. W. Renk and H. tom Dieck, Chem. Ber., 105, 1403 (1972).
8. E. G. McRae, J. Phys. Chem., 61, 562 (1962).
9. M. E. Baur and M. Nicol, J. Chem. Phys., 44, 3337 (1962).
10. H. Saito, J. Fujita, and K. Saito, Bull. Chem. Soc. Jap., 41, 863 (1968).
11. J. Burgess, Spectrochim. Acta, 26A, 1369 (1970).
12. J. Burgess, Spectrochim. Acta, 26A, 1957 (1970).
13. H. Kobayashi, B. V. Argarawala and Y. Kaizu, Bull. Chem. Soc. Jap., 48, 465 (1975).
14. J. Bjerrum, A. W. Adamson and O. Bostrup, Acta Chem. Scand., 10, 329 (1956).
15. A. A. Schilt, J. Amer. Chem. Soc., 82, 3000 (1960).
16. D. K. Hazra and S. C. Lahiri, Z. Phys. Chem. (Leipzig), 257, 497 (1976).

17. D. M. Adams, Report of the Conference Organized by the Hydrocarbon Research Group of Petrolium and held in London, The Institute of Petrolium, London, 1962.
18. H. tom Dieck, K. D. Franz and F. Hohmann, Chem. Ber., 108, 163 (1975).
19. J. Reinhold, R. Benedix, P. Berner and H. Hennig, Inorg. Chim. Acta, 33, 209 (1979).
20. J. A. Connor and C. Overton, Inorg. Chim. Acta, 65, L1 (1982)
21. M. S. Wrighton, H. B. Abrahamson and D. L. Morse, J. Amer. Chem. Soc., 98, 4105 (1976).
22. H. B. Abrahamson and M. S. Wrighton, Inorg. Chem., 17, 3385 (1978).
23. D. M. Manuta and A. J. Lees, Inorg. Chem., 22, 3825 (1983)
24. M. -T. Macholdt, R. van Eldik, H. Kelm and H. Elias, Inorg. Chim. Acta, 104, 115 (1985).
25. C. Reichardt, Angew. Chem. Internat., Edn., 4, 29 (1965)
26. S. Ernst and W. Kaim, J. Amer. Chem. Soc., 108, 3578 (1986).
27. D. Walther, J. Prakt. Chem., 316, 604 (1974).
28. R. W. Balk, D. J. Stufkens and A. Oskam, Inorg. Chim. Acta, 34, 267 (1979).
29. D. Walther, Z. Anorg. Chem., 396, 46 (1973).
30. R. W. Balk, D. J. Stufkens and A. Oskam, Inorg. Chim., Acta, 28, 133 (1978).
31. L. H. Staal, D. J. Stufkens and A. Oskam, Inorg. Chim. Acta, 26, 255 (1978).

32. H. tom Dieck and I. W. Renk, Chem. Ber., 104, 110 (1971).
33. J. A. Connor and C. Overton, J. Organomet. Chem., 277, 277 (1984).
34. C. Overton and J. A. Connor, Polyhedron, 1, 53 (1982).
35. S. Kohlman, S. Ernst and W. Kaim, Angew. Chem. Internat., Edn., 24, 684 (1985).
36. A. J. Lees, J. M. Fobare and E. F. Mattimore, Inorg. Chem., 23, 2709 (1984).
37. J. F. Skinner, E. L. Cussler and R. M. Fuoss, J. Phys. Chem., 72, 1057 (1968).
38. V. L. Goedken, J. Chem. Soc. Chem. Commun., 207 (1972).
39. B. C. Lane, J. E. Lestar and F. Basolo, J. Chem. Soc. A, 1618 (1971).
40. L. H. Staal, A. Terpstra and D. J. Stufkens, Inorg. Chim. Acta, 34, 97 (1979).
41. D. M. Adams, J. Chem. Soc., A, 87 (1969)
42. J. Chatt and H. R. Watson, J. Chem. Soc., 4980 (1961).
43. T. A. Magee, C. N. Matthews, T. S. Wang and J. H. Wotiz, J. Amer. Chem. Soc., 83, 8200 (1961).
44. W. Strohmeyer and F. Mulles, Chem. Ber., 100, 2812 (1967).
45. E. W. Abel, M. A. Bennett and G. Wilkinson, J. Chem. Soc., 2323 (1959).
46. L. E. Orgel, Inorg. Chem., 1, 25 (1962).
47. F. A. Cotton and C. S. Kraihanzel, J. Amer. Chem. Soc., 84, 4432 (1962).
48. J. A. Connor and C. Overton, J. Organomet. Chem., 282, 349 (1985)

49. C. N. Banwell,"Fundamentals of Molecular Specroscopy", McGraw-Hill, 2nd., 1972, p 277

50. L. F. Farnell, E. W. Randall and E. Rosenberg, Chem. Commun., 1078 (1971).

51. O. A. Gansow, B. Y. Kimura, G. R. Dobson and R. A. Brown, J. Amer. Chem. Soc., 93, 5922 (1971).

52. O. A. Gansow, D. A. Schexnayder and B. Y. Kimura, J. Amer. Chem. Soc., 94, 3406 (1972).

53. P. S. Braterman, D. W. Milne, E. W. Randal and E. Rosenberg, J. Chem. Soc., Dalton Trans., 1027 (1973).

54. A. F. Masters, R. T. C. Brownlee, M. J. O'Connor, A. G. Wedd and J. D. Cotton, J. Org. Chem., 195, C17 (1980).

55. E. C. Alyea, R. E. Lenkinski and S. Somogyvari, Polyhedron, 1, 130 (1982).

56. E. C. Alyea and A. Somogyvari, Inorg. Chim. Acta, 83, L49 (1984).

57. J. W. Faller and B. C. Whitmore, Organomet., 5, 752 (1986).

58. G. T. Andrews, I. J. Colquhoun, W. J. McFarlane, J. Chem. Soc., Dalton Trans., 2353 (1982).

59. J. T. Bailey, R. J. Clark, G. C. Levy, Inorg. Chem., 21, 2085 (1982).

60. A. M. Bond, S. W. Carr and R. Colton, Organomet., L49 (1984).

61. S. F. Gheller, M. Sidney, A. F. Masters, R. T. C. Brownlee, M. J. O'Connor and A. Wedd, Aust. J. Chem., 37, 1825 (1984).

CHAPTER 4

Solubilities and Transfer Chemical Potentials of Tetracarbonyldiiminemolybdenum(0) Complexes in Pure and Mixed-Solvents

4-1. Introduction

Information about the solvation of molybdenum(0) diimine complexes is very scarce. The only known work on this type of complexes has been reported on $Mo(CO)_4(bipy)$[1] and $Mo(CO)_4(btz)$[2], where bipy = 2,2'-bipyridyl and btz = 2,2'-bi(4H-5,6-dihydrothiazine), in conjunction with the analysis of the solvent effect on the reactivity of the complexes into initial state-transition state contributions. The results show that their transfer chemical potentials are, for aprotic solvents, decreased on going from a less to a more polar solvent.

Corresponding information can be obtained from the study of the analogous iron(II) diimine complexes,[3-5] in which most of the work has been carried out in aqueous methanol. The solvation of the complexes depends very much on the charge of the complex and the hydrophobicity of the diimine ligand present. It is understood that the higher the charge of the complex, the less it will tend to solvate in methanol.[6] The latter is rather interesting. For example, the extremely high negative of transfer chemical potential of $Fe(bsb)_3^{2+}$ complex (i.e. the complex is stablized), where bsb is bidentate Schiff base ligand derived from phenyl-2-pyridyl ketone and 3,4-dimethyl aniline, 1, on moving from water to methanol is due to a strong hydrophobic solvation of the ligand (or complex) by methanol.[7] On the other hand, the analogous complex of $Fe(gmi)_3^{2+}$, gmi = 2, only gives a little stabilization in the transfer chemical potential on going from water to methanol[8]. The latter

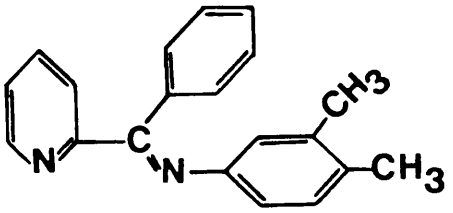

1

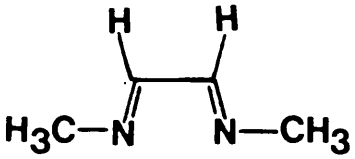

2

observation implies that the ligand gmi is considerably less hydrophobic. Later on, it is suggested that the changes in the hydrophobicity of the ligand are linked with their size.

In the present work, since we shall deal only with neutral complexes, the effect of changes in the ionic or charge character does not arise. The most significant effect is due to the diimine ligands. The solvation of the complexes will be studied in pure solvents and several binary mixtures; water-methanol, methanol-toluene, and toluene-heptane. In all cases, the transfer chemical potentials are determined from solubility measurements. The complexes are derived from $Mo(CO)_4(\widehat{N\ N})$ where $\widehat{N\ N}$ is a diimine ligand. The preparations of these complexes are as detailed in Chapter 2.

4-2. Experimental

The solubilities of the complexes were determined by dissolving the complexes in the corresponding solvents until

saturation. The solutions were placed in a thermostatted water bath at the required temperature for several hours and kept in the dark with frequent shaking. Unfortunately, most of the complexes are slightly unstable in certain solvents, such as dimethylsulphoxide (DMSO), acetonitrile and nitromethane,[1,2] due to solvolysis; the half life is 15-20 hours. In such solvents the solubility determinations were carried out in a shorter period, preferably within an hour. The saturated solutions were centrifuged, then diluted to the required concentration. Then their absorptions were measured, at the wavelength of maximum absorption of the charge tranfer spectrum, in a UV-VIS spectrophotometer (Pye-Unicam S.P.8-100). Finally these values were introduced into Beer-Lambert Equation (Eq 4-1) to calculate their solubilities (S)[9],

$$A = \epsilon l C \qquad \ldots \quad [4\text{-}1]$$

and

$$S = C.d \qquad \ldots \quad [4\text{-}2]$$

where A and C are the absorbance and concentration after dilution d, ϵ is the molar extinction coefficient, and l is the cell length. Prior to this, conformance to the Beer-Lambert Law was checked, and the molar extinction coefficient determined, for each complex.

4-3. Solubilities

The solubilities of the molybdenum(0) tetracarbonyl diimine complexes are relatively small in most of the solvents, though their high ϵ values mean that even dilute solutions exhibit intense colour. The results of our solubility determinations in pure solvents are given in Table [4-1]. These show that the solubilities of the complexes are significantly solvent dependent; in aprotic solvents they increase as the polarity of the solvent increases. However the lower solubilities reported for most of the complexes in methanol relative to its polarity suggest that the complexes also recognize differences between protic and aprotic media, similar to results of the solvent effect on the charge transfer spectra discussed in an earlier chapter. Those changes can be explained by two possible reasons. The first presumably is due to the presence of hydrogen bonding in methanol which leads to a smaller energy of solvation to be used for breaking down the bond between complex molecules. The second is based on the consideration that methanol has a property like-water[10] which is known to less favourably dissolve a neutral compound. Such evidence is consistent with the poor solubility of the present complexes in water ($<10^{-9}$ mol dm^{-3}).

The study of the solubilities of complexes in a binary system offers some basic information on selective solvation of the complexes. More detailed information can be obtained from the transfer chemical potential pattern discussed in the following section. The trends in heptane-toluene and

toluene-methanol show the effect of the medium composition on the solubility of the complex in the mixture of similar (protic-protic) and dissimilar (protic-aprotic) pairs of solvents respectively. It is informative to compare the solubility pattern in methanol-water with those for the iron(II)-diimine complexes which have been widely studied.

Solubilities in toluene-heptane are listed in Table [4-2] and illustrated in Figure [4-1]. These show that the solubilities of the complexes increase as the amount of toluene in the mixture increases. This observation corresponds to the fact that toluene has a better "solvating power" than heptane.[11] In contrast, the solubility trends in toluene-methanol give a maximum at the mixture 70-80% of toluene, Table [4-3]. In methanol-water mixtures, the complex clearly dislikes water; solubilities drop sharply in the presence of water. The solubility determinations listed in Table [4-4] indicate a sharp dropping in water-rich mixtures. In fact, most of them (above 50% water) are too sparingly soluble to be studied by the present method.

Apart from selective solvation, the solubility determination also offers an alternative method to estimate the enthalpy of solution,[12] ΔH_{sol}. This parameter is useful in analysing the ground state-transition state trend of the charge transfer spectra discussed in Chapter 3. A basic determination requires the measurement of solubility at various temperatures. Since the complexes are sparingly soluble in most of the solvents, the activity coefficients are assumed to be one and not to vary with temperature. The solubility determinations listed in Table [4-5] give a

straight line when the logarithm of solubility (ln(S)) is plotted against the reciprocal of temperature (1/T), as shown in Figure [4-2]. The enthalpies of solution are calculated from the slope of the graph according to Equation [4-3],

$$\frac{\delta \ln S}{\delta (1/T)} = \frac{-\Delta H_{sol}}{R} \qquad \ldots \quad [4\text{-}3]$$

where R is the Gas Constant. The results are also given in Table [4-5]. It is found that the enthalpies of solution increase as the polarity of the solvent increases and the size of the diimine ligand decreases. In the former, an extra solvation energy is required for opposing solvent-solvent interactions which increase as the polarity of a solvent increases. In the latter, with decrease in size, the complex molecules are pack more closely in their lattice and consequently increase their lattice energy.

4-4. Transfer Chemical Potentials

The transfer chemical potential, $\delta_m \mu^{\ominus}$, or Gibbs free energy of transfer, $\Delta G_t^{\ominus}$, is defined as the change in chemical potential, $\mu^{\ominus}$, of the particular compound on going from one solvent to another.[13]

$$\delta_m \mu^{\ominus}_{(X)} = \mu^{\ominus}_{1(X)} - \mu^{\ominus}_{2(X)} \qquad \ldots \quad [4\text{-}4]$$

where μ_1^{θ} and μ_2^{θ} are the chemical potentials in solvents 1 and 2 respectively. If $\mu_1^{\theta} > \mu_2^{\theta}$ the compound is stabilized on going from solvent 2 to 1, and vice versa. For an involatile compound, the transfer chemical potential can be obtained from the dependence of the solubility of the pure solid on solvent.[13] In this case the required quantities are given by Equation [4-5], where we have to make the usually reasonable assumption that the ratio of activity coefficients in both solvents is unity.

$$\delta_m\mu^{\theta}_{(X^{n\pm})} = RT \ln \left[\frac{\text{Solubility in Reference solvent}}{\text{Solubility in other solvent}}\right] \quad ..[4\text{-}5]$$

For neutral molecules, transfer chemical potentials can be calculated directly from solubilities, but for ionic species, $X^{n\pm}$, several assumptions have to be applied before the transfer chemical potential of a single ion $X^{n\pm}$, $\delta_m\mu^{\theta}_{(X^{n\pm})}$ can be calculated from the solubilities of its salt. The earliest efforts were based on assumptions that the solvation of the proton, H^+ was zero, and that the solvation of two opposite but equally charged ions of similar size such as K^+ and Cl^- were equal.[14] But recently the fashion has swung another way particularly for non-aqueous systems. Now large organic ions of the R_4N^+ and R_4B^- types are used as reference ions and it is assumed that the solvation parameters for one cation and one anion of

these types are both small and equal. Examples of these ions which are commonly used are tetraphenylarsonium and tetraphenylboronate ($Ph_4As^+ = Ph_4B^-$).[15] The assumption of equivalent solvation changes of ferrocene and ferrocinium is very similar.[16] Since our dealings involve only neutral compounds, the problem of single ions is avoided and transfer chemical potentials are directly calculated. Here they are referenced to those in methanol, or heptane for toluene-heptane mixtures. The results are summarized in the corresponding solubility table.

The transfer chemical potentials of some molybdenum(0) diimine complexes, $Mo(CO)_4(N\widehat{\ }N)$, in several pure organic solvents, as illustrated in Figure [4-3], generally give a parallel trend. The complexes are verywell solvated in dimethylsulphoxide, acetonitrile, and nitromethane but poorly in heptane. They are also poorly solvated in methanol, in fact, the chemical potentials of most of the complexes are lower in toluene than in methanol. Again, the presence of hydrogen bonding in the solvent limits solvation. However preferential solvation in both solvents varies according to the size of the complex. It is found that the biggest diimine ligands tend to increase their stabilization in toluene. Further discussion of the matter will be dealt with later in this section.

Better information about preferential solvation can be obtained from studies in binary solvents. In these systems, it is found that in some cases the complex shows maximum solvation in one of the pure solvents, but in others in their mixtures. Such behaviour is determined by the natures

of the solvents and complex being used. In aqueous methanol mixtures, for example, preferential solvation of all the molybdenum complexes clearly indicates their preference for methanol (Figure [4-4]). Their transfer chemical potentials are markedly positive on going from methanol to water and to all methanol-water mixtures, which reflects the poor solvation of such a neutral compound in water. The solvation of the complexes also varies according to the nature of the diimine ligand. The most significant effect is related to the concept of the hydrophobicity of the ligand. This concept is well established in explaining the solvation trends of the majority of iron(II) diimine complexes. In general, the term hydrophobic is used for a compound which has strong preferential solvation in organic solvent compared with water. Based on this, we can propose that the $Mo(CO)_4$(appi-OH) and $Mo(CO)_4$(bpni), where appi-OH (3) and bpni (4), complexes may be considered as weakly and strongly hydrophobic compounds respectively. The complete series of

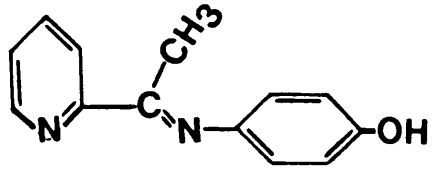

3

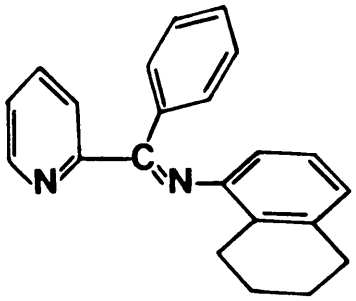

4

the hydrophobicity of the ligands is summarized in Table [4-7]. As for the iron(II) diimine complexes, it is found that the hydrophobicity of the ligand parallels the changes of the size of the ligand; it increases as the size of the ligand increases. Low hydrophobicity of $Mo(CO)_4$(appi-OH) is presumably due to a presence of the hydroxide group which have a potential to form hydrogen bonding to each other.

In methanol-toluene, the transfer chemical potential trend is completely different. The complexes are strongly stabilized in mixtures, 60-80% volume of toluene, rather than in their corresponding pure solvents, and increasingly stabilized on going from methanol to toluene as the size of the diimine ligand increases. Details of the trends are given in Figure [4-5]. The latter observation suggests that the complexes recognize preferential solvation in methanol-toluene similar to that in aqueous methanol. The concept of the hydrophobicity of the ligand still seems to be applicable to explain the solvation pattern in this system. Better preferential solvation of a bigger complex (more hydrophobic) in toluene reflects the behaviour of the solvent as a non-polar organic-solvent whereas methanol is sometimes referred as a water-like solvent (i.e. much stronger intermolecular forces in methanol than in toluene).

So for we have proved that the hydrophobicity of the ligand may be used to explain the pattern of the transfer chemical potentials either in aqueous methanol or methanol-toluene. Solubilities of the complexes in methanol-toluene are higher than in water-methanol. They

dissolve well in the whole range of methanol-toluene (0.1-0.001 mol dm^3). Therefore, it encourages us to carry out the study in this mixture for other complexes. For instance, we reported that the cyclohexane ring (e.g. as in $Mo(CO)_4$(cpi); cpi = 5) provides a somewhat more hydrophobic periphery than the corresponding aromatic phenyl and pyridyl rings. The effect of the substituent group has also been studied. It is found that the transfer chemical potential of the complexes $Mo(CO)_4$(bppi-X), bppi-X (6) with X = OCH_3 or CH_3, on moving from methanol to toluene are decreased more than that of $Mo(CO)_4$(bppi). On the other hand, the transfer chemical potential of $Mo(CO)_4$(appi-OH) complex decreases less on going from methanol to toluene compared to the corresponding transfer chemical potential of the $Mo(CO)_4$(appi) complex. The presence of the former group corresponds to the increase in the size of the ligand whereas the latter is dominated by hydrophilic nature of the hydroxide group.

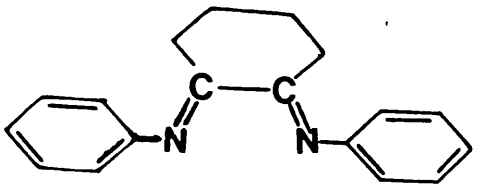

5

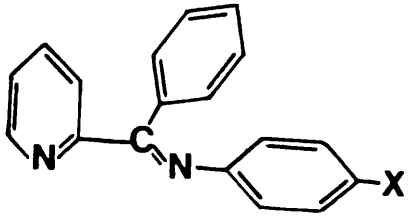

6

The transfer chemical potentials of the complexes in heptane-toluene are shown in Figure [4-6]. The trend indicates a strong stabilization on going from heptane to toluene. Unfortunately, it does not show any significant ligand dependence. Both solvents are similarly aprotic and both have only small intermolecular forces.

TABLE 4-1

Solubilities and transfer chemical potentials, $\delta_m\mu^{\ominus}$, of molybdenum(0) diimine complexes, $Mo(CO)_4(N\widehat{\ }N)$ in organic solvents at 298°K

N^N	*	Heptane	Methanol	Toluene	CH_3CN	CH_3NO_2	DMSO
bppi	S	8.1×10^{-5}	1.05×10^{-2}	7.65×10^{-2}	0.125	0.140	0.180
	TCP	12.03	0.00	-4.91	-6.13	-6.41	-7.03
cppi	S	3.30×10^{-5}	1.08×10^{-2}	2.23×10^{-2}	0.053	0.064	0.081
	TCP	14.33	0.00	-1.80	-3.93	-4.40	-4.95
appi	S	3.72×10^{-5}	9.05×10^{-3}	2.62×10^{-2}	0.055	0.071	0.094
	TCP	13.56	0.00	-2.62	-4.47	-5.10	-5.79
bpmi	S	1.85×10^{-4}	1.52×10^{-2}	0.095	0.112	0.124	0.143
	TCP	11.00	0.00	-4.53	-4.93	-5.19	-5.54
bpami	S	3.70×10^{-5}	3.30×10^{-2}	6.57x10	0.148	0.160	0.20
	TCP	16.80	0.00	-1.86	-3.71	-3.91	-4.46

*
S = solubility /mol dm^3
TCP= Transfer chemical potential $\delta_m\mu^0$/kJ mol^{-1}.

TABLE 4-2

Solubilities and transfer chemical potentials, $\delta_m\mu^{\theta}$, of molybdenum(0) diimine complexes, $Mo(CO)_4(\widehat{N\ N})$, in toluene-heptane mixtures at 298°K

$\widehat{N\ N}$	*	% volume Toluene					
		0	20	40	60	80	100
bppi	S	0.08	0.58	2.59	9.51	26.70	76.50
	TCP	0.00	-4.88	-8.57	-11.78	-14.34	-16.94
cppi	S	0.03	0.20	0.86	3.17	8.73	26.20
	TCP	0.00	-4.40	-8.08	-11.30	-13.80	-16.63
appi	S	0.04	0.28	1.22	3.85	10.30	26.20
	TCP	0.00	-4.97	-8.64	-11.47	-13.91	-16.22
bpami	S	0.04	0.38	1.94	8.13	27.00	65.00
	TCP	0.00	-5.73	-9.79	-13.34	-16.31	-18.48
bpmi	S	0.19	1.02	4.61	15.30	41.70	95.00
	TCP	0.00	-4.22	-7.95	-10.93	-13.40	-15.44
bpbui	S	0.82	5.02	23.40	85.50	220	-
	TCP	0.00	-4.47	-8.28	-11.47	-13.83	-
bppi -4F	S	0.20	1.03	4.64	16.80	36.90	71.50
	TCP	0.00	-4.09	-7.80	-10.09	-12.04	-14.60
bppi -4Cl	S	0.21	1.19	18.50	43.10	43.10	82.50
	TCP	0.00	-4.34	-7.84	-11.11	-13.21	-14.83

continued.

TABLE 4-2

N^N	*	% volume toluene					
		0	20	40	60	80	100
bppi-OCH_3	S	0.05	0.35	2.30	7.46	28.70	78.20
	TCP	0.00	-5.07	-9.74	-12.66	-15.98	-18.40
bppi-3,4Me	S	0.11	0.71	3.72	15.30	44.60	86.70
	TCP	0.00	-4.57	-8.66	-12.66	-14.81	-16.45
bppi-3,4MeCl	S	0.07	0.40	1.91	7.14	19.60	45.10
	TCP	0.00	-4.51	-8.36	-11.62	-14.13	-16.18
bpbei	S	0.07	0.27	1.18	3.93	12.10	30.40
	TCP	0.00	-3.49	-7.12	-10.11	-12.90	-14.75
bppei	S	0.05	0.26	1.03	3.58	9.75	23.50
	TCP	0.00	-3.98	-7.44	-10.52	-13.00	-15.17
bmi	S	0.41	1.96	7.38	18.10	29.20	49.00
	TCP	0.00	-3.89	-7.17	-9.39	-10.57	-11.85
gpi	S	0.17	0.60	1.19	4.74	10.80	21.5
	TCP	0.00	-3.19	-4.89	-8.30	-10.34	-12.04
ppi	S	0.26	1.02	3.79	9.67	22.30	42.30
	TCP	0.00	-3.37	-6.62	-8.94	-11.00	-12.59
bzmi	S	0.28	1.10	3.48	8.86	20.03	38.40
	TCP	0.00	-3.37	-6.22	-8.53	-10.58	-12.16

* S = solubility/ 10^{-3}mol dm^{-3}

TCP = Transfer chemical potential, $\delta_m \mu^{\ominus}$ / kJ mol^{-1}

TABLE 4-3

Solubilities and transfer chemical potentials, $\delta_m\mu^\theta$, of molybdenum(0) diimine complexes, $Mo(CO)_4(N\widehat{\ }N)$ in methanol-toluene mixtures at 298°K

N^N	*	% volume Toluene					
		0	20	40	60	80	100
bppi	S	1.05	2.65	5.71	8.42	1.15	7.65
	TCP	0.00	-2.29	-4.19	-5.12	-5.92	-4.91
cppi	S	1.08	2.20	4.10	5.18	5.11	2.62
	TCP	0.00	-1.76	-3.30	-3.88	-3.8	-2.20
appi	S	0.91	1.98	4.06	5.53	5.74	2.62
	TCP	0.00	-1.94	-3.71	-4.48	-4.5	-3.40
apmi	S	4.69	8.32	11.40	15.00	21.00	8.66
	TCP	0.00	-1.42	-2.20	-2.27	-3.71	-1.52
bpni	S	0.12	0.34	0.86	1.85	2.63	1.62
	TCP	0.00	-2.65	-4.95	-6.64	-7.79	-6.61
bppi -4Cl	S	1.72	5.00	8.90	1.53	1.75	9.31
	TCP	0.00	-2.64	-4.07	-5.41	-5.74	-4.19
appi -4OH	S	5.82	9.14	9.82	1.01	6.02	1.14
	TCP	0.00	-1.11	-1.29	-1.36	-0.10	4.03

continued.

TABLE 4-3

N^N	*	% volume toluene					
		0	20	40	60	80	100
bppi -OCH_3	S	0.81	2.43	6.20	7.37	13.60	7.82
	TCP	0.00	-2.72	-5.03	-5.46	-6.96	-5.64
bppi 3,4Me	S	7.00	1.81	5.10	7.60	11.30	7.96
	TCP	0.00	-2.35	-4.89	-5.91	-6.88	-6.01
bmi	S	7.35	9.38	10.90	12.10	12.20	4.90
	TCP	0.00	-0.60	-0.97	-1.23	-1.24	-1.00
cmi	S	3.89	9.02	16.20	28.70	28.80	17.90
	TCP	0.00	-2.08	-3.53	-4.94	-4.95	-3.98
dab	S	0.05	0.11	0.17	0.24	0.25	0.14
	TCP	0.00	-1.71	-2.92	-3.72	-3.82	-2.43
cpi	S	0.08	0.23	0.49	0.74	0.93	0.61
	TCP	0.00	-2.59	-4.52	-5.53	-6.11	-5.06

*

S = solubility / 10^2 mol dm^{-3}

TCP = Transfer chemical potential, $\delta_m \mu^{\ominus}$ / kJ mol^{-1}

TABLE 4-4

Solubilities and Transfer chemical potentials, $\delta_m\mu^{\ominus}$ of molybdenum(0) diimine complexes, $Mo(CO)_4(N\widehat{\ }N)$ in methanol-water mixtures at 298°K

N^N	*	% volume water							
		0	10	20	30	40	50	60	80
bppi	S	1.04×10^{-2}	2.50×10^{-3}	7.15×10^{-4}	1.67×10^{-4}	3.89×10^{-5}	1.41×10^{-5}	-	-
	TCP	0.00	3.53	6.73	10.23	13.83	16.51	-	-
appi	S	8.95×10^{-3}	2.96×10^{-3}	9.81×10^{-4}	2.84×10^{-4}	6.76×10^{-5}	2.51×10^{-5}	-	-
	TCP	0.00	2.67	5.41	9.47	12.02	14.53	-	-
apmi	S	5.21×10^{-2}	1.97×10^{-2}	8.15×10^{-3}	2.79×10^{-3}	8.10×10^{-4}	2.11×10^{-4}	8.58×10^{-5}	2.61×10^{-5}
	TCP	0.00	2.41	4.59	7.24	10.30	13.63	15.88	18.80
cppi	S	1.05×10^{-2}	3.61×10^{-3}	1.11×10^{-3}	2.38×10^{-4}	8.45×10^{-5}	3.93×10^{-5}	1.35×10^{-5}	-
	TCP	0.00	2.63	5.55	9.36	11.92	13.82	16.55	-
bpni	S	1.17×10^{-3}	1.64×10^{-4}	3.52×10^{-5}	7.13×10^{-6}	-	-	-	-
	TCP	0.00	4.86	8.67	12.61	-	-	-	-
bppi-$4OCH_3$	S	8.09×10^{-3}	2.14×10^{-3}	6.14×10^{-4}	1.49×10^{-4}	3.21×10^{-5}	-	-	-
	TCP	0.00	3.29	6.38	9.89	13.68	-	-	-
appi-$4CH_3$	S	1.38×10^{-3}	3.48×10^{-3}	8.90×10^{-4}	1.71×10^{-4}	2.90×10^{-5}	-	-	-
	TCP	0.00	3.41	6.78	10.86	15.25	-	-	-

continued

TABLE 4-4

$\widehat{N\ N}$	*	% volume water							
		0	10	20	30	40	50	60	80
bppi-4Cl	S	1.26×10^{-2}	2.46×10^{-3}	5.83×10^{-4}	1.36×10^{-4}	3.61×10^{-5}	-	-	-
	TCP	0.00	4.02	7.60	11.22	14.48	-	-	-
appi-4OH	S	5.82×10^{-2}	4.49×10^{-2}	2.25×10^{-2}	8.51×10^{-3}	3.43×10^{-3}	1.12×10^{-3}	3.47×10^{-4}	1.59×10^{-4}
	TCP	0.00	0.64	2.35	4.75	7.0	9.77	9.77	14.59
bppi-3,4Me	S	6.99×10^{-3}	1.66×10^{-3}	4.26×10^{-4}	6.65×10^{-5}	1.02×10^{-5}	-	-	-
	TCP	0.00	3.55	6.92	11.51	16.51	-	-	-
bppi-3,4MeCl	S	6.48×10^{-3}	1.33×10^{-3}	3.13×10^{-4}	5.64×10^{-5}	8.62×10^{-6}	-	-	-
	TCP	0.00	3.91	7.50	11.74	16.37	-	-	-
bmi	S	7.35×10^{-2}	2.78×10^{-2}	1.23×10^{-2}	4.18×10^{-3}	1.22×10^{-3}	-	1.32×10^{-4}	5.21×10^{-5}
	TCP	0.00	2.42	4.38	7.04	10.09	-	15.69	18.00
ppi	S	8.51×10^{-3}	2.21×10^{-3}	4.86×10^{-4}	1.31×10^{-4}	2.74×10^{-5}	1.31×10^{-5}	6.95×10^{-6}	-
	TCP	0.00	3.45	7.08	10.32	14.00	16.01	17.65	-
dab	S	5.51×10^{-4}	9.28×10^{-5}	2.41×10^{-5}	8.47×10^{-6}	-	-	-	-
	TCP	0.00	4.24	7.57	10.20	-	-	-	-
bzmi	S	4.88×10^{-3}	1.08×10^{-3}	2.38×10^{-4}	6.34×10^{-5}	1.65×10^{-5}	-	-	-
	TCP	0.00	3.74	7.47	10.74	14.07	-	-	-

*

S = solubility/mol dm^{-3}

TCP = Transfer chemical potential, $\delta_m \mu^{\ominus}$ / kJ mol^{-1}

TABLE 4-5

Temperature dependence on solubilities and enthalpies of Solution, ΔH_{sol} of $Mo(CO)_4(N\widehat{\ }N)$ complexes in several organic solvents

$N\widehat{\ }N$	Temp /°C	solubilities of $Mo(CO)_4(N\widehat{\ }N)$ in Heptane /10^{-5} M	Methanol /10^{-2} M	Toluene /10^{-2} M	CH_3CN /10^{-1} M	DMSO /10^{-1} M
bpami	25	3.89	3.30			
	30	3.89	3.91			
	35	8.37	4.68			
	40	11.51	5.50			
	ΔH /kJ mol^{-1}	56.10 ±5.0	25.11 ±3.0			
appi	25	3.51	0.90			
	30	5.89	1.04			
	35	7.62	1.20			
	40	10.97	1.34			
	ΔH /kJ mol^{-1}	52.37 ±6.0	20.77 ±3.0			
bppi	20				12.01	
	25	10.56	1.10	8.60	14.25	
	30	13.41	1.31	10.44	19.18	
	35	17.40	1.46	11.49	23.48	
	40	23.12	1.61	13.25	-	
	ΔH /kJ mol^{-1}	45.87 ± 5.0	19.39 ±2.5	18.55 ± 3.0	35.24 ±5.0	
bpni	25	2.84	0.12			
	30	3.41	0.13			
	35	4.40	0.14			
	40	5.02	0.15			
	ΔH /kJ mol^{-1}	33.81 ±4.0	13.22 ±1.5			

continued..

TABLE 4-5

N⌒N	Temp /°C	solubilities of $Mo(CO)_4(N\frown N)$ in Heptane /10^{-5}M	Methanol /10^{-2}M	Toluene /10^{-2}M	CH_3CN /10^{-2}M	DMSO /10^{-2}M
apmi	25	5.78	4.69			
	30	8.36	5.69			
	35	12.00	6.69			
	40	15.29	8.15			
	ΔH /kJ mol^{-1}	55.58 ± 5.0	27.11 ± 3.0			
bmi	20			4.28		
	25	29.92	7.35	5.81		
	30	40.92	9.07	7.85		
	35	51.04	10.20	10.65		
	ΔH /kJ mol^{-1}	41.06 ± 4.0	30.51 ±4.0	45.53 ±5.0		
gpi	20				2.75	
	25	26.57	0.63	3.13	3.32	
	30	33.14	0.756	3.28	4.02	
	35	39.43	0.876	3.39	-	
	ΔH /kJ mol^{-1}	30.08 ± 4.0	25.27 ±3.0	6.02 ±1.0	27.74 ±3.0	
dab	20				0.574	0.90
	25	-	0.043	1.30	0.665	1.04
	30	-	0.048	1.49	0.776	1.26
	35	-	0.054	1.68	-	-
	40	-	0.063	1.93	-	-
	ΔH /kJ mol^{-1}	-	20.57 ±2.0	19.97 ±2.0	22.13 ± 2.0	25.01 ± 3.0

$\Delta H = \Delta H_{sol}$

TABLE 4-6

Hydrophobicity of the Diimine Ligands.

INCREASING HYDROPHOBIC

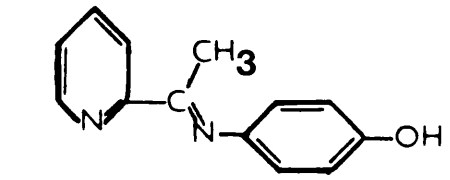

appi-OH

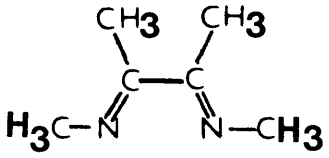

bmi

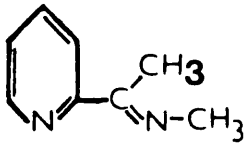

apmi

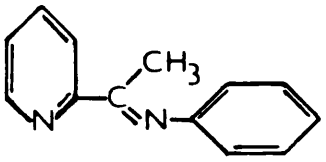

appi

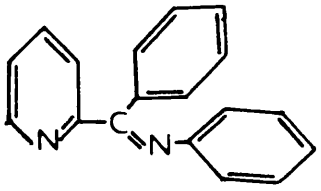

bppi

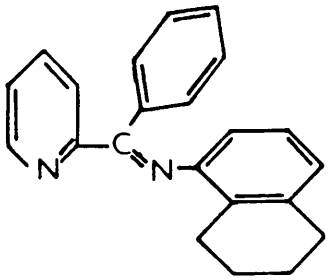

bpni

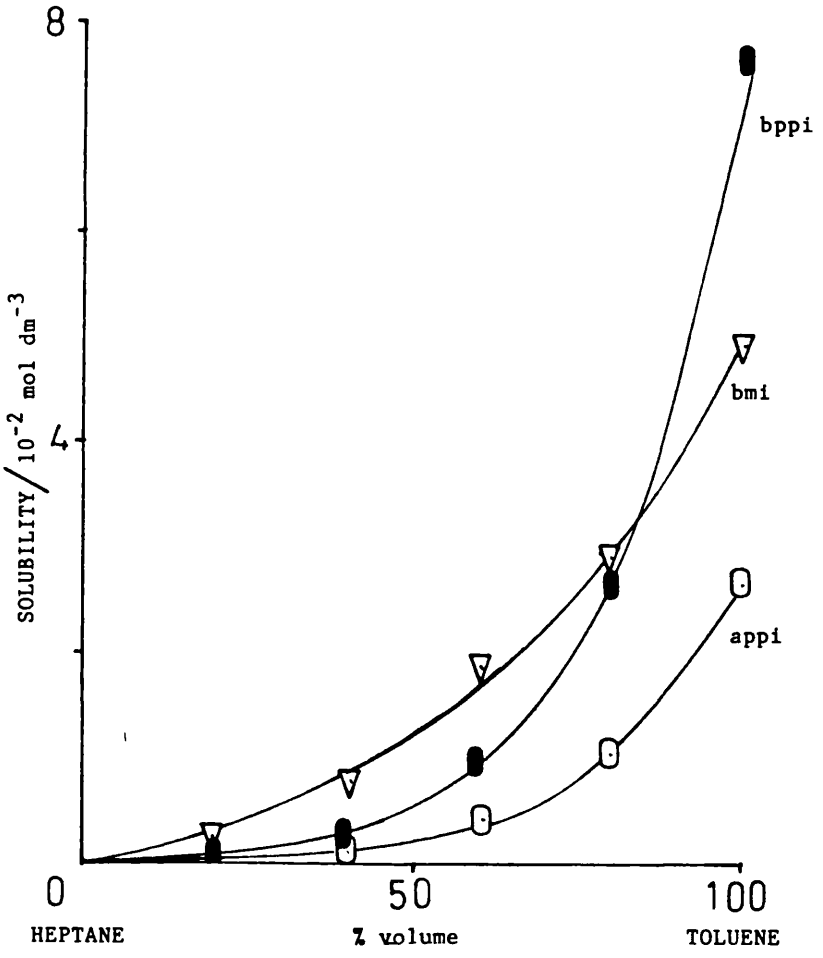

Figure [4-1] Solubilities of $Mo(CO)_4(\hat{N}\hat{N})$ complexes in heptane-toluene mixtures; ● $Mo(CO)_4$(bppi), ▽ $Mo(CO)_4$(bmi) and ○ $Mo(CO)_4$(appi).

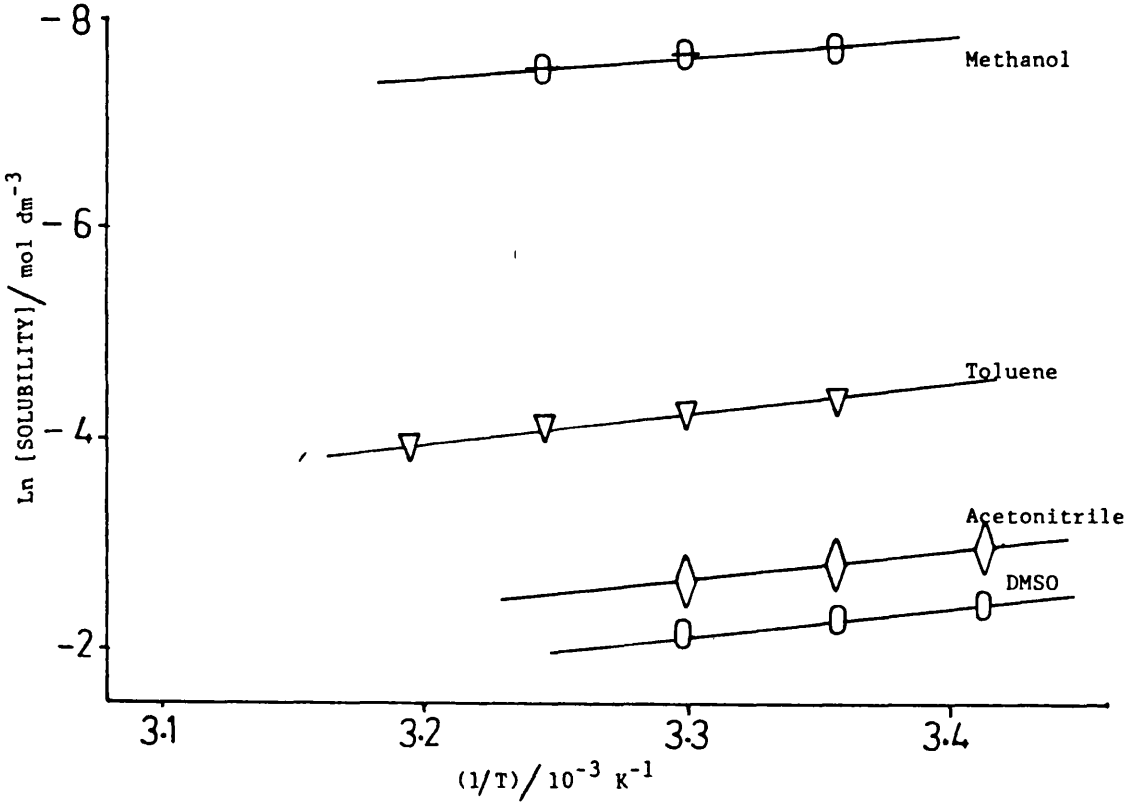

Figure [4-2] Plots of ln[solubility] against 1/T of the $Mo(CO)_4$(dab) in various organic solvents.

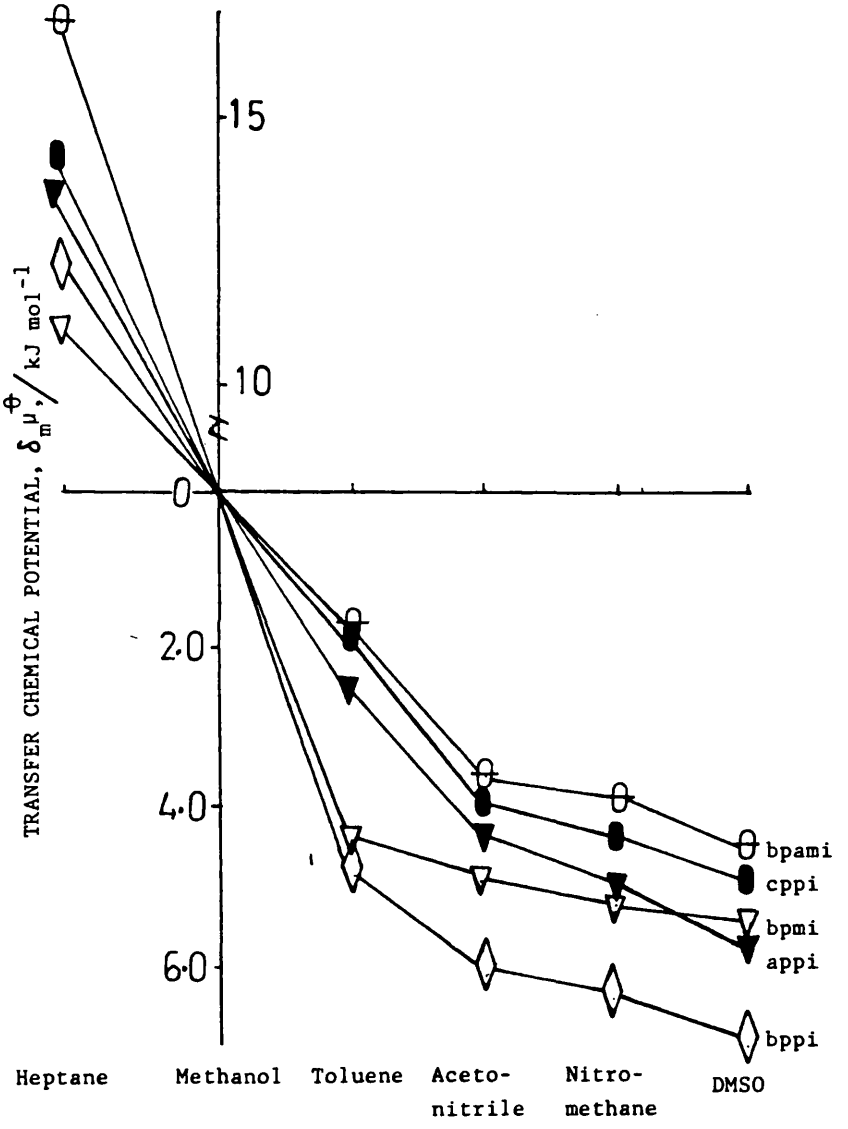

Figure [4-3] Transfer chemical potentials, $\delta_m\mu^{\ominus}$, of $Mo(CO)_4(N\hat{}N)$ complexes in several organic solvents with reference to methanol.

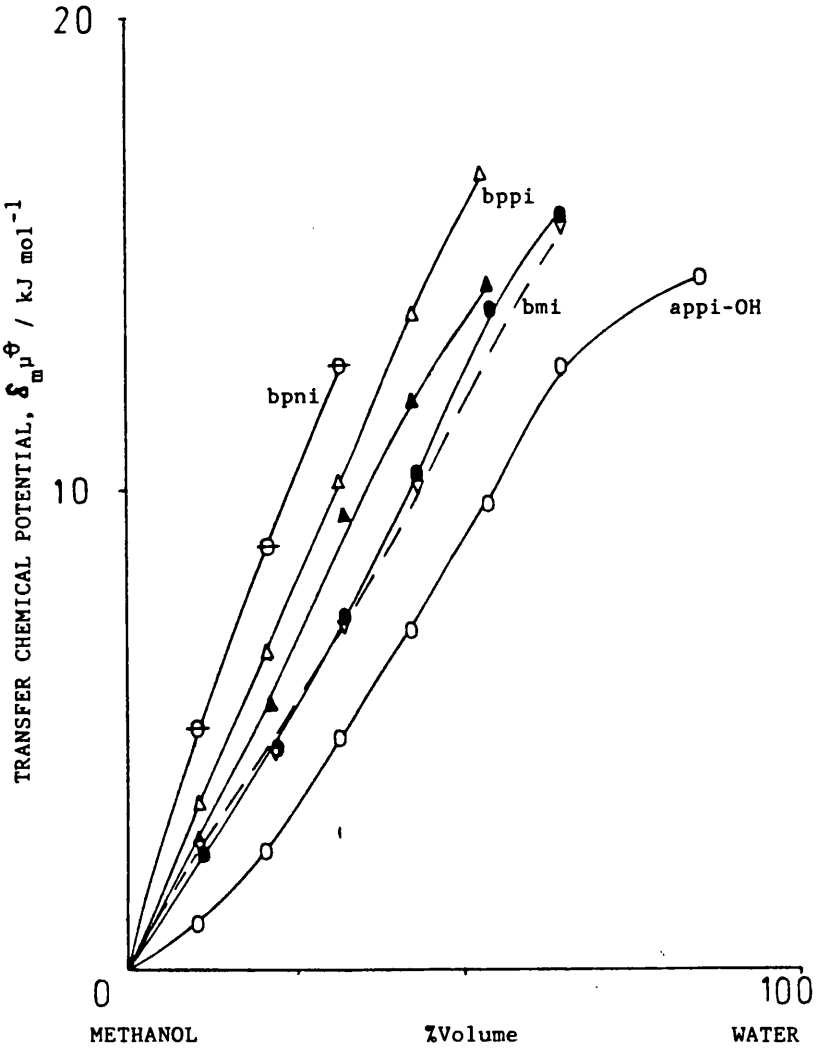

Figure [4-4] Transfer chemical potentials, $\delta_m\mu^\ominus$, of $Mo(CO)_4(N\hat{}N)$ complexes in aqueous methanol (reference to methanol); O $Mo(CO)_4$(appi-OH), ∇ $Mo(CO)_4$(bmi), Δ $Mo(CO)_4$(bppi), ● $Mo(CO)_4$(apmi), ▲ $Mo(CO)_4$(appi), ⊖ $Mo(CO)_4$(bpni).

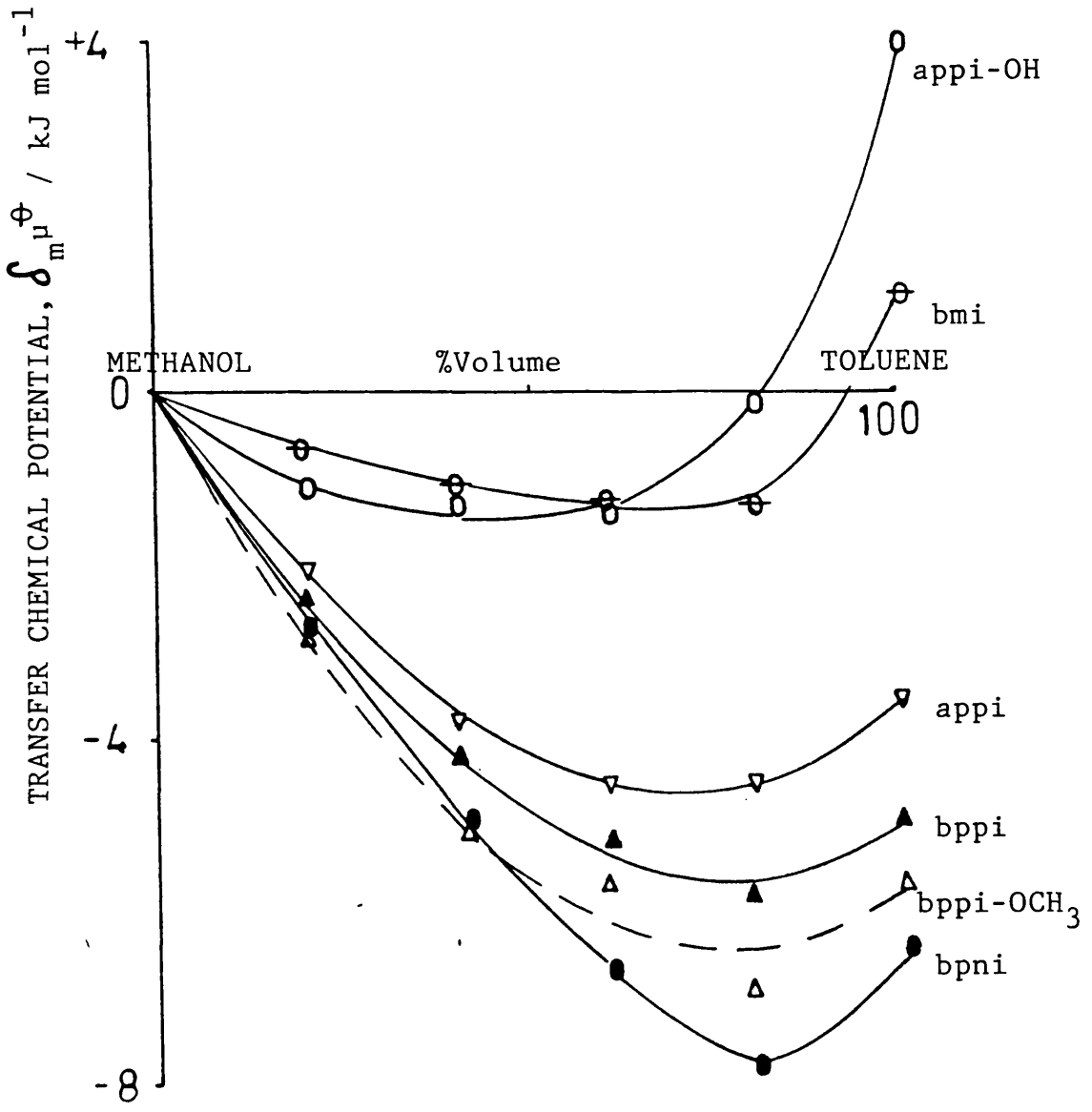

Figure [4-5] Transfer chemical potentials, $\delta_m\mu^\ominus$, of $Mo(CO)_4(N\hat{}N)$ in methanol-toluene mixtures (reference to methanol).

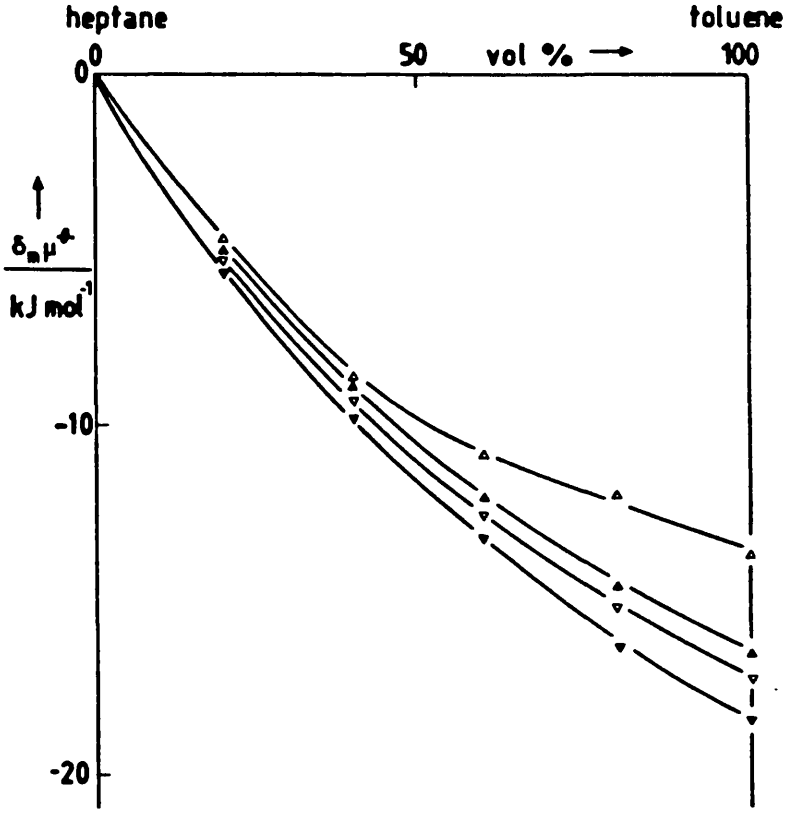

Figure [4-6] Transfer chemical potentials, $\delta_m\mu^\ominus$, of $Mo(CO)_4(N\hat{}N)$ complexes in heptane-toluene mixtures; △ $Mo(CO)_4$(bpbui), ▲ $Mo(CO)_4$(cppi), ▽ $Mo(CO)_4$(bppi), ▼ $Mo(CO)_4$(bppi-OCH_3).

4-5. References

1. M. J. Blandamer, J. Burgess, J. G. Chambers and A. J. Duffield, Transition Met. Chem., 6, 156 (1981).
2. M. J. Blandamer, J. Burgess, J. G. Chambers and T. Digman, Transition Met. Chem., 10, 274 (1985).
3. F. M. van Meter and H. M. Neumann, J. Amer. Chem. Soc., 98, 1382 (1976).
4. M. J. Blandamer, J. Burgess and A. J. Duffield, J. Chem. Soc., Dalton Trans., 1 (1980).
5. E. A. Abu-Garib, M. J. Blandamer, J. Burgess and N. Gosal, Transition. Met. Chem., 9, 306 (1984).
6. P. Krumholz, Structure and Bonding, 9, 139 (1971).
7. J. Burgess and C. D. Hubbard, J. Chem. Soc., Chem. Commun., 1482 (1983).
8. M. J. Blandamer, J. Burgess, B. Clack, P. P. Duce, A. W. Hakin, N. Gosal, S. Radulavic, P. Guardado, F. Sanchez, C. D. Hubbard and E. A. Abu-Garib, J. Chem. Soc., Faraday Trans. I, 82,1471 (1986).
9. H. H. Willard, L. L. Merritt, J. A. Dean and F. A. Settle,"Intrumental Methods of Analysis", 6ed., Van Nostrand, N.Y. 1981, Chaps. 2 and 3.
10. J. J. Lagowski (Edt),"The Chemistry of Non-aqueous Solvent", Academic Press, 1978, Vol: VA, p 9 (1978).
11. J. Burgess, J. Organomet. Chem., 19, 218 (1969).
12. J. Burgess, "Metal Ions In Solution", Ellis Horwood, 1978 Chap. 7.

13. M. J. Blandamer and J. Burgess, Coord. Chem. Rev., 31, 93 (1980).
14. D. R. Rosseinsky, Chem. Rev., 65, 467 (1965).
15. E. Grunwald, G. Baughman and G. Kohnstam, J. Amer. Chem. Soc., 82, 5801 (1960).
16. M. Alfenaar, J. Phys. Chem., 79, 2200 (1975).

CHAPTER 5

Kinetics of Reactions of Tetracarbonyldiiminemolybdenum(0) Complexes with Cyanide

5-1. Introduction

A considerable amount of information is available concerning the kinetics of reactions of the group VI hexacarbonyls, $M(CO)_6$, M = Cr, Mo and W,[1-4] but very much less is known about the kinetics of reactions of their diimine derivatives, $M(CO)_4(N\widehat{\ }N)$, where $N\widehat{\ }N$ is a diimine such as 1,10-phenanthroline or 2,2'-bipyridine. Our interest now is to investigate reactions involving the latter complexes centered on molybdenum(0) compounds, $Mo(CO)_4(N\widehat{\ }N)$, with cyanide. Some information regarding the reaction is available from the earlier studies on analogous compounds with 1,10-phenanthroline, 2,2'-bipyridine[5] and 2,2'-bi(4H-5,6-dihydrothiazine)[6] as diimine ligand. It is established that the complexes reacts with cyanide to give $Mo(CO)_4(CN)_2^{2-}$.[7] Even though the reaction is thought to involve a bimolecular mechanism, the process of substitution is still uncertained. It either occurs at metal atoms, carbonyl carbon or diimine ligand. Many instances are known of nucleophilic attack at the molybdenum atom of the hexacarbonyl;[1-3,8] several instances of attack, particularly by nitrogen nucleophiles such as azide[9], and primary amine[10] and lithium methyl,[11] at carbonyl carbon of the hexacarbonyl. There is also a steadily increasing body of evidence in favour of attack by hydroxide, methoxide or cyanide at diimine ligands coordinated to iron(II) or ruthenium(II)[12-14] and evidence for cyanide attack at coordinated benzene in the $Mo(CO)_3(C_6H_6)^+$ cation.[15] This uncertainty, however, will not interfere with the rate law for the reaction.

In most solvents, the overall rate law is given by Equation [5-1],

$$\frac{-d[Mo(CO)_4(N\widehat{\ }N)]}{dt} = \left[k_1 + k_2[CN^-]\right][Mo(CO)_4(N\ N)] \quad ..[5\text{-}1]$$

where k_1 presumably refers to a solvolysis pathway and k_2 to nucleophilic attack by cyanide. The solvolysis refers to a substitution reaction by solvent mólecules into the complex. The reaction is relatively slow, but it becomes apparent in solvents such as methanol, acetonitrile and dimethylsulphoxide. This observation concurs with the fact that these solvents have the ability to donate electrons.[16] Cyanide attack proceeds much more quickly, which is as expected since cyanide ion is a better attacking group.

In the present work, we shall examine similar reactions of some other molybdenum diimine derivatives as described in Chapter 1. Studies in several solvents have been carried out on at least one selected complex. These results are useful in interpreting solvent sensitivity on the rate of reaction.

Apart from solvent sensitivity, the kinetics of the reaction with cyanide also offer an alternative way to determine the relative order of coordinating ability among these diimine ligands. Since the reactions involved are substitution of diimine ligand in the complex by cyanide ion, therefore, energy is required for breaking the molybdenum-diimine bond. The increasing speed of substitution

reflects a weakening of the bond (i.e. the diimine compound is raken to have less ability to coordinate to the metal atom and vice versa).

Sufficient solubility is important to carry out the kinetic measurements by any method. The poor solubility of these molybdenum complexes in water and of cyanide salts in the vast majority of organic solvents limit the number of measurements that can be carried out in pure solvents. However, the use of tetraethylammonium cyanide provides sufficient cyanide concentration in many solvents. The reactivity of cyanide ion in this salt is found to be equivalent to that observed for other salts such as potassium cyanide etc.

5-2. Experimental

All tetracarbonyldiimine derivatives of molybdenum were prepared from the tetracarbonylbis(piperidine) complex as described in Chapter 2. The solubilities of the complexes were determined from their corresponding saturated solutions using the Pye-Unicam SP 8-100 spectrophotometer as described in Chapter 4. All cyanides used in this work were derived from tetraethylammonium cyanide (Fluka).

Kinetic runs at atmospheric pressure were carried out in 10mm silica cells in the thermostatted cell compartment of the Pye Unicam SP 1800 recording spectrophotometer. In all cases, the concentration of cyanide ion was kept in large excess over that of the molybdenum complex so that first order kinetics were observed. The reactions were monitored by following the

disappearance of the complex. Even though the reaction does not involve interaction between ions, the ionic strength was kept constant by using the chloride salt; tetraethylammonium chloride.

5-3. Solvent Effect

It is established that, apart from the molecule involved, the medium of the reaction also plays an important part in determining the rate of reaction. This observation has also been reported for the reaction of molybdenum complexes with cyanide. In the present study, we shall focus on the reaction of one of the molybdenum(0) family, that is 2-benzoylpyridinediiminetetracarbonylmolybdenum(0), $Mo(CO)_4$(bpami). The diimine ligand is prepared in situ in iso-propanol by the reaction of equivalent amount of 2-benzoylpyridine and concentrated ammonium hydroxide, based on Equation [5-2]. This complex is chosen because its

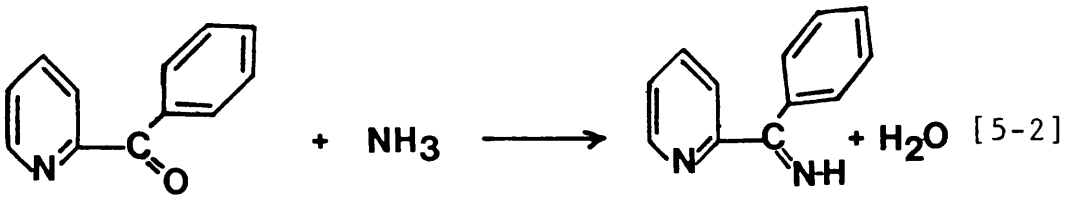

[5-2]

2-benzoylpyridine bpami

reactions with cyanide in the range of solvents studied occur in a reasonable time. Table [5-1] shows rate constants for the reaction of the complex with cyanide ion in various organic solvents. The reaction absolutely satisfies the rate law of Equation [5-1]. This result tells us that the overall reaction of the molybdenum compound with cyanide always occurs by two parallel pathways, namely cyanide attack k_2 and solvolysis k_1. In separate measurements, the first order rate constants obtained by solvolysis were within 10% of the expected value given by extrapolation to $[CN^-] = 0$. An investigation of the reaction at various temperatures, Table [5-2], showed that the $k_2[CN^-]$ term is dominant around room temperature, but at elevated temperatures the k_1 term becomes important. The changes correspond to the higher activation enthalpies reported for the solvolysis pathway. The entropies of activation of the two mechanisms have different signs, negative and positive for cyanide attack and solvolysis respectively. These results strongly support the argument for an associative mechanism for cyanide attack and dissociative for solvolysis. This mechanistic establishment is essential in interpreting the solvent effect on the rate of reaction. The results in Table [5-1] also indicate that the rate constants k_2 and k_1 are markedly solvent dependent. However, the intervention of the solvent in both pathways is rather different. In cyanide attack, the solvent acts as the medium providing the cyanide ion attacking the complex. The rate of reaction is determined by how the cyanide and complex are being solvated. On the other hand, in solvolysis the solvent molecule, apart from being the medium, also acts as the

incoming group. In the following we shall analyse the effect of solvent in both types of reaction separately.

An interpretation of the solvent effect on the rate constant of reaction in solution was given by Ingold.[17] In broad outline, he has shown how the rate constant of different nucleophilic substitution reactions of some organic compounds would change when the solvent is changed. He found that the acceleration or retardation of the reaction is determined by the difference in the stabilization of the starting material and the activated complex by solvation. Later on, several other attempts were made to explain solvent effects on rates of reactions. Most of them have analysed the effect on reactivity into initial state and transition state contributions.[18-27]

The principle of the analysis requires that the essential features of the reaction mechanism are well established, if this is not the case, quite misleading conclusions will be drawn. For example, we consider a reaction involving a single step of the type shown in Equation [5-3] where A and B are reactants and $AB^{\ddagger}$ is the transition state,

$$A + B \longrightarrow AB^{\ddagger} \longrightarrow \text{product} \qquad \ldots \quad [5\text{-}3]$$

The Gibbs activation function, $\Delta G^{\ddagger}$ (Equation [5-4]), at fixed temperature and pressure in a particular solvent is given by Equation [5-5],

$$\Delta G^{\ddagger} = -RT \ln k + RT \ln KT \quad \ldots \quad [5\text{-}4]$$

and

$$\Delta G^{\ddagger} = \mu^{\ddagger} - \mu^{\theta}_{react} \quad \ldots \quad [5\text{-}5]$$

where k is rate constant, K is Boltzmann's constant and h is Planck's constant. $\mu^{\ddagger}$ is the chemical potential of the transition state and μ^{θ}_{react} is the total of the standard chemical potentials of all the reactants contributing to the transition state.

For a first order reaction (e.g. $A \longrightarrow A^{\ddagger} \longrightarrow$ product) where only A contributes to the transition state, then $\Delta G^{\ddagger}$ is given by Equation [5-6].

$$\Delta G^{\ddagger} = \mu^{\ddagger} - \mu^{\theta}_{A} \quad \ldots \quad [5\text{-}6]$$

On the other hand, for second order, where both reactants A and B contribute to the transition state, then $\Delta G^{\ddagger}$ is given by Equation [5-7].

$$\Delta G^{\ddagger} = \mu^{\ddagger} - (\mu^{\theta}_{A} + \mu^{\theta}_{B}) \quad \ldots \quad [5\text{-}7]$$

However, in binary solvent mixtures, even though the dependence of the rate constant on solvent composition X leads to the corresponding dependence of $\Delta G^{\ddagger}$ on X, there is no obvious correlation reported between this dependence and the corresponding solvent dependences of $\mu^{\ddagger}$, μ_A^{θ} and μ_B^{θ}. Thus, the analysis is normally carried out by comparing these parameters in a particular solvent with those in the reference solvent. So the changes in rate constant or kinetic transfer parameter on going from reference solvent to another medium Y, $\delta_m \Delta G^{\ddagger}$, where δ_m is the medium operator, is given by Equation [5-8].

$$\delta_m \Delta G^{\ddagger} = RT \ln \left[\frac{\text{rate constant in reference solvent}}{\text{rate constant in solvent Y}} \right] \quad \ldots [5\text{-}8]$$

Similarly, the difference in transfer chemical potential on going from reference solvent to another solvent will be $\delta_m \mu^{\theta}$. Now the Equations [5-6] and [5-7] can be rewritten using the medium operator in conjunction with the transfer chemical potential:

$$\text{1st order:} \quad \delta_m \Delta G^{\ddagger} = \delta_m \mu^{\ddagger} - \delta_m \mu_A^{\theta} \quad \ldots [5\text{-}9]$$

$$\text{2nd order:} \quad \delta_m \Delta G^{\ddagger} = \delta_m \mu^{\ddagger} - (\delta_m \mu_A^{\theta} + \delta_m \mu_B^{\theta}) \quad \ldots [5\text{-}10]$$

If the rate constant increases on going from the reference

solvent to another, then $\delta_m \Delta G^{\ddagger} < 0$, but if the rate constant decreases, $\delta_m \Delta G^{\ddagger} > 0$. Again, if the solute (i.e initial state or transition state) is stabilized, $\delta_m \mu^{\ominus}$ (or $\delta_m \mu^{\ddagger}$) < 0 and if it is destabilized $\delta_m \mu^{\ominus}$ (or $\delta_m \mu^{\ddagger}$) > 0. An example of such present changes is shown diagramatically in Figure [5-1]. The diagram consists of two parallel chemical potential curves for similar reactions in different solvents (1 and 2).

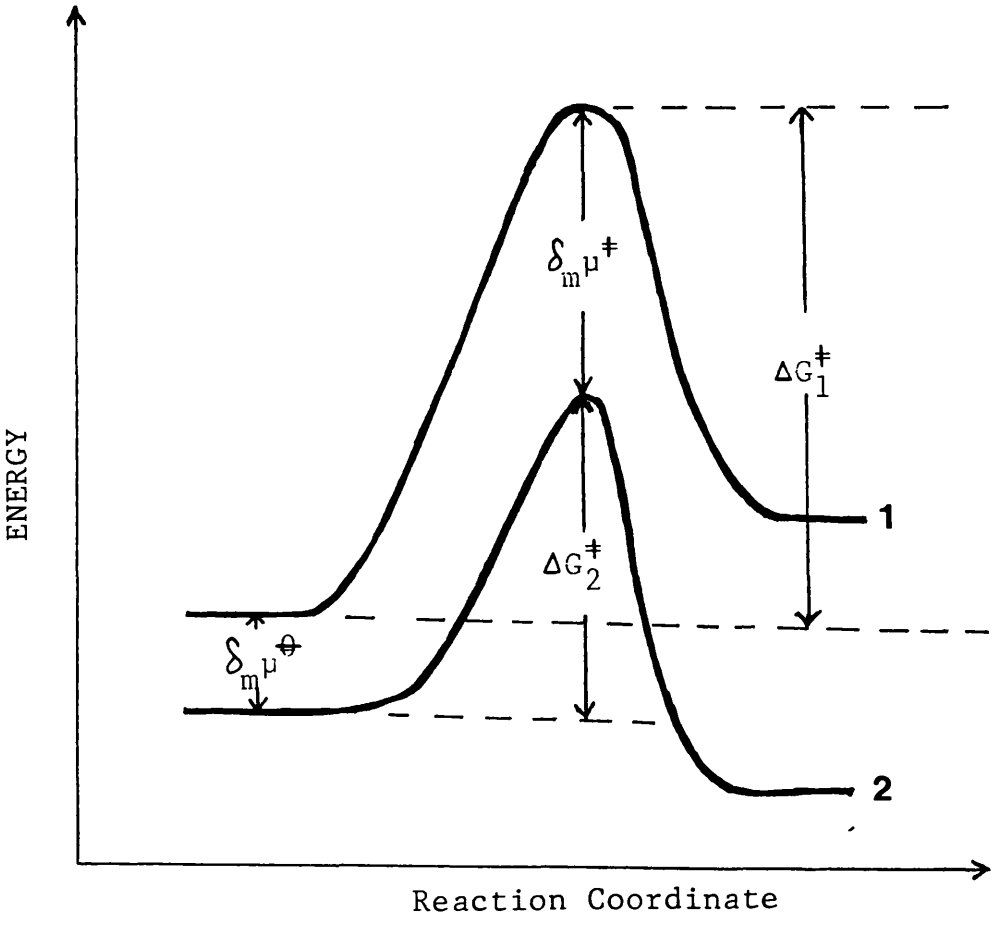

Figure [5-1] Schematic diagram of relations between transfer parameters on moving from solvent 1 to 2.

It becomes apparent that apart from kinetic data, the analysis of solvent effect into initial state-transition state component also requires thermodynamic information. For involatile reactants, (e.g. A in Equation [5-2]), $\delta_m\mu_A^\theta$ can be obtained from the dependence of solubility based on Equation [5-11], as described earlier in Chapter 4.

$$\delta_m\mu_A^\theta = RT \ln \left[\frac{\text{solubility in reference solvent}}{\text{solubility in solvent Y}} \right] \quad ..[5\text{-}11]$$

Table [5-3] displays the dissection of solvent effects on reactivity into initial state-transition state components for cyanide attack and solvolysis of $Mo(CO)_4$(bpami) in a series of non-aqueous solvents. For cyanide attack, the observed solvent effect on rate constant, k_2, is analysed based on a simple second order bimolecular process whereas, for comparison, the solvolysis is analysed as a first order unimolecular process. The solubilities of the compound determined by uv-visible spectroscopy are reported in Table [5-3], from which the transfer chemical potentials $\delta_m\mu^\theta$ are calculated (Equation [5-11]). Values for $\delta_m\mu^\theta_{(CN^-)}$, derived from solubilities of potassium cyanide have been calculated based on the assumption that $Ph_4As^+ = Ph_4B^-$,[28] and are also included in the Table. In all cases, transfer chemical potentials are calculated using methanol as the reference solvent. The analysis of Table [5-3] for cyanide attack is displayed diagramatically in Figure

[5-2]. It shows that the trends in the transfer chemical potentials of cyanide ion and molybdenum compound are in opposite directions. The ionic character of the cyanide ion makes it very much destabilized in organic solvents, but the molybdenum compound is slightly stabilized. Thus the solvation changes and trends will be dominated by cyanide in nucleophilic attack by this ion.

The changes in transfer chemical potentials of initial state-transition state are parallel, with both being destabilized from methanol to organic solvent. This indicates that the coordinated cyanide ion present in the transition state is a major factor in decreasing the interaction with solvent molecule. The cyanide ion dominates over the molybdenum compound in determining the transfer chemical potential of the initial state, resulting in a solvent effect larger on the initial state than on the transition state. The increase in rate constant, k_2, of cyanide attack in organic solvents is presumably caused by a decrease in the electrostriction effect on cyanide ion.[29,30] Thus it increases the potential for cyanide ion attacking the molybdenum compound.

A similar analysis is also reported in water. In the present case, the cyanide ion is highly solvated so that the rate of the reaction would be slower. Unfortunately, the solubility of the molybdenum compound in water is very small and below the required amount for kinetic studies by the present method. This prevents us from monitoring the reaction. However, the situation in water may be different from that in other solvents. Now the transfer chemical potential of the

molybdenum compound is very high and would become an important factor in determining the transfer chemical potential of the initial state and transition state. The expected reactivity in water can be derived from the study in binary aqueous solvents. Examples of such studies are listed in Table [5-4] showing the results of the reaction of cyanide attack on $Mo(CO)_4$(bpami) in aqueous dimethylsulphoxide mixtures. The reactivity pattern as shown in Figure [5-3] again is reported to be similar to those in pure solvents where both states are stabilized in the presence of a small quantities of water. The solvent effect is somewhat larger on the initial state than on the transition state. The situation is changed in water-rich mixtures in which the transfer chemical potential of molybdenum is dominant and is sharply increased (large positive) but that for cyanide is only slightly decreased (small negative). Consequently, the initial state as a whole is destablized. Such behaviour is similar to that reported on trisbipyridineiron(II) complex attacked by cyanide ion in aqueous solvent mixtures where in a water-rich mixture the initial state and transition state are dominated by the iron(II) compound.[31,32] In the present case, the solvent effects on initial state-transition state of cyanide attack are parallel and identical; presumably the increase of electrostriction on the cyanide ion is counterbalanced by a decrease of electrostriction on the molybdenum compound.

The study of solvent effects on reactivity for cyanide attack on $Mo(CO)_4$(bpami) can be extended to non-aqueous solvent mixtures. Unfortunately, we are unable to measure the transfer chemical potential of cyanide in those

mixed-solvents. Therefore, it is not possible to complete the analysis. Nevertheless, the information which is derived from the transfer kinetic parameter, $\delta_m \Delta G^{\ddagger}$, might be useful to support the present discussion. Some of those results are displayed in Table [5-5] and Figure [5-4]. It shows that in all types of co-solvents the kinetic transfer parameters are increased from methanol to another solvent. Since the transfer chemical potential of the molybdenum compound is small, therefore the transfer chemical potential of the initial state is dominated by cyanide ion. For instance, in methanol-acetone and methanol-toluene mixtures, the kinetic transfer parameters are increased sharply in acetone- or toluene-rich mixtures. This observation is presumably related to an extremely large destabilization of cyanide ion in both solvents (acetone and toluene).

The reactivity patterns for cyanide attack are interestingly compared with the corresponding patterns in the solvolysis pathway. The rate constants of this latter process in the vast majority of solvents are related to the rate constants of k_1 in Equation [5-1]. The dissections into initial state-transition state components of solvolysis of $Mo(CO)_4$(bpami) are given in Table [5-3] and displayed diagramatically in Figure [5-5]. The trend is in the opposite direction to that for cyanide attack in which both states are parallel towards stabilization in organic solvents. The solvent effect is somewhat larger in the transition state than in the initial state. The increase in rate constant of solvolysis, k_1, is closely related to the ability of the solvent molecule to coordinate with the complex. Thus, for

example, dimethylsulphoxide and toluene are good and poor coordinating solvents respectively. In the presence of dimethylsulphoxide the rate of solvolysis increases but, on the other hand, it decreases in toluene. A general picture for the present changes is given in Table [5-6] and Figure [5-6] showing that the solvolysis is sharply decreased in toluene-rich mixture.

5-4. Metal-Diimine Bond

It is recognized that the strength of the metal-diimine bond reflects the stability and better coordinating ability of the diimine ligand to form a bond with the metal atom in the complex. Such strength has been estimated from the energy of dissociation or formation of the bond which has been experimentally measured by thermochemical, spectroscopic and kinetic studies.[33] In the present work, we shall examine the relative strengths of the metal-diimine bonds in $Mo(CO)_4$(diimine) complexes based on kinetic measurements involving cyanide attack on the complex. As mentioned earlier, the reaction is known to involve a bimolecular process, thus the rate determining step is given by the slower step of breaking the molybdenum-diimine bond which is balanced by forming molybdenum-cyanide bond. Here, the increasing speed of reaction reflects a weakening of the bond, so such a diimine compound is considered to have poor coordinating ability to the metal atom in the complex.

Table [5-7] shows the rate constants of cyanide attack on several molybdenum(0) tetracarbonyldiimine complexes, which

have been carried out in 80% aqueous dimethylsulphoxide mixture at 25°C. The results lead to a series of increasing coordinating ability of ligand as:

gpi,1 < ppi,2 < bpami,3 < bzmi,4 ≃ dab,5 ≃ bppi,6 < cmi,7 < bmi,8 < bpmi,9 < apmi,10 < bipy

The high stability reported for 2,2'-bipyridine suggests that the aromatic ligand contributes a somewhat better coordinating ability.

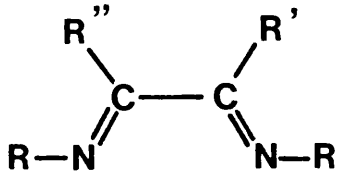

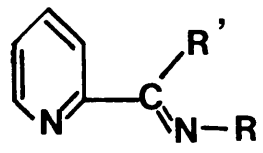

1. R' = R'' = H; R = Ph
2. R' = H; R'' = Me; R = Ph
3. R' = Ph; R = H
4. R' = R'' = Ph; R = Me
5. R' = R'' = Me; R = Ph
6. R' = R = Ph
7. R'—R'' =  ; R = Me
8. R' = R'' = R = Me
9. R' = Ph; R = Me
10. R' = R = Me

In view of the strength of the metal-diimine bond in molybdenum diimine complexes, it is established that the total strength of the bond comes mainly from two conventional σ- and π-bonds. The formation of the σ-bond is due to the ability of the ligand to donate and share its lone pair of electrons with the metal atom. In normal cases, the ligand is also referred to as the nucleophile. The σ-bond strength increases as the ability of the ligand to donate its lone pair of electrons increases. In contrast, the π-bond arises from the back-donation of electrons from the t_{2g}-orbital of the metal to the π^*-orbital of the ligand. A better π-acceptor ligand increases the formation of π-bonding in the complex. Some estimations of π-acceptor ability of ligands have been carried out based on the stretching frequency of carbonyl in such complexes,[34,35] and theoretical calculations of the energies of π^*-orbitals of diimine ligands.[36] A direct estimation can be obtained from the wavelength of maximum absorption in the charge transfer spectruma of the complex. Details of the relation are given in Chapter 3. The plot of rate constant ($\ln k_2$) against wavenumber of maximum absorption of charge transfer is shown in Figure [5-7]. The result indicates that aromatic ligands are somewhat poorer π-acceptors. This completely opposite trend suggests that the σ-bond is the most significant factor in determining the strength of the bond. The most common estimation of σ-donation is obtained from the pK_a of the ligand. However, the present result is sufficient to show that the σ-donation trend is opposite to that of the π-acceptor but identical to the metal-diimine bond strength. Such argument is in a good

agreement with the result reported on phosphine derivatives.[37] The highest stability of $Mo(CO)_4$(bmi) in the aliphatic group corresponds to the presence of four methyl groups in the ligand molecule, which is thus expected to be a good electron donor. On the other hand, the poorest stability of $Mo(CO)_4$(gpi) is related to the weaker donating ability for hydrogen and phenyl groups. A similar argument can also be used to explain the higher stability reported for $Mo(CO)_4$(apmi) and lower for $Mo(CO)_4$(bpami) complexes.

The effects of substituent group X (Cl and CH_3), on the rate constant of cyanide attack on $Mo(CO)_4$(bppi-X) (bppi-X = 11) complexes, have also been studied. The results, as listed in Table [5-7], are almost similar to that of $Mo(CO)_4$(bppi). This observation suggests that the presence of these substituent groups give only a small effect on stabilization of metal-diimine bond. Their wavenumber of maximum absorption of charge transfer spectra are also identical. Thus, it is concluded that such groups of the diimine ligand are considered to have compensating π-acceptor and σ-donor behaviour.

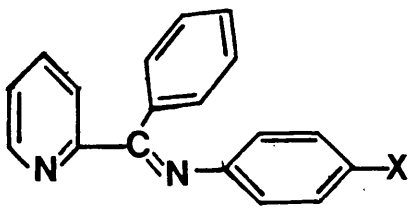

11

TABLE 5-1

The Kinetic of the reaction of $Mo(CO)_4(bpami)$ with cyanide in several organic solvents,

$[Mo(CO)_4(bpami)] = 1x10^{-4}M$

at 298°K

Solvent	$10^5k_{obs}/\ s^{-1}$ with $10^2[CN^-]/M$											10^4k_2	10^5k_1
	0.2	0.3	0.4	0.5	1.0	1.5	2.0	2.5	10.0	15.0	20.0	$/M^{-1}s^{-1}$	$/s^{-1}$
DMSO	-	-	-	8.00	13.71	20.01	26.03	-	-	-	-	120.80	1.84
CH_3CN	-	-	-	7.51	13.32	19.18	24.91	-	-	-	-	116.20	1.72
DMF	-	-	-	5.82	9.98	13.96	18.02	-	-	-	-	81.20	1.80
CH_3NO_2	-	-	-	3.51	5.01	7.14	8.63	-	-	-	-	35.00	1.70
Ethanol	-	-	-	0.32	0.41	0.49	-	-	-	-	-	1.70	0.23
i-propanol	-	-	-	0.35	-	0.74	-	1.12	-	-	-	3.85	0.16
n-butanol	-	-	-	0.50	-	0.92	-	1.35	-	-	-	4.25	0.17
Acetone	8.61	12.26	16.67	-	-	-	-	-	-	-	-	403.00	0.52
Methanol	-	-	-	-	-	-	-		1.81	2.58	3.41	1.60	0.25

TABLE 5-2

Temperature dependence of rate constant of $Mo(CO)_4$(bpami) with cyanide in several organic solvents at 298°K

Temp /°C	Methanol					DMSO				Acetonitrile				
	$10^5 k_{obs}$ with [CN]			$10^4 k_2$	$10^5 k_1$	$10^4 k_{obs}$ with [CN]			$10^4 k_2$	$10^5 k_1$	$10^5 k_{obs}$ with [CN]			$10^4 k_2$	$10^5 k_1$
	0.10	0.15	0.20	$/M^{-1}s^{-1}$	$/s^{-1}$	0.01	0.015	0.020	$/M^{-1}s^{-1}$	$/s^{-1}$	0.010	0.015	0.02	$/M^{-1}s^{-1}$	$/s^{-1}$
25	1.81	2.58	3.41	1.61	0.25	13.71	20.01	26.03	120.80	1.84	13.32	19.18	24.91	116.2	1.72
35	5.57	7.85	10.08	4.51	1.07	32.57	44.12	56.54	309.70	8.46	34.42	43.96	51.05	266.3	7.55
45	18.12	22.84	28.31	10.19	5.28	81.10	117.1	157.15	767.5	32.10	86.10	120.39	165.66	591.4	28.60
$\Delta H^{\ddagger}$ /kJ mol^{-1}				72.9 ±8	123.4 ±10				72.7 ±6	112.8 ±10				66.5 ±5	110.7 ±10
$\Delta S^{\ddagger}$ /J $K^{-1}mol^{-1}$				-80.4 ±10	53.9 ±5				-45.3 ±5	35.6 ±5				-74.7 ±7	27.9 ±3

TABLE 5-3

Solvent effect on reactivity trend of cyanide attack and solvolysis on $Mo(CO)_4$(bpami) in several organic solvents

solvent	cyanide attack							solvolysis			
	$10^4 k_2$	$\delta_m \Delta G^{\ddagger}$	$10^2 S$	$\delta_m \mu^{\theta}_{Mo}$	$\delta_m \mu^{\theta}_{CN}$	$\delta_m \mu^{\theta}_{is}$	$\delta_m \mu^{\theta}_{es}$	$10^5 k_1$	$_m\Delta G^{\ddagger}$	$\delta_m \mu^{\theta}_{is}$	$\delta_m \mu^{\theta}_{es}$
Methanol	1.60	0.00	3.30	0.00	0.00	0.00	0.00	0.25	0.00	0.00	0.00
Ethanol	1.66	-0.10	2.35	0.90	-1.40	-0.50	-0.60	0.23	0.21	0.90	1.11
DMSO	120.80	-10.69	20.11	-4.46	26.70	22.26	11.57	1.84	-4.94	-4.46	-9.40
CH_3CN	116.20	-10.60	14.80	-3.71	26.30	22.59	11.99	1.72	-4.77	-3.71	-8.48
DMF	81.20	-9.71	16.00	-3.91	27.50	23.59	13.88	1.80	-4.88	-3.91	-8.79
Acetone	403.00	-13.67	10.50	-2.86	39.40	36.54	22.87	0.52	-1.81	-2.86	-4.67

$\Delta G^{\ddagger}$ of cyanide attack and solvolysis in methanol are 101.40 kJ mol^{-1} and 116.6 kJ mol^{-1} respectively.

S = solubility (mol dm^{-3}); $\delta_m \Delta G^{\ddagger}$ (kJ mol^{-1}); $\delta_m \mu^{\theta}$ (kJ mol^{-1}); k_2 ($M^{-1} sec^{-1}$); k_1 (sec^{-1}).

TABLE 5-4

Solvent effect on reactivity trend of cyanide attack on $Mo(CO)_4$(bpami) complex in aqueous DMSO at 298°K

Solvent %DMSO(V)	$10^3 k$ /$M^{-1}s^{-1}$	$\delta_m \Delta G^{\neq}$ /kJ mol^{-1}	$10^2 S$	$\delta_m \mu^{\ominus}_{Mo}$ /kJ mol^{-1}	$\delta_m \mu^{\ominus}_{CN}$ * /kJ mol^{-1}	$\delta_m \mu^{\ominus}_{is}$ /kJ mol^{-1}	$\delta_m \mu^{\ominus}_{es}$ /kJ mol^{-1}
100	12.08	0.00	20.11	0.00	0.00	0.00	0.00
95	6.29	1.61	-	-	-	-	-
90	4.15	2.64	5.93	3.02	-9.80	-6.78	-4.14
80	2.50	3.90	1.51	6.40	-15.20	-8.80	-4.90
70	2.02	4.42	0.12	12.67	-19.90	-7.23	-2.81
60	2.07	4.36	0.003	21.79	-25.00	-3.21	1.15
0	-	-	-	-	-35.30	-	-

* reference (28)

S = solubility (mol dm^{-3}) of molybdenum complex

TABLE 5-5

The reactivity trend of cyanide attack on $Mo(CO)_4$(bpami) in non-aqueous binary mixtures (methanol mixture) at 298°K

Solvent	DMSO		Acetone		Iso-propanol		Toluene	
$\%CH_3OH$ (Vol)	10^4k_2 /$M^{-1}s^{-1}$	$\delta_m\Delta G^{\ddagger}$ /kJ mol^{-1}	10^4k_2 /$M^{-1}s^{-1}$	$\delta_m\Delta G^{\ddagger}$ /kJ mol^{-1}	10^4k_2 /$M^{-1}s^{-1}$	$\delta_m\Delta G^{\ddagger}$ /kJ mol^{-1}	10^4k_2 /$M^{-1}s^{-1}$	$\delta_m\Delta G^{\ddagger}$ kJ mol^{-1}
0	120.80	-10.69	403.00	-13.68	3.85	-2.17	-	-
10	47.10	-8.37	12.40	-5.07	-	-	23.20	-6.61
20	18.30	-6.03	4.55	-2.59	-	-	5.20	-2.92
40	9.15	-4.31	2.03	-0.60	2.23	-0.82	2.08	-0.65
60	4.07	-2.31	1.57	0.05	-	-	1.62	-0.03
80	2.36	- 0.95	1.50	0.13	1.54	0.10	1.39	0.35
100	1.60	0.00	1.60	0.00	1.60	0.00	1.60	0.00

TABLE 5-6

The reactivity trend of solvolysis process of $Mo(CO)_4$(bpami) in non-aqueous binary mixtures (methanol mixture) at 298 °K

Solvent	DMSO		Acetone		Iso-propanol		Toluene	
%CH_3OH (Vol)	$10^5 k_1$ /$M^{-1}s^{-1}$	$\delta_m \Delta G^{\ddagger}$ /kJ mol^{-1}	$10^5 k_1$ /$M^{-1}s^{-1}$	$\delta_m \Delta G^{\ddagger}$ /kJ mol^{-1}	$10^5 k_1$ /$M^{-1}s^{-1}$	$\delta_m \Delta G^{\ddagger}$ /kJ mol^{-1}	$10^5 k_1$ /$M^{-1}s^{-1}$	$\delta_m \Delta G^{\ddagger}$ kJ mol^{-1}
0	1.84	4.94	0.52	1.80	0.16	1.11	-	-
10	1.35	4.17	0.62	2.25	-	-	-	-
20	1.25	3.98	0.54	1.90	-	-	-	-
40	1.25	3.98	0.35	0.83	0.20	0.55	0.07	-3.15
60	0.76	2.75	0.24	-0.10	-	-	0.18	-0.03
80	0.54	1.90	0.26	0.10	0.10	0.10	0.36	0.90
100	0.25	0.00	0.25	0.00	0.25	0.00	0.25	0.00

TABLE 5-7

Rate constant of cyanide attack on $Mo(CO)_4(\hat{N}N)$ in 80% aqueous-DMSO at 298°K with their respective wavenumber of charge transfer spectra in DMSO

$\hat{N}N$	$10^4 k_2$ /$M^{-1}s^{-1}$	$10^{-3}\nu_{max}$ /cm^{-1}
gpi	26800.00	17.82
ppi	5210.00	18.65
cpi	342.00	19.15
dab	8.10	19.84
bzmi	10.40	19.82
cmi	4.15	21.05
bmi	3.15	21.74
bipy	0.51	22.78
apmi	0.73	22.15
bpmi	1.21	21.10
bpami	2.50	20.10
bppi	9.94	20.05
bppi-4F	11.91	19.85
bppi-3Me	9.65	19.96
bppi-4Me	8.65	19.92
bppi-3,4-Me	7.15	20.20

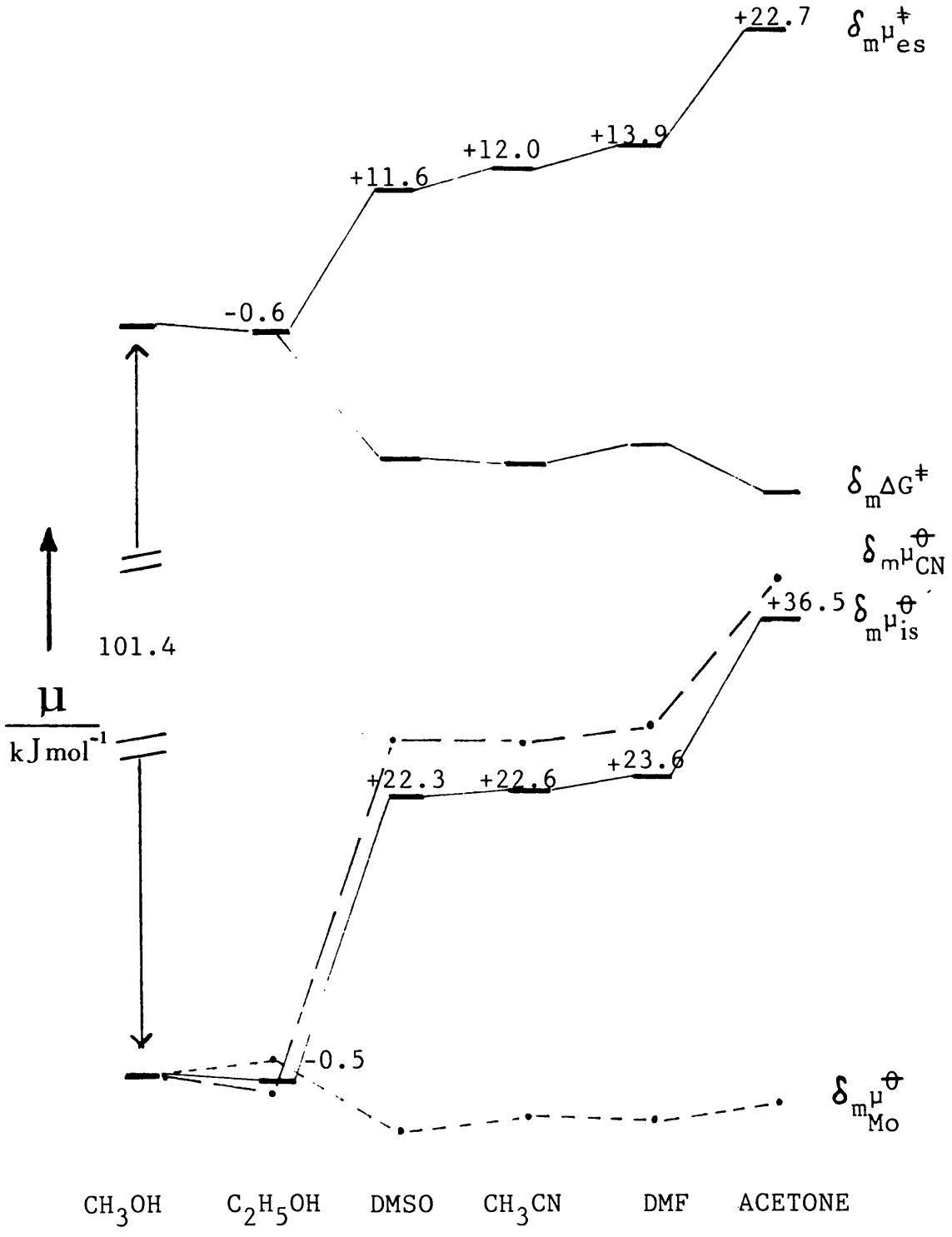

Figure [5-2] Initial state-transition state analysis of solvent effect on the reactivity of cyanide attack on $Mo(CO)_4$(bpami) in pure solvents relative to that in methanol.

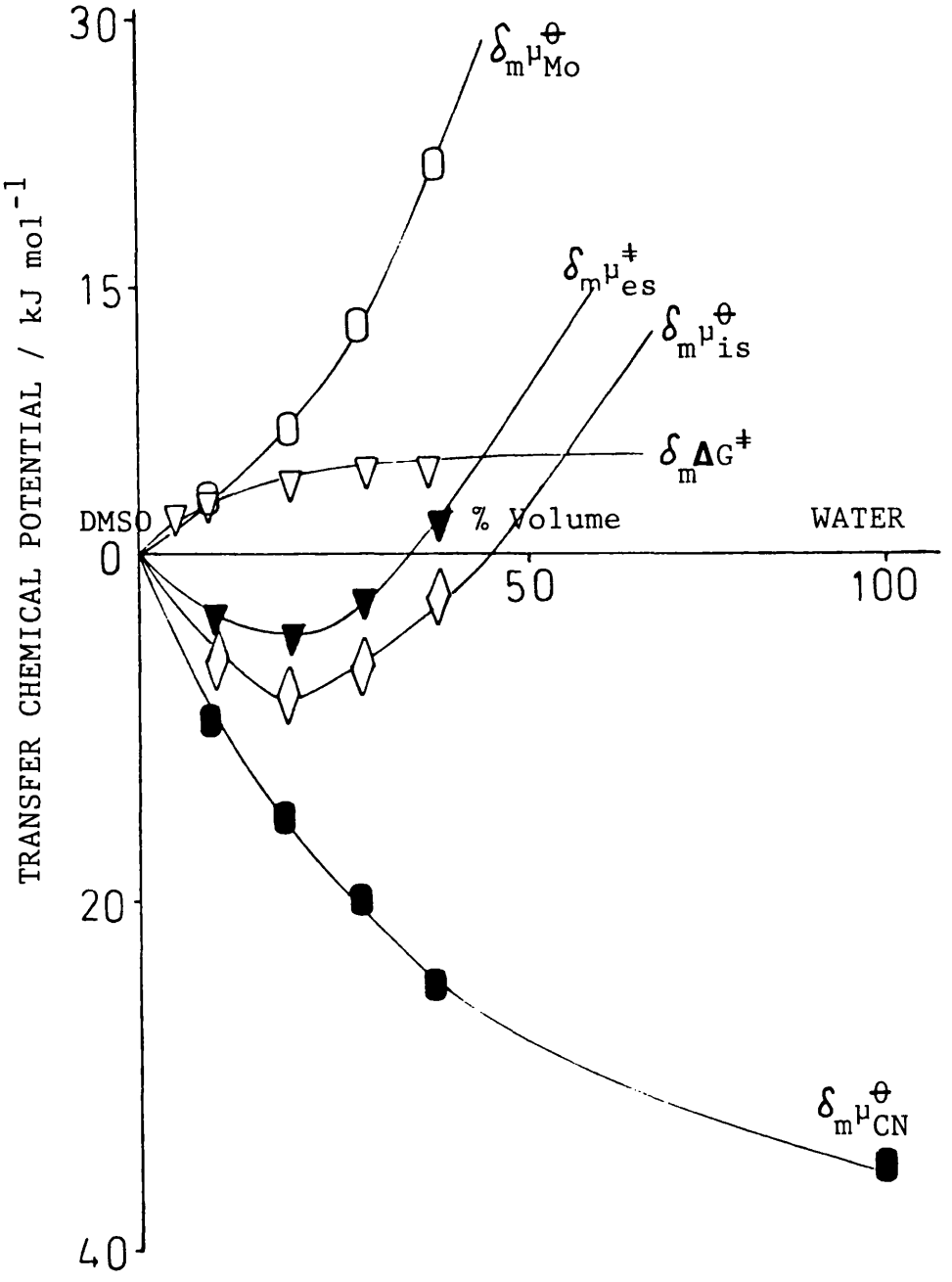

Figure [5-3] Initial state-transition state analysis of solvent effect on cyanide attack on $Mo(CO)_4$(bpami) in water-DMSO mixtures.

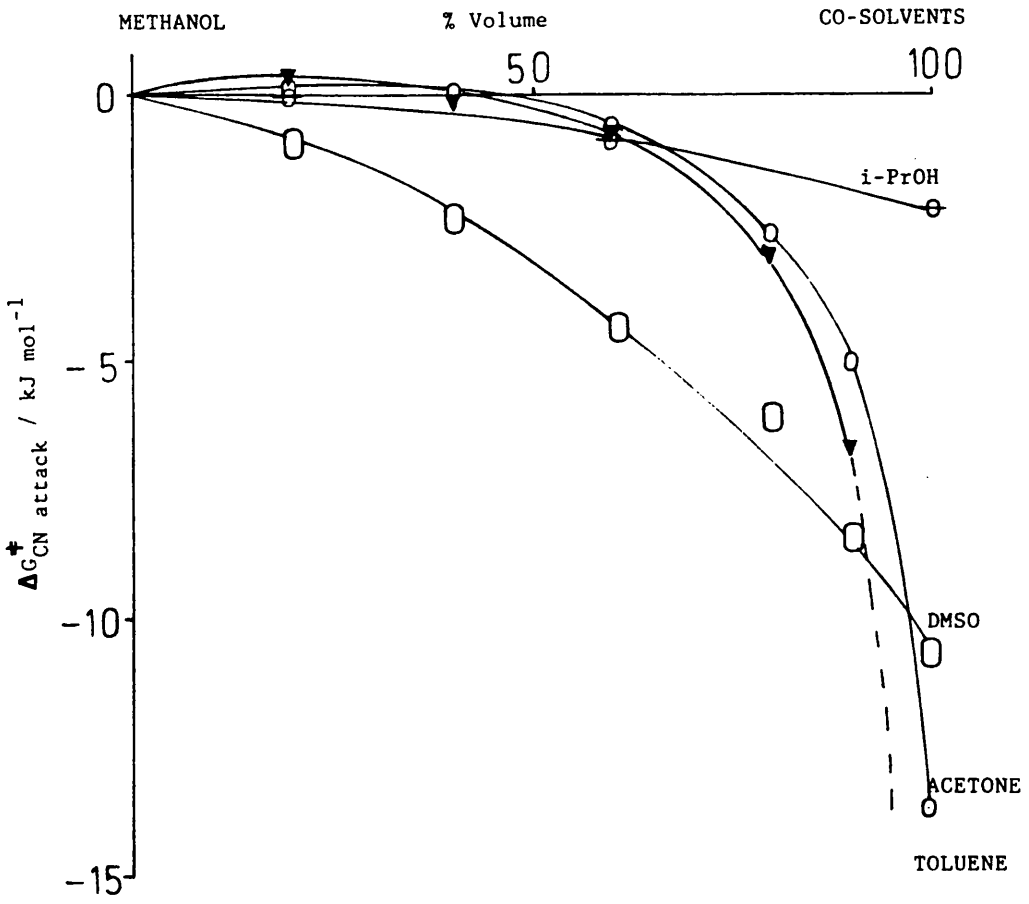

Figure [5-4] The solvent effect pattern on reactivities of cyanide attack on $Mo(CO)_4$(bpami) in non-aqueous mixtures.

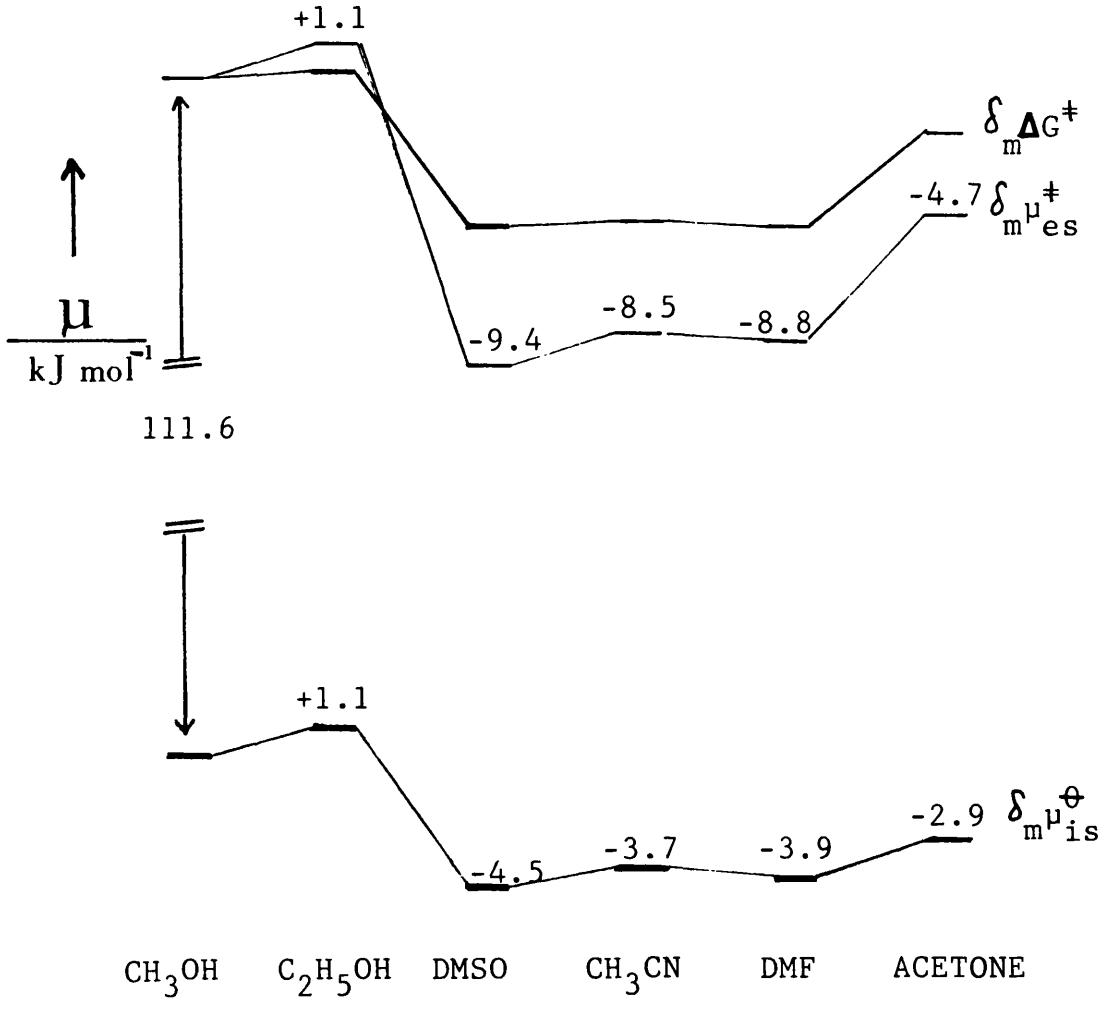

Figure [5-5] Initial state-transition state analysis of solvent effect on solvolysis of $Mo(CO)_4$(bpami) in several organic solvents.

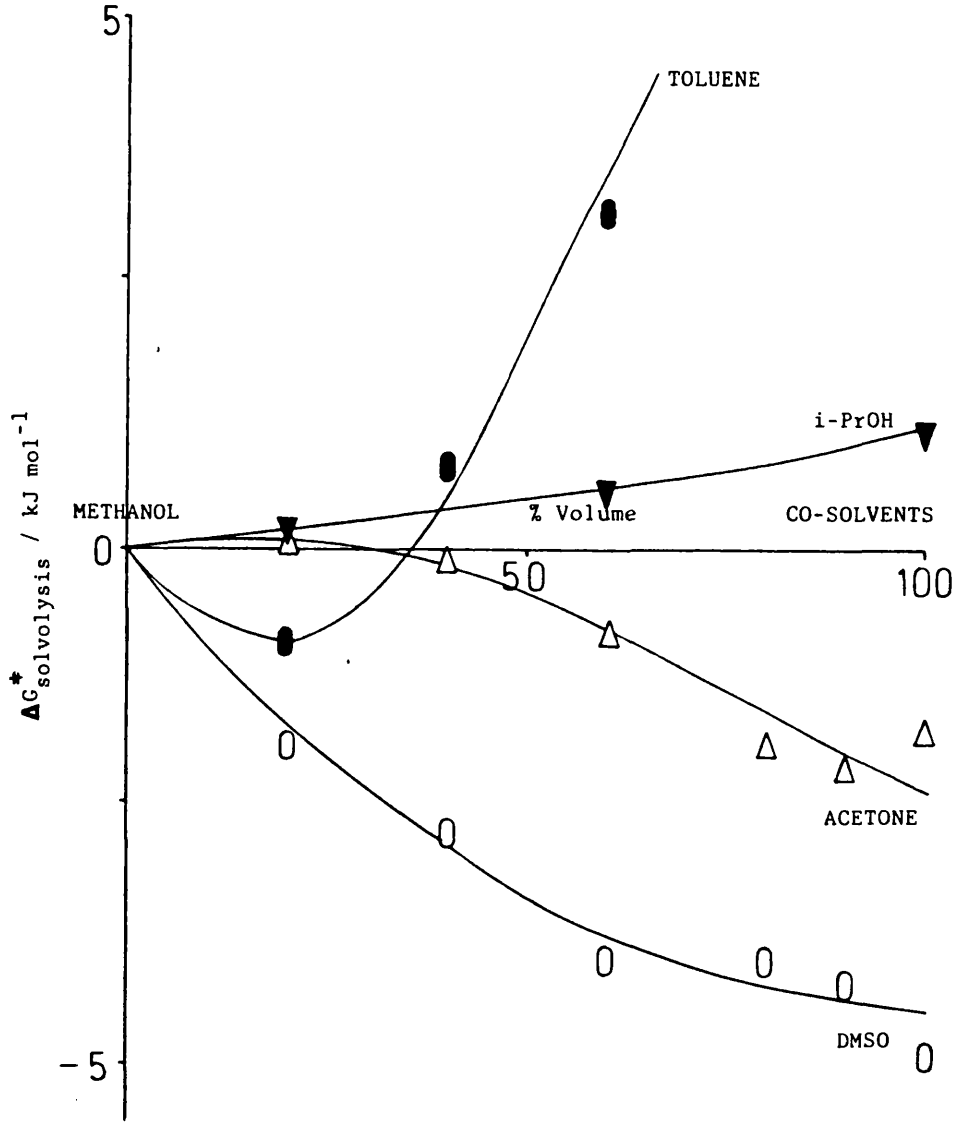

Figure [5-6] Plots of kinetic transfer parameter, $\Delta G^{\ddagger}$, for the solvolysis process of $Mo(CO)_4$(bpami) in binary methanol mixtures.

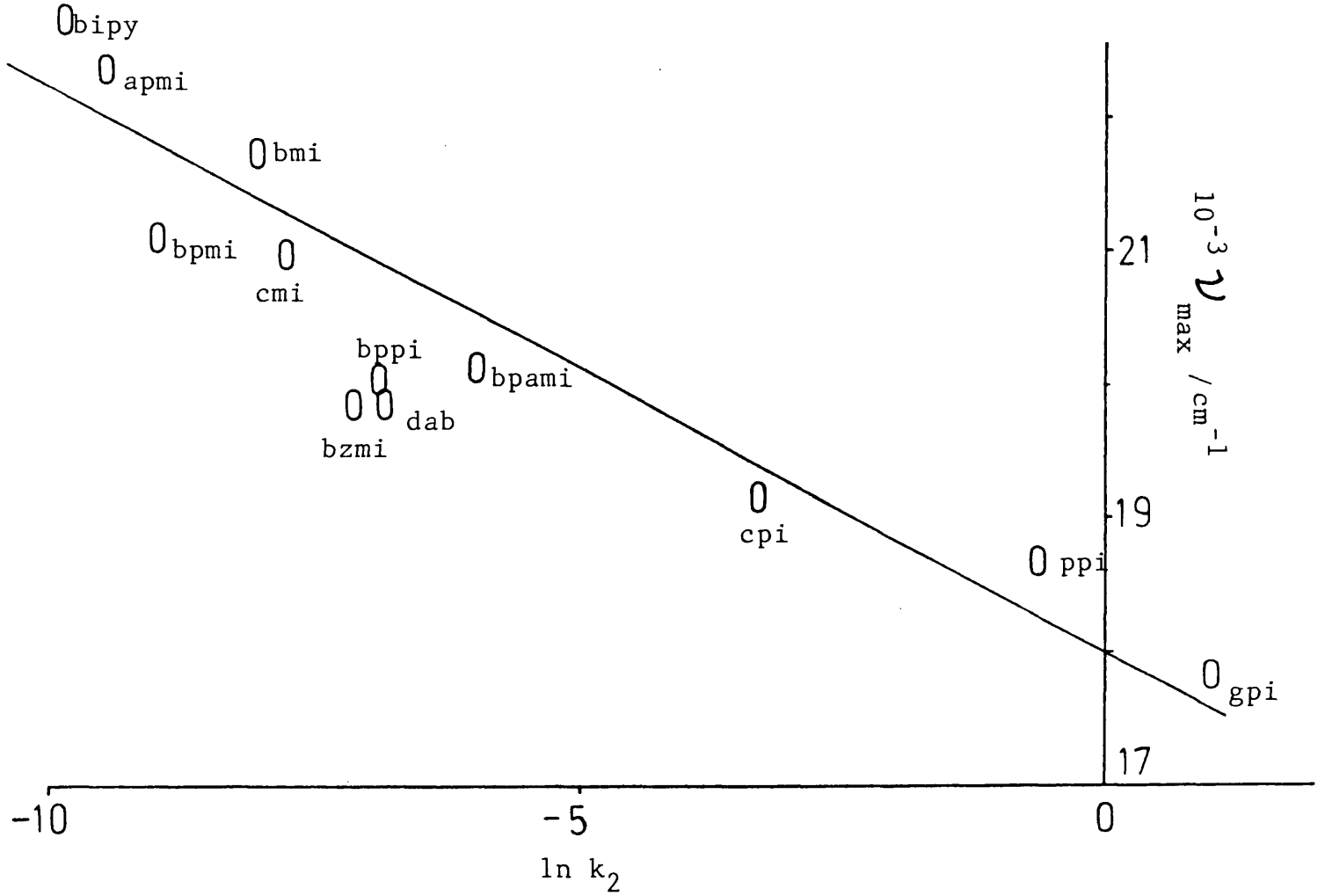

Figure [5-7] Plot of rate constants of cyanide attack (ln k_2) on various $Mo(CO)_4(N\widehat{\ }N)$ complexes against their corresponding ν_{max} of charge transfer in DMSO.

5-5. References

1. J. Burgess and R. D. W. Kemmitt, Inorg. React. Mechanism, 1, 266 (1971).
2. R. D. W. Kemmitt and M. A. R. Smith, Inorg. React. Mechanism, 3, 354 (1974).
3. J. L. Davidson, Inorg. React. Mechanism, 6, 346 (1979).
4. M. H. B. Stiddard, J. Chem. Soc., 4712 (1962).
5. M. J. Blandamer, J. Burgess, J. G. Chambers and A. J. Duffield, Transition Met. Chem., 6, 156 (1981).
6. M. J. Blandamer, J. Burgess and T. Digman, Transition Met. Chem., 10, 274 (1985).
7. F. A. Cotton and G. Wilkinson, "Advanced Inorg. Chem., 3rd Edit., Wiley, New York 1972, p 707.
8. G. R. Dobson, Accts. Chem. Res., 9, 300 (1976).
9. W. Beck, H. Werner, H. Engelmann and H. S. Smedal, Chem. Ber., 101, 2142 (1968).
10. R. D. Adams, D. F. Choddosh and N. M. Golembeski, Inorg. Chem., 17, 266 (1978)
11. J. R. Paxson and G. R. Dobson, J. Coord. Chem., 1, 321 (1972).
12. R. D. Gillard, Coord. Chem. Rev., 16, 67 (1975).
13. R. D. Gillard, Transition Met. Chem.,2, 247 (1977).
14. R. D. Gillard, J. Chem. Soc., Dalton Trans., 190, 193 (1979).
15. P. J. C. Walker and R. J. Mawby, Inorg. Chim. Acta, 7, 621 (1973).

16. J. J. Lagowski (edt.),"The Chemistry of Non-aqueous solvents", Academic Press ,1978), Vol: VA, p 9.
17. C. K. Ingold, "Structure and Mechanism in Organic Chemistry", G. Bell, London (1953).
18. A. J. Parker, Chem. Rev., 69, 1 (1969).
19. M. J. Blandamer and J. Burgess, Coord. Chem. Rev., 31, 93 (1980)
20. M. J. Blandamer and J. Burgess, Pure and Applied Chem., 54, 2285 (1982).
21. M. J. Blandamer, J. Burgess and J. G. Chambers, J. Chem. Soc., Dalton Trans., 60 (1977).
22. E. Pelizzetti, Inorg. Chem., 18, 1386 (1979).
23. E. Pelizzetti and P. Giordano, J. Inorg. Nucl. Chem., 43, 2463 (1981).
24. E. Pelizzetti, E. Pramauro, M. J. Blandamer, J. Burgess and N. Gosal, Inorg. Chim. Acta, 102, 163 (1985).
25. M. H. Abraham, G. F Johnston, J. F. C. Oliver and J. A. Richards, Chem. Commun., 930 (1969).
26. M. H. Abraham, J. Chem. Soc., A, 1061 (1971).
27. M. H. Abraham, Chem. Commun., 1307 (1969).
28. M. J. Blandamer, J. Burgess and A. J. Duffield, J. Chem. Soc., Dalton Trans., 1 (1980).
29. J. W. Akitt, J. Chem. Soc., A, 2347 (1971).
30. J. Burgess, "Metal Ions in Solution", Ellis Horwood, 1978, p 194.
31. M. J. Blandamer, J. Burgess. J. G. Chamber, R. I. Haines and H. E. Marshall, J. Chem. Soc., Dalton Trans, 165 (1977).

32. M. J. Blandamer, J. Burgess and J. G. Chambers, J. Chem. Soc., 60 (1977).
33. T. L. Cottnell, "The Strengths of Chemical Bond", 2ed., Butterworth Sciencetific Pub., 1958.
34. W. D. Horrocks and R. C. Taylor, Inorg. Chem., 2, 723 (1963).
35. W. Strohmeyer and F. Muller, Chem. Ber., 100, 2812 (1967).
36. J. Reinhold, R. Benedix, P. Birner and H. Hennig, Inorg. Chim. Acta, 33, 209 (1979).
37. L. W. Yarbrough and M. B. Hall, Inorg. Chem., 17, 2269 (1978).

CHAPTER 6

Kinetics of Substitution Reactions of Pentacarbonyl(4-cyanopyridine)molybdenum(0), $Mo(CO)_5(4CNpy)$

6-1. Introduction

In the last Chapter, we discussed reactions involving the substitution of the diimine ligand, (N^N), in $Mo(CO)_4(N\hat{}N)$ complexes by cyanide ion. That process has been shown to be bimolecular. In the present study, we shall deal with another pattern of reaction which is considerably different; the substitution reaction of $Mo(CO)_5(4CNpy)$ with a diimine compound, N^N, leading to the formation of the $Mo(CO)_4(N\hat{}N)$ complex.

$$Mo(CO)_5(4CNpy) + N\hat{}N \longrightarrow Mo(CO)_4(N\hat{}N) + 4CNpy + CO \quad ..[6\text{-}1]$$

This type of reaction can be used as a synthetic route to the tetracarbonyldiiminemolybdenum(0) complexes, though it is much less convenient than the cis-$Mo(CO)_4(pip)_2$ route.

Since the final product is $Mo(CO)_4(N\hat{}N)$, it is therefore expected that the reaction involves two consecutive processes. The first is probably the replacement of the 4-cyanopyridine and later on this is followed by the elimination of one of the adjacent carbonyl groups by the diimine ligand. Thus the observed rate constant will be dominated by one of these processes or both depending on their relative values.

The work presented here will focus on finding out the slowest path which may represent the rate controlling step and then later on trying to establish its possible mechanism. Some related reactions include those of

pentacarbonylaminemolybdenum(0), $Mo(CO)_5(amine)$, complexes with monodentate non-nitrogen-coordinated incoming ligands.[1-4]

$$Mo(CO)_5(amine) + L \longrightarrow Mo(CO)_5L + amine \quad ..[6-2]$$

where L= PR_3, AsR_3 and SbR_3. The rate law of these reactions is given by the total of first and second-order terms;

$$rate = k_1[Mo(CO)_5(amine)] + k_2[L][Mo(CO)_5(amine)]..[6-3]$$

where k_1 and k_2 represent dissociative (S_N1) and associative (S_N2) mechanisms respectively. Other relevant information can be obtained from the substitution reaction of cis-tetracarbonylbis(pyridine)molybdenum(0), cis-$Mo(CO)_4(py)_2$, where two molecules of pyridine are replaced by a diimine ligand.[5] This reaction has been shown to proceed through a purely dissociative process and the rate determining step is the dissociative elimination of the first pyridine group.

The majority of the kinetic measurements on the reactions studied here were carried out in toluene. Therefore, self-decomposition of the starting complex (mainly by solvolysis) is minimised. Like any other reaction, apart from the rate law, the mechanistic establishment of the process will be assisted by several other kinetic results, such as the volume of activation and mass law retardation.

6-2. Experimental

(a). Ligands and solvent

Most of the required incoming ligands were commercially supplied; 2,2'-bipyridine and pyrazine (Aldrich), 1,10-phenanthroline and 5-nitro-1,10-phenanthroline (Sigma). 1,4-Diphenyl-diazabutadiene (dab) and its derivatives were prepared by condensation of 2,3-butadione with aniline (and derivatives), as described in Chapter 2. The solvent, toluene, was dried over 4°A molecular sieve before used.

(b). Preparation of pentacarbonyl(4-cyanopyridine)-molybdenum(0); $Mo(CO)_5(4CNpy)$

The $Mo(CO)_5(4CNpy)$ was synthesized from molybdenum hexacarbonyl, $Mo(CO)_6$, by a thermal method.[6]

A 100 cm^3 one-neck round-bottomed flask equipped with a condenser was flushed with nitrogen. About 50 cm^3 of toluene, 1.5 g of molybdenum(0) hexacarbonyl (Aldrich) were placed in the flask. The reaction mixture was refluxed using a water bath for about two hours (the flask was covered with aluminium foil to exclude light). Finally a dark-red solution appeared. The reaction mixture was allowed to cool at room temperature and then at 0°C. The solution was filtered to removed unreacted molybdenum(0) hexacarbonyl and the volume reduced to 5 cm^3 by using a rotary evaporator. About 25 cm^3 of heptane were added to the residue,and the precipitated solid was then filtered off. The light brown $Mo(CO)_5(4CNpy)$ was collected and

washed with 10 cm^3 of heptane. The compound was dried overnight in a vacuum desiccator.

The collected complex is not pure. It still contains some impurities, mainly unreacted molybdenum(0) hexacarbonyl. Further purification by vacuum sublimation at 30-35°C eliminates the molybdenum(0) hexacarbonyl.

Melting point : 126-128°C

Analysis :

	%C	%N	%H
Theoretical	38.82	8.24	1.18
Found	37.24	7.97	1.67

λ_{max} in toluene: 398 nm (ϵ = 7000 cm^2 mol^{-1})

Infrared (ν_{CO}) : 2070, 1940 and 1925cm^{-1} (Figure [6-1](a)).

^1H NMR (δ) : 8.90 and 7.50 (Figure [6-1](b)).

(c) Kinetic measurements.

The kinetic measurements at ambient pressure were conducted (in a thermostatted quartz cell) by using a UV-Visible spectrophotometer (Pye-Unicam SP 1800). The formation of the product $Mo(CO)_4(N\widehat{\ }N)$ was followed at the corresponding wavelength of maximum absorption in toluene (Chapter 3) as shown in Figure [6-2]. In all cases, the reactions were carried out with a large excess of the incoming ligand so that the first-order rate law was observed. The observed rate constants, k_{obs}, were calculated from the slope of $\ln(A_\infty - A)$ against time (for at least two and half half-lives) by computer. The kinetics at higher pressure were

monitored as described in Chapter 2.

6-3. Results and Discussion

As mentioned earlier, studies of the kinetics of the substitution reaction of $Mo(CO)_5(4CNpy)$ with diimine ligands have been carried out in toluene at 25°C with various concentrations (large excess) of the incoming ligand. The observed first-order rate constants, k_{obs}, are summarized in Table [6-1]. Looking at the data obtained, for example, at various concentrations of 2,2'-bipyridine one recognizes that at a given temperature k_{obs} is independent of the excess concentration of the entering ligand. It follows furthermore that at a given temperature the average rate constants, $\overline{k}_{obs}$, for other incoming ligands such as 5-nitro-phen, dab and its derivatives, are very close. This means that the rate of the reaction in Equation [6-1] is almost independent of the nature of the attacking group.

The experimental rate equation for the reaction therefore is given by the Equation [6-4];

$$\text{rate} = \frac{d[Mo(CO)_5(4CNpy)]}{dt} = k_1\,[Mo(CO)_5(4CNpy)] \quad \ldots\ [6\text{-}4]$$

This observed rate law suggests that the reaction proceeds through a dissociative process. This would be either I_d, or a limiting dissociative (or D-) mechanisms in which the complex

itself will first form an intermediate with a lower coordination number[7]. The estimated volume of activation (2.7 ± 1.0 cm^3 mol^{-1}) is close to that for the reaction between cis-$Mo(CO)_4(py)_2$ and a diimine (3.6 ± 0.5 $cm^3 mol^{-1}$). This observation suggests that both reactions proceed by a similar mechanism (i.e. D-mechanism)[5]. However, in some reactions there will be more than one process taking place, thus it is essential to recognize the process which controls the rate. In the present case, as mentioned earlier, the reaction is expected to occur by two consecutive processes. The first is the entering of one end of the diimine compound at the leaving site of the 4-cyanopyridine and secondly , this is followed by the ring closure at the other end of the diimine ligand by pushing out the carbonyl group which is adjacent to it (Scheme [6-1]).

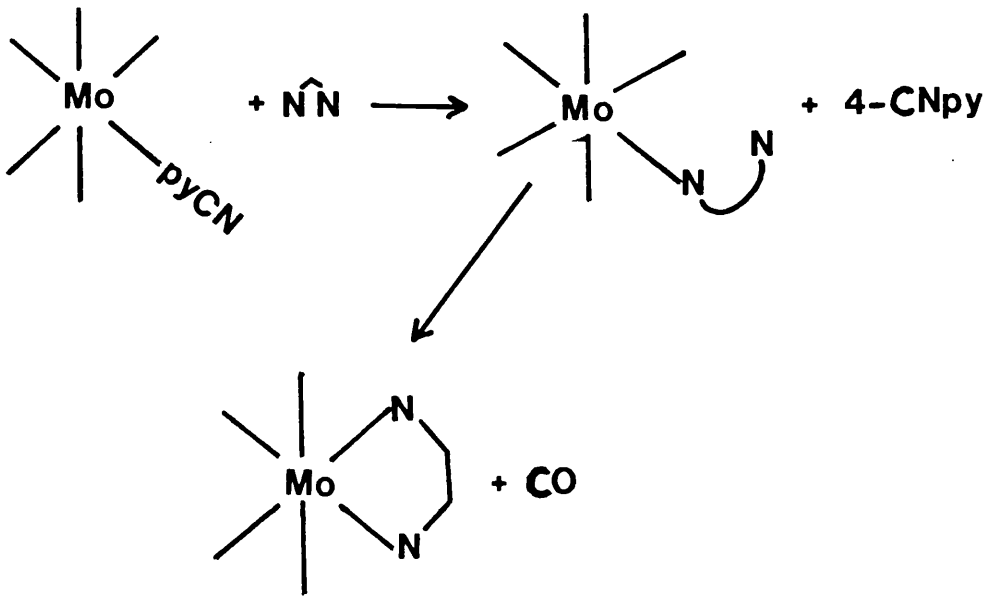

Scheme 6-1

Evidence for the formation of the monodentate intermediate $Mo(CO)_5LL$ where LL is bidentate phosphorus and arsenic donor ligands has long been known.[8,9] Staal et al.[10] reported the formation of a monodentate intermediate species of diimine ligand (1,4-diphenyl-1,4-diazabutadiene). They observed a transient green colour during the substitution reaction of the corresponding $Mo(CO)_5(THF)$ complex (where THF is tetrahydrofuran) with the diimine ligand at -60°C. Later, rapid-scanning Fourier transform infrared spectroscopy techniques have provided spectral evidence for the formation of such species.[11] In general, such an intermediate was observed to react rapidly at room temperature to form $Mo(CO)_4(N\ N)$. Schadt and Lees [12] recently carried out work to estimate the rate of ring closure from the product of fast photolysis of molybdenum(0) hexacarbonyl, $Mo(CO)_6$, to form intermediate $Mo(CO)_5(N\widehat{\ }N)$. The rate of the reaction reported by them is found to be very much faster than the rate reported here; the rate constant of ring closure $Mo(CO)_4(N\widehat{\ }N)$ where $N\widehat{\ }N$ is 2,2'-bipyridine in benzene* at 20°C is bigger than $0.4s^{-1}$. This observation strongly supports the argument that the second step proceeds very much more quickly and the rate controlling step is the dissociation of 4-cyanopyridine.

---

* It is found that the properties of benzene are similar to those of toluene.

$$Mo(CO)_5(4CNpy) \underset{k_{-1}}{\overset{k_1}{\rightleftharpoons}} Mo(CO)_5 + 4CNpy \qquad \text{slow} \qquad ..[6\text{-}6]$$

$$Mo(CO)_5 + N\widehat{\ }N \xrightarrow{k_2} Mo(CO)_5(N\widehat{\ }N) \qquad \text{medium} \qquad ..[6\text{-}7]$$

$$Mo(CO)_5(N\widehat{\ }N) \xrightarrow{k_3} Mo(CO)_4(N\widehat{\ }N) + CO \qquad \text{fast} \qquad ..[6\text{-}8]$$

Direct evidence to test the validity of the process can be obtained by the reaction with a monodentate amine ligand where no ring closure process take place. In Table [6-1], we also include results of the kinetics of reaction between $Mo(CO)_5(4CNpy)$ and monodentate pyrazine. These show that the rate constant for the reaction is identical with those given by the bidentate ligands. Its observed rate constant, k_{obs}, is independent of concentration of pyrazine and equivalent to the rate given by the bidentate diimine ligands. This observation suggests that the reaction involving carbonyl extrusion has not occurred. If it does the process is expected to be slower. Thus,

$$Mo(CO)_5(4CNpy) \underset{k_{-1}}{\overset{k_1}{\rightleftharpoons}} Mo(CO)_5 + 4CNpy \qquad \text{slow} \qquad ..[6\text{-}9]$$

$$Mo(CO)_5 + pyz \xrightarrow{k_2} Mo(CO)_5(pyz) \qquad \text{faster} \qquad ..[6\text{-}10]$$

However, the application of the steady-state approximation for concentration of the five coordinate $Mo(CO)_5$ for both systems

leads to a similar rate expression as shown in Equation [6-11]

$$\text{rate} = \frac{k_1 k_2 [N][Mo(CO)_5(4CNpy)]}{k_{-1}[4CNpy] + k_2[N]} \quad \ldots [6\text{-}11]$$

and

$$k_{obs} = \frac{k_1 k_2 [N]}{k_{-1}[4CNpy] + k_2[N]} \quad \ldots [6\text{-}12]$$

where N is the incoming ligand. This rate law pattern is identical to that reported for the formation of $Fe(CN)_5L^{3-}$,[14-24] $Ru(NH_3)_5L^{2+}$[25-27] and $Co(CN)_5L^{3-}$[7], where L is monodentate amine, from their aquo-complexes in water.

Theoretically, a plot of k_{obs} against the concentration of the incoming ligand, N, based on Equation [6-11], gives a curve rising from origin and finally asymptotic to limiting rate constant k_1, as shown in Figure [6-3].

At higher concentrations of incoming ligand, the Equation [6-11] can be reduced to,

$$\text{rate} = k_1[Mo(CO)_5(4CNpy)] \quad \ldots [6\text{-}13]$$

or

$$k_{obs} = k_1 \quad \ldots [6\text{-}14]$$

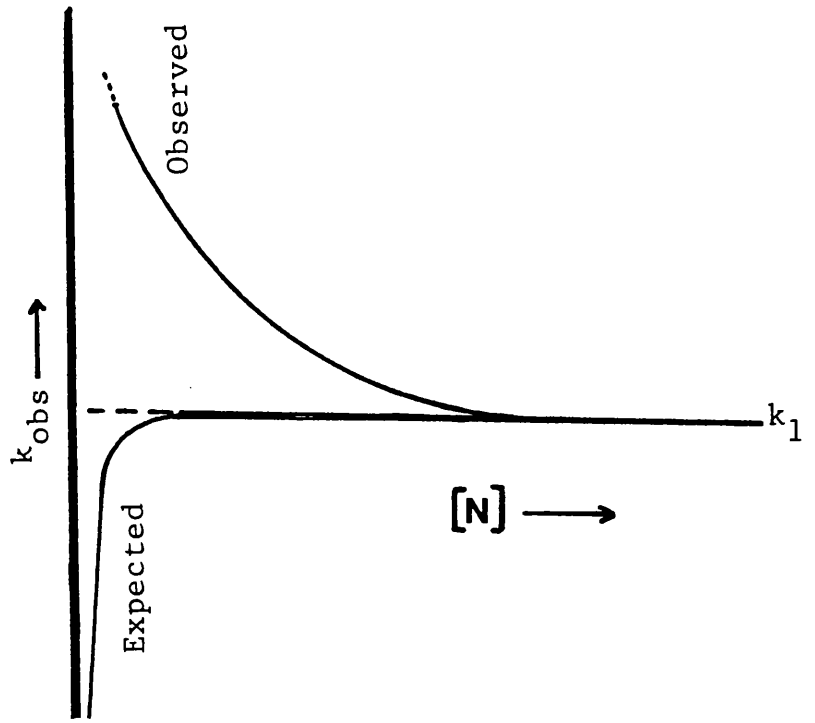

Figure [6-3] Expected and observed rate constant trends for dissociative or D-mechanism [Eq. [6-12]].

This expression explains that the process of occupying the vacant coordination site in $Mo(CO)_5$ is dominated by incoming ligand to yield a product. Thus the reaction leads to a limiting rate at k_1. On the other hand, at very low concentrations of incoming ligand the process of occupying the vacant coordination site in $Mo(CO)_5$ is hindered by growing competition from liberated 4-cyanopyridine to force the reaction back to the starting complex. Under such circumstances, the rate of the formation of the product is expected to be slower. Unfortunately, the latter pattern proved difficult to observe, since at this concentration, the growing competition of 4-cyanopyridine forces the reaction to stop before reaching completion. Therefore, their rate constants will be increased instead of decreased. This

expected pattern was clearly observed by Toma and Malin[28-30] in their study on the substitution reaction of $[Fe(CN)_5(DMSO)]^{3-}$ with N-methyl pyrazinium in aqueous solution.

Our data summarized in Table [6-1] are analysed. The plot of the observed first-order rate constant, k_{obs}, against the concentration of the incoming ligand is displayed in Figure [6-4]. The result shows that the reactions have a limiting rate constant of about $((1.50-1.35)\pm 0.2)\times10^{-4}sec^{-1}$, except for 1,10-phenanthroline which has a limiting rate of about $(2.10 \pm 0.3)\times10^{-4}sec^{-1}$. The pattern exemplified by this type of plot sometimes can be used to estimate the relative reactivity of the various incoming ligands compared to 4-cyanopyridine. The present analysis reveals that 1,10-phenanthroline, 2,2'-bipyridine and pyrazine are considered to be better coordinating ligands. They indicate little sign of deviation from the limiting rate constant k_1 even at lower concentrations. Presumably these ligands have sufficient ability to force the reaction to go to completion. The situation is different for dab and its derivatives, in which the observed rate constants at lower concentrations of dab are faster. The result can be associated with the formation of equilibrium rather than completion. At this point, some amount of reactants stay in solution without being converted to product. The possible explanation of the relation between the effect of equilibrium and rate constant of the reaction is shown in the schematic diagram of Figure [6-5]. It shows that how three reactions of equal concentration of complex with different concentrations of incoming ligand could yield different amount of product. Due to equilibrium, two of the

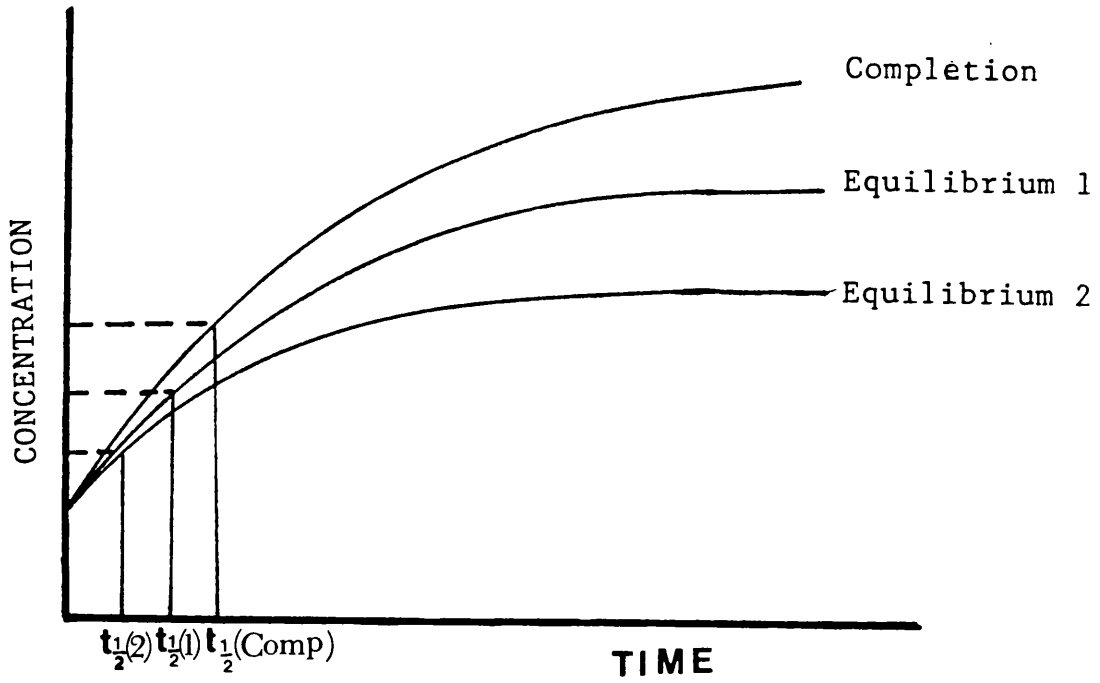

Fig.[6-5]. A schematic diagram of relative rate constant (half-life) of the reaction at various stages of concentration of product.

reactions (with lower concentration of incoming ligand) do not convert all starting complex to product and their rate constant (based on half-life) become faster as the amount of product formation is less. The amount of product formation varies depending on the nature of the incoming ligand as well as its concentration. The ligand which has less coordinating ability leads to an equilibrium position further from completion than a better one. The ligands dab, dab-Cl, and dab-OCH_3 are good examples to illustrate this. In this case, dab-Cl is expected to have the poorest coordinating ability in this group. The plot of k_{obs} against its concentration , as shown in Figure [6-4], deviates to higher k_{obs} values from the limiting rate constant, k_1, earlier compared to dab and

dab-OCH_3. As expected, the presence of methoxide, OCH_3, increases the coordinating ability of dab-OCH_3, thus it deviates later than the other ligands. A good estimation of the coordinating ability of the ligand can be obtained from the study of the kinetic effect of the mass law retardation which will be discussed later in this Chapter. The effect of concentration leads to a similar result; the presence of a lower amount of incoming ligand reduces its ability to converted completely into product. Here again the problem of not reaching completion arises, and an increased rate constant will be observed.

The trend given by the reaction with dimethylsulphoxide (DMSO) is rather interesting. It was recognized long ago that dimethylsulphoxide, apart from being a solvent, also has the ability to donate its electrons to form a complex.[31-33] In the present case, the dimethylsulphoxide is expected to act as a monodentate incoming ligand to replace the 4-cyanopyridine molecule in $Mo(CO)_5$(4CNpy). A plot of k_{obs} versus concentration of DMSO, Figure [6-4], shows a minimum point indicating that the reaction slows down as the concentration of DMSO decreases, and then increases at yet lower concentrations. This observation suggests that the reaction probably satisfies the expected trend in the beginning but at the lower concentration the reaction tends to reach equilibrium rather than go to completion.

So far we have established that the reaction of Equation [6-1] proceeds through a D-mechanism. The rate controlling step is determined by the dissociation of $Mo(CO)_5$(4CNpy) to form a five coordinate complex, $Mo(CO)_5$, and 4-cyanopyridine.

According to the absolute mass law the dissociation process is controlled by changing the concentration of 4-cyanopyridine. A higher concentration of 4-cyanopyridine increases its competition with the diimine ligand to coordinate with the intermediate complex, $Mo(CO)_5$; thus the prosess will slow down. Such a kinetic effect is called mass law retardation. Data in Table [6-2] summarize the effect. As expected, the rate constant decreases as the concentration of the 4-cyanopyridine increases. This is parallel to the reaction given by Equation [6-12]. In fact, in certain circumstances, this effect is used as an alternative technique to test the validity of the dissociative or D-mechanism.

Rearrangement of Equation [6-12] leads to Equation [6-15].

$$\frac{1}{k_{obs}} = \frac{1}{k_1} + \frac{k_{-1}[4\text{-CNpy}]}{k_2 k_1 [N]} \qquad \ldots [6\text{-}15]$$

Thus a plot of $(1/k_{obs})$ against the ratio [4CNpy]/[N] is expected to be a straight line. Figure [6-6] shows the application of such a plot for several incoming groups. The rate constant k_1, which should be independent of the nature of the incoming group, is estimated at [4CNpy]/[N] = 0. The ratios k_{-1}/k_2 describing the relative reactivity of the incoming group with respect to 4-cyanopyridine are calculated from the slope of the line. All these results are compiled in Table [6-3]. It shows that the ratio of k_{-1}/k_2 for all types

of incoming group are less than one, which means that the present incoming groups are better nucleophiles than 4-cyanopyridine. This ratio can also be used to estimate the relative coordinating ability of the ligand as indicated by rate constant k_2(rel). It is found that the monodentate pyrazine shows somewhat better coordinating ability than the bidentate ligands. As expected, the presence of the substituent group chloride in dab-Cl clearly reduces the coordinating ability which , on the other hand, increases in the presence of the methoxide, OCH_3 group.

In conclusion, the mass law retardation not only provides a characteristic feature of a D-mechanism but also offers an alternative technique for estimating the relative abilities of ligands to form metal-ligand bonds. The mass law retardation is not observed for other mechanisms.

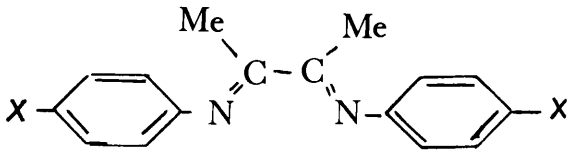

X = H ; dab

X = OCH_3 ; dab-OCH_3

X = Cl ; dab-Cl

TABLE 6-1

Rate constants at 298°K for ligand substitution of $Mo(CO)_5(4CNpy)$ with several incoming ligands N in toluene ; initial $[Mo(CO)_5(4CNpy)] = 2x10^{-4}M$.

N	$10^4 k_{obs}/s^{-1}$ with $[N]/10^{-3}M$						$\bar{k}_{obs}$
	0.5	1.0	2.0	3.0	4.0	5.0	$/s^{-1}$
1,10-phen	2.14	2.13	2.12	2.08	2.06	2.16	2.11
1,10-phen $-5NO_2$	1.55	1.54	1.58	1.60	1.58	1.63	1.58
2,2'-bipy	1.42	1.42	1.50	1.53	1.49	1.55	1.49
dab-OCH_3	1.67	1.28	1.36	1.35	1.44	1.43	1.41
dab	1.97	1.45	1.36	1.36	1.34	1.38	1.39
dab-Cl	2.08	1.71	1.31	1.31	1.33	1.32	1.38
pyrazine	1.48	1.46	1.51	1.57	1.56	1.55	1.52
DMSO	-	-	0.89	0.89	1.16	1.26	-

TABLE 6-2

The effect of addition of 4-cyanopyridine on the rate constant for the substitution reaction of $Mo(CO)_5(4CNpy)$ with incoming ligands N in toluene at 298°K; initial $[Mo(CO)_5(4CNpy] = 2x10^{-4}M$; $[N] = 5x10^{-3}M$.

N	$10^4 k_{obs}/s^{-1}$ in presence of $[4CNpy]/10^{-3}M$						
	0.0	2.0	5.0	10.0	20.0	30.0	50.0
2,2'-bipy	1.53	1.47	1.35	1.18	0.90	0.85	0.54
dab-OCH_3	1.43	1.37	1.18	0.97	0.66	0.59	0.36
dab	1.42	1.30	1.07	0.82	0.59	0.42	-
dab-Cl	1.40	1.20	0.91	0.63	0.42	0.31	-
Pyrazine	1.53	1.49	1.43	1.31	1.10	1.05	0.82

TABLE 6-3

Rate constants at 298°K derived for ligand substitution of $Mo(CO)_5(4CNpy)$ by several incoming ligands ,N in toluene based on Equation [6-15] and Figure [6-2].

N	$10^4 k_1$ /s^{-1}	k_{-1}/k_2 [a]	k_2 (rel) [b]
2,2'-bipy	1.58	0.18	0.56
dab-OCH_3	1.55	0.32	0.31
dab	1.37	0.41	0.24
dab-Cl	1.43	0.57	0.11
Pyrazine	1.56	0.10	1.00

[a] Obtained by multiplication of the slope of the straight line of Figure [6-2] with k_1 according to $(k_{-1}/k_2)x(1/k_1)$.

[b] Obtained by dividing the ratio (k_{-1}/k_2) for pyrazine by other corresponding (k_{-1}/k_2);(rel= relative)

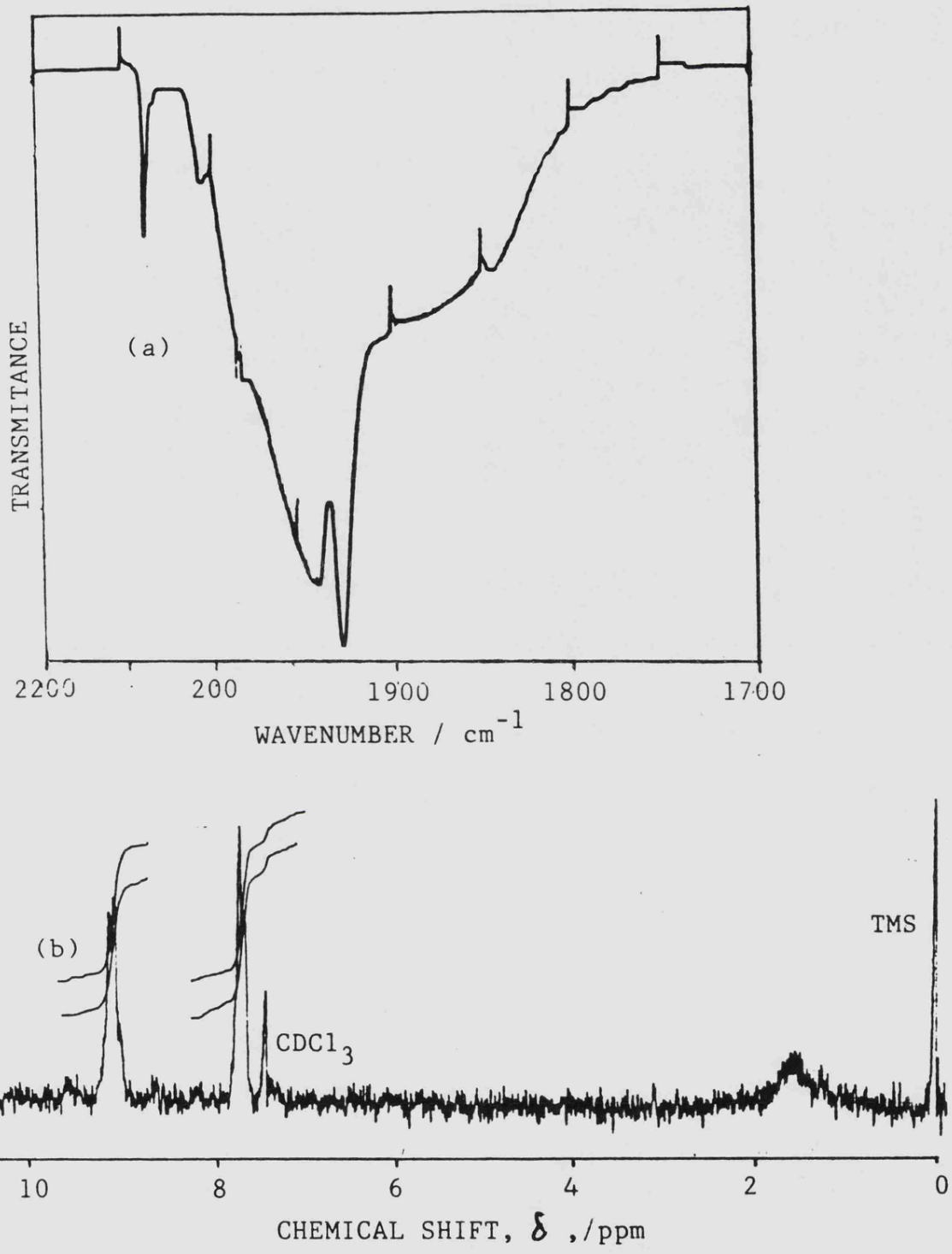

Figure [6-1] Infrared and proton NMR analysis on $Mo(CO)_5$(4CNpy) complex; (a) carbonyl stretching fequencies in KBr and (b) proton NMR in $CDCl_3$.

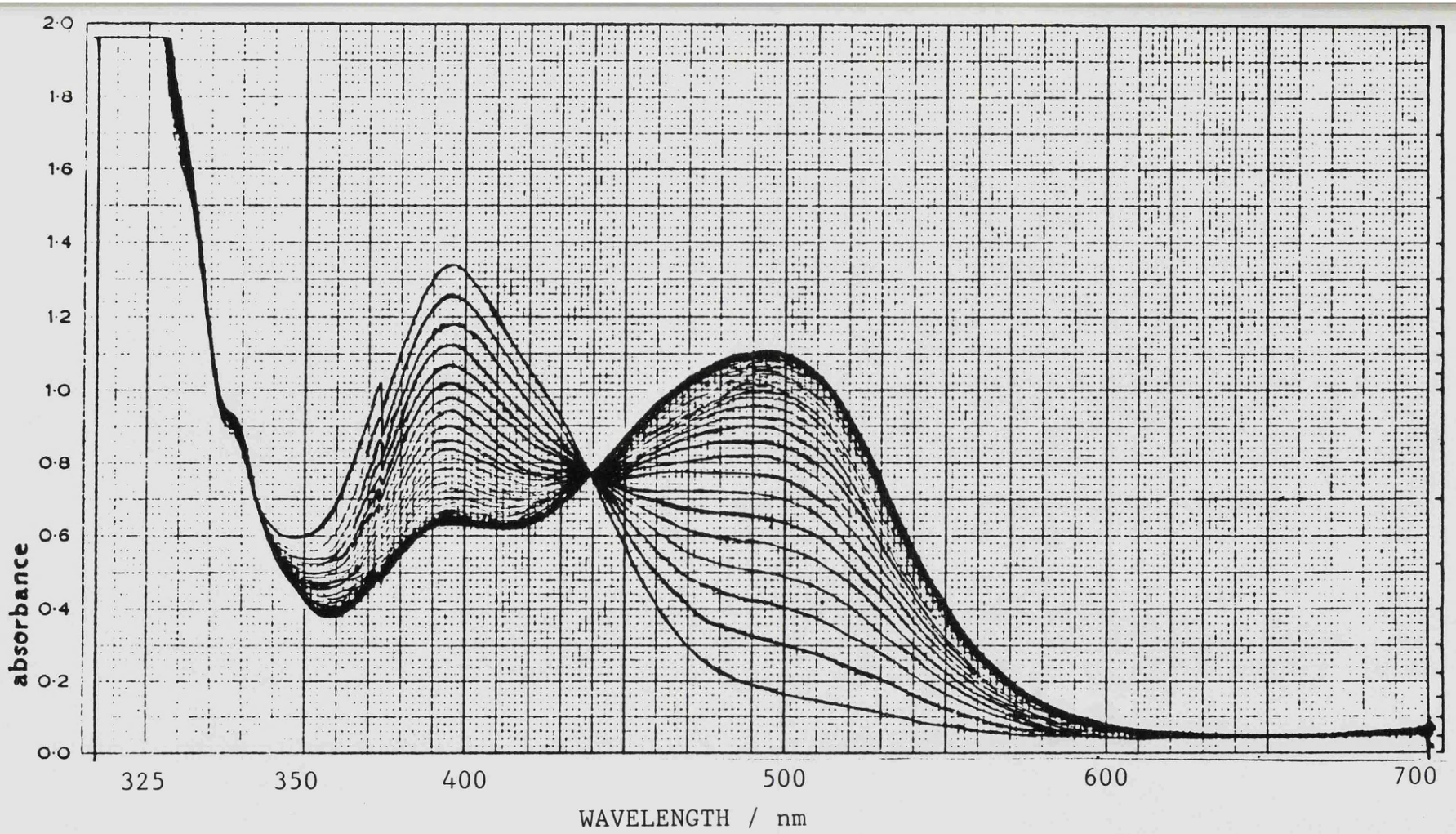

Figure [6-2] A scanning spectrum for the reaction between $Mo(CO)_5(4CNpy)$ and 2,2'-bipyridine (bipy) in toluene at 298°K; initial $[Mo(CO)_5(4CNpy)] = 2x10^{-4}M$, $[bipy] = 3x10^{-3}M$. A peak at $\lambda = 495$ nm corresponds to absorption for $Mo(CO)_4(bipy)$.

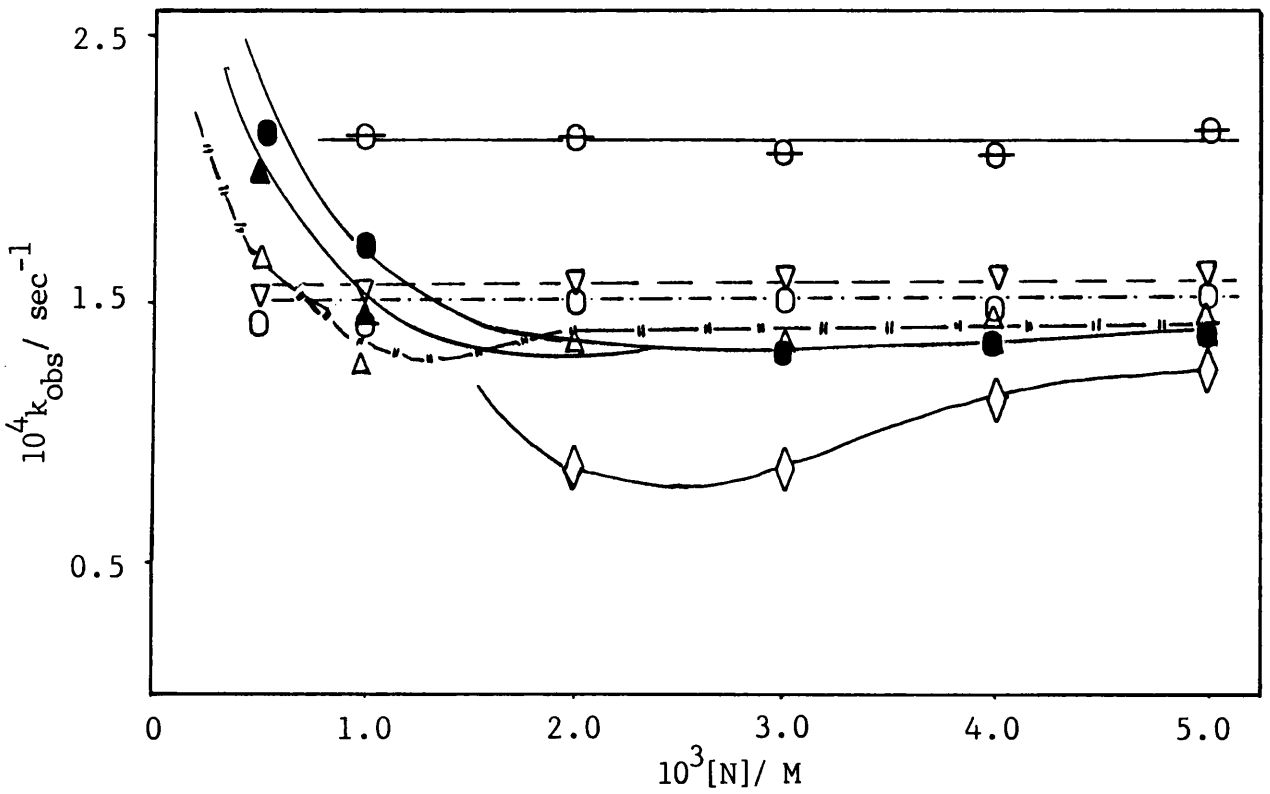

Figure [6-4] Plots of k_{obs} against concentration of incoming ligands, [N], of the substitution reaction of $Mo(CO)_5(4CNpy)$ in toluene at 298°K; ⊖ 1,10-phen, ▽ 5-nitro-1,10-phen, O bipy, Δ dab-OCH_3, ▲ dab, ● dab-Cl O pyrazine and ◇ DMSO.

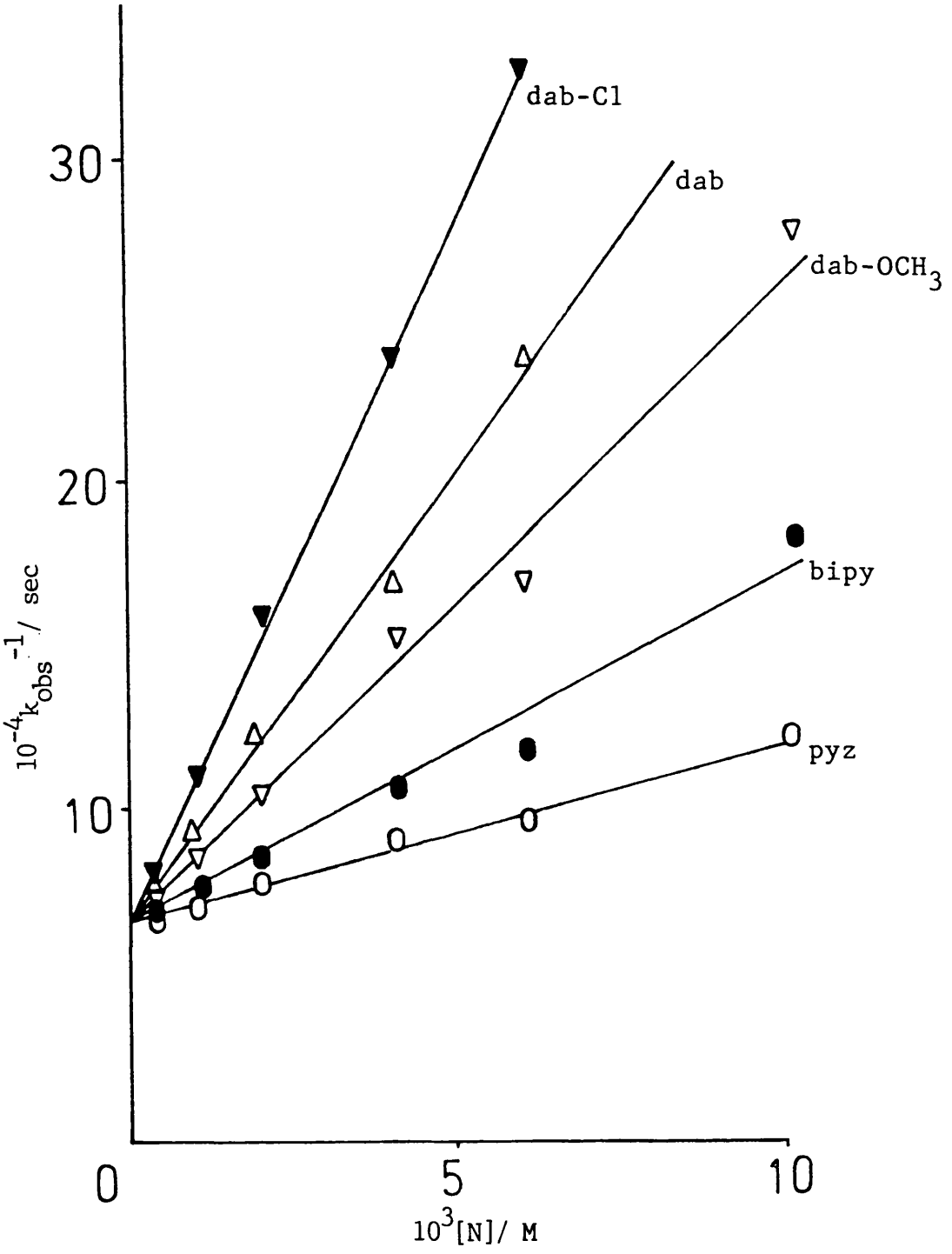

Figure [6-6] Plot of the reciprocal rate constant, k_{obs}^{-1} versus the concentration ratio [4CNpy]/[N] for the reaction between $Mo(CO)_5(4CNpy)$ and incoming ligands at various concentration of 4-cyanopyridine; initial $[Mo(CO)_5(4CNpy)] = 3x10^{-4}M$, $[N] = 3x10^{-3}M$

6-4. References

1. C. M. Ingemanson and R. J. Angelici, Inorg. Chem., 7, 2646 (1968).
2. D. J. Darensbourg and T. L. Brown, Inorg. Chem., 7, 1679 (1968).
3. W. D. Convey and T. L. Brown, Inorg. Chem., 12, 2820 (1973).
4. D. J. Darensbourg and J. A. Ewen, Inorg. Chem., 20, 4168 (1981).
5. H. -T. Macholdt and H. Elias, Inorg. Chem., 23, 4315 (1984).
6. R. J. Dennenberg and D. J. Darenbourg, Inorg. Chem., 11, 72 (1972).
7. F. Basolo and R. G. Pearson,"Mechanisms of Inorganic Reactions", Wiley, 1958, p 98.
8. J. A. Connor, J. P. Day, E. M. Jones and G. K. McEwen, J. Chem. Soc., Dalton Trans., 347 (1973).
9. J. A. Connor and G. A. Hudson, J. Organomet. Chem., 73, 351 (1974).
10. L. H. Staal, D. J. Stufkens and A. Oskam, Inorg. Chim. Acta, 26, 255 (1978).
11. R. J. Kazlauskas and M. S. Wrighton, J. Amer. Chem. soc., 104, 5784 (1982).
12. M. J. Schadt and A. J. Lee, Inorg. Chem., 25, 672 (1986).
13. M. A. Blesa, J. A. Olabe and P. J. Aymonino, J. Chem. Soc., Dalton Trans., 1196 (1976).

14. M. A. Blesa, I. A. Funai, P. J. Morando, J. A. Olabe, P. J. Aymonino and G. Ellenrieder, J. Chem. Soc., Dalton Trans., 845 (1977).
15. N. E. Katz, M. A. Blesa, J. A. Olabe and P. J. Aymonino, Inorg. Chim. Acta, 27, L65 (1978).
16. N. E. Katz, M. A. Blesa, J. A. Olabe and P. J. Aymonino, Inorg. Chim. Acta, 17, 556 (1978).
17. T. R. Sullivan, D. R. Stranks, J. Burgess and H. I. Haines, J. Chem. Soc., Dalton Trans., 1460 (1977)
18. M. J. Blandamer, J. Burgess and R. I. Haines, J. Chem. Soc., Dalton Trans., 1293, (1976).
19. M. J. Blandamer, J. Burgess and H. I. Haines, J. Chem. Soc., Dalton Trans., 244 (1978).
20. I. Murati, D. Pavloric, A. Sustra and S. Avperger, J. Chem. Soc., Dalton Trans., 500 (1978).
21. M. L. Bowers, D. Kovacs and R. E. Shepherd, J. Amer. Chem. Soc., 99, 6555 (1977).
22. A. R. Garafalo and G. Davies, Inorg. Chem., 15, 1787 (1976).
23. A. D. James and R. S. Murray, J. Chem. Soc., Dalton Trans., 1182 (1976).
24. P. C. Ford, Coord. Chem. Rev., 5, 75 (1970).
25. P. C. Ford, D. F. P. Rudd, R. G. Grauder and H. Taube, J. Amer. Chem. Soc., 90, 1187 (1968).
26. J. N. Armor and H. Taube, J. Amer. Chem. Soc., 92, 6170 (1970).
27. H. E. Toma and J. M. Malin, Inorg. Chem., 12, 2080 (1973).

28. J. M. Malin, H. E. Toma and E. Giesbrecht, J. Chem. Educ., 54, 386 (1977).

29. J. M. Malin, H. E. Toma and E. Giesbrecht, Inorg. Chem., 12, 2084 (1973).

30. D. Martin, A. Weisen and H. J. Niclas, Angew. Chem. Internat., Edn., 6, 318 (1967).

31 H. L. Schlafer and W. Schaffernicht, Angew. Chem., 72, 618 (1966).

32. W. L. Reynolds, Progr. Inorg. Chem.,12, 1 (1970).

CHAPTER 7

Kinetics of The Reaction of $Mn(CO)_5Br$ with Diimine Compounds and Charge Transfer Spectra of $Mn(CO)_3(bipy)Br$

7-1. Introduction

The discovery of dimanganese decacarbonyl, $Mn_2(CO)_{10}$, was soon followed by an observation that it reacted fairly readily with iodine to give pentacarbonyl iodine, $Mn(CO)_5I$. This reaction proceeds conveniently by heating the mixture of both compounds at 140°C in an evacuated, sealed tube[1]. Preparations of the bromide and chloride are rather easier. These are carried out by the action of halogen on a solution of dimanganese(0) decacarbonyl at lower temperatures than that required for the iodide, at about 40°C and 0°C for the bromide and the chloride respectively, to produce manganese(I) pentacarbonyl halides, $Mn(CO)_5X$.

$$Mn_2(CO)_{10} + X_2 \longrightarrow 2Mn(CO)_5X \quad .... [7\text{-}1]$$

At higher temperature further reaction may convert the product to a dimeric compound $[Mn(CO)_4X]_2$[2],

$$2Mn(CO)_5X \longrightarrow [Mn(CO)_4X]_2 + 2CO \quad .... [7\text{-}2]$$

which is analogous to the corresponding ruthenium complexes[3].

The manganese(I) pentacarbonyl halides are very important because they have been widely used as starting materials to prepare other manganese(I) carbonyl derivatives. Most of the

complexes which have been synthesized are grouped into three general formulae, $Mn(CO)_4XL$, $Mn(CO)_3XL_2$[4] and $Mn(CO)_3X(L\text{-}L)$,[5,6] where L and L-L are monodentate and bidentate ligands respectively. The formation of these types of complexes suggests that the reaction involves the extrusion of carbonyl rather than halide.

So the question now arises as to which of the carbonyl groups in the complex will be involved in the substitution process. The structure of $Mn(CO)_5X$ shows that there are two types of carbonyl present; four of them are cis and one trans to the halogen as shown in 1. Theoretical explanation by Wilkinson and coworkers[2,3] suggests that the carbonyl group trans to halogen in the complex may have higher stability than that in the corresponding cis-position. This is because of a greater amount of π-bonding of carbonyl compared to the halogen group. In d^6-octahedral systems of this type, there is a back donation of d_{xz}, d_{xy} and d_{yz} pairs of electron via π-bonding into vacant π^*-orbitals, with ligands trans to each other competing for the same set of d-orbitals. Therefore, the carbonyl trans to halogen is only in competition with halogen and as a result, is more π-bonded than it would be if in competition with carbonyl for the d-orbital electrons. In fact, the analysis of the product from isotopic ^{13}CO exchange with $Mn(CO)_5X$[7] and infrared studies[8,9] proved that the exchange process might have occured at any four of the carbonyl groups cis to halogen to form cis-$Mn(CO)_4LX$ (2) similar to those reported in substitution processes of $Ru(CO)_5X$.

The same argument can be used also to explain the formation of fac-$Mn(CO)_3L_2X$ (3) in the bisubstitution process

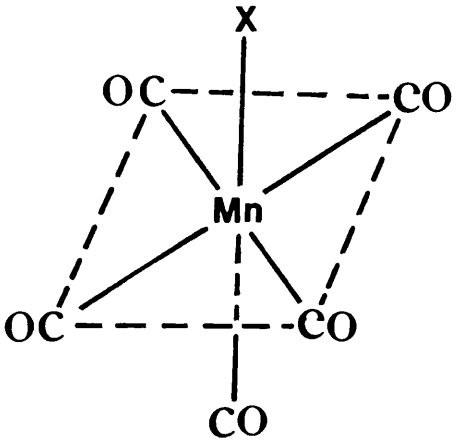

1

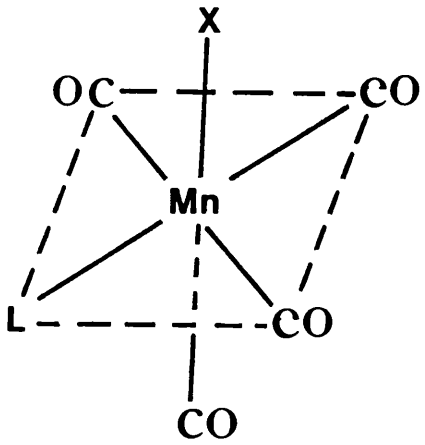

2

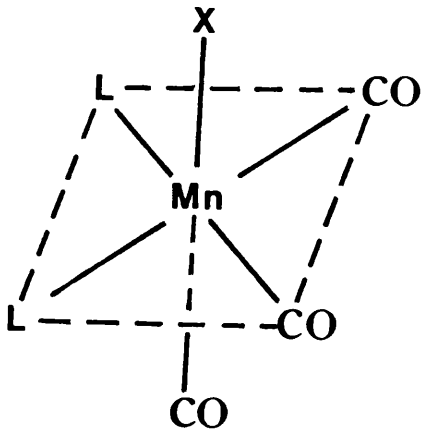

3

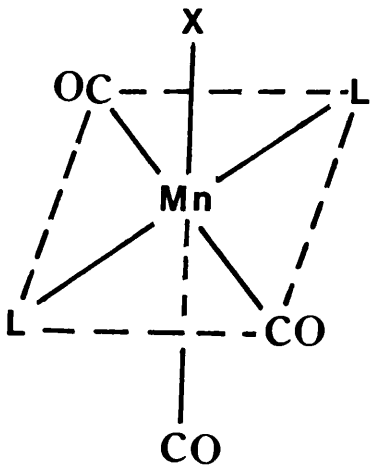

4

of $Mn(CO)_5X$ by monodentate ligand L. In this case, the carbonyls trans to halogen and monosubstituted group L are considered to be more stable than those trans to carbonyl. Therefore, the exchange process of the second carbonyl may occur at either of two carbonyl groups trans to each other. Although some mer-$Mn(CO)_3L_2X$ (4)[10] complexes have been reported, they only form via reduction of Mn(II) complexes.

Apart from preparation and spectroscopy studies of the manganese(I) carbonyl derivatives, several studies also have been done to monitor the kinetics of some of the preparative reactions based on Equations [7-3] and [7-4],[11-17]

$$Mn(CO)_5X + L \longrightarrow cis\text{-}Mn(CO)_4LX + CO \quad \ldots [7\text{-}3]$$

$$cis\text{-}Mn(CO)_4LX + L' \longrightarrow fac\text{-}Mn(CO)_3LL'X + CO \quad \ldots [7\text{-}4]$$

where L and L' are monodentate incoming ligands. It is found that both reactions follow a similar dissociative mechanism (always D- or sometimes I_d-mechanisms) in which the rate constant for of the reaction is independent of the nature as well as concentration of the incoming group, with the latter process proceeding much more slowly. For example, the rate constants for the reaction of $Mn(CO)_5Br$ and of $Mn(CO)_4(P(OCH_2)_3CCH_3)Br$ with $P(OCH_2)_3CCH_3$ in chloroform at 40°C are 2.56×10^{-4} sec^{-1} and 4.0×10^{-6} sec^{-1} respectively. This result implies that the presence of the other substituent

group strengthens the metal-carbonyl bond. The rate determining step involving the dissociation of carbonyl seems likely in the reaction to form the five-coordinated intermediate, followed by rapid occupation of the vacant site by the entering ligand L to form a product as shown in Scheme 7-1.

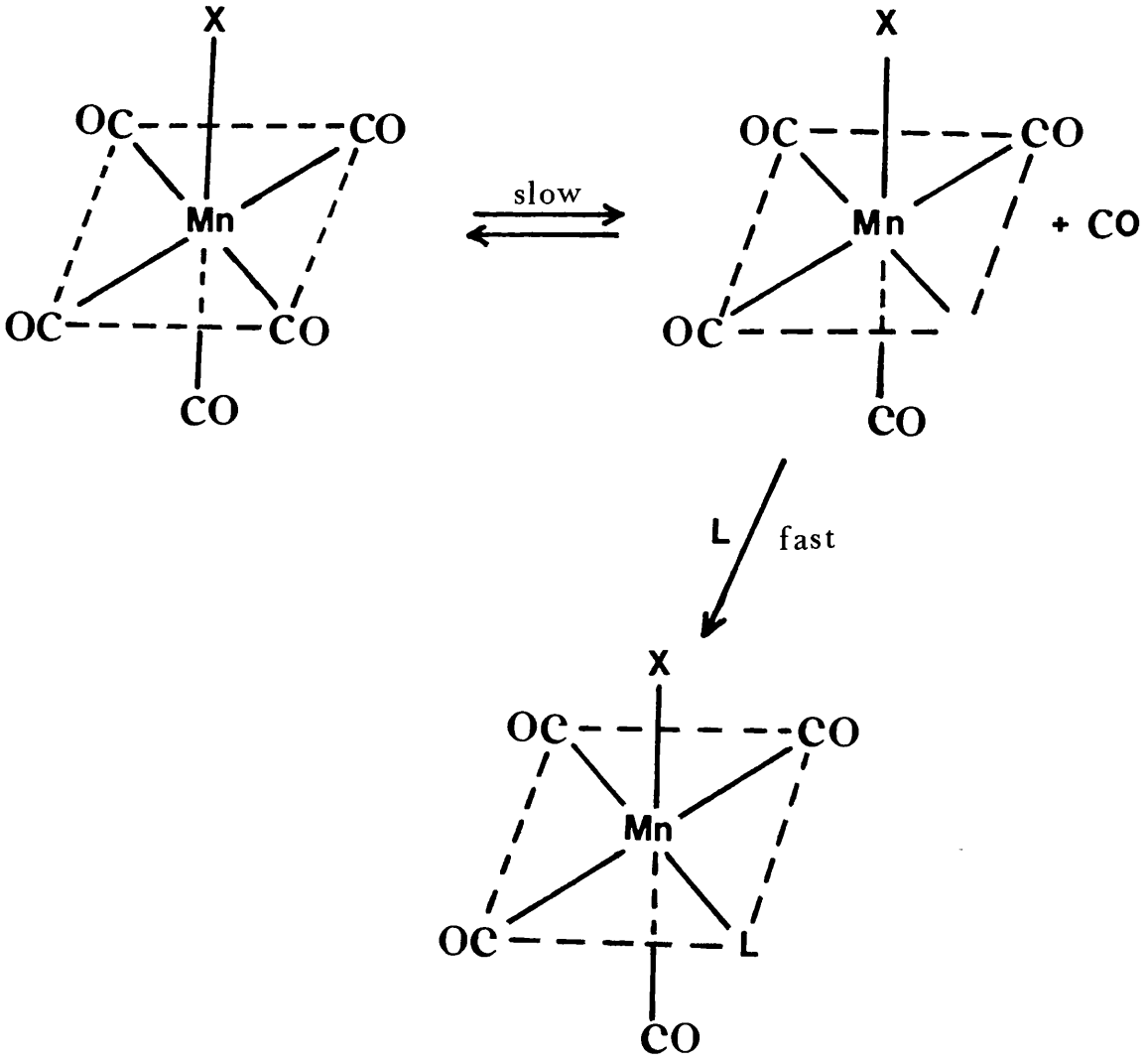

Scheme 7-1

The objective of the present work is to examine the reaction involving one of the manganese(I) carbonyl halides (i.e. $Mn(CO)_5Br$) with some bidentate diimine ligands ($N\widehat{\ }N$) such as 2,2'-bipyridine, 1,10-phenanthroline, etc. Apart from establishing the mechanism we shall also be looking at how the solvent influences the rate of the process. The product of the reaction is usually $Mn(CO)_3(bipy)Br$. This type of complex is expected to produce metal to ligand charge transfer spectra which are similar to those reported for ternary iron(II) and molybdenum(0) diimine complexes. Thus, the present study will also undertake some discussions on solvatochromism of this complex.

7-2. Experimental

(i) Preparative

(a) Preparation of $Mn(CO)_5Br$[18]

A tube, about 100 cm^3 capacity, equipped with a magnetic stirring bar, was flushed with nitrogen. Dimanganesedecacarbonyl, $Mn_2(CO)_{10}$ (2.0 g, 5.13 mmol) and cyclohexane (50 cm^3) were added, under a nitrogen flush, and the mixture was stirred for about ten minutes under nitrogen. Some of the $Mn_2(CO)_{10}$ remained undissolved, but this did not affect the reaction. A solution of Br_2 (0.35 cm^3, 6.3 mmol) in 20 cm^3 of cyclohexane was then added under nitrogen from an equipressure dropping funnel over a period of 20-30 minutes; some of the product began to precipitate during this time.

Stirring was continued for an additional hour. The dark red mixture was then evaporated under reduced pressure to give an orange powder.

The crude product was stirred with 150 cm^3 of dichloromethane, and the orange solution was filtered. Hexane (60 cm^3) was added, and the solution was slowly evaporated under reduced pressure to about 30 cm^3. The yellow-orange, microcrystalline $Mn(CO)_5Br$ was filtered off, washed with cold (0 °C) pentane, and dried in vacuo.

(b) Preparation of $Mn(CO)_3(bipy)Br$

In a 100 cm^3 round-bottomed flask fitted with a condenser, manganese(I) pentacarbonylbromide (1.0 g) was dissolved in 25 cm^3 of dioxan, and then 2,2'-bipyridine (0.7 g) was added. The solution was refluxed for an hour, leaving a yellow precipitate when it was left to cool to room temperature. The solution was filtered, and the precipitate washed with ether and dried in vacuo.

(ii) Kinetic Measurements

Kinetic runs for the reactions between manganese(I) pentacarbonyl bromide and 2,2'-bipyridine (Aldrich) and 1,10-phenanthroline (Sigma) at atmospheric pressure were carried out in 10 mm silica cells in the thermostatted cell compartment of a Pye-Unicam SP 1800 recording spectrophotometer. Kinetic runs at higher pressures were carried out in a thermostatted pressure vessel as described in

Chapter 2. In all cases, the concentration of incoming group was kept in large excess over that of the manganese compound so that first-order kinetics were observed. The reactions were monitored by following the appearance of the absorption of the product. Methanol was distilled and dried over 4^{o}A molecular sieve.

7-3. Kinetics of the Reactions of $Mn(CO)_5Br$ with Diimines (N^N)

The substitution reactions of $Mn(CO)_5X$ by several monodentate ligands have been the subject of several investigations. There was no information about kinetics of the reaction between $Mn(CO)_5X$ and bidentate diimine ligands (N^N), even though the complex $Mn(CO)_3$(bipy)I had been reported a long time ago.[2] It was not until recently that Schmidt[19] carried out preparative and kinetic studies of some of these reactions of $Mn(CO)_5X$ with bidentate diimine ligands, such as 2,2'-bipyridine, 1,10-phenanthroline, etc, in toluene and chloroform. He found that the final product of the reaction consisted of the complex $Mn(CO)_3(N\hat{}N)X$. Using evidence as reported on monodentate substituted ligands, he expected that the complex would preferably form as fac-$Mn(CO)_3(N\hat{}N)X$ (5). The reaction in both solvents is found to follow a similar mechanism as given by monodentate substitution (D-mechanism), independent of the nature of the diimine ligand. Based on the molecular structure of the final product it can be suggested that there are two consecutive processes taking place involving elimination of two carbonyl groups. The rate of the

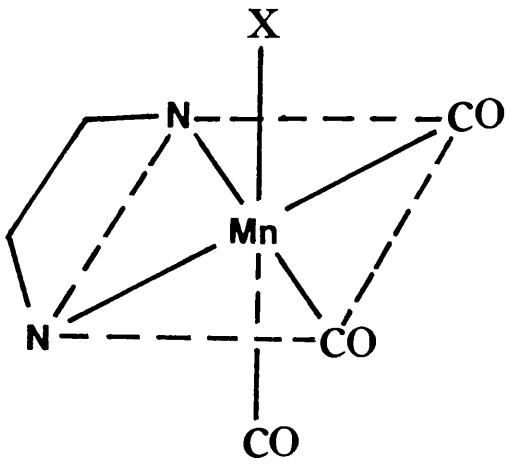

5

reaction is identical to the rate of monosubstitution by monodentante ligands (Equation [7-1]). Therefore, it is suggested that the rate determining-step of the process is given by the dissociation of the first carbonyl group, whereas the elimination of the second carbonyl and ring closure are known to proceed more quickly (Scheme 7-2).

Our present investigation of the reaction will concentrate on the role of solvent in controlling the mechanism and rate of the reaction. Some ideas about the solvent sensitivity of substitution reactions of $Mn(CO)_5X$ can be obtained from the earlier work by Angelici and Basolo.[16] They reported that the rate constant for the reaction between $Mn(CO)_5Br$ and $As(C_6H_5)_3$ decreases as the dielectric constant of solvent increases, except in polar solvents such as nitromethane and p-nitrotoluene. Burgess and Duffield[17] studied the rate of the reaction of $Mn(CO)_5Br$ with amino acids (β-alanine and glycine) in aqueous mixtures. They proposed that the rate of the reaction is given by two parallel processes, first-order and second-order.

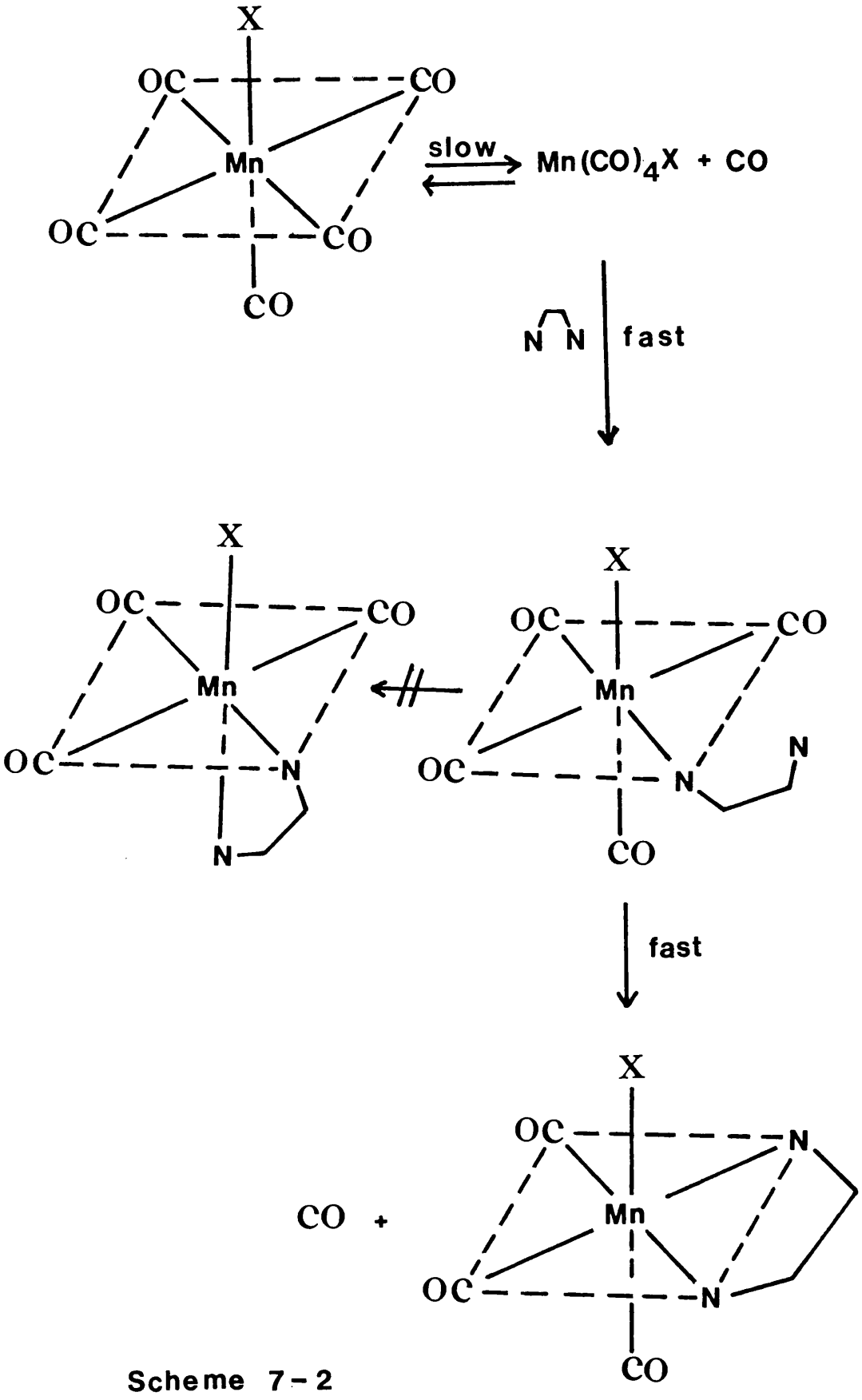
X
OC
CO
Mn
CO
OC
CO
CO
slow
Mn(CO)4X + CO
N N
fast
X
OC
CO
Mn
OC
N
N
X
OC
CO
Mn
OC
N
N
CO
fast
X
OC
N
Mn
CO +
OC
N
CO

Scheme 7-2

$$- \frac{d[Mn(CO)_5Br]}{dt} = \left[k_1 + k_2[\text{Amino acid}] \right][Mn(CO)_5Br] \quad ..[7\text{-}5]$$

where k_1 is the rate constant for self-decomposition of the complex and k_2 represents nucleophilic attack by the incoming ligand.

Our data in Table [7-1] include results for the observed rate constant, k_{obs}, of the reaction between $Mn(CO)_5Br$ and a large excess of diimine ligand (2,2'-bipyridine and 1,10-phenanthroline) in pure methanol and 50% (by volume) aqueous methanol mixture. The reaction in both solvents satisfies the rate law of Equation [7-5]. The plot of the observed rate constant against the concentration of the incoming ligand (N^N) in methanol (Figure 7-1) gives a straight line intercepting the vertical axis where [N^N]=0 at $(3.92 \pm 0.10)\times10^{-5}$ sec^{-1}. The bimolecular rate constant, k_2, for the reaction with incoming ligand 1,10-phenanthroline ($(2.80 \pm 0.10)\times10^{-4}$ M^{-1}sec^{-1}) is bigger than with 2,2'-bipyridine ($(1.22 \pm 0.10)\times10^{-4}$ M^{-1}sec^{-1}), indicating that the former group exhibits better nucleophilicity as expected because it is a stronger base. We also studied the pressure effect on the rate of the reaction, (Table [7-2]) which leads to an estimation of the volume of activation, $\Delta V^{\ddagger}$ as $+19.0 \pm 0.5$ cm^3 mol^{-1} (the kinetics at high pressure were carried out in methanol between $Mn(CO)_5Br$ (0.3 mM) and 2,2'-bipyridine (5 mM)). This large positive volume of

activation strongly indicates that the transition state is being dominated by the formation of a lower coordinated complex through a dissociative mechanism. Indeed, almost 98% of the observed rate constant at the diimine concentration used in these experiments is associated with rate constant k_1.

In aqueous methanol, even though the rate law remains unchanged, both self-decomposition and nucleophilic attack are quicker than in methanol, $(8.96 \pm 0.5)\times10^{-5}\,sec^{-1}$ and $(6.03\pm0.03)\times10^{-2}\,M^{-1}sec^{-1}$ for self-decomposition and 2,2'-bipyridine attack processes respectively. It is found that the self-decomposition rate constant is very close to the rate of the reaction of $Mn(CO)_5Br$ with β-alanine[17] (Figure [7-2]). In contrast, the reaction with β-alanine has shown no signs of the nucleophilic attack process, presumably the ligand is solvated very well in this medium. The determination of the rate of the reaction at various pressures between $Mn(CO)_5Br$ (0.3 mM) and 2,2'-bipyridine (5 mM) leads to an estimation of activation volume of the process as -18.0 ± 2.0 $cm^3\,mol^{-1}$. This large negative volume of activation suggests that the transition state is being dominated by bimolecular interchange. The larger contribution of rate constant for bipyridine attack (80%) on the observed rate constant at the measured point of high pressure kinetics is in good agreement with a negative volume of activation. Considering that process proceeds through elimination of carbonyl, the bimolecular interchange dominating the reaction seems to be relevant to the poor solvation of $Mn(CO)_5Br$ and carbonyl leaving group in this solvent.

However, a quicker rate of reaction of self-decomposition

in this solvent than in methanol, which has clearly broken away from the general trend (the rate decreases as dielectric constant increases), leaves a little doubt about the real process involved. This is because, in some cases, the reaction may also be considered to proceed by elimination of bromide. Several compounds basically derived from this process have been widely reported.[20-31] The formation of $Mn(CO)_5(MeCN)^+$,[22-24] for example, when treating $Mn(CO)_5Br$ in acetonitrile is one of the earlier indications of this reaction. Singh and Angelici[27] proposed that when $Mn(CO)_5Br$ is dissolved in a highly polar and coordinating solvent, the complex may dissociate the bromide group to form a solvento-complex.

$$Mn(CO)_5Br + Sol \longrightarrow Mn(CO)_5(Sol)^+ + Br^- \quad .... [7\text{-}6]$$

This suggestion follows from observations that the bromide catalyses the reaction between $Mn(CO)_5Br$ and aziridine ($\overline{HNCH_2CH_2}$) in acetonitrile leading to formation of metal-carbene complexes, but a similar mixture has not been observed in dichloromethane except after the addition of a bromide salt. Snow and Wimmer[28] reported the transfering of a yellow colour due to $Mn(CO)_5(ClO_4)$ from dichloromethane to an aqueous phase after shaking. The yellow colour of the aqueous solution is then assigned to the aquo complex $Mn(CO)_5(H_2O)^+$.

It has now become apparent that the process of bromide elimination from $Mn(CO)_5Br$ in aqueous solution cannot be simply ignored. In fact, our observation of gradual formation

of a more intense yellow solution at λ=390nm of $Mn(CO)_5Br$ in this solvent is probably associated with this process. Unfortunately, this product could not be isolated pure, therefore further analysis cannot be carried out. The presence of 2,2'-bipyridine may give a bromide elimination process, but rather quicker. Since the observed rate constant, k_{obs}, of the reaction indicates dependence on concentration of 2,2'-bipyridine, it can reasonably be suggested that the rate determining step of the process is given by associative interchange, followed by a quick ring closure and carbonyl elimination, to form $Mn(CO)_4(bipy)^+$. This suspected species gives absorption maximum in 50% aqueous methanol at λ = 413 nm which is higher than that for the corresponding $Mn(CO)_3(bipy)Br$ in similar solvent, where λ=402nm. This complex is very soluble. Behrens et al.[30-31] have been able to isolate the complex as the $[Mn(CO)_4(bipy][ZnCl_3]$ salt. But our attempt to prepare the complex in aqueous methanol was disappointing because a mixture was formed consisting of a small amount of $Mn(CO)_4(bipy)^+$, presumably as its bromide, and mainly $Mn(CO)_3(bipy)Br$. On treatment with toluene, some of the sample dissolved to give a yellowish orange solution (λ = 438 nm) which is associated with $Mn(CO)_3(bipy)Br$. On treatment with water, again some of the sample dissolved, this time giving a yellowish solution (λ=411 nm) which probably contains $Mn(CO)_4(bipy)^+$. In contrast, an authentic sample of $Mn(CO)_3(bipy)Br$ prepared in dioxan shows no sign of dissolving in water.

Thus the substitution process of $Mn(CO)_5Br$ may give two possible reactions, either carbonyl or bromide elimination,

depending on the nature of the solvent. It is expected that both elimination processes are always complementary, in that in low polarity solvents the carbonyl elimination is dominant whereas in high polarity solvents the favoured process is bromide elimination.

The process of bromide elimination is the best reason to be used in explaining for the unexpected observation of a negative volume of activation and dissociative mechanism for the reaction of $Mn(CO)_5Br$ and β-alanine in 50% aqueous methanol.[17] This result shows that the volume of the transition state is depressed very much, presumably due to solvation changes. In the ground state, the complex is neutral, thus solvation in this solvent is small. But the situation is changed in the transition state where the ionic species is formed, leading to much more solvation, consequently depressing the overall volume.

7-4. Charge Transfer Spectra of $Mn(CO)_3(bipy)Br$

As with their kinetics, the charge transfer spectra of complexes of the type $Mn(CO)_3(N\widehat{\ }N)X$ with X = Cl, Br or I and $N\widehat{\ }N$ a bidentate diimine ligand, have not been investigated even though the complex $Mn(CO)_3(bipy)I$ was identified quite early.[2] Schmidt[19] in monitoring the kinetics of the reaction of $Mn(CO)_5X$ with diimine ligands in toluene found a new band with higher intensity appearing in the visible region. This new band is associated with a charge transfer spectrum which arises from the transition of electrons from the metal t_{2g} -orbitals of metal to the lowest unoccupied orbitals (π^*)

of the diimine ligand (MLCT). This type of transition is analogous to those reported for the corresponding diimine complexes of molybdenum(0)[32-35] and iron(II).[36-38]

Table [7-2] includes the wavenumbers of maximum absorption of the charge transfer spectra of $Mn(CO)_3(bipy)Br$ in various organic solvents. The complex clearly exhibits solvatochromism; the wavenumber of maximum absorption increases as the polarity of the solvent increases. The plot of the wavenumber of maximum absorption against the respective polarities of solvent (based on E_T values from Reichardt)[39] gives two separate lines as shown in Figure [7-3]. This observation suggests that the solvent sensitivity of the $Mn(CO)_3(bipy)Br$ complex also needs to be considered in terms of two types of solvents, aprotic and protic. The slope of the plot for protic (154 ± 20) is larger than that for aprotic (104 ± 15) groups. Such order of the slope implies that the aprotic solvent gives a somewhat larger effect on charge transfer spectra of the complex, which is opposite to the trend reported earlier for $Mo(CO)_4(\widehat{N\ N})$ complexes. Figure [7-4] shows a plot of the wavenumber of maximum absorption of charge transfer spectra of $Mn(CO)_3(bipy)Br$ in various solvents against the corresponding wavenumber of maximum absorption of $Mo(CO)_4(bipy)$. Again, it is found that the graph shows two lines classifying, corresponding to the two groups of solvents. The slopes of the plots are 0.50 ± 0.02 and 1.03 ± 0.03 for aprotic and protic groups respectively. This result suggests that the aprotic solvents have a somewhat similar effect on charge transfer spectra for both complexes.

There is no satisfactory theory to explain the

differences of the solvent sensitivity on charge transfer spectra of both complexes. For the moment, we presume that such variation is largely due to differences in solvation behaviour of the complexes. For example, we have already seen that the complex $Mo(CO)_4(bipy)$ is relatively very well solvated in aprotic, less well solvated in protic solvents, in relation to their polarities. The situation probably changes for manganese(I) complex in which we expect that the presence of the hydrophilic bromide group in $Mn(CO)_3(bipy)Br$ will make the complex less preferably solvated in aprotic or non-polar solvents. This may explain the difference in wavenumber shift behaviour for these two compounds in series of polar and of non-polar solvents.

TABLE 7-1

Rate Constants for the Substitution Reaction of $Mn(CO)_5Br$ by Diimine Ligands in Methanol and 50% Aqueous-Methanol* at 298°K; initial $[Mn(CO)_5Br] = 3.0 \times 10^{-4}$ M.

$[N\frown N]$ $/10^{-3}$M	$10^5 k_{obs}/s^{-1}$ in MeOH		$10^4 k_{obs}/s^{-1}$ in 50% MeOH-Water
	bipy	phen	bipy
0	-	-	9.0
1.0	3.83	-	15.1
3.0	4.11	4.22	24.9
5.0	3.96	4.65	39.1
10.0	4.25	4.95	-
20.0	4.25	5.27	-
30.0	4.40	5.77	-
40.0	4.55	-	-

*
Solvent composition by volume prior to mixing.
$N\frown N$ = Diimine ligand

TABLE 7-2

Rate Constants for the Substitution Reaction of $Mn(CO)_5Br$ with 2,2'-bipyridine in Methanol and 50% Aqueous-Methanol at 298°K at various pressures; initial $[Mn(CO)_5Br] = 3.0 \times 10^{-4}$ M; $[bipy] = 5.0 \times 10^{-3}$ M

Solvent	$10^5 k_{obs}/s^{-1}$			$\Delta V^{\ddagger}$ / $cm^3\ mol^{-1}$
	at P_{atm}	at P_{340}	at P_{680}	
Methanol	4.31	3.21	-	+19.0 ± 0.5
	4.09	-	2.13	
50% Methanol-Water	59.1	99.3	-	-18.0 ± 2.0

P (Pressure) in bar.

TABLE 7-3

Wavenumbers of maximum absorption spectra, ν_{max}, of $Mn(CO)_3(bipy)Br$ and $Mo(CO)_4(bipy)$ in various organic solvents, with the corresponding solvent E_T values

Solvent	E_T/ kcal mol^{-1}	$10^{-3}\nu_{max}/cm^{-1}$ $Mn(CO)_3(bipy)Br$	$10^{-3}\nu_{max}/cm^{-1}$ $Mo(CO)_4(bipy)$
Methanol	55.5	24.75	21.79
Ethanol	51.9	24.30	21.32
n-Propanol	50.7	23.95	20.92
i-Propanol	48.6	23.75	21.00
n-Butanol	50.2	23.85	20.75
i-Butanol	-	23.75	-
Benzyl-alcohol	51.9	24.05	-
DMSO	45.0	24.20	22.78
DMF	43.8	24.15	22.62
CH_3NO_2	46.3	24.20	22.57
Ethylene-carbonate	46.6	24.10	-
CH_3CN	46.0	24.05	22.52
Acetone	42.2	23.90	22.08
Methyl ethyl-ketone	41.3	23.75	21.83
Acetophenone	41.3	23.85	21.79
Cyclohexanone	40.8	23.90	21.69
CH_2Cl_2	41.1	23.35	21.23
CH_2Cl-CH_2Cl	41.9	23.25	21.37
Ethyl acetate	38.1	23.50	21.23
Anisole	37.2	23.30	21.10
Chlorobenzene	37.5	23.00	20.66
Chloroform	39.1	23.10	20.58
Diethyl ether	34.6	23.00	20.24
Dioxan	36.0	23.25	-
Toluene	34.9	22.85	20.12
CCl_4	32.5	22.75	19.50

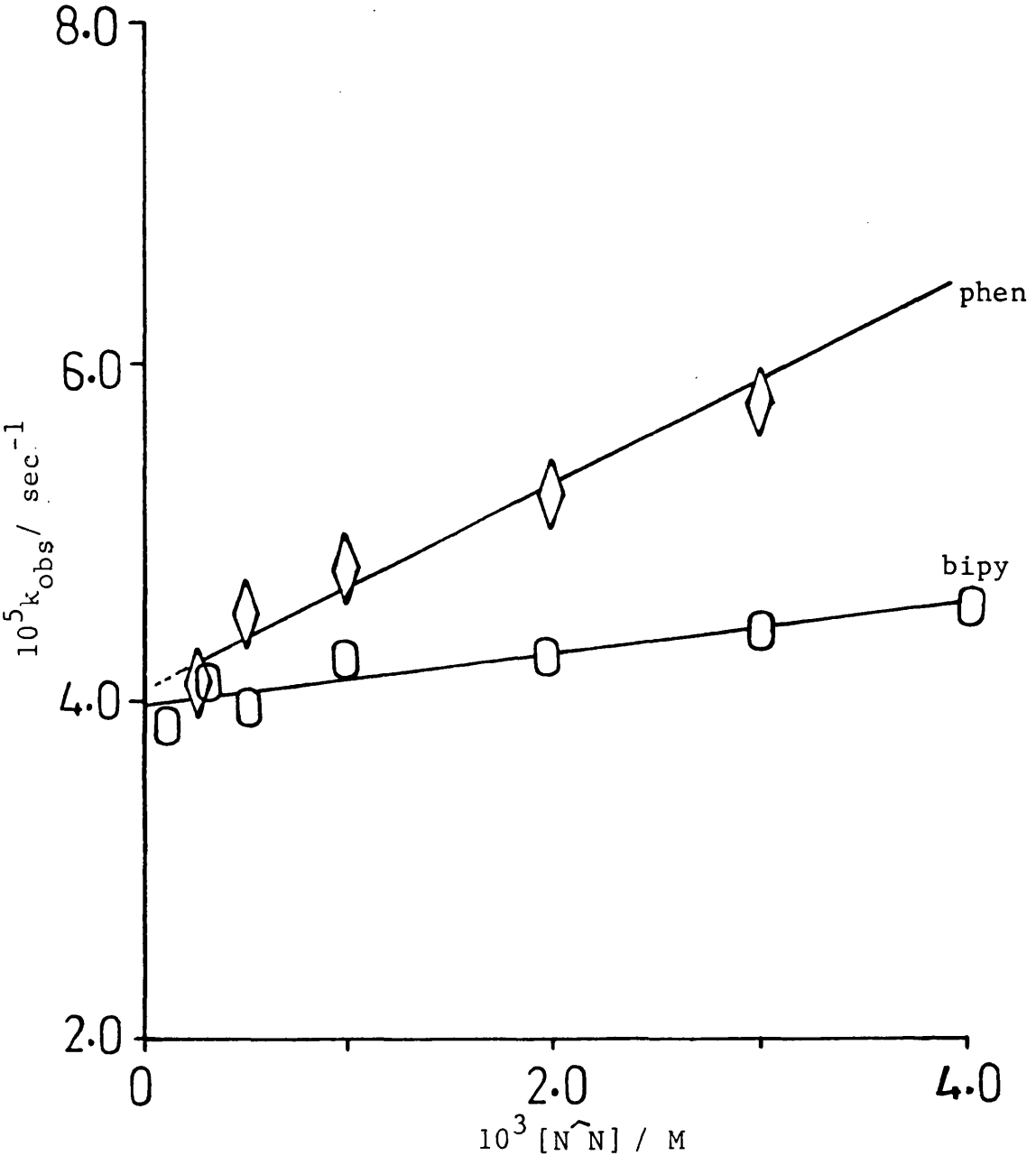

Figure [7-1] A plot of k_{obs} against concentration of incoming ligand [N^N] for the reaction between $Mn(CO)_5Br$ and diimine ligands in pure methanol at 298°K ; initial $[Mn(CO)_5Br] = 3x10^{-4}M$.

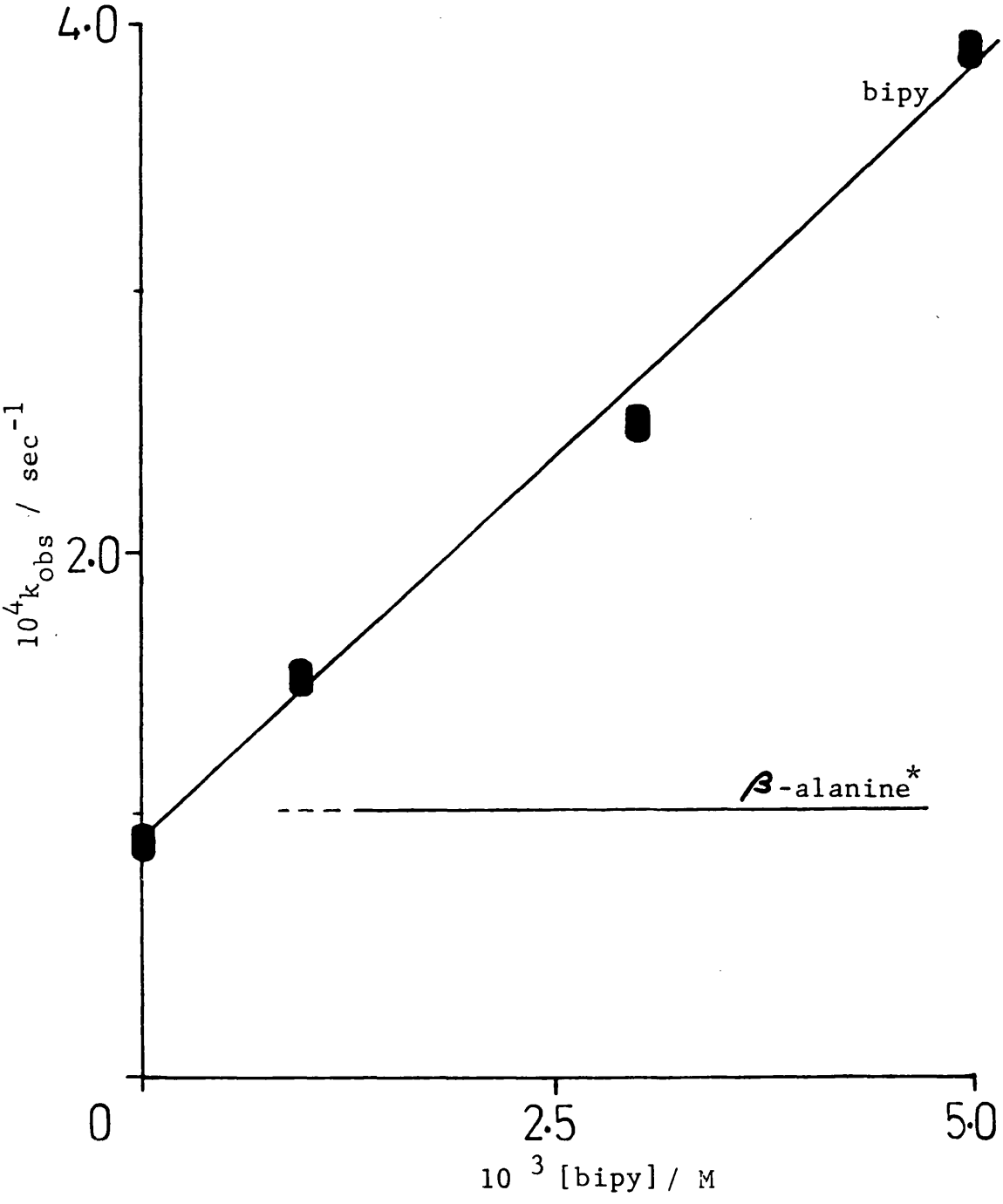

Figure [7-2] Graph of k_{obs} against [bipy] for the reaction between $Mn(CO)_4Br$ and 2,2'-bipyridine in 50% (volume) aqueous methanol at 298°K; initial $[Mn(CO)_5Br] = 3 \times 10^{-4}$M.

*Reference 17.

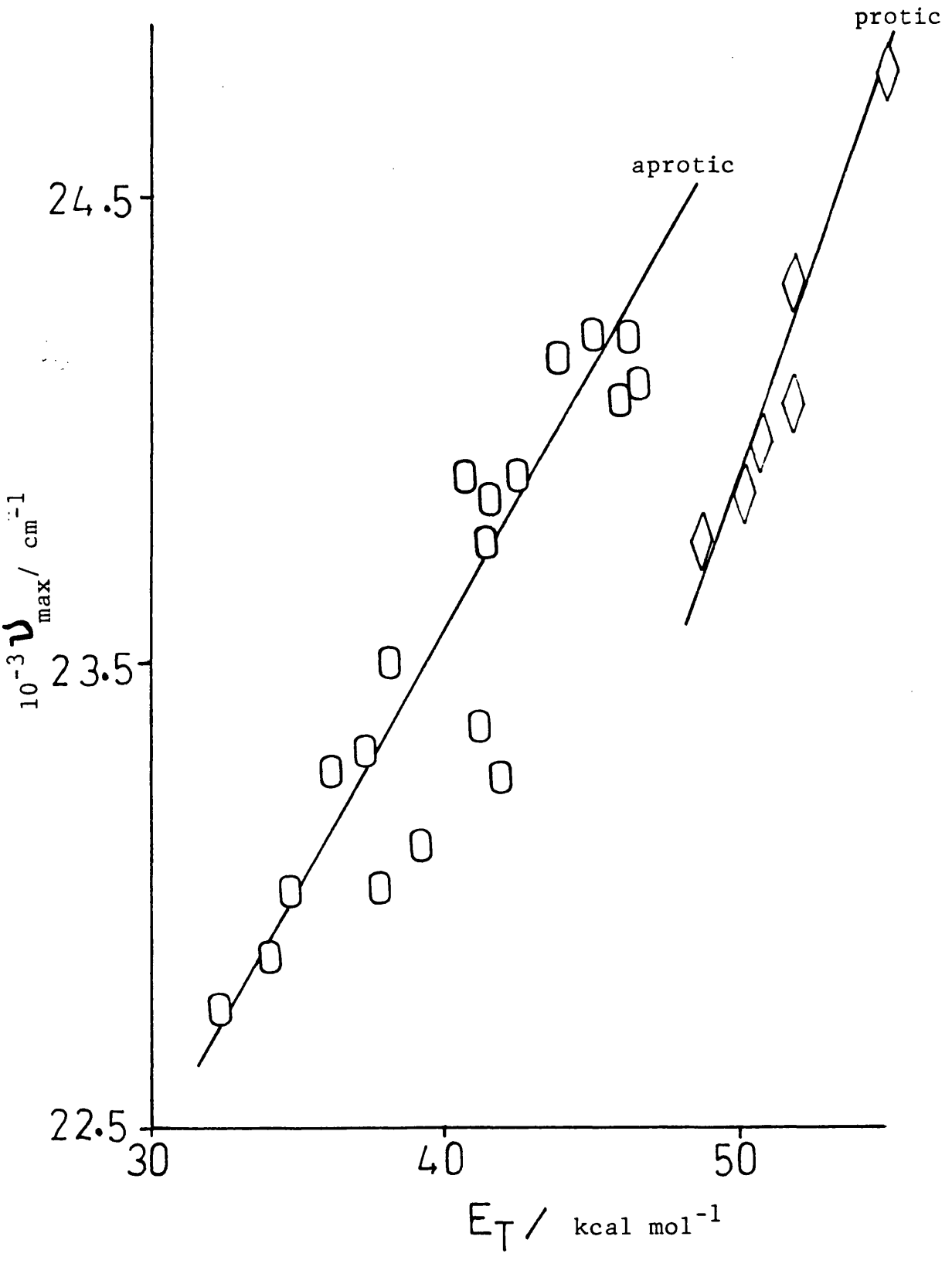

Figure [7-3] Plot of wavenumbers of maximum absorption, ν_{max}, of charge transfer spectra of $Mn(CO)_3(bipy)Br$ in various organic solvents against the corresponding E_T values.

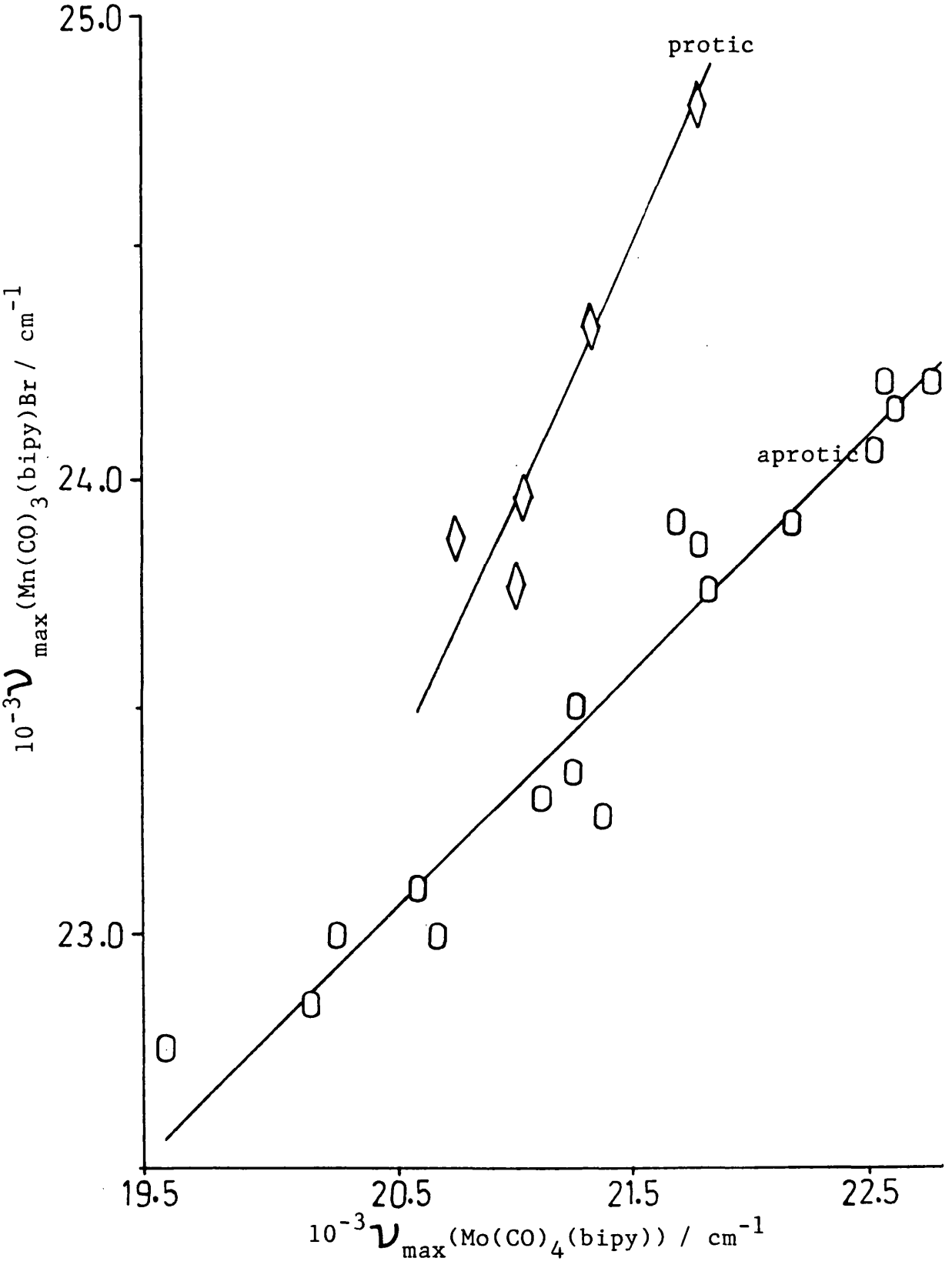

Figure [7-4] Plot of wavenumbers of maximum absorption ν_{max}, of charge transfer spectra of $Mn(CO)_3(bipy)Br$ in various organic solvents against the corresponding absorption for $Mo(CO)_4(bipy)$.

7-5. References

1. F.O. Brimm, M. A. Lynch and W. J. Sesny, J. Amer. Chem. Soc., 76, 3831 (1954)
2. E. W. Abel and G. Wilkinson, J. Chem. Soc., 1501 (1959)
3. (a) E. W. Abel, Hargreaves and G. Wilkinson, J. Chem. Soc., 3149 (1958).
   (b) A. M. Sladkov, N. A. Vasneva, A. A. Johansson, and V. V. Derunov, Inorg. Chim. Acta, 25, L97 (1977).
4. R. J. Angelici, F. Basolo and A. J. Poe, J. Amer. Chem. Soc., 85, 2215 (1963)
5. A. M. Bond, R. Colton and M. J. McCormik, Inorg. Chem., 16, 155 (1977)
6. A. M. Bond, B. S. Grabaric and Z. Grabaric, Inorg. Chem., 17, 1013 (1978)
7. J. D. Atwood and L. Brown, J. Amer. Chem. Soc., 97, 3380 (1975)
8. R. J. Angelici, Inorg. Chem., 3, 1099 (1964)
9. I. F. Wuyts and G. P. Vander Kelen, Inorg. Chim. Acta, 23, 19 (1977)
10. A. M. Bond, R. Colton and M. E. McDonald, Inorg. Chem., 17, 2842 (1978)
11. A. Wajcicki and F. Basolo, J. Amer. Chem. Soc., 83, 525 (1961)
12. B. F. G. Johnson, J. Lewis, J. R. Miller, B. H. Rabinson and A. Wojcicki, J. Chem. Soc.,A, 522 (1968)
13. T. L. Brown, Inorg. Chem., 7, 2673 (1968)
14. A. Berry and T. L. Brown, Inorg. Chem., 7, 2673 (1972)

15. A. J. Angelici and F. Basolo, J. Amer. Chem. Soc., 84, 2495 (1962)
16. A. J. Angelici and F. Basolo, Inorg. Chem., 2, 728 (1963)
17. J. Burgess and A. J. Duffield, J. Organomet. Chem., 177, 435 (1979)
18. D. F. Shriver (Edt.),"Inorganic Synthesis", Wiley, Vol: VI, 1979, p. 160.
19. G. Schmit, Diplomarbeit, Technische Hochshule Darmstard, 1985.
20 D. Palmer and H. Kelm, Coord. Chem. Rev., 36, 89 (1981)
21. D. J. Darensbourg, Adv. Organomet. Chem., 21, 113 (1982)
22. N. G. Connelly and L. F. Dahl, Chem. Commun., 880 (1970)
23. N. G. Connelly and J. D. Davies, Organomet. Chem., 38, 385 (1972)
24. R. H. Reimann and E. Singleton, J. Chem. Soc., Dalton Trans., 2638 (1973)
25. R. H. Reimann and E. Singleton, J. Chem. Soc., Dalton Trans., 808 (1973)
26. G. Wilkinson, F. G. A. Stone and E. W. Abel (Edts.), "Comprehensive Organometallic Chemistry", Pergamon Press, 1982, Vol:4, p. 63.
27. M. M. Singh and R. J. Angelici, Inorg. Chem., 23, 2699 (1984)
28. F. L. Wimmer and M. R. Snow, Aust. J. Chem., 31, 267 (1978)
29. F. L. Wimmer and M. R. Snow, Inorg. Chim. Acta, 44, L189 (1980)
30. H. Behrens, R. J. Lampe, P. Merback and M. Moll, J. Organomet. Chem., 159, 201 (1978)

31. H. Behrens, E. Lindner, D. Maertens, P. Wild and R. J. Lampe, J. Organomet. Chem., 34, 367 (1972)
32. H. Saito, J. Fujita and K. Saito, Bull. Chem. Soc. Jap., 41, 863 (1968)
33. J. Burgess, J. Organomet. Chem., 19, 218 (1969).
34. H. Bock and H. tom Dieck, Angew. Chem. Internat. Edn., 5, 520 (1966).
35. J. Burgess, J. G. Chambers and R. I. Haines, Transition Met. Chem., 6, 145 (1981).
36. J. Bjerrum, A. W. Adamson and O. Bostrup, Acta Chem. Scand., 10, 329 (1956)
37. J. Burgess, Spectrochim. Acta, A26, 1369, 1967 (1970)
38. H. Kabayashi, B. V. Agarwala and Y. Kaizu, Bull. Chem. Soc. Jap., 48, 465 (1975)
39. C. Reichardt, Angew. Chem. Internat. Edn., 4, 29 (1965).

CHAPTER 8

Kinetics of Substitution Reactions of Bis(cyclopentadienyl)dichloro-Titanium(IV), -Vanadium(IV) and -Zirconium(IV)

2-1. Introduction

The formation of compounds of the type $M(Cp)_2X_2$, where M =Ti(IV), V(IV), or Zr(IV), X = F, Cl, Br, I, SCN, N_3 etc and Cp = cyclopentadienyl (η^5-C_5H_5), has long been known.[1-7] The complexes are pseudo-tetrahedral[8] in which six π-electrons in the system of the cyclopentadienyl ion are bound to the metal atom as in ferrocene, $Fe(Cp)_2$.[9,10] In the beginning, due to the formation of a complex between $Ti(Cp)_2Cl_2$ and aluminium chloride and alkyl-aluminium chloride,[11] the complex was thought to be dimeric in solution. However, estimation of the molecular weight of the complex in various solvents confirms that it is mainly monomeric. The d-orbitals of the metal atoms of the complexes, except for vanadium(IV), are empty (vanadium(IV)-d^1, titanium(IV) and zirconium(IV)-d^0). This configuration makes the complexes unlikely for vanadium(IV) and impossible for titanium(IV) and zirconium(IV) to be stabilized by metal to ligand back-bonding. This argument is consistent with no reported a formation of complexes of the metals at this oxidation state with carbonyl and other strong π-acceptor ligands.[12,13] A vacant d-orbital, on the other hand, renders the metal atom in the complex more open to nucleophilic attack. This behaviour has been the subject of several previous studies as well as the present one.

Jensen and Basolo[14] first investigated kinetic behaviour by studying the substitution process of $Ti(Cp)_2Br_2$ with different sources of chloride in benzene and in tetrahydrofuran (THF), leading to the formation of $Ti(Cp)_2Cl_2$. They reported that the reaction with quaternary ammonium

chloride salts proceeds through a bimolecular (i.e. second order) process but is nearly unimolecular (i.e. first order) with lithium chloride. This observation implies that the reactivity of the chloride ion as the attacking group varies from one salt to another. Presumably the first step involves attack on the complex by the predominant ion-pairs of chloride and the accompanying cation. This suggestion is probably reasonable since titanium(IV) can increase its coordination number and thus provides a lot of space for large incoming ligands.

Langford and Aplington[15] extended the study to other dihalide titanium(IV) complexes $Ti(Cp)_2Br_2$ with several incoming groups, Y, in acetone. They showed that the rate law for all reactions generally consists of two parallel mechanisms with first and second order terms.

$$\text{rate} = \left\{k_1 + k_2[Y]\right\}[Ti(Cp)_2X_2] \quad \ldots \quad [8\text{-}1]$$

k_1 is a rate constant due to halide dissociation, which may well be solvent assisted, whereas k_2 represents nucleophilic attack by the incoming ligand Y. This kinetic pattern is similar to that reported for $Ti(acac)_2Cl_2$ complex.[16]

The work presented here is mainly centred on the study of the substitution reactions of the dihalide complexes (Equation [8-2]) in acetonitrile. This solvent was chosen as a compromise between minimising solvolysis and maximising solubility of salts of incoming anionic nucleophiles.

$$M(Z\text{-}Cp)_2Cl_2 + 2Y^- \longrightarrow M(Z\text{-}Cp)_2Y_2 + 2Cl^- \quad \ldots [8\text{-}2]$$

Apart from the mechanism, we also planned to study the comparative reactivities among various changes of complexes. These include the effect of varying the complex (M = Ti(IV), V(IV), or Zr(IV) and Z = H or CH_3), incoming group Y^-, and solvent (mixtures containing small amounts of water and toluene).

8-2. Experimental

(i) Preparative

(a) Starting Complexes

All the dichloro complexes of $M(Z\text{-}Cp)_2Cl_2$ where M = Ti(IV), V(IV) or Zr(IV), and Z = H or CH_3 were prepared by Dr. A. T. Casey of the University of Melbourne. Their analysis are summarized in Table [8-4].

(b) Dithiocyanatobis(η^5-cyclopentadienyl)titanium(IV); $Ti(Cp)_2(NCS)_2$.

About 0.5 g of $Ti(Cp)_2Cl_2$ was dissolved in 50 cm^3 of acetonitrile and then 0.6 g of KNCS was added. The solution was stirred in a beaker, using a magnetic stirrer, at 40-50°C while the solvent evaporated for about an hour. More solvent

was removed using a rotary evaporator until 5-10 cm^3 remained; then 25 cm^3 of water was added. The red precipitate of $Ti(Cp)_2(NCS)_2$ appeared. The solution was filtered and the precipitate washed with 5 cm^3 of cooled distilled water.

A similar procedure was used to prepare $Ti(Cp)_2Br_2$ from lithium bromide (0.5 g). Analysis results are also given in Table [8-4].

(ii) Kinetic Measurements

All materials used in kinetic experiments were analytical grade: potassium thiocyanate (Hopkin and Williams), lithium bromide and lithium iodide (BDH) and tetraethylammonium cyanide (Fluka). Acetonitrile and toluene were dried using 0.4 mm molecular seive.

The kinetics of the reaction were monitored by using a thermostatted quartz cell in an HP 8551A spectrophotometer. The formation of the product was followed at the corresponding wavelength of maximum absorption. In all cases, the reactions were carried out with a large excess of incoming ligand so that the first-order rate law was obeyed. The observed rate constants, k_{obs}, were calculated by computer from the slope of $\ln(A_\infty - A)$ against time for at least two and half half-lives.

8-3. Results

All the kinetic measurements were carried out in acetonitrile or acetonitrile-rich mixtures at 25°C and 1 atm pressure. It is found that the rate constants of the reaction

are dependent on the nature of the entering group, the complex, and the solvent. In the following we shall describe the results of the kinetics of the reactions based on these natures separately.

(a) Entering Group

The effect of the entering group was studied for the reaction of $Ti(Cp)_2Cl_2$ in acetonitrile. The entering groups include I^-, Br^-, NCS^-, and CN^-. The salts used were LiBr, LiI, KNCS, and Et_4NCN, with the choice of cation governed by solubility considerations. Table [8-1] lists results for the reactions involving various concentrations of the entering groups. It shows that the observed rate constant, k_{obs}, increases as the concentration of the entering group increases. A plot of k_{obs} against concentration of the entering group gives a straight line as displayed in Figure [8-1]. This observation leads to the conclusion that the rate law of the reaction is similar to that given by Equation [8-1], where

$$k_{obs} = k_1 + k_2[Y] \qquad \ldots [8\text{-}3]$$

The rate constants k_1 and k_2 are estimated from extrapolation to [Y] = 0 and from the slope of the plot respectively. These results are also summarized in Table [8-1].

As expected, the rate constant, k_1, is insensitive to the

nature of the incoming group. The value remains similar for all types of group. The plots of Figure [8-1] for several incoming ligands intercept the vertical axis where [Y] = 0 at a single point $\bar{k}_1 = (2.81\pm0.05)\times10^{-3}s^{-1}$. The rate constant k_2 is rather different. It depends very much on the nature of the incoming group and thus it is suggested that the process proceeds through a bimolecular interaction. Such typical rate constants have been widely used in many types of reactions to estimate the relative nucleophilicity among incoming groups. In this case, the higher the rate constant for a given incoming group the better is its nucleophilicity, increasing as follows:

$$Cl^- < Br^- < I^- << NCS^- < CN^-$$

(b) Complex

The effect of varying the complex was studied using $M(Z\text{-}Cp)_2Cl_2$ where Z= H or CH_3 and M = Ti(IV) , V(IV), or Zr(IV), with thiocyanate (NCS^-) in acetonitrile leading to the formation of $M(Z\text{-}Cp)_2(NCS)_2$:

$$M(Z\text{-}Cp)_2Cl_2 + 2NCS^- \longrightarrow M(Z\text{-}Cp)_2(NCS)_2 + 2Cl^- \ldots [8\text{-}4]$$

The observed rate constants, k_{obs}, of the the reactions are summarized in Table [8-2] and plotted against concentration of

thiocyanate as shown in Figure [8-2]. The result clearly indicates that for all types of complex the rate law of the reaction follows a similar pattern, given by Equation [8-1]. The calculated rate constants k_1 and k_2 are also listed in Table [8-2]. It is found that these rate constants decrease as M is changed from titanium(IV) to vanadium(IV) and Z from hydrogen to methyl. In this work, we also intended to measure the kinetics of the reaction involving zirconium(IV). However, it was impossible to follow this reaction because the complex reacts very fast leading to instant formation of a cloudy white solution.

The effect of changing the metal atom from titanium(IV) to vanadium(IV) retards the rate of thiocyanate attack, k_2, and of self-dissociation, k_1, by 20 and 15 times respectively. The presence of methyl groups in cyclopentadienyl also retards the reaction but the effect is smaller; 4 times for thiocyanate attack and 2.5 times for self-dissociation processes.

(c) Solvent

The experiments reported in this section are concerned with the effect of adding co-solvents, namely protic (water) and aprotic (toluene) to the main medium (acetonitrile) on the rate of reaction of $Ti(Cp)_2Cl_2$ with thiocyanate. The observed rate constants, k_{obs}, of the reactions at various concentration of thiocyanate are summarized in Table [8-3]. The reactions satisfy the rate law of Equation [8-1]. The plot of the observed rate constant, k_{obs}, against the concentration

of thiocyanate gives a straight line as shown in Figure [8-3] from which the rate constants for thiocyanate attack, k_2, and self-dissociation, k_1, can be estimated. These results are also listed in Table [8-3]. It is found that the presence of water in the reaction medium retards the rate of the thiocyanate attack but enhances the rate of self-dissociation. The presence of toluene, on the other hand, accelerates thiocyanate attack but retards the self-dissociation process. Plots of the rate constants k_1 and k_2 against percentage volume of co-solvent are displayed in Figure [8-4]. These trends indicate that the roles of water and toluene in solvating the reactants are always opposite.

8-4. Discussion

(a) Mechanism

As mentioned earlier, the main aim of this study was to ascertain the kinetics of the substitution reaction

$$M(Z\text{-}Cp)_2Cl_2 + 2Y^- \longrightarrow M(Z\text{-}Cp)_2Y_2 + 2Cl^- \qquad \ldots [8\text{-}5]$$

The uv-visible and elementary analysis studies on the yield of the reaction, as summarized in Table [8-4], confirm that the final product consists of $M(Z\text{-}Cp)_2Y_2$. This observation suggests that the overall reaction might proceed by two consecutive displacement processes.

$$M(Z\text{-}Cp)_2Cl_2 + Y^- \longrightarrow M(Z\text{-}Cp)_2YCl + Cl^- \quad \ldots [8\text{-}6]$$

$$M(Z\text{-}Cp)_2YCl + Y^- \longrightarrow M(Z\text{-}Cp)_2Y_2 + Cl^- \quad \ldots [8\text{-}7]$$

Jensen and Basolo[14] found a single rate determining step in their kinetic study of chloride exchange. In our system, in order to find out the rate determining step, we recorded the absorption spectrum of the reaction between $Ti(Cp)_2Cl_2$ with lithium bromide at various times during the reaction. The reaction goes almost to completion with two isobestic points as shown in Figure [8-5]. On examining the spectra, we found that there is no significant trace of the intermediate $Ti(Cp)_2BrCl$; the initial and final spectra were essentially identical with $Ti(Cp)_2Cl_2$ and $Ti(Cp)_2Br_2$ respectively. Presumably the latter step proceeds very quickly to form a product. So the rate of the controlling step is given by the first process, Equation [8-6].

The kinetic studies of all the reactions give a rate law indicating two parallel processes; unimolecular and bimolecular.

$$\text{rate} = \left\{k_1 + k_2[Y]\right\}[M(Z\text{-}Cp)_2Cl_2] \quad \ldots [8\text{-}8]$$

k_1 is the rate constant given by the dissociation process presumably due to interaction with the solvent. An indication of the interaction can be seen clearly as in the presence of water k_1 increases but decreases in the presence of toluene.

k_2 represents the rate constant of nucleophilic attack. The rate of reaction is determined by how easily the incoming group approaches and attacks the metal atom in the complex. The proposed mechanism of the reaction is shown in Scheme [8-1].

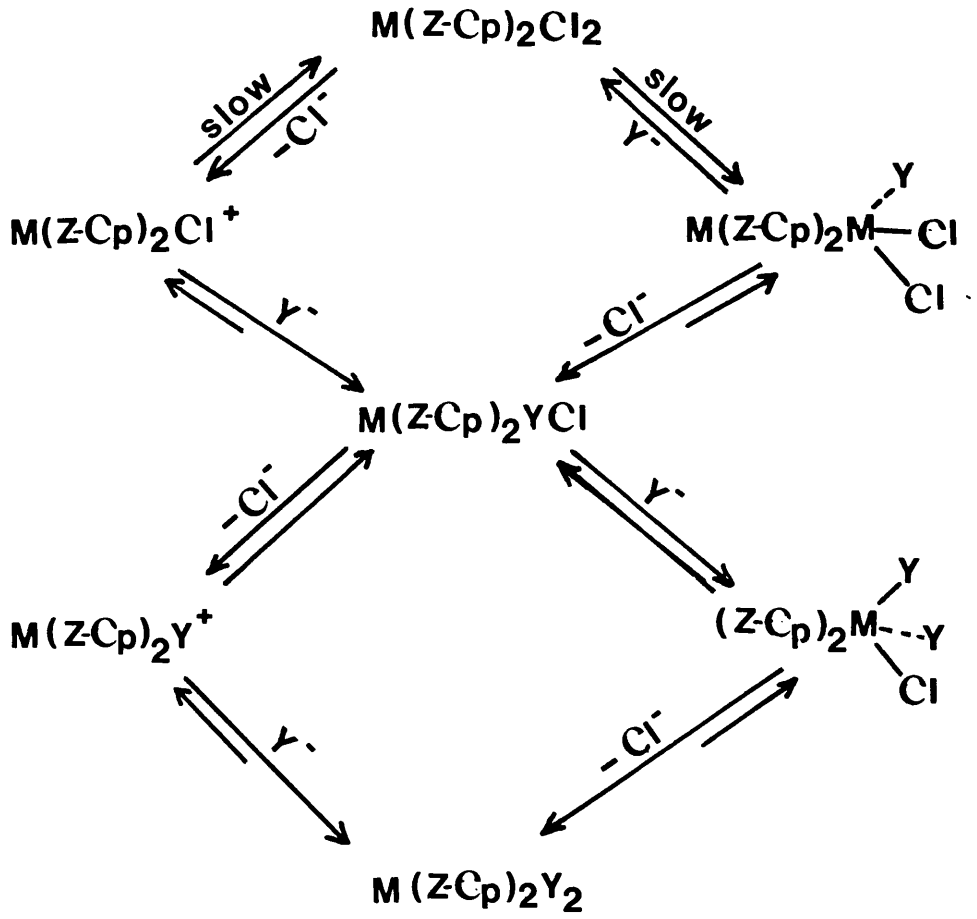

Scheme 8-1

(b) Nucleophilicity

A study of the reaction between $Ti(Cp)_2Cl_2$ and various incoming ligands leads to a series of increasing nucleophilicity as follows:

$$Cl^- < Br^- < I^- << NCS^- << CN^-$$

Thiocyanate reacts very well with $Ti(Cp)_2Cl_2$ to give the intense colour of $Ti(Cp)_2(NCS)_2$. Our result indicates that it reacts almost twenty times more quickly than bromide and fifteen times more quickly than iodide. This observation suggests that the thiocyanate is more nucleophilic than the halides. Thus thiocyanate was used as the incoming group when monitoring the other effects on the rate of the reaction.

The reactions with bromide and iodide, on the other hand, only give good results at large concentrations of bromide and iodide. The problem arises, as suggested by Jensen and Basolo,[14] due to the reverse process taking place, e.g.:

$$Ti(Cp)_2Cl_2 + 2Br^- \longrightarrow Ti(Cp)_2Br_2 + 2Cl^- \quad \ldots [8\text{-}9]$$

Unlike the halides, the thiocyanate is triatomic. It may coordinate to the metal in the complex $M(Cp)_2(NCS)_2$ through the nitrogen atom M-NCS or sulphur M-SCN. Vibrational studies on metal-thiocyanate indicate that M-NCS is the more probable bonding in the complex.[17-22] Our kinetic measurements show that the mixing of the complex and cyanide ion is followed by rapid

disappearance of the colour of the dichloro complex. We were unable to follow this reaction with our present apparatus. This observation indicates that cyanide ion is the strongest nucleophile.

(c) Stability of the Complex

Different reactivities for different complexes reflect changes in stability which normally follow from the arrangement of the electrons in the complex. In this work, we have looked at such an effect from the reaction between $M(Z\text{-}Cp)_2Cl_2$, where Z = H or CH_3 and M = Ti(IV) or V(IV), with thiocyanate in acetonitrile. It is found that the rate of reaction decreases as M changes from titanium(IV) to vanadium(IV) and Z from hydrogen to methyl groups.

In the former case, changing the metal atom in the complex from titanium(IV)-d^0 to vanadium(IV)-d^1 results in the addition of a single electron to the system. Since the d-orbitals in the complex are split into various energy levels, as predicted by the Crystal Field theory,[23,24] the single electron in vanadium(IV) will occupy the lowest energy d-orbital. Such a configuration leads to some crystal field stabilization of the complex. Again, as predicted by Crystal Field theory, the lowest d-orbital in a complex points to an area between metal-ligand bonds, in which a possibility of nucleophilic attack takes place. The presence of a single electron of vanadium(IV) in this orbital screens the metal atom from being approached and attacked easily by an incoming group (NCS^-).

The effect of the methyl substituent in the cyclopentadienyl group may be explained by two possible reasons. The first is based on the consideration that the methyl group is a good electron donor. The presence of the group in cyclopentadienyl may result in the reduction of the positive charge on the metal atom, thus reducing interaction with the negatively charged incoming group (NCS^-). The second explanation is based on a screening effect by the methyl group. As mentioned earlier, the cyclopentadienyl group is bonded to the metal atom through its π-orbital, so that the plane of the cyclopentadienyl ring is directly facing the metal atom in the centre, Figure [8-6]. This position allows the ligand to occupy a large space around the metal atom in the complex which sterically protects the metal atom from being attacked by the incoming group. The presence of a methyl group on the cyclopentadienyl ring increases the size of the ligand and consequently increases the steric protection of the metal atom.

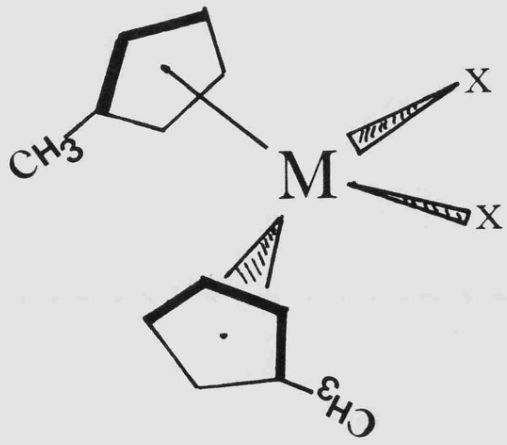

Figure [8-6] Molecular structure of $M(CH_3\text{-}Cp)_2X_2$

(d) Role of the Solvent

The effect of solvent on the rate of reaction of several organic and inorganic compounds has been widely reported.[25-29] The majority of reactions exhibit solvent dependence. A recent explanation suggests that reactivity in a particular solvent is associated with the solvation behaviour of the reactants. In the present study, we report the effect of the addition of a small amount of water or toluene to the main medium (acetonitrile) on the rate of the reaction of $Ti(Cp)_2Cl_2$ with thiocyanate. The results indicate solvent dependence . However, since the overall reaction involves two parallel mechanisms, dissociative and thiocyanate attack, it is convenient to explain the effect on both pathways separately. Our observation shows that the solvent has opposite effects on the two mechanisms. In the presence of water and toluene the rate of dissociative process increases and decreases respectively. However, the rate of thiocyanate attack decreases in the presence of water and increases in the presence of toluene.

In thiocyanate attack, the rate of reaction reflects the ability of a thiocyanate group to approach and attack the metal atom in the complex. The present result suggests that the solvation of thiocyanate is a dominant factor in influencing the process. If the thiocyanate group is strongly solvated, as expected in the presence of water, it will be massively surrounded by the solvent molecules, thus it will be less able to attack and the rate will be slower. Similarly, in the presence of toluene, the thiocyanate group is expected to

be less solvated so the process goes more quickly.

In contrast, the rate constant k_1, obviously unaffected by the solvation of thiocyanate, may be expected to be influenced by solvation of the leaving group. This argument is related to the observation by Jensen and Basolo[14] that the rate constant of the dissociative process of $Ti(Cp)_2Br_2$ increases in presence of water. In fact, recent reports prove that these types of complexes are quickly hydrolysed in water.[30] As expected, the chloride leaving group in $Ti(Cp)_2Cl_2$ is increasingly solvated in the presence of water. Thus the rate of Ti-Cl bond-breaking is faster. Such a reaction pattern is similar to that reported for the solvolysis of tert-butyl chloride.[31,32] In the presence of toluene, on the other hand, the chloride leaving group will be less solvated, so the potential for bond breaking is less and the reaction becomes slower.

TABLE 8-1

Kinetics of substitution of $Ti(Cp)_2Cl_2$ in acetonitrile with various incoming group, Y , at 298°K.

Y[a]	$10^3 k_{obs}/s^{-1}$ in [Y]/ M						
	0.01	0.03	0.05	0.08	0.10	0.15	0.20
NCS^-	3.89	8.54	11.21	19.63	23.22	32.94	39.52
I^-	-	3.97	3.59	-	3.68	4.89	5.40
Br^-	-	3.51	2.92	-	2.83	3.41	3.85
CN^-	The reaction goes very fast[b]						

[a] Added in the form of KNCS, LiBr, LiI and Et_4NCN.

[b] Give a lower limit or a rough estimate for k_{obs}.

TABLE 8-2

Kinetics of substitution of $M(Z\text{-}Cp)_2Cl_2$ in acetonitrile with NCS^- at 298°K; M = Ti and V and Z = H or CH_3.

Complex	$10^3 k_{obs}/s^{-1}$ with various $[NCS^-]/M$							$10^2 k_2$	$10^3 k_1$
	0.01	0.03	0.05	0.08	0.10	0.15	0.20	$/M^{-1}s^{-1}$	$/ M^{-1}$
$Ti(Cp)_2Cl_2$	3.89	8.54	11.21	19.63	23.22	32.94	39.52	19.23	2.82
$Ti(CH_3\text{-}Cp)_2Cl_2$	1.50	2.44	4.20	-	6.87	9.41	11.34	5.28	1.21
$V(Cp)_2Cl_2$	-	-	0.58	-	1.03	1.66	1.98		

TABLE 8-3

Kinetic of substitution reaction of $Ti(Cp)_2Cl_2$ with NCS^- in acetonitrile-water and acetonitrile-toluene mixtures at 298°K

(a) Acetonitrile-water

solvent %(volume) CH_3CN	10^3 k_{obs}/s^{-1} with $[NCS^-]/M$								10^2 k_2 $/M^{-1}s^{-1}$	10^3 k_1 $/ s^{-1}$
	0.01	0.02	0.03	0.05	0.08	0.10	0.12	0.15		
100	3.89	5.71	8.54	11.21	19.63	23.22	25.11	32.94	19.23	2.82
99	4.34	-	8.56	11.52	17.11	20.91	-	27.68	16.77	3.28
97	9.67	-	12.71	17.18	22.31	22.88	-	-	15.66	8.49
95	18.52	20.76	21.49	22.54	24.11	31.82	-	-	14.41	17.20

TABLE 8-3

(b) Acetonitrile-toluene

Solvent %volume CH_3CN	$10^3\ k_{obs}/s^{-1}$ with $[NCS^-]/M$						$10^2\ k_2$ $/M^{-1}s^{-1}$	$10^3\ k_1$ $/\ s^{-1}$
	0.01	0.03	0.05	0.08	0.10	0.15		
95	3.86	8.66	13.86	22.14	25.67	40.73	26.11	8.74
90	3.81	8.91	14.98	25.73	33.73	-	33.44	0

TABLE 8-4

UV-Visible spectroscopic data and microanalysis of some $M(Z\text{-}Cp)_2X_2$; Z = H or CH_3 , M = Titanium(IV) or Vanadium(IV) and X = Cl, Br,I or NCS

Complex		Microanalysis			Wavelength	
		%C	%H	%N	Acetonitrile /nm	Acetone /nm
$Ti(Cp)_2Cl_2$	calculated observed	48.19 48.43	4.02 4.24	0.00 0.00	393 (2300)	392 (2150)
$Ti(Cp)_2Br_2$	calculated observed	35.50 35.86	2.96 3.05	0.00 0.02	426 (3200)	-
$Ti(Cp)_2I_2$	-	-	-	-	450	-
$Ti(Cp)_2(NCS)_2$	calculated observed	48.98 48.86	3.43 3.56	9.52 9.21	436 (12800)	440 (12400)
$Ti(Z\text{-}Cp)_2Cl_2$	calculated observed	51.99 49.36	5.02 4.87	0.00 0.04	392 (2500)	-
$V(Cp)_2Cl_2$	calculated observed	47.81 47.96	3.93 4.05	0.00 0.02	482 (4000)	-

Numbers in bracket indicate molar extinction coefficients.

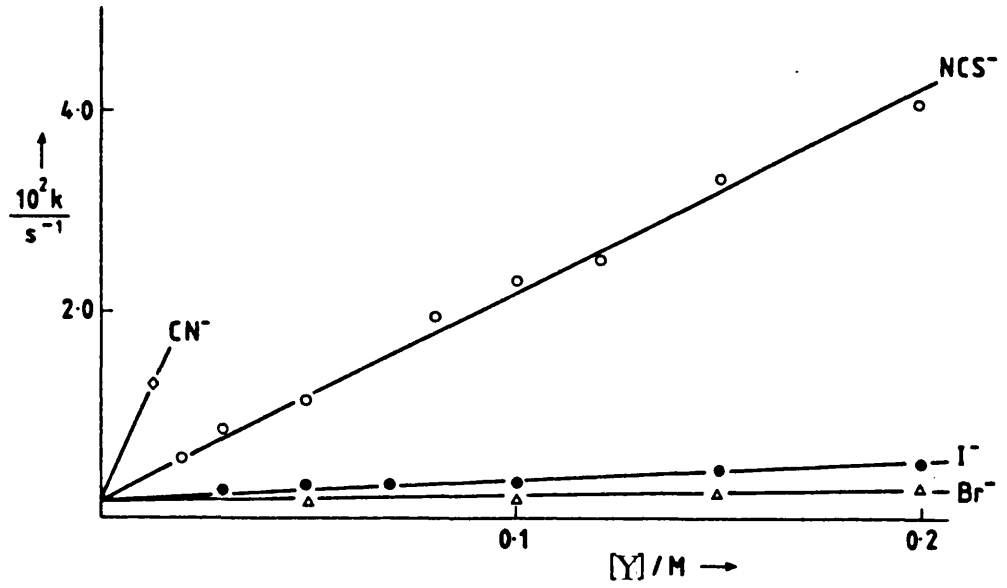

Figure [8-1] Plots of observed rate constants, k_{obs} against the concentration of incoming ligand, Y, for substitution reaction of $Ti(Cp)_2Cl_2$ complex with various Y in acetonitrile at 298°K.

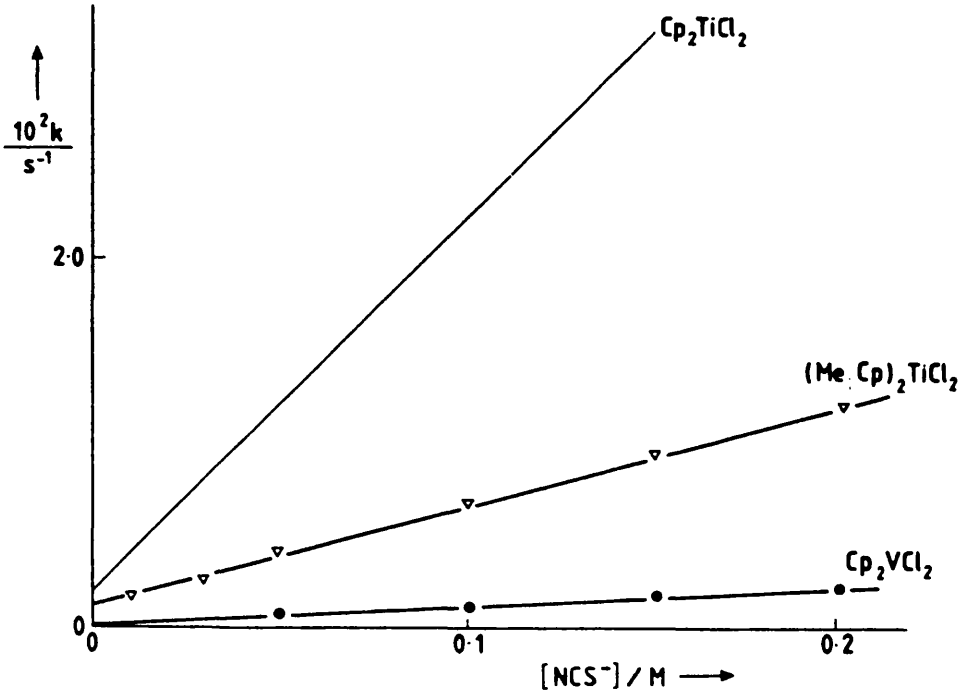

Figure [8-2] Plots of observed rate constants, k_{obs}, versus $[NCS^-]$ in acetonitrile for the reaction between $M(Z\text{-}Cp)_2Cl_2$ complexes with NCS^-; M = Ti(IV), or V(IV) and Z = H or Me, at 298°K.

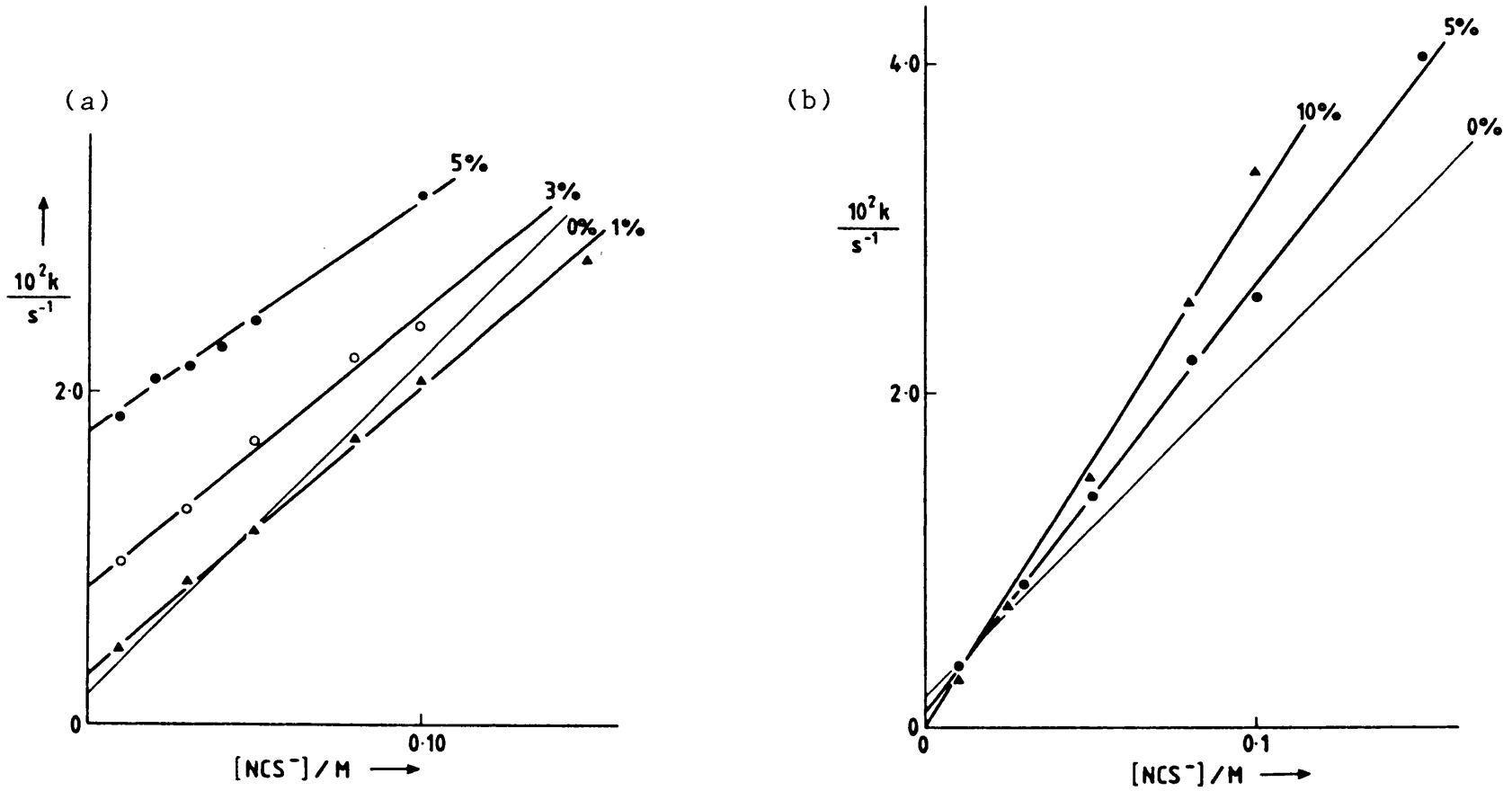

Figure [8-3] Plots of observed rate constants, k_{obs}, against $[NCS^-]$ for the reaction of $Ti(Cp)_2Cl_2$ with NCS^- at 298°K in binary mixtures; (a) acetonitrile-water and (b) acetonitrile-toluene.

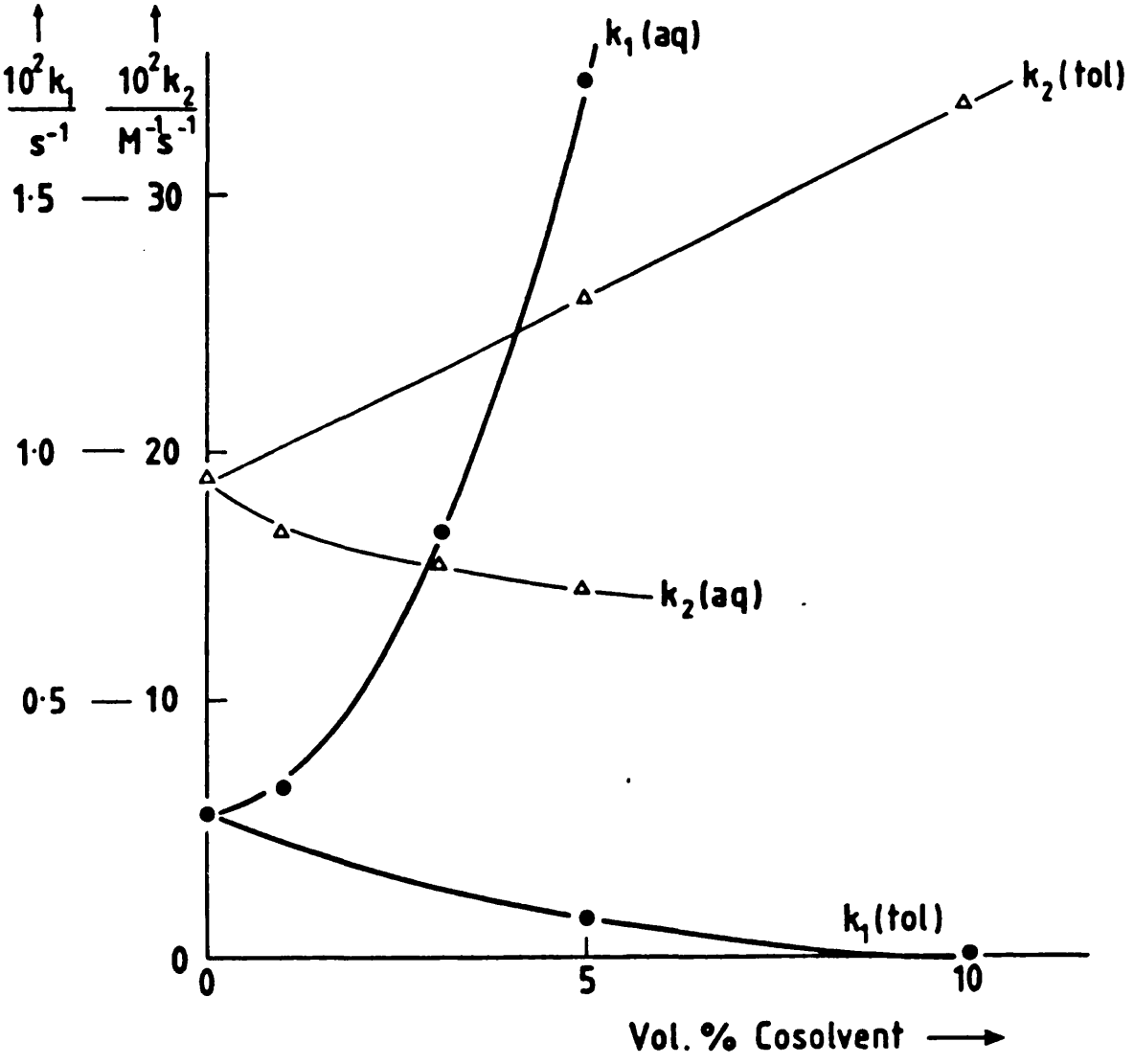

Figure [8-4] Plots of rate constants for thiocyanate attack (k_2) and self-decomposition (k_1) of $Ti(Cp)_2Cl_2$ complex against percentage volume of co-solvents to acetonitrile; water and toluene.

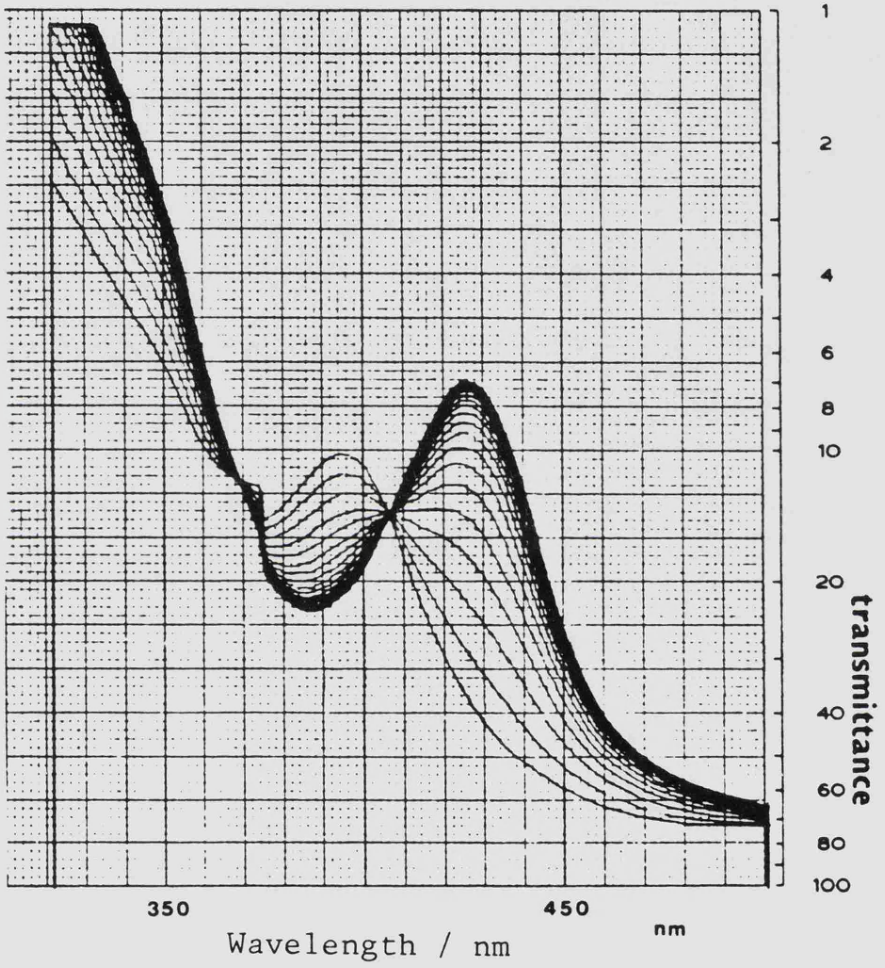

Figure [8-5] Continuous recording spectra for every one minutes of the reaction between $Ti(Cp)_2Cl_2$ complex with Br^- in acetonitrile at 298°K; $[Ti(Cp)_2Cl_2] = 5x10^{-4}M$ and $[Br^-] = 0.1M$.

8-5. References

1. G. Wilkinson and J. M. Birmingham, J. Amer. Chem. Soc., 76, 4281 (1954).
2. S. A. Griddings, Inorg. Chem., 6, 849 (1967).
3. J. L. Burmeister, E. A. Deardorff and C. E. van Dyke, Inorg. Chem., 8, 170 (1969).
4. G. Doyle and R. S. Tobias, Inorg. Chem., 7, 2479 (1968).
5. J. W. C. Chien, J. Amer. Chem. Soc., 85, 2477 (1963).
6. A. Clearfield, D. K. Warner, C. H. S. Molona, R. Ropal and I. Bernal, Can. J. Chem., 53, 1622 (1975).
7. R. K. Tuli, K. Chandra, R. K. Sharma, N. Kumar and B. S. Garg, Transition Met. Chem., 5, 49 (1980).
8. W. Moffitt, J. Amer. Chem. Soc., 76, 3386 (1954).
9. A. D. Liehr and C. J. Ballhausen, Acta Chem. Scand., 11, 207 (1957).
10 J. W. Linnett, Trans Faraday Soc., 52, 904 (1956).
11. W. P. Long, J. Amer. Chem. Soc., 81, 5312 (1959).
12. J. G. Murray, J. Amer. Chem. Soc., 83, 1287 (1961)
13. H. Alt and M. D. Rausch, J. Amer. Chem. Soc., 96, 5936 (1974).
14. A. Jensen and F. Basolo, J. Amer. Chem. Soc., 81, 5312 (1959).
15. C. F. Longford and J. P. Aplington, J. Organomet. Chem., 4, 271 (1965).
16. J. M. Bull, M. J. Frazer and J. Measures, Chem. Commun., 1310 (1968).
17. J. L. Burmeister, Coord. Chem. Rev., 1, 205 (1966).
18. J. L. Burmeister, Coord. Chem. Rev., 3, 225 (1968).

19. J. S. Thayer and R. West, Adv. Organomet. Chem., 5, 115 (1967)

20. P. C. H. Mitchell and R. J. P. Williams, J. Chem. Soc., 1912 (1960).

21. A. Sabatini and I. Bertini, Inorg. Chem., 4, 956 (1965).

22. R. S. P. Coutts and P. C. Wailess, Aust. J. Chem., 19, 2069 (1966).

23. S. F. A. Kettle,"Coordination Chemistry", Nelson, 1969, p. 177

24. F. A. Cotton and G. Wilkinson,"Advanced Inorganic Chemistry", 4th Edit., Wiley, New York (1980), p. 682.

25. C. K. Ingold,"Structure and Mechanism in Organic Chemistry", Bell, London, 1953.

26. A. J. Parker, Chem. Rev., 69, 1 (1969)

27. M. J. Blandamer and J. Burgess, Coord. Chem. Rev., 31, 93 (1980).

28. M. J. Blandamer and J. Burgess, Pure and Applied Chem., 54, 2285 (1982).

29. E. Pelizzetti and P. Giordano, J. Inorg. Nucl. Chem., 43, 2463 (1981).

31. J. H. Toney and T. J. Marks, J. Amer. Chem. Soc., 107, 947 (1985).

32. E. M. Arnett, W. G. Bentrude and McDuggleby, J. Amer. Chem. Soc., 87, 2048 (1965).

33. S. Winstein and A. H. Fainberg, J. Amer. Chem. Soc., 79, 5937 (1957).

CHAPTER 9

Binuclear Complexes

9-1. Introduction

In discussing electron transfer processes, we shall meet two established mechanisms which operate in such reactions. In the first, commonly termed outer-sphere reactions, orbital interaction between the oxidant and the reductant at the time of electron transfer is small and they go through the process with their coordination spheres intact. The second type of reaction, which is termed inner-sphere, requires that the oxidant and the reductant are firmly bonded during the act of electron transfer and a bridge formed by at least one ligand that is common to the coordination shells of the oxidant and the reductant. This bridge serves as the channel through which the electron is transmitted. The demonstration of such a mechanism in which a firm ligand bridge was shown to be present at the time of electron transfer was made most elegantly by Taube[1]. He chose a reacting system whereby the reduced forms of the redox system were substitutionally labile and the oxidized forms substitutionally inert. In this way the bridging ligand was passed from the oxidant to the oxidized form of the reductant.

The classical reaction was

$$Co(NH_3)_5Cl^{2+} + Cr(H_2O)_6^{2+} \longrightarrow Co(aq)^{2+} + 5NH_4^+ + Cr(H_2O)_5Cl^{2+}$$

inert	labile	labile	inert
d^6-low spin	d^4-high spin	d^7	d^3

Careful isolation of the product showed that virtually all of the chromium(III) was in the form of $Cr(H_2O)_5Cl^{2+}$ and, working with radioactive chloride, it could be shown that all of the chloride come from the original $Co(NH_3)_5Cl^{2+}$ and none from free chloride ion in solution. Thus the reaction is proposed to have a mechanism as shown in Scheme 9-I,

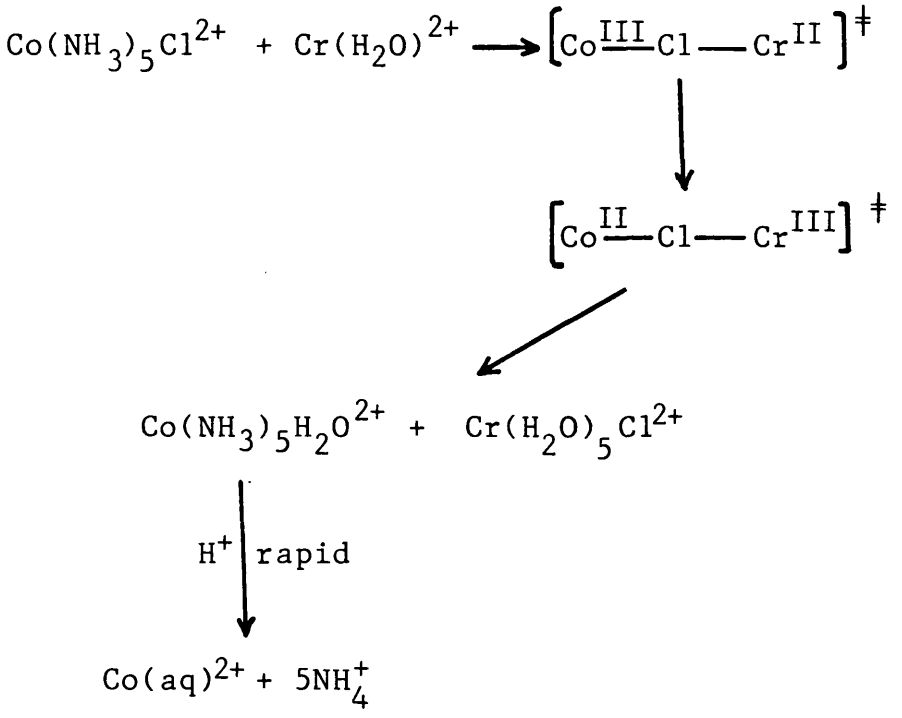

Scheme 9-I

This latter process has become a subject of several studies, especially in finding out the behaviour of this intermediate bridging complex which is often known as precursor. The most characteristic features of the complex are that its stability is sensitive to the natures of the oxidant, the reductant and the bridging ligand. Thus, for example, the

rate constant for electron transfer reaction to $Co(NH_3)_5Cl^{2+}$ from chromium(II) is 10^8 quicker than that from iron(II).[2] This is in agreement with a stronger reducing action of chromium(II) than iron(II); $Cr^{3+/2+}$ = -0.38 V and $Fe^{3+/2+}$ = +0.77 V.[3] The effect of the bridging ligand on the stability of the complex offers another great interest to several workers. There are many species (other than monoatom) which are known to be bridging ligands, but only those with conjugated π-orbitals can allow an electron to be transferred readily from one metal to another. Cyanide and thiocyanate are two examples of the group where two metal complexes are linked to each other by the group through two positions; carbon or nitrogen for cyanide and sulphur or nitrogen for thiocyanate.

N-Heterocyclic aromatic compounds such as pyrazine are another series of well-known compounds which have the ability to act as bridging ligands (1).[4,5] The presence of the delocalized π-orbital in their aromatic ring may allow for an electron to be transferred through the system. These features of the compound became a subject of several studies for almost a decade.

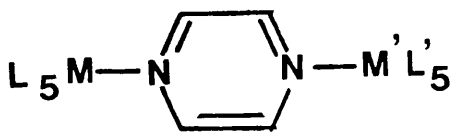

1

In general, the binuclear complexes can be classified into two groups; hetero- and homobinuclear. In heterobinuclear complexes two different metal complexes are linked by a bridging ligand (e.g. with conjugated π-orbital). If they are different in chemical potential, nett electron transfer may take place. Taube and co-workers[6-9] have reported in a series of papers on the rate of intramolecular electron transfer in redox active complexes of inner sphere type

$$[(NH_3)_5Ru\ ---LL---Co\ (NH_3)_5]^{5+}$$

with various N-heterocyclic aromatic bridging groups, LL, such as pyrazine or 4,4'-bipyridine. Haim[5,11-17] and Malin[4,18] and co-workers have subsequently developed a system that also allowed the measurements of intramolecular electron transfer rate constants using the $Fe^{II}(CN)_5^{3-}$ moiety as reductant in precursor complexes of the type

$$[(CN)_5Fe\ ---LL---Co\ (NH_3)_5]$$

where LL is one of the same N-heterocyclic aromatic bridging ligands as were used in the Ru(II)-Co(III) system. The electron transfer process through such bridging ligands is much slower than that given by a chloride bridge; presumably a longer bridge of an aromatic N-heterocyclic ligand delays the

process. This allows the formation and decomposition of the complex to be kinetically measured separately. In this case the substitutionally inert $Co^{III}(NH_3)_5L^{2+}$ is mixed with substitutionally labile $Fe^{II}(CN)_5H_2O^{3-}$ or $Ru^{II}(NH_3)_5H_2O^{2+}$, similar to Scheme [9-1]. The formation of the binuclear complex is indicated by the appearance of an intense colour. It then slowly disappears due to decomposition.[4,19,20] This intense colour is associated with metal to ligand charge transfer (MLCT) from a t_{2g}-orbital of the metal, Fe^{II} or $Ru^{II}(d^6)$, to a π^*-orbital of the ligand, similar to that reported for mononuclear complexes.

The situation in homobinuclear complexes, where two metal complexes, such as Fe-Fe,[21-25] Ru-Ru[26-31] and Mo-Mo[32-34] are linked, is rather different. There are two possible situations which may be observed. The first is that when both metal atoms in the complex have an equivalent oxidation state. An example of the group includes $(CO)_4Mo(bipym)Mo(CO)_4$ (2), $(CO)_5Mo$-LL-$Mo(CO)_5$, $(CN)_5Fe$-LL-$Fe(CN)_5^{6-}$ and $(NH_3)_5Ru$-LL-$Ru(NH_3)_5^{4+}$, where LL is pyrazine or 4,4'-bipyridine 3. In such system, there will be no electron transfer takes place but their metal to ligand charge transfer spectra will be maintained. The second is that when two equivalent metal complexes of different oxidation state are linked by a bridging group such as $(CN)_5Fe^{II}$-LL-$Fe^{III}(CN)_5^{5-}$ and $(NH_3)_5Ru^{II}$-LL-$Ru^{III}(NH_3)_5^{5+}$, where LL is pyrazine or 4,4'-bipyridine. Such a complex, which is often called a mixed valence compound, apart from exhibiting the metal-to-ligand charge transfer spectrum,[22] may also produce an intervalence charge transfer (IVCT) spectrum caused by a rapid electron transfer from metal to metal. Such typical intervalence charge

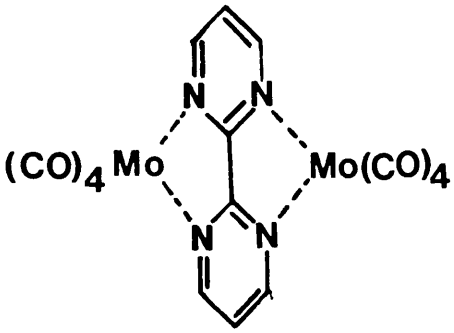

2

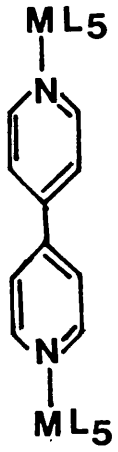

3

transfer spectra are reported to appear at lower energy, normally in the near-infrared region.

The aim of the present work is to synthesize and characterize some of the known binuclear complexes comprising metal-d^6 and some potentially binucleating ligands such as 2,2'-bipyrimidine, pyrazine and pyrazine derivatives. Metal-to-ligand charge transfer spectra observed in these complexes will be compared with those for their corresponding mononuclear analoguse. We shall also report the kinetics of electron transfer in one of the Fe^{II}/Co^{III} binuclear system, obtained by monitoring the rate of its decomposition. The effect of solvent on these phenomena form the main subjects of the present discussion.

9-2. Experimental

(a) μ -(2,2'-bipyrimidine)octacarbonyldimolybdenum(0)

In a 100 cm^3 round-bottomed flask fitted with a condenser was placed 0.74 g (2 mmol) of $Mo(CO)_4$(bipym) and 0.89 g (2.1 mmol) of cis-$Mo(CO)_4(pip)_2$ in 50 cm^3 of heptane. The reaction mixture was refluxed for five hours, during which a black precipitate appeared. The solution was filtered while still hot. The black residue was recrystallized from acetone, precipitated by the addition of ether.

(b) μ -(bisacetylpyridine-1,3 diaminopropane)octacarbonyl-bimolybdenum(0); μ-$Mo_2(CO)_8$(bapdi)

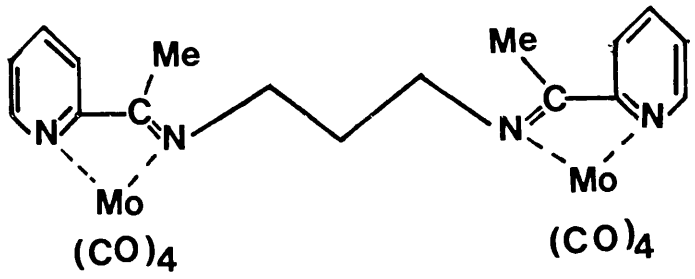

4

In a 100 cm^3 round-bottomed flask fitted with a condenser was placed 0.3 cm^3 of 2-acetylpyridine and 0.12 cm^3 of 1,3-diaminopropane in 25 cm^3 of iso-propanol. The solution was heated for 20 minutes, and then 1.0 g cis-$Mo(CO)_4(pip)_2$ was slowly added. A red colour appeared. The reaction mixture was

refluxed for two hours. The solution was left to cool overnight at room temperature. The red-orange crystals were collected, dried, and kept in a desiccator away from light.

(c) Sodium μ-(pyrazine)decacyanobiiron(II);
$Na_6[Fe_2(CN)_{10}(pyz)]$

The complex was prepared by mixing equimolar amounts of $Na_3[Fe(CN)_5(pyz)]$ and $Na_3[Fe(CN)_5(NH_3)]$ in water and then leaving the solution overnight to evaporate slowly at room temperature. A dark-red crystalline solid was collected

(d) μ-(pyrazine)decacarbonylbimolybdenum(0);
$Mo_2(CO)_{10}(pyz)$

The complex was prepared by refluxing for about 30 minutes a 2:1 mole mixture of $Mo(CO)_5(pip)$ and pyrazine in heptane. A dark brown precipitate was collected.

(e) Sodium pentacyanoammoniairon(II) trihydrate;
$Na_3[Fe(CN)_5(NH_3)] .3H_2O$

In a 250 cm^3 conical flask was dissolved 20 g of sodium nitroprusside in 100 cm^3 of ammonia solution (SG 0.88). The solution was left overnight, yielding a yellow solution which was then filtered. An equal volume of methanol was added to the solution; a yellow precipitate was appeared. The solution was filtered, the precipitate washed with methanol and dried in a vacuum desiccator.

(f) Pyrazine-2-carboxylatobis(ethylenediamine)cobalt(III) perchlorate, $[Co(en)_2(pyzCOO)](ClO_4)_2$

3.0 g of cobalt nitrate dissolved in 5 cm^3 of water were mixed with 15 cm^3 of solution containing 1.46 g of sodium pyrazine-2-carboxylate and 1.6 cm^3 of ethylenediamine (BDH). The reddish solution was treated with 3 cm^3 of hydrogen peroxide (30 Volume) in small amounts and heated on a steam bath for one hour, without stirring. The orange-red solution was filtered through a sintered glass filter, mixed with 5 g of $LiClO_4$ and evaporated on a steam bath until crystallization started. The solution was allowed to cool for one day at room temperature. The orange crystals were separated by filtration, washed with 20 cm^3 of 1:1 ethanol-water solution and finally with pure ethanol. A similar method was used to prepare $[Co(trien)(pyzCOO)](ClO_4)_2$.

(g) Kinetics and Charge Transfer Spectra

The kinetics of the intramolecular electron transfer in the binuclear complex

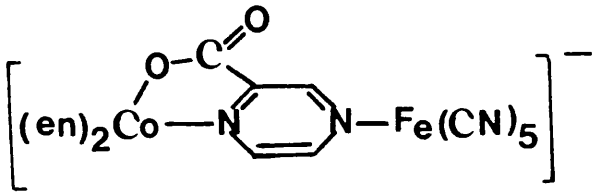

in water and water-mixtures were monitored in 10 mm silica cells in the thermostatted cell compartment of an HP 8451A

spectrophotometer. The complex was prepared by mixing equimolar ($2x10^{-4}$M) solutions of $Co(en)_2(pyzCOO)^{2+}$ and $Fe(CN)_5(H_2O)^{3-}$ (the complex of $Fe(CN)_5(H_2O)^{3-}$ was prepared by dissolving $Fe(CN)_5(NH_3)^{3-}$ in water which lead to a rapid substitution of NH_3 by water)[35]. An intense blue colour due to the binuclear species was immediately apparent. Its formation was complete after 3-4 minutes and it then slowly decomposed to reduced-oxidized products. The rate of the electron transfer process was followed from the disappearance of the blue band (fromr 5 minutes after mixing) for at least 2 1/2 half-lives. The computed results give a good first-order plot. The kinetics at high pressure were monitored by the method described in Chapter 2.

The wavenumber of maximum absorption of charge transfer of this binuclear species and related mononuclear complexes were measured using a Pye-Unicam SP 800 spectrophotometer as described in Chapter 3.

9-3. Charge Transfer Spectra

It is well documented that ligands (LL) such as 2,2'-bipyrimidine (bipym)[32,36], pyrazine (pyz)[37,38], apart from being mononucleating ligands, can also act as bridging ligands linking two metal complexes:

X M —LL— M'X'.

The metal-to-ligand charge transfer which is normally observed for mononuclear complexes of metal-d^6 with these ligands is also reported for binuclear complexes. Some of these features were illustrated by Overton and Connor[32] in their preparation of several binuclear complexes of metal-d^6 carbonyls of group VI with 2,2'-bipyrimidine as a bridging group.

Complexes with pyrazine also exhibit similar behaviour. The features of this ligand have been recognized and exploited by several workers. Several series of binuclear complexes involving homonuclear -d^6 and -d^5 metals have been reported. These include pentaamine ruthenium(II)/(III),[26-31] pentacyanoiron(II)/(III),[21-25] pentaamine osmium(II)/(III)[39] complexes (group VIII), pentachloroiridium(III)/(IV) complexes (group IX), pentacarbonyl -chromium(0), -molybdenum(0) and -tungsten(0) complexes[33,34,40-43] (group VI) and cyclopentadienylbiscarbonylmanganese(I) complex[44] (group VII). The presence of the lower unoccupied π^* molecular orbital in pyrazine and 2,2'-bipyrimidine leads to the formation of charge transfer spectra similar to those for corresponding mononuclear complexes but these occur at a rather lower energy. This observation suggests that the energy level of the lower unoccupied π^* molecular orbital of the bridging ligand is being lowered as a result of bonding to the metal complex at the other end. The complex is relatively unstable and steadily decomposes when in solution, presumably to mononuclear products.

In contrast, the binuclear complexes in the system shown in 4 with molybdenum exhibit charge transfer spectra in the visible region but at exactly the same wavelength as its

mononuclear parent. The situation in this system is rather different from that with 2,2'-bipyrimidine or pyrazine. In this system each metal atom is bonded to a binucleating ligand which has two isolated delocalized π-systems. Thus each of the lower unoccupied molecular orbitals, π^*, of each system remained unchanged even after being bonded to a metal complex at the other end. Details of the results are summarized in Table [9-1]. The associated charge transfer spectra of the binuclear complex $Mo_2(CO)_8$(bipym) consist of two peaks which are similar to those reported for $Mo(CO)_4$(bipym). The charge transfer spectrum for $Mo_2(CO)_{10}$(pyz) is rather different from its mononuclear analogue, $Mo(CO)_5$(pyz). It is found that the $Mo(CO)_5$(pyz) gives only a single peak, for example at 386 nm in toluene, but two peaks appear for binuclear $(OC)_5Mo(pyz)Mo(CO)_5$ (386 nm and 450 nm). Lees et al.[43] suggested that the single peak for $Mo(CO)_5$(pyz) is actually comprised of two overlapping absorption spectra (charge transfer and d-d) in which both excited states (π^* and e_g) are almost identical. The formation of the binuclear complex lowers the π-acceptor ability of pyrazine as well as the energy level. (Figure [9-1]).

As for the mononuclear complexes, the charge transfer spectra of the binuclear complexes of this type also exhibit solvent dependence (solvatochromism). The results listed in Table [9-2] show that their wavenumbers of maximum absorption increases as the polarity of the solvent increases. It is found that the solvent sensitivity for molybdenum binuclear complexes is somewhat larger than the corresponding solvent sensitivity for mononuclear complexes. The plot of wavenumber

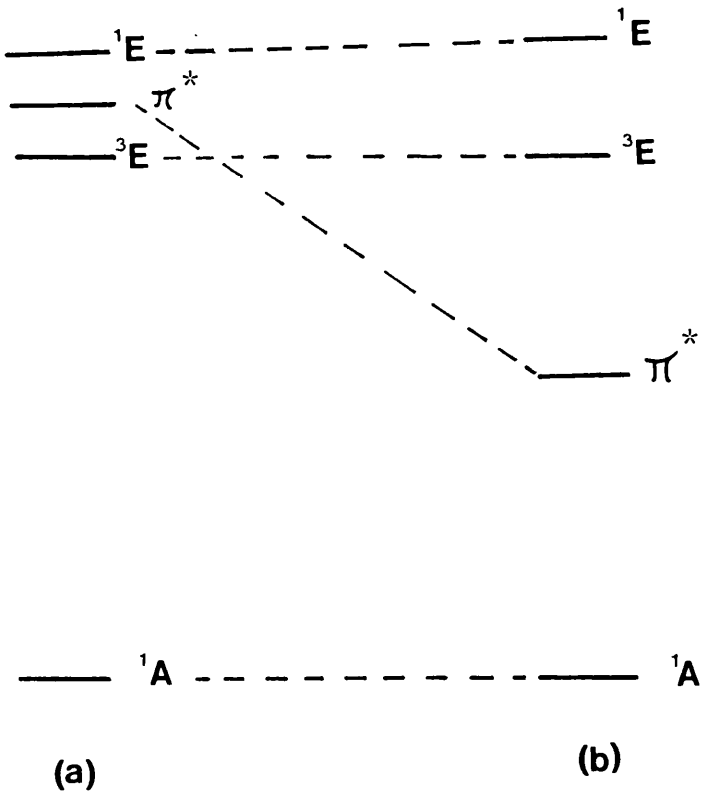

Figure [9-1] Relatives energies of the excited states observed in the absorption spectra of (a) $M(CO)_5(pyz)$ (b) $(OC)_5M(pyz)M(CO)_5$

of maximum absorption of charge transfer of $Mo_2(CO)_8(bipym)$ in various solvents against the corresponding wavenumber for $Mo(CO)_4(bipym)$, as shown in Figure [9-2], gives a straight line with slope 2.61±0.05. The effect is even larger with pyrazine bridging ($Mo_2(CO)_{10}(pyz)$). It is found that the charge transfer spectrum of the mononuclear complex is almost unshifted on changing solvent but that of the binuclear complex clearly varies.

The situation seems to be reversed for iron(II) complexes; $Fe_2(CN)_{10}(pyz)^{6-}$. Even though both mono and binuclear complexes

exhibit a blue shift as the solvent become more polar, the solvent sensitivity appears to be larger for the mononuclear complex. However, this is only based on two solvents (water and methanol) because of the difficulty of dissolving in other organic solvents. In the present work, we have also tried to study the properties of binuclear complexes of mixed-metal atoms; iron(II)-molybdenum(0). We found that the mixing between two metal complexes in which one has a potential bridging ligand was always followed by a rapid transfer of bridging ligand from one metal to another. This observation is based on the electronic absorption of the product which is identical with the absorption spectrum of an authentic sample of ligand-transferred complex. For example, when a complex of $Mo(CO)_4(bipym)$ is mixed with Fe^{2+} in aqueous methanol, the absorption spectrum of the product is identical to that of the mononuclear iron(II)-bipym complex. Conversely, when the complex of $Fe(bipym)_3^{2+}$ is mixed with $cis\text{-}Mo(CO)_4(pip)_2$ in a similar solvent, the absorption spectrum of the product is identical with that of $Mo(CO)_4(bipym)$.

9-4. Kinetics of the Electron Transfer Process in Precursor Complexes

It is well documented that when aqueous solutions of $Co(NH_3)_5(pyz)^{3+}$ and $Fe(CN)_5(NH_3)^{3-}$ are mixed a strong visible absorption band at λ = 630 nm appears spontaneously. This band then slowly disappears to form as final products Co^{2+}, NH_4^+ and $Fe(CN)_5(pyz)^{2-}$. The result shows that the reaction involves transfer of an electron as well as the pyrazine group taking

place. This type of reaction is analogous to the reaction of $Co(NH_3)_5Cl^{2+}$ with Cr^{2+} which has been demonstrated to proceed through the inner-sphere mechanism. The appearance of the band at λ = 630 nm is due to formation of the pyrazine-bridged precursor or binuclear complex whereas the disappearance of the band corresponds to the rate of the electron transfer process as thereafter the binuclear species produced quickly decomposes to mononuclear products, as shown in Scheme 9-2.

Under normal condition, the electron transfer process from iron(II) to cobalt(III) via the pyrazine π-system is relatively slow, compared with the rate of formation of the precursor (e.g. at 298°K, $k_f = 7.0 \times 10^3\ M^{-1}\ sec^{-1}$ and $k_{et} = 5.5 \times 10^{-2}\ sec^{-1}$).[4] This is because the transferring of an electron to cobalt(III) has to take place into an e_g-orbital (d_{z^2} or $d_{x^2-y^2}$ of low-spin-d^6 for cobalt(III)). As electron transfer usually takes place through a ligand orbital π-system, there is a large barrier to the transfer of an electron into the d_{z^2} or $d_{x^2-y^2}$ orbital as shown in the diagram of Figure [9-3].

A large difference between rates of binuclear formation and of electron transfer allows the estimation of both processes to be carried out separately by using conventional kinetic techniques. In all cases, it is found that the mechanism of the formation of precursor complex is similar to the reaction of $Fe(CN)_5(H_2O)^{3-}$ with non-complexed pyrazine to form $Fe(CN)_5(pyz)^{3-}$. The reaction is very fast (half-life is about a few milliseconds under normal conditions), whereas the electron transfer reaction is much slower, unimolecular and only begins after the formation of the precursor.

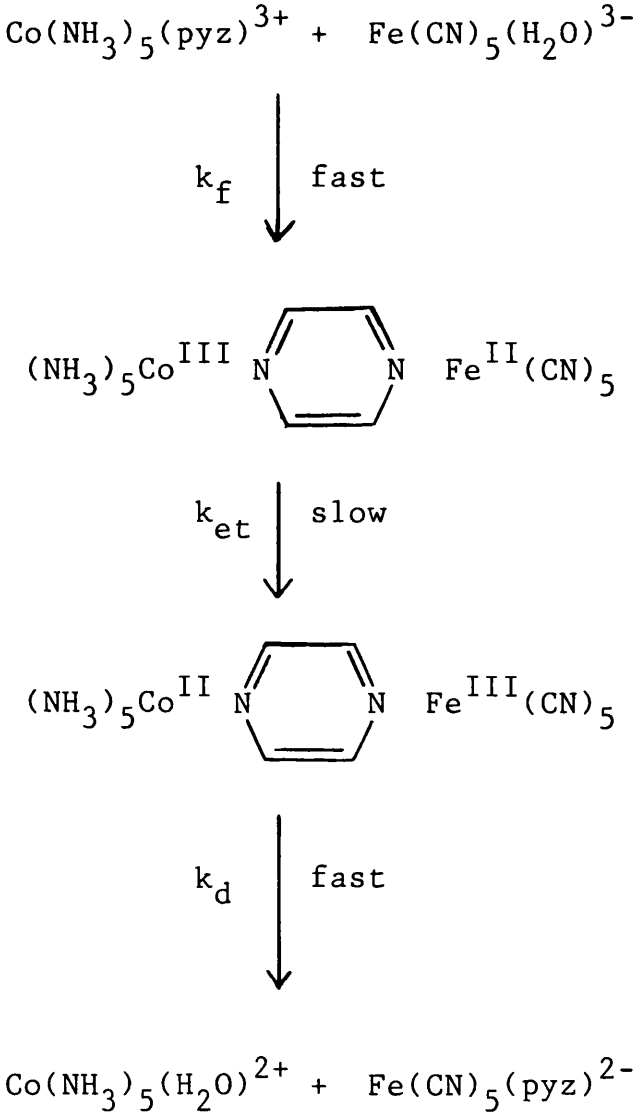
Co(NH3)5(pyz)3+ + Fe(CN)5(H2O)3-
kf
fast
(NH3)5CoIII N N FeII(CN)5
ket
slow
(NH3)5CoII N N FeIII(CN)5
kd
fast
Co(NH3)5(H2O)2+ + Fe(CN)5(pyz)2-

Scheme 9-2

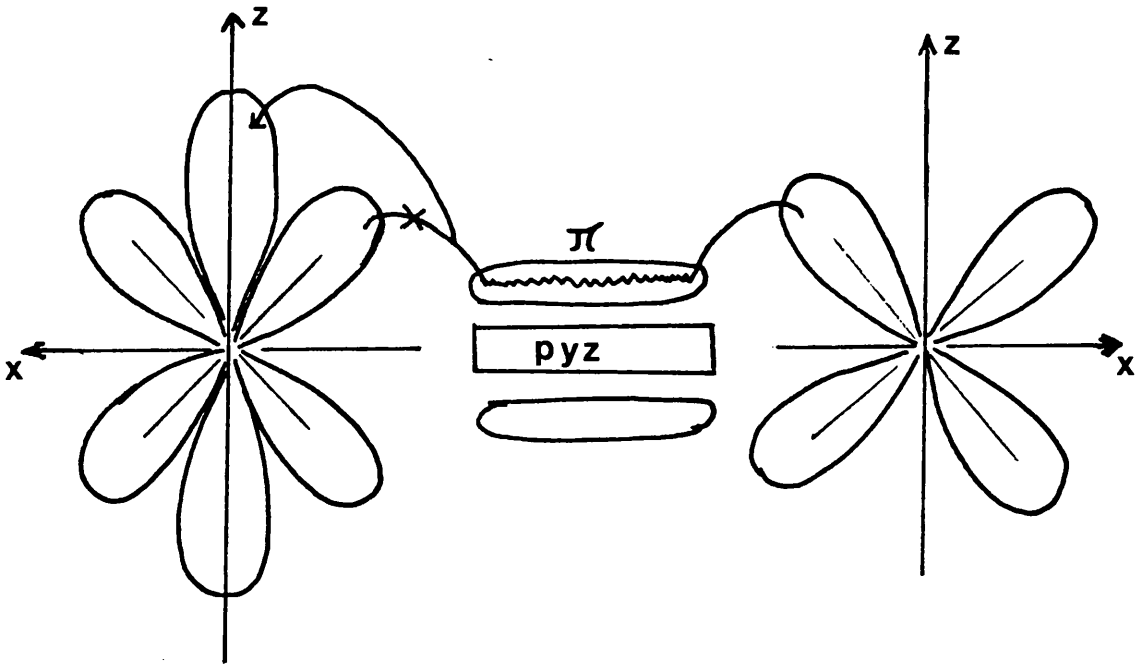

Figure [9-3] Schematic diagram for the electron transfer process from cobalt(III) to iron(II) complexes via pyrazine as bridging ligand

In the present discussion, we shall deal with the kinetics of the electron transfer of the analogous process involving $Co(en)_2(pyzCOO)^-$ and $Fe(CN)_5(H_2O)^{3-}$, where en is ethylenediamine and $pyzCOO^-$ is pyrazine-2-carboxylate, in various binary aqueous mixtures. The system in which the electron transfer process occurs through pyrazine-2-carboxylate bridging group is shown in 5. The distinguishing feature of this reaction is that the pyrazine-2-carboxylate group bonds to the cobalt(III) as a bidentate ligand, through one of the pyrazine nitrogens and one of the carboxylate oxygens. We also carried out a few

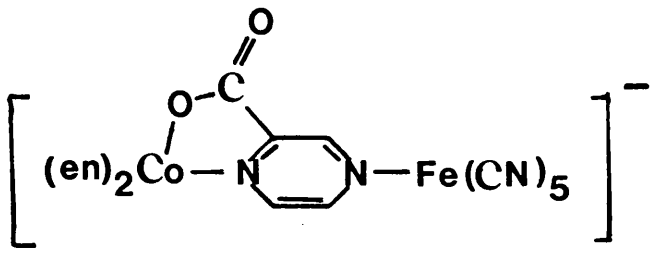

5

reactions of $Co(trien)(pyzCOO)^-$ with $Fe(CN)_5(H_2O)^{3-}$ in water, from which the effect of the non-bridging ligand can be assessed. In general, the rate of the electron transfer process of the system studied here is slow and convenient to be monitored by our present spectrophotometer. The measurement is carried out by mixing equimolar solutions of the two reactants, as described earlier, leading to formation of the precursor.[19] This complex, like the pyrazine precursor, gives a strong absorption band in the visible region (600-635 nm) whose position varies with the nature of the medium of the reaction (solvatochromism) similarly to other binuclear complexes (Table [9-3]). The measurement of the rate of the electron transfer process is begun soon after the formation of the precursor is completed (normally 3-4 minutes after mixing), by monitoring the disappearance of the precursor band (Figure [9-4]). All the reactions satisfy first-order kinetics for at least two and a half half-lives.

The results summarized in Table [9-4] show that the rate constant for the electron transfer process varies depending on the nature of the non-bridging ligand present and of the

medium (solvent) of the reaction. It is found that the rate constant for the electron transfer process decreases as the order of chelating of the non-bridging ligand increases. For example, the rate of the reaction decreases by 130 times on changing from ammonia to ethylenediamine (en) in water and 15 times on changing from ethylenediamine to triethylenetetramine (trien). These large differences in rate constants indicate that the energy barrier to placing an electron into an e_g-orbital of cobalt become larger as denticity increases. The observation apparently reflects a larger crystal field energy (Dq) of the cobalt complex with ethylenediamine than ammonia and of triethylenetetramine than ethylenediamine. The result also follows from a difference in chemical potentials of cobalt complexes; e.g. $Co(NH_3)_6^{3+/2+}$ = +0.11 V, $Co(en)_3^{3+/2+}$ = +0.18 V.[3]

The interpretation of solvent sensitivity on electron transfer reactions is limited compared with other reactions.[45-47] The most common interpretation of solvent effect on electron transfer reactions is based on Marcus-Hush theory.[48-50] This says that the Gibbs free energy change for solvation changes associated with the electron transfer is given by the two equations below:

$$\Delta G_{out}^{\ddagger} = \frac{e^2}{4r_{\ddagger}}\left[\frac{1}{D_{op}} - \frac{1}{D}\right]$$

or

$$\Delta G_{out}^{\ddagger} = e^2\left(\frac{1}{2r_A} + \frac{1}{2r_B} \div \frac{1}{r_{\ddagger}}\right)\left[\frac{1}{D_{op}} - \frac{1}{D}\right]$$

where D_{op} and D are the optical and static dielectric constants respectively, r_A and r_B are the radii of the corresponding reactants A and B, and $r_{\ddagger}$ is a distance between them in the transition state. Thus a plot of $\Delta G^{\ddagger}$ or ln k_{et} against $(1/D_{op} - 1/D)$ is expected to be linear. This relation is assumed for electron transfer processes for binuclear series of Ru^{II}-LL-Ru^{III} complexes in which the kinetic result is taken from non-kinetic measurement, that is solvatochromism of intervalence charge transfer (IVCT) spectra. However the validity of the equation for slow electron transfer processes has not been assessed.

In the present discussion, we shall concentrate on how the rate constant for electron transfer between $Co(en)_2(pyzCOO)^{2+}$ and $Fe(CN)_5(H_2O)^{3-}$ in the binuclear intermediate in a series of aqueous methanol mixtures could be related with Marcus-Hush theory and other solvent parameters. Figure [9-5](a) shows an application of the Marcus-Hush equation. The rate constant trend for electron transfer within $[(en)_2Co(pyzCOO)Fe(CN)_5]^-$ confirms this expectation only in the range 0 to 20% methanol. Thereafter the rate constant trend deviates markedly, decreasing greatly from 60% to 80% methanol whereas the Marcus-Hush treatment forecasts a small rate increase. Logarithms of rate constants correlate less badly with 1/D than with $(1/D_{op} - 1/D)$ (Figure [9-5](b)), but reactivity is clearly not directly controlled by solvent dielectric properties. The plot against solvent Y values,[51] in other words against rate constants for t-butyl chloride solvolysis, Figure [9-5](c), is also included to give an idea of the large magnitude of the solvent effect on reactivity at

high methanol contents.

We also established the dependence of rate constant of the reaction on pressure in water and 40% methanol-water which leads to estimation of volumes of activation, $\Delta V^{\ddagger}$. In both cases, large positive values of $\Delta V^{\ddagger}$ are reported (24.0± 2.0 $cm^3 mol^{-1}$ and 7.0 ±1.0 $cm^3\ mol^{-1}$ in water and 40% methanol-water respectively). These positive value of $\Delta V^{\ddagger}$ are apparently consistent with a positive value of $\Delta S^{\ddagger}$ reported for analogous reaction involving $(dien)Co^{III}$-LL-$Fe^{II}(CN)_5^{2-}$ complexes, where LL = pyrazine-2,6-dicarboxylate (32 cal K^{-1} mol^{-1}).[17] The large positive value of $\Delta V^{\ddagger}$ in water suggests considerably desolvation of the binuclear complex on going to the transition state. This desolvation behaviour is, in contrast to intramolecular redox within a dicobalt-μ-peroxide complex, decreased in methanol.[52] The intrinsic part of the complex contributing to $\Delta V^{\ddagger}$ on going from initial state to transition state is not known, but is most likely given by cobalt-ligand bond stretching since iron-cyanide bond lengths are essentially equal for $Fe(CN)_6^{4-}$ and $Fe(CN)_6^{3-}$.[53] To find out the reactivity trend, we first analyse it by assuming that the initial state for the intramolecular electron transfer process is a total of the transfer chemical potentials (measured from solubilities) of the two isolated complexes $Co(en)_2(pyzCOO)^{2+}$ and $Fe(CN)_6^{4-}$, but the analysis does not give a satisfactory result. The trend shows a large destabilization in methanol which is in contrast with a slower rate. The other way of probing solvation of the initial state for the electron transfer process is through solubility studies and derived

transfer chemical potentials for a very closely related non-redox model, such as $[(en)_2Cr^{III}(pyzCOO)\text{-}Fe^{II}(CN)_5]^-$. Again, this type of analysis is dependent on success in synthesis of the model binuclear complex.

So far, we have discussed details of the behaviour of binuclear complexes including charge transfer spectra and kinetics of the electron transfer reaction. The solvent effect on the charge transfer spectra of the complexes seems to be similar to that reported for their corresponding mononuclear analogues. In kinetic aspects, the $\Delta V^{\ddagger}$ for the electron transfer process of our system in water (24 ± 2.0 cm^3 mol^{-1}) is similar to outer-sphere processes $Co(NH_3)_5X^{2+}$ plus $Fe(CN)_6^{4-}$ system ((27-30) cm^3 mol^{-1}), where X = H_2O, pyridine and DMSO.[54] Presumably, the solvation effects on inner- and outer-sphere mechanisms are similar. But, it is disappointing that the analysis of solvent effects, based on initial state-transition state, of our system cannot be completed successfully. At the present stage, we can only summarize some problems and suggestions which might be useful for future treatment in analysing the effects.

TABLE 9-1

The comparison between wavenumbers of maximum absorption, ν_{max}, for mono- and related binuclear complexes.

Complex	Solvent	$10^{-3}\nu_{max}/cm^{-1}$	Ref
$Mo(CO)_4(bipym)$	CH_2Cl_2	26.30, 19.80	31, a
$Mo_2(CO)_8(bipym)$	CH_2Cl_2	22.50, 14.90	-
$Mo(CO)_5(pyz)$	toluene	25.90	a
$Mo_2(CO)_{10}(pyz)$	toluene	25.90, 20.35	a
$Fe(CN)_5(pyz)$	water	19.70	20
$Fe_2(CN)_{10}(pyz)$	water	18.55	20
$Ru(NH_3)_5(pyz)$	water	21.10	25
$Ru(CN)_5pyz$-$Ru(NH_3)_5$	water	19.16	16
$Mo(CO)_4(apmi)$	toluene	19.40	a
$Mo_2(CO)_8(apmi)$	toluene	19.40	a

[a] This work

TABLE 9-2

The wavenumbers of maximum absorption of binuclear and corresponding mononuclear complexes in various solvents.

Solvent	$10^{-3}\,\nu_{max}$ / cm^{-1}					
	$Mo_2(CO)_8$ (bipym)	$Mo(CO)_4$ (bipym)	$Mo_2(CO)_{10}$ (pyz)	$Mo(CO)_5$ (pyz)	$Fe_2(CN)_{10}$ (pyz)	$Fe(CN)_5$ (pyz)
Water	–	–	–	–	19.80	22.00
Methanol	–	–	–	–	18.55	19.70
DMSO	18.10	21.74	–	–	–	–
CH_3CN	17.62	21.60	–	–	–	–
Acetone	17.40	21.10	–	–	–	–
Me-Et-ketone	– 17.00	– 21.05	–	–	–	–
CH_2ClCH_2Cl	15.25	19.95	20.65	25.72	–	–
CH_2Cl_2	14.90	19.80	20.55	25.75	–	–
Anisole	–	–	20.95	25.85	–	–
C_6H_5Cl	–	–	20.15	25.70	–	–
$CHCl_3$	–	–	19.65	25.70	–	–
Et_2-ether	–	–	20.80	25.65	–	–
Toluene	–	–	20.35	25.61	–	–
Dioxan	–	–	21.25	25.70	–	–
CCl_4	–	–	19.00	25.50	–	–

TABLE 9-3

The wavenumbers of maximum absorption of $Na[(en)_2Co(pyzCOO)\text{-}Fe(CN)_5]$ compared to $Na_4(Fe(CN)_5(pyzCOO))$, its final product (after electron transfer process) and $Na_3(Fe(CN)_5(pyzCOO))$ in various solvents

Solvent	$10^{-3}\,\nu_{max}$ / cm^{-1}			
%volume water	$Na_4Fe(CN)_5$-(pyzCOO)	Binuclear	product	$Na_3(Fe(CN)_5$-(pyzCOO))
100	22.00	15.72	21.65(m)	21.60
80-water 20-MeOH	21.15	15.87	21.37(m)	21.50
60-water 40-MeOH	20.42	16.03	21.90(b)	21.32
40-water 60-MeOH	20.03	16.23	21.05(b)	21.23
20-water 80-MeOH	19.83	16.34	20.96(b)	21.05
60-water 40-Aceto-ne	-	16.75	20.00(vb)	20.62
60-water 40- BuOH	-	16.53	very broad	20.41

Prepared by oxidizing $Na_2(Fe(CN)_5(pyzCOO)$ with bromine.
m = medium; b = broad; vb = very broad.

TABLE 9-4

Rate constants for electron transfer within $[(en)_2Co(pyzCOO)Fe(CN)_5]^-$ in aqueous mixtures at 298°K

% volume cosolvent	$10^5 k_{et}$ / s^{-1}		
	MeOH	t-BuOH	Acetone
20	12.5	-	-
40	12.3	-	-
60	7.6	1.5	8.8
80	1.7	-	-

Rate constants in water at 298°K for electron transfer within:

$[(NH_3)_5Co(pyzCOO)Fe(CN)_5]^- = 5.5 \times 10^{-2}\ s^{-1}$

$[(en)_2Co(pyzCOO)Fe(CN)_5]^- = 10.4 \times 10^{-5}\ s^{-1}$

$[(trien)Co(pyzCOO)Fe(CN)_5]^- = 7.3 \times 10^{-6}\ s^{-1}$

TABLE 9-5

The rate constants for the intramolecular electron transfer, k_{et}, within $[(en)_2Co(pyzCOO)Fe(CN)_5]^-$ in aqueous mixtures at 298°K and corresponding solvent parameters; $(1/D_{op}-D)$, $1/D$, and Y values.

$10^5 k_{et}$ /s^{-1}	Solvent % (V) co-solvent	$(1/D_{op}-D)$	$(1/D)$	Y
10.4	water	0.551	0.0122	3.44
12.5	20-MeOH	0.545	0.0136	3.08
12.3	40-MeOH	0.539	0.0154	2.56
7.6	60-MeOH	0.535	0.0186	1.64
1.7	80-MeOH	0.535	0.0232	0.48
1.5	60-t-BuOH	-	0.0196	1.66
8.8	60-acetone	-	0.0168	2.20

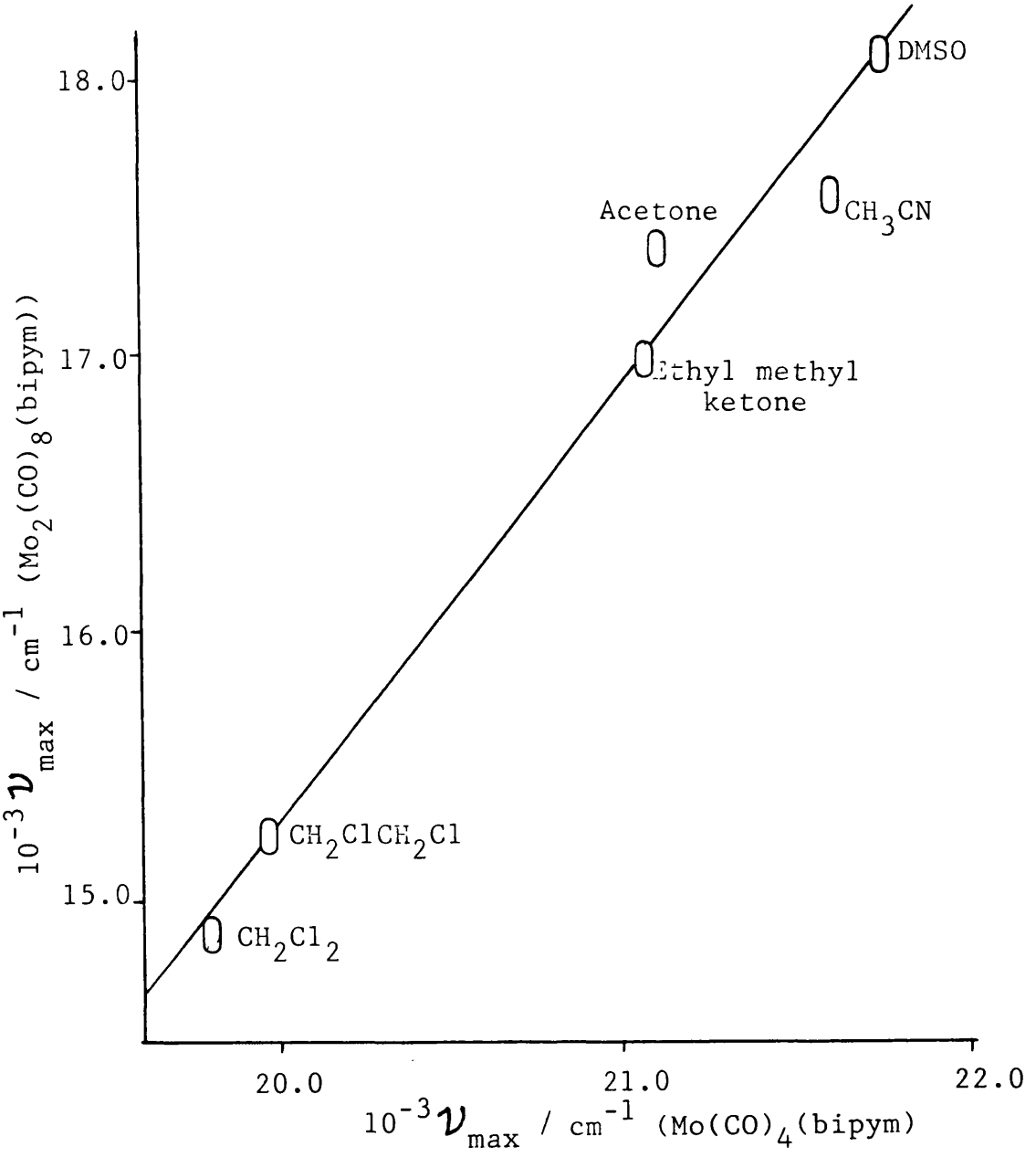

Figure [9-2] A plot of ν_{max} for $Mo_2(CO)_8$(bipym) against that for the corresponding absorption for $Mo(CO)_4$(bipym) in various organic solvents.

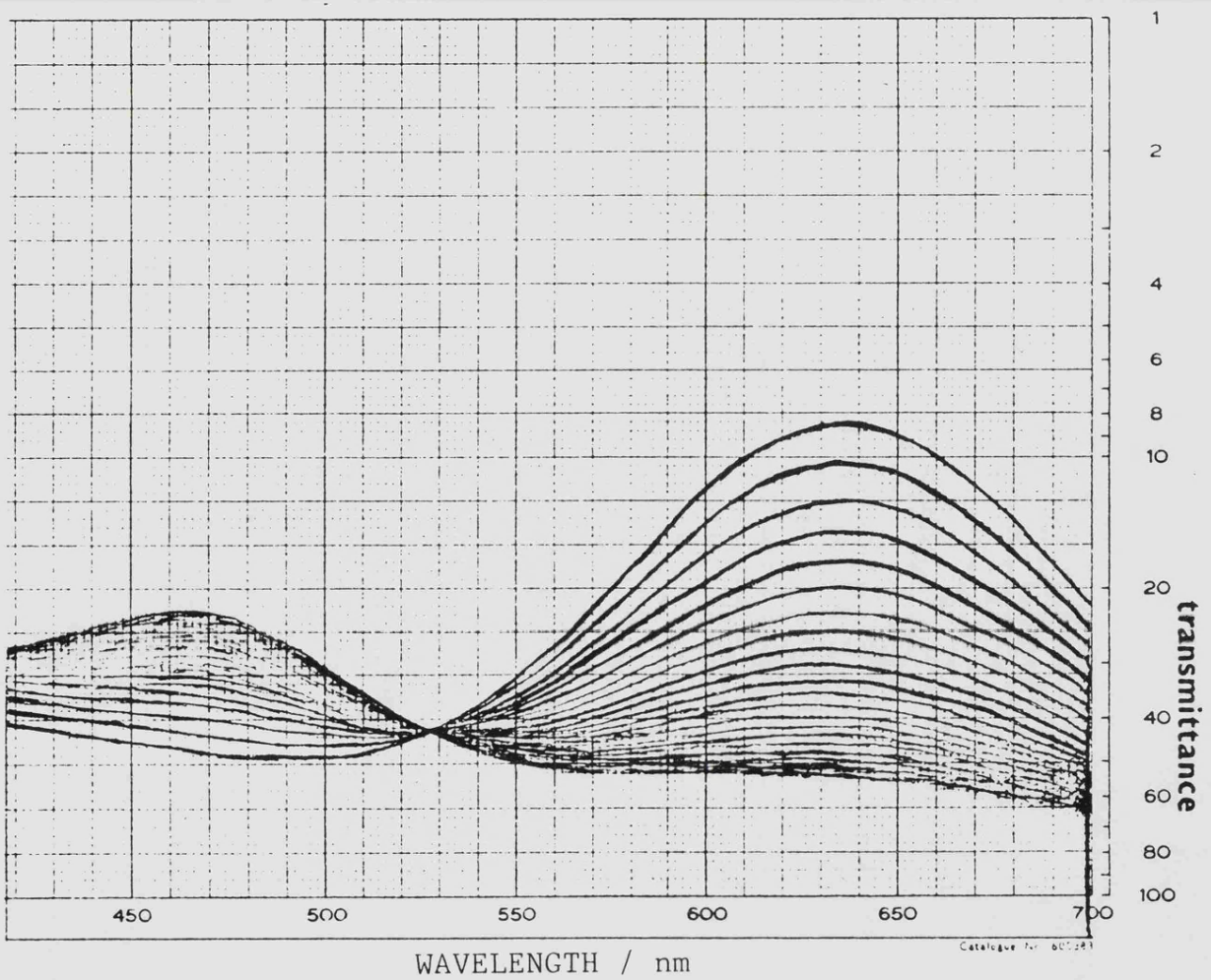

Figure [9-4] A scanning spectrum showing the progress of the intramolecular process of $(en)_2Co(pyzCOO)Fe(CN)_5^-$ in water at 298°K; initial $[(en)_2Co(pyzCOO)Fe(CN)_5^-] = 2x10^{-4}M$; interval scanning time = 15 minutes.

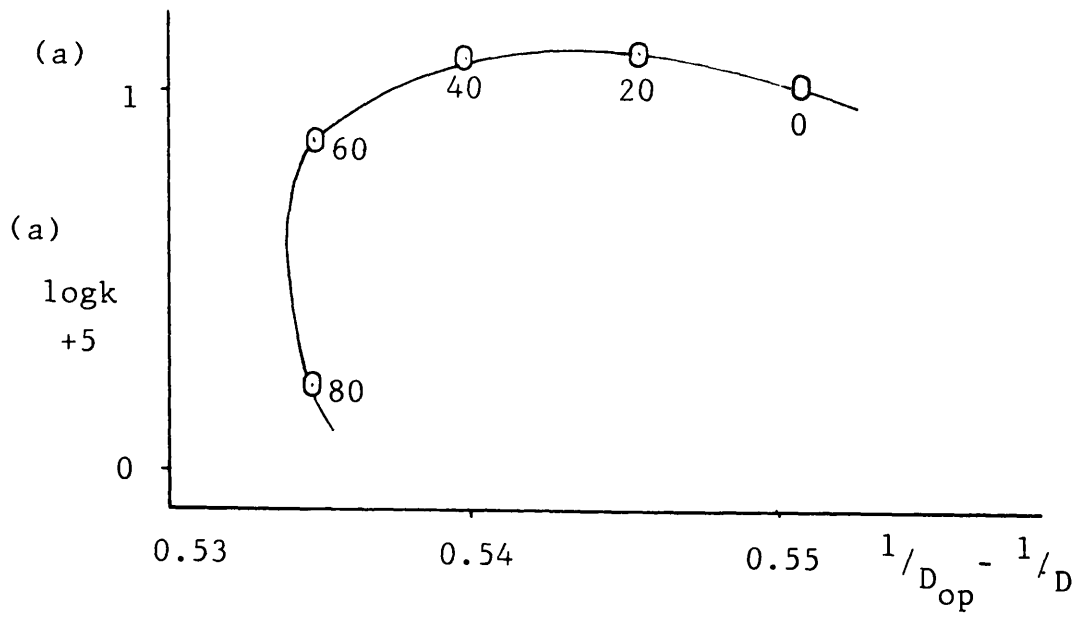
(a)
1
40
20
0
60
(a)
logk
+5
80
0
0.53
0.54
0.55
1/Dop - 1/D

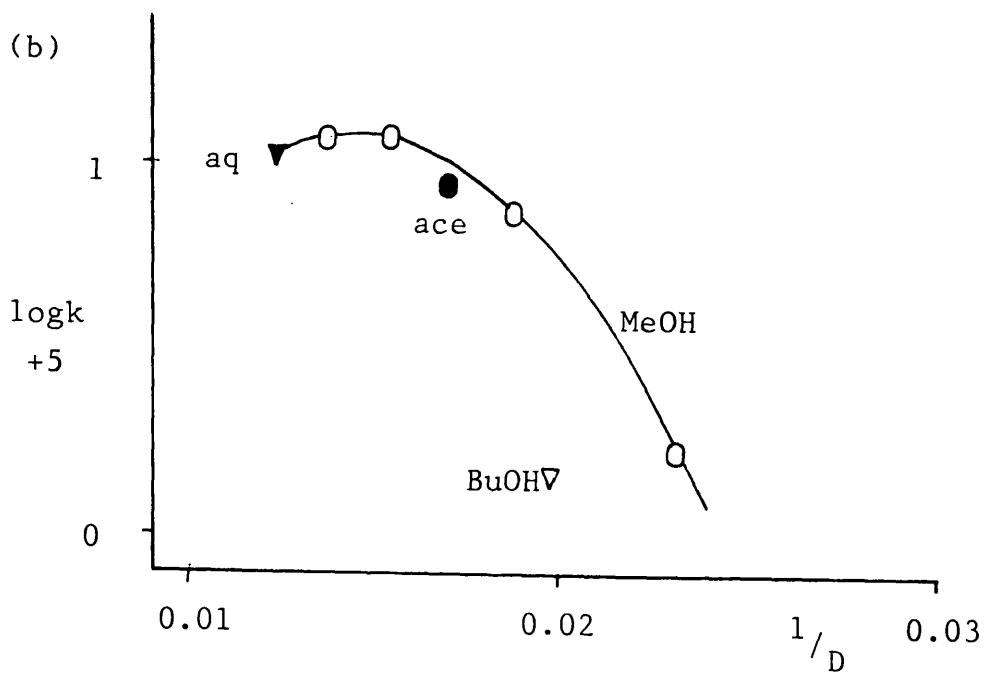
(b)
1
aq
ace
MeOH
logk
+5
BuOH∇
0
0.01
0.02
0.03
1/D

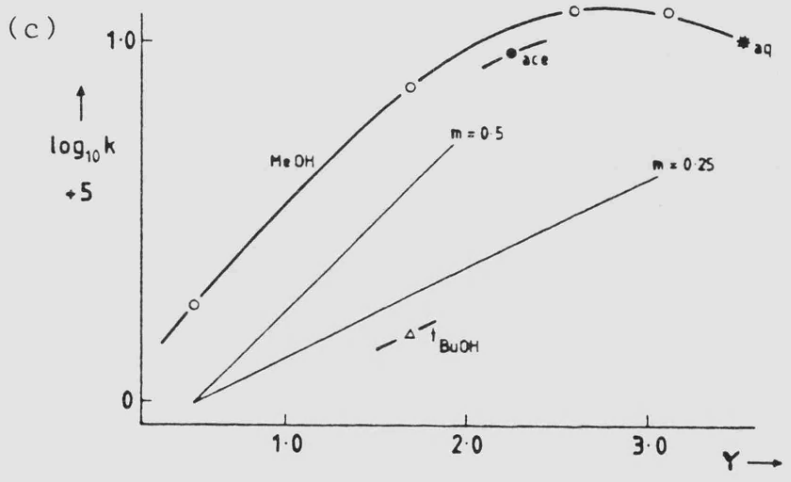

Figure [9-5] Plots showing the relation between log k for the intramolecular electron transfer process in $(en)_2Co(pyzCOO)Fe(CN)_5^-$ and various solvent parameters; (a) against $(1/D_{op} - 1/D)$ (b) against 1/D and (c) against Y.

9-5. References

1. H. Taube, Adv. Inorg. Chem. Radiochem., 1, 1 (1959).
2. M. L. Tobe,"Inorganic Reaction Mechanisms", Nelson (1972),p 136
3. G. Milazzo and S. Caroli, "Tables of Standard Electrode Potentials", Wiley, New York, 1978.
4. J. M. Malin, D. A. Ryan, T. V. O'Halloran, J. Amer. Chem. Soc., 100, 2097 (1978)
5. D. Gaswick and A. Haim, J. Amer. Chem. Soc., 96, 7845 (1974)
6. S. S. Isied, and H. Taube, J. Amer. Chem. Soc., 95, 8198 (1973)
7. H. Fischer, G. M. Toma and H. Taube, J. Amer. Chem., Soc., 98, 5512 (1976)
8. K. Riederk and H. Taube, J. Amer. Chem. Soc., 99, 7891 (1977)
9. S. K. S. Zawacky, J. Amer. Chem. Soc., 103, 3379 (1981)
10. S. S. Iseid and C. G. Kuehn, J. Amer. Chem. Soc., 100, 6754 (1978)
11. J. Jwo and A. Haim, J. Amer. Chem. Soc., 98, 1172 (1976)
12. A. Szecsy and A.Haim, J. Amer. Chem. Soc.,103, 1679 (1981)
13. A. Szecsy and A. Haim, J. Amer. Chem. Soc., 104, 3063 (1982)
14. J. Jwo, P. L. Gaus and A. Haim, J. Amer. Chem. Soc., 101, 6189 (1979)

15. A. Haim, Pure and Applied Chem., 55, 89 (1983)
16. A. Haim, Progr. Inorg. Chem., 30, 273 (1973)
17. A. Yeh and A. Haim, J. Amer. Chem. Soc., 107, 369 (1985)
18. D. A. Piering and J. M. Malin, J. Amer. Chem. Soc., 98, 6045 (1976)
19. H. E. Toma , J. Inorg. Nucl. Chem., 37, 785 (1975)
20. A. Neves, W. Herrmann, and K. Wieghardt, Inorg. Chem., 23, 3435 (1984)
21. F. Felix, U. Hauser, H. Siegenthaler, F. Wenk and A. Ludi, Inorg. Chim. Acta, 15, L7 (1975)
22. F. Felix and A. Ludi, Inorg. Chem., 17, 1782 (1978)
23. J. M. Malin, C. F. Schmidt and H. E. Toma, Inorg. Chem., 14, 2924 (1975)
24. R. Glauser, U. Hauser, F. Herren, A. Ludi, P. Roder, E. Schmidt, H. Siegenthaler and F. Wenk, J. Amer. Chem. Soc., 95, 8457 (1973)
25. A. B. Altabef, S. A. Brandan, and N. E. Katz, Polyhedron, 4, 227 (1985)
26. C. Creutz and H. Taube, J. Amer. Chem. Soc., 95, 1086 (1973)
27. D. K. Lavallee and E. B. Fleischer, J. Amer. Chem. Soc., 94, 2583 (1972)
28. G. M. Tom, C. Creutz and H. Taube, J. Amer. Chem. Soc., 96, 7827 (1974)
29. R. W. Callahan, G. M. Brown and T. J. Meyer, Inorg. Chem., 14, 1443 (1975).
30. K. Krentzien and H. Taube, J. Amer. Chem. Soc., 98, 6379 (1976)

31. M. J. Powers and T. J. Meyer, Inorg. Chem., 17, 1785 (1978)
32. C. Overton and J. A. Connor, Polyhedron, 1, 53 (1982)
33. R. Ernhoffer, R. E. Shepherd, J. Chem. Soc., Chem. Commun., 859 (1978).
34. K. H. Pannell and R. Iglesias, Inorg. Chim. Acta, 33, L161 (1979).
35. A. D. James, R. S. Murray, and W. C. E. Higginson, J. Chem. Soc., Dalton Trans., 1273 (1974).
36. R. H. Petty, B. R. Welch, L. J. Wilson, L. A. Bottomly and K. M. Kadish, J. Amer Chem. Soc., 102 611 (1980)
37. E. V. Dose and L. J. Wilson, Inorg. Chem., 17, 2660 (1978)
38. M. Hunziker and A. Ludi, J. Amer. Chem. Soc., 99, 7390 (1977)
39. R. H. Magnuson, P. A. Lay and H. Taube, J. Amer. Chem. Soc., 105, 2507 (1983).
40. H. Diaaman, H. van der Poel, D. J. Stufkens and A. Oskam, Thermochim. Acta, 34, 69 (1978)
41. H. Diaaman, D. J. Stufkens and A. Oskam, Inorg. Chim. Acta, 39, 75 (1980)
42. S. Chun, D. C. Palmer, E. F. Mattimore and A. J. Lees, Inorg. Chim. Acta, 77, L119 (1983)
43. A. J. Lees, J. M. Fobare, E. F. Mattimore, Inorg. Chem., 23,2709 (1984)
44. R. Gross and W. Kaim, Inorg. Chem., 25, 498 (1986)
45. C. K. Ingold,"Structure and Mechanism in Organic Chemistry", G. Bell, London, 1953.

46. A. J. Packer, Chem. Rev., 69,1 (1969)

47. M. J. Blandamer and J. Burgess, Coord. Chem. Rev., 31, 93 (1980)

48. (a) R. A. Marcus, J. Chem. Phys., 24,966 (1956), (b) N. S. Hush, Progr. Inorg. Chem. 8, 391 (1967) (c) R. A. Marcus and N. Sutin, Biochem. Biophys Acta, 811, 265 (1985)

49. N. Sutin, Progr. Inorg. Chem., 30, 441 (1983)

50. A. P. Szecsy and A. Haim, J. Amer. Chem. Soc., 103, 1683 (1981)

51. E. Grunwald and S. Winstein, J. Amer. Chem. Soc., 70, 846 (1948)

52. M. Kenesato, M. Ebihara, Y. Sasaki and K. Saito, J. Amer. Chem, Soc., 105, 5711 (1983)

53. A. G. Sharpe, "Inorganic Chemistry", Longman, London, 1981, p. 587.

54. I. Krack and R. van Eldik, Inorg. Chem., 25, 1743 (1986).

Spectroscopy, Solvation and Reactivity of Transition Metal Complexes with π-Acceptor Ligands

by Razak Bin Ali

ABSTRACT

Information from solubility, spectroscopy and kinetic studies has been used to characterize solvation for three groups of complexes. These three groups include metal-d^6 diimine complexes, metallocenes ($M(Cp)_2Cl_2$ where M = Ti(IV), V(IV) and Zr(IV)), and binuclear complexes involving d^6-metal ions with π-acceptor bridging ligands.

The discussion of the first group deals mainly with Mo(0), and also with a few Mn(I) analogues. Solubilities, from which transfer chemical potentials are derived, have been measured in various pure and mixed solvents. Information about charge transfer spectra, carbonyl stretching frequencies and n.m.r chemical shifts (several nuclei) are reported. The results clearly indicate solvent dependence. Kinetics of substitution reactions involving formation from $Mo(CO)_5(4CNpy)$ or from $Mn(CO)_5Br$ and substitution of $Mo(CO)_4(diimine)$ complexes have been studied in various solvents. The solvent sensitivities of reactivity of the latter process are analysed, based on initial state-transition state contributions for these reactions of well-established mechanism. Pressure effects on reactivity, and on charge transfer spectra of complexes in this first group, have been investigated.

Kinetics of reaction between $M(Cp)_2Cl_2$ with NCS^- in acetonitrile have been used to assess the solvation of the complexes. The rate law for this reaction contains first-order and second-order terms. The effect of addition of water or toluene to the main medium on the rate constant is reported.

The binuclear complexes of d^6-metal ions with π-acceptor bridging ligands, like mononuclear complexes of the first group, also exhibit charge transfer spectra. Absorption occurs at rather lower energy and shows higher solvent sensitivities than mononuclear analogues. The majority of the complexes are relatively unstable. The rate of decomposition of the pyrazine carboxylate bridged $[(en)_2Co(pyzCOO)Fe(CN)_5]^-$ anion, which follows intramolecular electron transfer, has been measured in binary aqueous solvent media. Its rate constant is markedly solvent dependent; no correlation with Marcus-Hush theory is observed.